

NN 0201, 1687

**Quantifying the impact of soil and climate variability on
rainfed rice production**

BIBLIOTHEEK LANDBOUWUNIVERSITEIT
POSTBUS 9100
6700 HA WAGENINGEN
NEDERLAND

CENTRALE LANDBOUWCATALOGUS



0000 0609 1181

Promotor: dr. ir. J. Bouma
hoogleraar in de bodeminventarisatie en landevaluatie

Co-promotor: dr. M.J. Kropff
gewascoloog, International Rice Research Institute (IRRI)
Los Baños, Philippines

pN08201, 1687.

Quantifying the impact of soil and climate variability on rainfed rice production

Marco C. S. Wopereis

Proefschrift
ter verkrijging van de graad van doctor
in de landbouw- en milieuwetenschappen
op gezag van de rector magnificus
dr. C.M. Karssen
in het openbaar te verdedigen
op vrijdag 29 oktober 1993
des namiddags te half twee in de Aula
van de Landbouwuniversiteit te Wageningen

180 : 587110.

CIP-DATA KONINKLIJKE BIBLIOTHEEK, DEN HAAG

Wopereis, Marco C. S.

Quantifying the impact of soil and climate variability on
rainfed rice production / Marco C.S. Wopereis. - [S.l. :
s.n.]

Thesis Wageningen. - With ref. - With summary in Dutch.

ISBN 90-5485-147-3

Subject headings: rice production / soil hydraulic
properties.

The study reported here results from the project 'Soil Management for Increased and Sustainable Rice Production' (RA 89/950), a collaboration between the Winand Staring Centre for Integrated Land, Soil and Water Research (SC-DLO), the Department of Soil Science and Geology of the Wageningen Agricultural University, and the International Rice Research Institute in the Philippines. Part of the work was continued during the third phase of the project 'Simulation and Systems Analysis for Rice Production' (SARP), which is a joint research project of the Centre for Agrobiological Research (CABO-DLO), the Department of Theoretical Production Ecology of the Wageningen Agricultural University, and the International Rice Research Institute.

The research was partly financed by the Netherlands' Ministry for Development Co-operation (DGIS).

Stellingen

- 1 Het handhaven van een zo dun mogelijk waterlaagje op een rijstveld vermindert vooral bij een relatief doorlatende ondergrond het waterverlies, omdat preferente stroming naar slecht gepuddelde plekken en onder 'bunds' (dijkjes) wordt afgeremd.
Tabbal, D.F., Lampayan, R.M. and Bhuiyan, S.I., 1992. Water-efficient irrigation technique for rice. In: Murthy, V.V.N. and Koga, K. (Eds), Soil and Water Engineering for Paddy Field Management. AIT, Bangkok, Thailand, pp. 146-159.
Dit proefschrift
- 2 Het vermelden van de waterdoorlatendheid van een gepuddelde rijstgrond heeft alleen zin indien de bodemfysische omstandigheden waaronder de meting plaatsvond goed zijn gedefinieerd.
Dit proefschrift
- 3 Bemonsteringsstrategieën voor bodemhydrologische parameters en de keuze van interpolatietechnieken kunnen het beste gebaseerd worden op verkennende metingen, gevolgd door simulatie- en gevoeligheidsanalyses van het effect van bodem- en klimaatsverschillen op bijvoorbeeld gewasproductie.
Dit proefschrift
- 4 Critici van het gebruik van simulatiemodellen beseffen vaak niet dat het ontwikkelen van een voor de praktijk relevant model voornamelijk tijd en financiële armslag vereist voor het verzamelen van gegevens.
Thomas, G.W., 1992. In Defense of Observations and Measurements. Soil Sci. Soc. Am. J. 56 (6): 1979.
Dit proefschrift
- 5 Regionale toepassing van gewassimulatiemodellen komt in Azië onder andere moeizaam van de grond door het gebrek aan betrouwbare bodem- en weersgegevens.
Dit proefschrift
- 6 Twee jaar na uitbarsting van Mt. Pinatubo is internationale hulp aan het getroffen gebied meer dan ooit noodzakelijk omdat steeds meer dorpjes en landbouwgrond onder gigantische hoeveelheden 'lahar' (modder) bedolven dreigen te raken.
- 7 De eeuwenoude, zeer arbeidsintensieve, kleinschalige rijstbouw in Azië is door de sterk veranderende economische situatie en de snelle bevolkingstoename niet meer van deze tijd.
'The new rice crisis', Asiaweek, May 26, 1993.

- 8 Vanwege de wereldwijde belangstelling voor gewassimulatie is het verantwoord een internationaal netwerk op te zetten voor uitwisseling en standaardisatie van gegevensbestanden voor validatie en toepassing van simulatiemodellen.
- 9 Door de grote aandacht voor de temperatuurstijging van onze atmosfeer over de afgelopen 30 jaar ('global climate change'), wordt het werkelijke probleem, een toename van de wereldbevolking van 5 naar 8 miljard in de komende 30 jaar, ondergesneeuwd.
- 10 Het gegeven dat slechts 37% van de Filipijnse bevolking haar informatie ontleent aan dagbladen wijst op het bedroevend lage peil van nieuwsgaring en verslaggeving als gevolg van corruptie, chantage en gebrek aan journalistieke scholing.
'An outsider's view: Reckless reporting flaws Philippine press'. Press Forum newsletter Philippine Press Institute, 1st Quarter 1993.
- 11 De term 'brown-out' die in de Filipijnen gebruikt wordt voor de dagelijks terugkerende zes tot acht uur durende stroomonderbrekingen in dat land is niet zwart-wit genoeg.
- 12 Het feit dat een Hollander in Nederland woont maar een Nederlander niet noodzakelijkerwijs in Holland, klinkt iedere buitenlander als 'double Dutch' in de oren.
- 13 Uit het organiseren van twee tweekampen om de wereldtitel blijkt eens te meer dat een patstelling in de schaakwereld nooit een winnaar kan opleveren.
- 14 Als Jacques Delors in Europa niet wordt gewisseld voor Ruud Lubbers, scoort Ruud Lubbers in Azië nooit zo hoog als Ruud Gullit.

Marco C.S. Wopereis

Quantifying the impact of soil and climate variability on rainfed rice production

Wageningen, 29 oktober 1993

Abstract

Quantifying the impact of soil and climate variability on rainfed rice production (Het bepalen van de invloed van bodem- en klimaatsverschillen op niet-geïrrigeerde rijstproductie) - Wopereis, M.C.S., 1993.

Methods and sampling strategies for measurement of soil hydraulic functions in puddled and non-puddled rice soils are discussed. A method was developed to measure in situ water percolation rate and soil water pressure head gradients in puddled soils. The number of measurements needed to estimate field-average infiltration rates was determined using a sequential *t*-test. It was concluded that sampling strategies for soil hydraulic functions and the choice of spatial interpolation techniques are best based on preliminary simulation and sensitivity analyses of the impact of soil heterogeneity and weather variability on yield variability and associated cost/benefit calculations. Several possibilities for water saving in rice-based cropping systems are discussed. Field and laboratory experiments indicated that the use of a pre-tillage operation before reflooding a dry, cracked rice field may allow earlier transplanting and reduce the risk of late drought. Maintaining shallow depths of ponded water and construction of extra bunds after puddling the field, close to bunds that are left undisturbed from year to year, may also reduce water use. Drought stress responses of two lowland rice cultivars to temporary drought at different growth stages were studied. Drought in the vegetative phase delayed flowering and maturity. Drought in the reproductive phase resulted in large yield reductions. The following morphological and physiological responses to soil moisture content were quantified: (1) rate of leaf production, (2) rate of leaf rolling, (3) rate of senescence and (4) relative transpiration rate. A simulation model for rainfed rice growth was developed, validated and used to estimate regional rice yield losses due to drought in a province of the Philippines, as a function of soil and climate variability.

The results of this study are discussed in relation to the increasing use of simulation models in rice growing countries for estimation of potential and water limited yields, priority setting in research and extrapolation of new technologies.

additional key words: soil hydraulic properties, rice production, modelling, GIS, environmental characterization.

Aan mijn ouders

Preface

Many people have contributed to the research that is described in this thesis. I am very grateful for their support.

The work reported here was conducted at the International Rice Research Institute (IRRI) in Los Baños, Philippines and was partly financed by the Netherlands' Ministry for Development Co-operation. Research activities started in April 1989 with the implementation of the project 'Soil Management for Increased and Sustainable Rice Production' (SMISRIP, Project Nr. RA 89/950), a collaboration between the Winand Staring Centre for Integrated Land, Soil and Water Research, the Department of Soil Science and Geology of the Wageningen Agricultural University and IRRI. The project ended on 1 June 1992. Project co-ordinators at IRRI were Dr. T. Woodhead (until 1 July 1991) and Dr. M.J. Kropff (after 1 July 1991), and in the Netherlands, Dr. J.H.M. Wösten (until 1 September 1991) and Dr. A.L.M. van Wijk (after 1 September 1991). Prof. Dr. J. Bouma chaired a backstopping committee for the project in the Netherlands, which consisted of Dr. J.H.M. Wösten, Dr. A. Stein, Dr. H.F.M. ten Berge, Dr. W. Andriesse, Dr. E. Smaling and Dr. J.J.B. Bronswijk. After completion of the SMISRIP project, research was continued during the third phase of the project 'Simulation and Systems Analysis for Rice Production' (SARP), a collaboration between the Centre for Agrobiological Research, the Department of Theoretical Production Ecology of the Wageningen Agricultural University and IRRI.

My promoter Johan Bouma did a great job despite the 12,000 kilometers separating Wageningen and Los Baños. He wrote numerous letters, faxes and E-mails and gave very valuable advice during intensive work visits to IRRI. We were also able to discuss research progress at conferences in Thailand and Japan and of course during my yearly home leave in the Netherlands. His willingness to comment on draft papers and reports within one or two days was very stimulating. This was especially important during my stay in the Netherlands in 1992, when we were preparing the final report of the SMISRIP project, and again this year (mainly via E-mail) when I was working on parts of this thesis.

At IRRI, my co-promoter Martin Kropff has given day-to-day support and guidance to the research activities. His systems approach to research has been very important for me. He encouraged me to look beyond the 'soil horizon' and study the implications of changes in soil-water status of the root zone on rice growth. I have enjoyed our discussions a lot. They often lasted until late in the evening and were then almost inevitably stopped at the tennis court or continued at the Kropff's residence with a bottle of San Miguel. Martin's comments on draft papers and chapters of this thesis have been extremely valuable to me. I am grateful to Nynke and Martin for their hospitality and friendship.

Gon van Laar has been a very stimulating and pleasant office mate at IRRI. Also

outside work we have spent a lot of time together, often trying out the Philippine cuisine in small restaurants in- and outside Los Baños. I am very much indebted to her for all her help in finalizing the manuscript. Hein ten Berge has followed the research described here from the start. We had many stimulating discussions in the Netherlands, at IRRI and during a very interesting two weeks visit to SARP teams in India, where he took the cover photo of this thesis. His comments on an earlier draft of this thesis, and his advice on modelling of the soil water balance of puddled rice soils are gratefully acknowledged. I wish to thank Marco van den Berg for providing excellent computer network and E-mail facilities, which made life a lot easier, and for commenting on excessive working hours. I am grateful to Lucille and Marco for their hospitality and friendship. Terry Woodhead's guidance in research and administrative matters and the pleasant working atmosphere he created during the first two years of the SMIS RIP project have been very important for a smooth progress of the project. I wish to thank Frits Penning de Vries for his interest in my research work during his stay at IRRI. George Pateña kindly provided greenhouse facilities at IRRI in 1991 and 1992 for our drought stress experiments. T.P. Tuong and Bas Bouman gave very valuable comments on parts of this thesis.

Henk Wösten and Alfred Stein were closely involved with the SMIS RIP project. They visited IRRI a number of times, and in 1991 were obliged to stay one week longer than originally planned, after the eruption of Mt. Pinatubo. Henk's advice on use of various measurement techniques for soil hydraulic properties and his help in setting up laboratory facilities at IRRI were very important. During the first two years of the project he also took care of administrative matters dealing with the project in the Netherlands. I am very grateful to Alfred for his fast ways of solving statistical problems and his advice on use of geostatistics in part of the research work. Aad van Wijk made one timely trip to IRRI at the end of the SMIS RIP project. This turned out to be a busy but very fruitful visit. Aad has done a lot of administrative work during the second half of the project. I am also very grateful for his comments on drafts of the SMIS RIP final report which were very valuable and often given in one or two days. I am grateful to Wim Andriesse, Hans Bronswijk and Eric Smaling for their input during discussions on research progress at IRRI (Wim) and in the Netherlands. Peter Finke kindly provided the sequential *t*-testing software used in this study.

Armel Maligaya has done a great job in assisting and supervizing numerous field and laboratory experiments. Her good mood, jokes and attempts to teach me Tagalog always guaranteed a relaxed working atmosphere. Marlon Calibo, Lino Tatad, Ray Galang and Jessie Baraquio have formed a perfect team over the years at IRRI. Their innovative ways to facilitate research have helped to speed up the work considerably. I could fill a few pages here on the good time we spent together during day and evening hours in Los Baños, Bulacan and Tarlac.

Willy Sanidad from the Philippine Bureau of Soil and Water Management joined us on most field trips to Tarlac and translated many questions for rice farmers into Ilocano. It is safe to say that without his help we would have had a lot more trouble to find our way in Tarlac. A. Micosa kindly provided the soil maps of the Tarlac province.

I am grateful to Susan Telosa for all the secretarial work she did and especially for the smooth and efficient way with which she kept track of the logistics of numerous SARP workshops and meetings held at IRRI and outside the Philippines. Say Calubiran-Badrina did a perfect job in improving most of the figures for this thesis. I am thankful to Lee Hunt for plotting the soil and yield probability maps for the Tarlac study. I am grateful to Karel Hulsteijn for making the cover lay-out.

I wish to thank the research group of the Crop Simulation Modeling - Climate Unit group at IRRI for creating a pleasant work atmosphere and for organizing numerous despedidas, ice-cream parties, family days, New Year and Christmas parties and a very special 'dry-run' for my PhD defence. IRRI has provided excellent research and sports facilities and an opportunity to live and work in an international community which was very enjoyable. On the Wageningen side I am grateful to Henriette Drenth for her advice on research or administrative matters related to SARP.

Outside work, Myra, Dylan, Edna, Hugo, Ian, John, Lammert, Olivier, Tim and many others assured that there was a healthy balance between work and social life. They were always in for a Greenway party, a hike to Mt. Makiling, a sailing trip on Lake Taal, a diving expedition to Mindoro, or to participate in an AFSTRI / IRRI / UPLB sporting event, which was a lot of fun.

Last, but not least, I wish to thank my parents. They have always shown a lot of interest in the work I was doing in the Philippines and have given me full support during my often hectic visits to the Netherlands.

Maraming salamat po!

Marco Wopereis

Wageningen, September 1993

Account

Part of this thesis have been included, in part or in whole, in the following publications:

- Chapter 2 Wopereis, M.C.S., Wösten, J.H.M., Bouma J. and Woodhead, T., 1992. Hydraulic resistance in puddled rice soils: measurement and effects on water movement. *Soil and Tillage Research* 24: 199-209.
- Chapter 3 Wopereis, M.C.S., Stein, A., Bouma, J. and Woodhead, T., 1992. Sampling number and design for measurements of infiltration rates into puddled rice fields. *Agricultural Water Management* 21: 281-295.
- Chapter 4 Wopereis, M.C.S., Kropff, M.J., Wösten, J.H.M. and Bouma, J., 1993. Sampling strategies for measurement of soil hydraulic properties to predict rice yield using simulation models. *Geoderma* 59: 1-20.
- Chapter 5 Wopereis, M.C.S., Wösten, J.H.M., ten Berge, H.F.M., Woodhead, T. and de San Agustin, E.M., 1993. Comparing the performance of a soil-water balance model using measured and calibrated hydraulic conductivity data: a case study for dryland rice. *Soil Science*, in press.
- Chapter 6 Wopereis, M.C.S., Stein, A., Kropff, M.J. and Bouma, J., 1993. Spatial interpolation of soil hydraulic properties and simulated rice yield. *Soil Technology*, submitted.
- Chapter 7 Wopereis, M.C.S., Bouma, J., Kropff, M.J. and Sanidad, W., 1993. Reducing bypass flow through a dry, cracked and previously puddled rice soil. *Soil and Tillage Research*, in press.
- Chapter 9 Wopereis, M.C.S., Bouman, B.A.M., Kropff, M.J., ten Berge, H.F.M. and Maligaya, A.R., 1993. Understanding the water use efficiency of flooded rice fields. I. Detailed modelling. *Agricultural Water Management*, submitted.

Contents

Chapter 1	General introduction	1
Chapter 2	Hydraulic resistance in puddled rice soils: measurement and effects on water movement	19
Chapter 3	Sampling number and design for measurements of infiltration rates into puddled rice fields	27
Chapter 4	Sampling strategies for measurement of soil hydraulic properties to predict rice yield using simulation models	39
Chapter 5	Comparing the performance of a soil-water balance model using measured and calibrated hydraulic conductivity data: a case study for dryland rice	55
Chapter 6	Spatial interpolation of soil hydraulic properties and simulated rice yield	67
Chapter 7	Reducing bypass flow through a dry, cracked and previously puddled rice soil	81
Chapter 8	Drought stress responses of two lowland rice cultivars	91
Chapter 9	Understanding the water use efficiency of flooded rice fields	103
Chapter 10	Modelling the soil-plant water balance of rainfed lowland rice	115
Chapter 11	Case study on regional application of crop growth simulation models to predict rainfed rice yields: Tarlac province, Philippines	135
Chapter 12	General discussion	153
	Summary	165
	Samenvatting	169
	References	173
	Other related publications of the author	187
	Curriculum vitae	188

Chapter 1

General introduction

The extra amount of rice that has to be produced by 2020 to cope with growing populations has been estimated at 65% (IRRI, 1993). By now, 76% of the consumers depend on rice produced in irrigated ecosystems and 17% on rice produced in rainfed lowland systems. Expansion of the production area is generally not an option, due to increasing urban and industrial demand for water and land. Therefore, the extra rice needed has to come from increased production per unit area. Fortunately, yields are still increasing in most irrigated areas, presumably as a result of improved varieties and crop and soil management. In the past decades, the yield increase was around 2.3% in Asia (IRRI, 1989).

Rice is grown under very diverse climatic, hydrological and edaphic conditions. If categorized according to water regime four major rice ecosystems can be distinguished: (i) irrigated ecosystem, (ii) rainfed lowland ecosystem, (iii) upland ecosystem, and (iv) deepwater and tidal wetland ecosystem.

Definitions for 'upland' and 'lowland' rice have been given in many ways in different parts of the world. 'Dryland rice' and 'riz pluvial' are other terms found in literature for upland rice, and 'wetland rice' is often regarded as equivalent to 'lowland rice'. The following definitions for the four ecosystems are generally accepted (IRRI, 1989):

- (i) Irrigated rice lands are those areas that have assured irrigation for one or more crops per year, with some areas served only by supplementary irrigation in the wet season.
- (ii) Rainfed lowland rice is grown in banded fields where water depth does not exceed 50 cm for more than 10 consecutive days and the fields are inundated for at least part of the season. Such fields have no access to an irrigation system but may have on-farm rainwater conservation facilities.
- (iii) Upland rice is grown in rainfed banded or unbanded fields with naturally well-drained soils and no surface water accumulation.
- (iv) Deepwater rice areas are those where rice grows under rainfed dryland or shallow flooding conditions for 1 - 3 months, then is subjected to flooding with water depths of over 50 cm for a month or longer. Where water levels are over 100 cm, the crop is usually called floating rice. Tidal wetlands occur where water levels in the rice fields fluctuate under the influence of tides.

Moormann and van Breemen (1978) categorized rice lands based on landscape position, natural water source and impact of human action on the natural water regime. Their terminology is less confusing but not widely used.

In lowland ecosystems, water is a major factor as up to 5000 kg of water may be

needed to produce 1 kg of rice. In irrigated ecosystems, the area of land that can be serviced by a particular irrigation facility is determined by water availability. In rainfed lowland systems, rainfall largely determines the attainable yield. Efficient management of soil-water, whether its source is rainfall or irrigation, is thus vital for global rice production.

In Asia, contributing 90 - 95% of world rice production (Pathak and Gomez, 1991), rice in irrigated and rainfed lowland environments is mostly grown under flooded conditions. To achieve this, fields are banded and soils are puddled by plowing at water-saturated conditions, followed by harrowing and levelling. This process leads to a destruction of soil aggregates and macropore volume (Moorman and van Breemen, 1978) and a decrease in water-percolation rate, due to compaction, settling and consolidation of dispersed clay particles (Sharma and De Datta, 1985a). Long-term puddling induces the formation of a compact subsurface layer. It may take 3 to 200 years for such layers to form, depending on soil type, climate, hydrology, and puddling frequency (Moorman and van Breemen, 1978). Many names have been given to subsurface compact layers, e.g. plowpan, traffic pan, hard layer, compacted layer, restricting layer, impermeable layer, and least permeable layer. The compact subsurface layer can be a problem for non-rice crops grown after rice, because it may cause waterlogging and may impede deep rooting.

Deliberate or unavoidable drying of a previously submerged puddled soil creates soil cracks that may extend through the puddled layer. This may cause a radical change in the seasonal water balance. Especially during land preparation, water loss as a result of preferential flow down through deep soil cracks can be high. Irrigated rice production may require as much as 2000 mm of water per crop, a third to a half of which is needed for land preparation (IRRI, 1978; Hardjoamidjojo, 1992; Valera, 1977).

The response of crops in water-limited environments can be quantified through field experiments. However, field experimental research is often restricted, because of time and expenses involved. Experiments have to be conducted over a series of years and planting dates and on relevant soil types, to obtain results that can be used for recommendations. This is especially the case in many rainfed rice environments where rainfall is extremely erratic. Moreover, extrapolation of the research findings to other areas is difficult.

Research findings can be extrapolated if the crop-soil-weather system is understood quantitatively, and if changes in any component of the system can be evaluated properly. Systems approaches are required for that purpose. Systems analysis is concerned with resolution of a complex system into a number of simpler components and subsequent synthesis into a symbolic representation (diagram, flow chart) and ultimately a mathematical process model of the whole system (Nix, 1976).

The research described in this study was conducted to improve our quantitative understanding of the soil-crop-weather system in rice ecosystems, with emphasis on rainfed lowland rice. Detailed studies were conducted to analyse the water dynamics of lowland puddled rice soils and the response of the crop to drought. Based on the results

of these studies, a process based simulation model was developed, evaluated for the system and subsequently used to analyse its potential at a regional level.

Soil component

Soils in regions where rice is grown can be extremely variable in space. At a certain location, a very distinct plow pan may have developed in the soil profile, due to many years of rice cultivation, while sugarcane may be grown nearby on a well-drained sandy soil. For a specific field, one soil attribute, like clay content of the top 0 - 20 cm of the soil profile, may be relatively constant whereas another soil attribute, e.g. depth to an impenetrable soil layer for roots, may vary considerably. Soil characteristics also change in time, especially in puddled rainfed lowland systems. Soil attributes that are time dependent are e.g. soil temperature and soil moisture content.

Spatial variation

Two types of spatial models to classify soils can be considered (Bregt, 1992): discrete spatial models and continuous spatial models. The discrete spatial model or choropleth map model (Burrough, 1986) separates areas of equal value by distinct boundaries. Both quantitative and qualitative data can be mapped using the discrete spatial model. Examples are soil maps and land-use maps. Each mapping unit on a soil map is characterized by a representative soil profile description, assigning one specific value to each soil attribute. Additional information on within-variance of the soil attribute in a mapping unit can be given, but soil information for any point within a mapping unit will be the same.

Quantitative data can be also mapped using a continuous spatial model. Results are usually displayed as isolines or contours, i.e. lines connecting points of equal value. A variety of continuous spatial models is available. A well known example is the geostatistical model, based on the regionalized variable theory (Burgess et al., 1981; McBratney et al., 1981).

Especially for larger areas, it may have advantages to combine discrete and continuous models. Stein et al. (1988) subdivided a survey area into well-defined subregions (strata) using a soil map. Within each stratum, a continuous spatial model was used to describe spatial variability and to carry out predictions for specific locations. Combining both models has the advantage that a continuous model is not used to describe spatial variability across boundaries of clearly different mapping units. This avoids for example that predictions of clay content are made across the boundary of a well-drained sandy soil and a poorly drained heavy clay soil.

Measurements of soil properties are often very costly and time consuming. One has to find a balance between the number of observations that can be afforded and the required 'coverage' of the target area with sample points. An efficient sampling procedure obtains a maximum of information with a minimum of effort and cost. Sampling can often be improved using geostatistics, which defines soil heterogeneity and allows a

quantitative estimate of variability obtained as a function of observation density (e.g. Burgess et al., 1981).

Temporal variation

For crop growth, temporal variability of soil properties like temperature and water content of the root zone are of crucial importance. In this study, emphasis was on characterization of the variability of soil water content in time. A variety of systems approaches may be chosen to describe such variability. Simple empirical relationships may prove very useful in practice. Mathematical process-based simulation models may also be used. Simple modelling approaches include balance-sheet models that describe water-retention and in- and outflow of water for a soil profile over time (van Diepen et al., 1991). If focused on soil-water management, the following levels of systems approaches may be distinguished (after Bouma et al., 1993):

- Level 1 Farmer's knowledge
- Level 2 Expert knowledge
- Level 3 Integral models
- Level 4 Differential models
- Level 5 Complex differential models for subprocesses.

Levels 1 and 2 can be seen as purely descriptive, empirical approaches. Levels 3 - 5 are increasingly explanatory, all using the soil-water balance as a starting point.

The possibilities of using these levels of systems approaches in water-limited environments and associated soil data needs are discussed below. Going from level 1 to 5, data needs increase strongly (Table 1.1).

Farmer's knowledge

Rice farmers may be able to give rules of thumb for dates of transplanting or sowing and can provide useful information about crop yield, crop varieties, planting densities, use of fertilizer, pesticides, water losses, soil profile etc. However, information from farmers is often difficult to describe in reproducible terms and hard to extrapolate.

Important empirical information on water management may be derived, especially if the area under study has not been visited before. For example, in areas where rainfed rice is grown on terraces, some farmers will grow up to three crops per year on the lowest terraces, whereas they can grow only one crop at the highest elevations. Wet season rainfall is often collected from a catchment area and stored in ponds or farm reservoirs. This water can be used for supplementary irrigation for a rice crop in the wet season, or for growing a second crop in the dry season. Seedbeds are located at the lowest terraces, if possible near natural wells. In general, landscape position of a particular field will give an indication of runoff/on and surface and internal drainage.

Plow pans or traffic pans may have developed in soils where lowland rice has been grown for a long time (at least 5 - 50 years depending on soil type). This plow pan usually hinders downward flow, and therefore helps water conservation.

In the dry season, when upland crops are grown, farmers may try to conserve water

Table 1.1 Soil-data needs for the five input levels distinguished in systems analysis (after: Bouma et al., 1993).

Level 1	Local experience; difficult to describe in reproducible terms and to extrapolate
Level 2	Soil texture; local experience in terms of descriptive land qualities (water availability, workability, trafficability, root zone aeration etc.)
Level 3	Field capacity, wilting point, thickness root zone, bulk density, water table depth, if any
Level 4	Hydraulic conductivity, moisture retention, water table depth if any, empirical relations for bypass flow, soil shrinkage characteristics
Level 5	As 4, but with hysteresis characteristics, soil-root contact, accessible relative soil volumes for roots

in the topsoil by mulching or by shallow surface tillage. This tillage also removes weeds that are competing for water.

Farmers may also invest in water pumps if the groundwater is sufficiently shallow, depending on fuel prices, interest rates, etc.

Expert knowledge

Experts from national agricultural research centres and national soil survey institutes develop a set of decision rules to investigate possibilities for crop growth in a given area of land. Such an 'expert system' may include information on land qualities like water availability, workability, trafficability, drainage class, salinity etc.

Simple mathematical rules of thumb are also considered as 'expert knowledge' in this overview. Doorenbos and Kassam (1979) found a linear relationship between relative evapotranspiration deficit and relative yield reduction for 26 agricultural crops. The slope of the graph (yield response factor) differed between crops and between specific growth stages. These relationships can be used to predict effects of water deficits at different growth stages on crop yield.

The concept of the water balance is one of the greatest advances in understanding the response of crops in water-limited environments, both when used alone, and as a component in crop growth models (Angus, 1991). A soil water balance determines gain and loss of water (in mm d⁻¹) over a specified soil depth, such as the root zone. Rainfall or irrigation (*I*) and capillary rise (*C*) increase soil water storage *W*; runoff (*R*), deep drainage (*D*), seepage (*S*), evaporation from the soil or water surface (*E*) and crop transpiration (*T*) decrease *W*:

$$dW = I + C - R - D - E - T - S \quad (1.1)$$

Rice farmers in Asia will try to minimize R through levelling and bunding of their fields and D and S through thorough puddling of the soil. At the start of the growing season E will be large, but it gradually decreases due to shading by the growing crop. In contrast, T will be small at the start of the growing season, but increases rapidly as the crop grows. A schematic representation of the soil-water balance of a lowland rice field is given in Fig. 1.1. Eqn 1.1 is often used to calculate irrigation requirements (i.e. I) for agricultural crops. Examples are given by Doorenbos and Kassam (1979). Evapotranspiration ($ET = E + T$) is estimated, usually from a reference ET_0 measured with an evaporation pan, and a crop coefficient.

Doorenbos and Kassam (1979) estimated dW using soil water depletion fractions p , i.e. the fraction to which the total available soil water can be depleted, before actual evapotranspiration rates ET_a drop below maximum evapotranspiration rates ET_m , and an estimate for the rooting depth. 'Total available soil water' (S_a) was defined as the soil water volume between field capacity (i.e. soil moisture content at pressure heads ranging from -10 to -20 kPa) and wilting point (i.e. soil moisture content at pressure head of -1.5 MPa). They gave rough estimates of S_a for three soil textural classes (heavy, medium and coarse textured soils) but stressed the need for field measurements.

The magnitude of C (capillary rise) in Eqn 1.1 is difficult to determine and is often ignored. This leads to erroneous results when a shallow groundwater table influences the moisture condition of the root zone.

Tabal et al. (1992) measured I , R and $D + S$ (both percolation and lateral seepage) and estimated E and T to derive water losses over a cropping season for a large number of rice fields in the Philippines. Water requirements ranged from 1000 to 4000 mm per rice crop. Such large water losses indicate the importance of lateral seepage through bunds or preferential flow through poorly puddled areas in paddy rice fields. In the

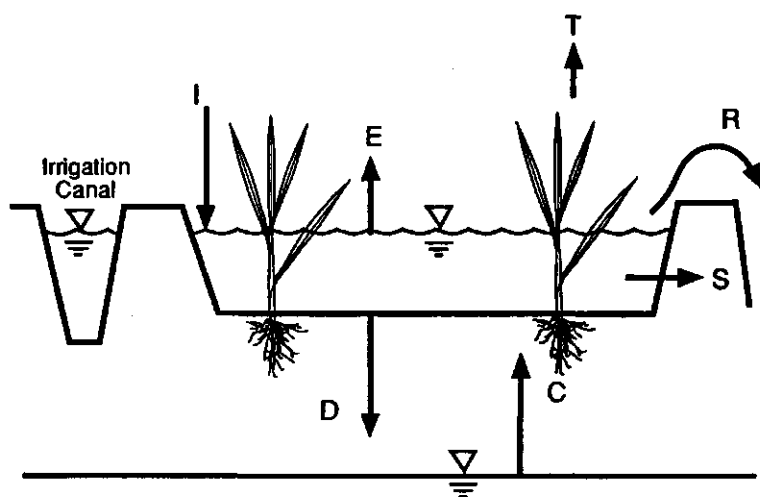


Fig. 1.1 Water balance of a paddy rice field.

tropics, preferred percolation rates are 1 - 3 mm d⁻¹ in rainfed or inadequately irrigated lands. In irrigated temperate rice lands higher percolation rates may be needed (5 - 15 mm d⁻¹) to leach organic toxins that persist from year to year in cooler climates. Walker and Rushton (1984) developed a numerical model that simulates lateral water losses from irrigated rice fields.

Integral models

Integral models (ten Berge et al., 1992) are defined here as models that describe water transport in soils partly by integrating (over time and/or depth) calculations rather than by solving the *general flow equation*, which combines Darcy's law and an expression for conservation of mass.

In many integral models, the root zone can be seen as a 'box' which contains water within two predefined critical pressure heads: field capacity and wilting point. When water is applied to the soil, it is assumed to be rapidly redistributed when the water content is above field capacity. The excess water flows downward. Water can be extracted to the wilting point; water held at lower pressure heads is unavailable for plants. 'Field capacity' is often determined by flooding a field and measuring water content after two days while avoiding evaporation. Similarly, the wilting point is estimated by growing a crop and by observing the moisture content at which wilting occurs (e.g. IBSNAT, 1988). These procedures are very laborious and hard to control. Formerly, the water content at -1.5 MPa pressure was taken to represent the permanent wilting point but this value has correctly been criticized because wilting of plants depends not only on the soil water state but also on the type of plant and the evaporative demand. Distinction of arbitrary 'field capacity' and 'wilting point' values poses a scientific problem in view of the continuous processes of water transport and uptake in nature.

The CERES crop growth model used by the International Benchmark Sites Network for Agrotechnology Transfer (IBSNAT) project (Jones and O'Toole, 1987) and the WOFOST crop growth model of the Centre for World Food Studies (van Keulen and Wolf, 1986; van Diepen et al., 1988) use integral soil-water balance modules.

Some models developed at the International Rice Research Institute (IRRI) in Los Baños, Philippines such as IRRIMOD (Angus and Zandstra, 1980) and PADDYWATER (Bolton and Zandstra, 1981) assume a constant percolation rate through the puddled top-soil and are, therefore, also integral models.

Differential models

Differential soil-water balance models are defined here as models that describe water distribution in soils by solving the general flow equation (usually numerically). Such models require both hydraulic conductivity ($k(h)$) and moisture retention data ($h(\theta)$) to calculate boundary fluxes between layers in the soil (where h is the pressure head, θ the soil moisture content and k the hydraulic conductivity). Differential models are generally preferable if the soil-water system does not reach an equilibrium state within the period of one time step of the main (crop growth) simulation model (ten Berge et al., 1992).

Usually the soil profile is divided into a number of compartments, each having its own soil hydraulic characteristics, i.e. soil hydraulic conductivity and water retention functions. Upper boundary conditions include daily values for rainfall and potential evapotranspiration. Lower boundary conditions can be depth to a groundwater table or the assumption of free drainage.

Differential models are very suitable for simulation of water dynamics in puddled rice fields. However, because of the need to determine hydraulic conductivity and water retention characteristics, a simple integral model using a constant percolation rate will be often preferred.

In Europe, negative effects of soil compaction on agricultural production could be explained using differential models, after measuring both hydraulic conductivity and water retention data of the compacted layer and of surface and subsurface soil horizons (Bouma, 1990). Examples of multiple layer differential soil water balance models are SWATRE (Belmans et al., 1983) and SAWAH (ten Berge et al., 1992), which was used in this study. Time steps in SAWAH are independent from time steps used in the main (crop) model. Bronswijk (1988a) presented the simulation model FLOCR in which shrinkage characteristics of soils are included as hydraulic parameters that can be specified for each soil layer. FLOCR can simulate the soil water balance of swelling and shrinking soils.

Complex differential models for subprocesses

In the field, most soils show 'non-ideal' behaviour with preferential water flow along the walls of macropores or cracks. Irregular wetting may occur due to effects of microrelief or hydrophobicity (Dekker and Jungerius, 1990). Irregular flow patterns may be caused by the occurrence of contrasting soil horizons. Clayey soils with natural, large aggregates often show rooting patterns that leave water inside aggregates inaccessible. Standard flow theory and existing models for water extraction by roots do not consider these phenomena. For very detailed studies more complex simulation models are sometimes needed. Input requirements for such models may include measures for effective soil-root contact, hysteresis characteristics, and accessible relative soil volumes for roots, in addition to data on soil water retention, soil hydraulic conductivity, and possibly soil shrinkage characteristics.

Data needs

Data needs for the five levels in systems analysis distinguished above are summarized in Table 1.1. A distinction can be made between internal and external variables. Internal variables can be subdivided into system parameters (like hydraulic conductivity functions) and state variables (like root zone water content). System parameters are assumed to be constant; state variables change over time. For rice, system parameters like soil hydraulic conductivity may however change drastically during one growing season, due to crop and soil management procedures or soil cracking. External variables are boundary conditions, like a time series of groundwater table depth.

Differential models (Levels 4 and 5) require knowledge of soil hydraulic conductivity and water retention characteristics. They should be only used if simpler integral type models (Level 3) are not applicable.

Since soil-water parameters are difficult to measure, it is extremely helpful that they can be derived from more easily obtained soil characteristics, determined during routine soil surveys. This results in substantial savings in research time and effort. Deriving complex soil information, like hydrological data from other soil data is referred to as applying 'pedo-transfer functions'. This term is generally accepted and is also used in this thesis. It is however confusing as a function in itself transfers information from one variable to another. Class pedo-transfer functions relate physical data to soil horizons. A standard series of 360 conductivity/retention curves for surface- and subsoils of some 150 soil profiles is being used in the Netherlands (Wösten et al., 1987a; Wösten et al., 1990). Such data sets can be used for studies carried out for large areas, like in zonation studies. Much work has been done to derive continuous pedo-transferfunctions, i.e. to relate soil hydraulic characteristics to simple soil characteristics such as texture, bulk density, and organic matter content. Examples are presented by Brooks and Corey (1964), Bloemen (1980), Wagenet et al. (1991) and Vereecken et al. (1990). Measurements of soil-water parameters will usually be more precise and accurate than estimates. However, depending on the degree of detail of the question being pursued, estimates of soil data may be quite satisfactory. Such a judgment can only be made, however, when the relative importance of the variable is known, and when the accuracy of an estimate of its value is known (Bouma et al., 1993).

Crop component

Rice plants that are exposed to drought try to conserve water by various morphological and physiological responses. Chaudry and McLean, cited in De Datta et al. (1973) observed that non-flooded conditions caused a delay in flowering. Severe stress in the vegetative stage may delay heading by up to 40 days (Inthapan and Fukai, 1988; Puckridge and O'Toole, 1981). Water deficits in the vegetative phase may reduce plant height, tiller number and leaf area and may cause retarded growth, but yield may not be affected if the plant is able to recover before flowering (Yoshida, 1981). A similar observation was done by Aragon et al. (1987) who even found higher yields in plots not irrigated for three weeks during the vegetative phase, compared with continuously flooded plots. On the other hand, Cruz et al. (1986) observed a reduction in leaf area index and grain yield as a result of water deficit in the vegetative phase. According to Yoshida (1981) rice is most sensitive to drought 0 - 2 weeks before heading, as it may cause grain sterility.

Drought strongly affects the morphology of the rice plant. Leaf expansion and leaf area development may be hampered, and tillering and panicle development may be reduced (e.g. O'Toole and Cruz, 1980; O'Toole and Baldia, 1982). Very clear symptoms

of drought stress in rice are leaf-rolling and early leaf senescence. An important characteristic of rice is its desynchronized tillering, i.e. not all tillers emerge at the same time. The number of affected tillers may, therefore, be small if the duration of drought is relatively short (O'Toole and Chang, 1979; O'Toole, 1982).

The rooting depth of irrigated rice normally does not exceed 15 - 20 cm. Drought may stimulate more rapid root growth to explore deeper soil layers for water (O'Toole and Chang, 1979; O'Toole and Moya, 1981). However, rice rooting may be restricted by wet-tillage-induced compacted layers (Hasegawa and Woodhead, 1990).

Physiological processes that are affected by drought are closing of stomata, reduction of photosynthesis, reduction of respiration and reduced translocation of assimilates to the grains (e.g. Fukai et al., 1985; Turner, 1986).

Crop modelling

In the past 20 - 30 years, crop growth simulation models have been developed to integrate the available knowledge about processes determining plant growth, which is needed to understand the system. Once validated, they allow quantitative estimates of plant growth and production under varying agro-ecological conditions, as shown by e.g. de Wit et al. (1978), Feddes et al. (1978), Penning de Vries and van Laar (1982), France and Thornley (1984), van Keulen and Wolf (1986), and Penning de Vries et al. (1989).

Crop growth simulation models have been developed for different production situations. Four production situations can be distinguished (de Wit and Penning de Vries, 1982):

- Production Situation 1: Potential production, where yield is determined by radiation, temperature and crop and varietal characteristics,
- Production Situation 2: Water-limited production for at least part of the growing season,
- Production Situation 3: Water and/or nitrogen-limited production for at least part of the growing season, and
- Production Situation 4: Water, nitrogen and/or other nutrients limited production for at least part of the growing season.

Going from Production Situation 1 to 4, crop production generally decreases and the number of variables required to describe the system increases. At all these situations, growth reducing factors like pests, diseases and weeds can interfere. Models for all production situations exist, although models for the first two situations are further developed than models for situations three and four. In this thesis, focus will be on Production Situations 1 and 2 only.

The crop growth simulation models used in this study were ORYZA1 (Kropff et al., 1993a) and MACROS (Penning de Vries et al., 1989), which both are based on SUCROS (Spitters et al., 1989; van Laar et al., 1992). The general structure of these models is given in Fig. 1.2.

Crop growth simulation models have been used to estimate yield potential of several crops under a range of weather conditions and for different soil types (see e.g. van Wijk

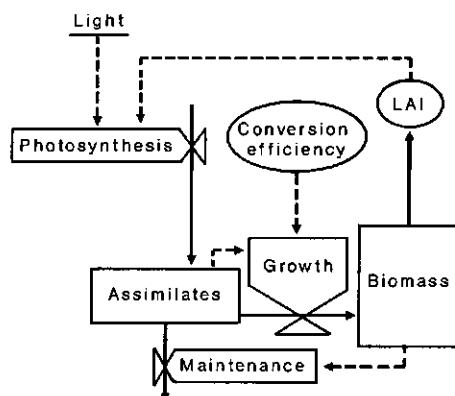


Fig. 1.2 Relational diagram of a system in Production Situation 1. Boxes are state variables, valves are rate variables, circles are intermediate variables. Solid lines are flows of material, dotted lines are flows of information (after: Kropff and van Laar, 1993).

and Feddes, 1986; Feddes and van Wijk, 1990; de Wit and van Keulen, 1987; van Lanen et al., 1991). Regional estimation of crop performance in water limited environments in response to crop, soil or water management can be very useful for extension and planning purposes. Numerous examples are given by Bunting (1987) and Muchow and Bellamy (1991). The use of simulation models for decision-making in water management for cropping systems within Europe were summarized by Feyen (1987). Irrigation requirements for wheat in Bangladesh were estimated by van Keulen and Wolf (1986). Muchow et al. (1991) used a crop simulation model with 100 years of weather data in a feasibility study on introducing farming in parts of Australia. Another example is the analysis of production constraints of sorghum in Burkina Faso. Crop simulations showed that fertilizer input and not water shortage was the main production constraint and that attempts to improve sorghum yields should focus on improvement of soil fertility, despite low and erratic rainfall (van Keulen et al., 1987).

Data needs

Input requirements for the model ORYZA1 that is parameterized for rice, in Production Situation 1 are:

- Daily weather data for solar radiation and temperature,
- Plant density,
- Date of crop emergence or transplanting, and
- Parameters that describe the morphological and physiological characteristics of the crop species.

Models that are used in Production Situation 2 often assume that the ratio between actual and potential transpiration decreases linearly from 1 to 0, if the root zone water content drops from saturation to wilting point (soil pressure head is -1.5 MPa). Drought stress reduces the rate of photosynthesis and development rate and changes the partitioning of carbohydrates over shoots and roots. This is done by multiplying the corresponding rates with a level of stress, defined as the ratio of actual over potential transpiration (Penning de Vries et al., 1989). In such models, drought does not affect the morphology of the plant. Sinclair (1986) and McCree and Fernandez (1989) used empirical relationships to describe several morphological and physiological responses of soybean to soil-water status.

Weather component

Rice is cultivated under tremendously different climatic conditions. It is grown at latitudes from 35°S (New South Wales, Australia) to 53°N (north-east China) and at elevations ranging from below sea level (Kerala, India) to more than 2,000 m (Kashmir, India and Nepal). Temperatures during the growing season vary widely. Low temperature problems, like delayed flowering, spikelet sterility and delayed seedling emergence, may occur in e.g. Australia, China, Japan and Nepal. High temperatures ($> 35^{\circ}\text{C}$) may cause spikelet sterility in dry season crops in e.g. Thailand (Yoshida, 1981).

For irrigated rice, yields are generally higher in the dry season than in the wet season, because of higher levels of solar radiation. In Indonesia, dry season yields are lower than wet season yields, possibly because of negative effects of high temperature. In eastern and northeastern India wet season yields are comparatively low due to cloudiness. Cultivars adapted to low-light stress are indispensable in these regions that receive less than 300 hours of sunshine during the wet season (Murty and Sahu, 1987).

Long-term daily weather data are important for calculating reliable average crop yields with simulation models. Unfortunately, in many rice growing countries, such data sets are often not available, or common years between meteorological stations are non-existent. The use of average climatic data (e.g. monthly averages) does not give reliable predictions. Erratic occurrences of drought periods may have severe implications for crop growth. Weather generators can generate daily weather data from monthly averages, or can be used to create additional years of weather from a small complete set of years.

Interpolation of weather data from point to area can be done by a variety of techniques (Brinkman and Stein, 1987). Kriging (Webster, 1985) seems the most appropriate interpolation method, in that it provides an unbiased prediction with minimum prediction variance. If possible, stratification of the study area into clear climatic zones should be done beforehand, to avoid for example using rainfall data from mountainous or coastal areas to predict rainfall for inland plains. For drought experiments at key sites, rainfall measurements and monitoring of groundwater table depth in the experimental field, in addition to data obtained from the weather station are important.

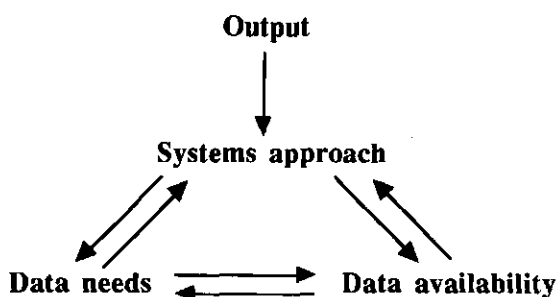


Fig. 1.3 Interdependency of output definition, selected systems approach, associated data needs and data availability in systems analysis.

Linking crop, soil and weather components

To quantify the impact of soil and weather conditions on rainfed rice production the crop, soil and weather components have to be linked.

In the previous sections different levels of systems approaches and different models to analyse water-limited environments were presented. The question which of these models / approaches to use, depends on the required output of the study, on data needs and on data availability. It is very important to define the required output of the study first before a systems approach is chosen. A systems approach may be altered depending on data needs and data availability (Fig. 1.3).

The following two examples will illustrate the importance of this methodology.

Example 1:

Output:	Insight in variability of rice yield as a function of transplanting date under intensive irrigated cultivation.
Systems approach:	Production Situation 1 model parameterized for rice.
Data needs:	Long-term weather data (daily data on solar radiation; minimum and maximum temperatures); Crop characteristics.

Example 2:

Output:	Feasibility study to investigate possibilities to grow maize on a free draining soil under rainfed conditions.
Systems approach:	Production Situation 2 model parameterized for maize coupled to a simple integral soil water balance model.
Data needs:	Long-term weather data (daily data on solar radiation; minimum and maximum temperatures, wind speed, relative humidity and rainfall);

Crop characteristics, including drought stress responses;
Soil data (moisture contents at field capacity, wilting point).

The first example deals with irrigated rice, where no water limitations occur, and the soil, therefore, does not play a role. In the second example, maize yield is simulated under rainfed conditions. Because the soil is freely draining, a simple capacity soil water balance model is chosen, with limited soil data needs.

In general, the simpler the model the less input parameters are needed. A complex model will provide more information but may be less accurate, if for some input parameters only rough estimates can be made.

Combined use of crop simulation models and GIS

Regional application of models requires a means to extend point-information over wider geographic areas and to combine data sets from different disciplines. A Geographic Information System (GIS) can be used for this purpose. A GIS is a structured framework for acquisition, storage, retrieval, analysis and display of data within some common spatial referencing system (Nix, 1987). It is in fact a combination of cartographic data, software to manipulate these data, and the computer hardware.

Combined use of Geographic Information Systems (GIS) and crop growth simulation modelling offers unique possibilities for the interpretation of extensive data sets derived from various disciplines to answer questions at the regional level. It can help in the extrapolation of research results and in the identification of research priorities. Models need to be tested at very carefully selected key sites. These key sites should represent the full range of situations regarding water limited, nitrogen limited and pest/diseases limited production. Testing will imply improvement of the models and often a better specification of the data input.

Quantitative understanding of the rainfed lowland rice system

Quantification of responses of rice to drought stress is essential for predicting the impact of soil and weather conditions on rice production. The link between soil-water status and crop response is crucial. For lowland rice, grown in puddled soils, hardly any information on this aspect is available, although drought periods as a result of erratic rainfall is a major cause of yield loss in rainfed rice production systems. Existing rice growth simulation models use standard drought stress responses derived for other crops and are not validated with field experimental data.

The man-made puddled layer in lowland rice soils is often very effective in reducing water losses through percolation to deeper soil layers. The effect of puddling on the hydraulic conductivity of the various layer is however not well understood. Drying of a previously submerged rice soil creates cracks that may extend through this puddled layer. This can cause a drastic and often irreversible increase in water losses due to increased

percolation rates. Quantitative understanding of the physical changes in a drying lowland puddled soil is needed. Existing soil-water balance models do not consider such changes and are not directly applicable to puddled rainfed lowland rice soils.

The spatial interdependence of soil hydraulic properties can be determined through geostatistical techniques. This dependence can be used in data collection operations to optimize sampling strategies and to support interpolation techniques, like kriging. The optimization of sampling strategies can result in substantial savings of time and money, and interpolations allow quantitative predictions with known precision. An expression of the spatial variability of parameters to be used in simulation modelling is crucial to obtain realistic results for field conditions.

Pedotransfer functions are not widely used in rice growing countries in Asia. Only if hydrological data can be derived from readily available soil data, it will be possible to simulate water regimes and rice production across large areas of rice land. To do such simulations an effective link between the crop growth simulation model and a GIS is needed.

Research objectives and approach

The specific objectives of the study were:

- Identification and adaptation of methods of measurement of soil-physical properties for use in rice soils,
- Development of methods to estimate basic physical parameters from relatively simple, available soil data (pedotransfer functions),
- Quantitative characterization of the spatial variability of rice-soil physical properties and specification of sampling strategies,
- Development of procedures for regional application of crop growth simulation models using GIS,
- Quantification of drought stress responses of lowland rice cultivars grown in puddled soil, and
- Development of a rainfed lowland rice simulation model.

Outline of the thesis

The structure of the thesis is presented in Fig. 1.4. Chapters 2 - 7 and 9 discuss various aspects of the soil component of the rainfed rice ecosystem.

The effect of the puddled layer on soil hydrology in lowland puddled rice soils is of crucial importance when modelling rainfed rice growth. A technique was developed to measure *in situ* the hydraulic resistance of the puddled layer (Chapter 2). Measurements of physical parameters needed for simulation should preferably be made *in situ*, using methods that are relatively simple, accurate and cheap. Chapter 3 explains the use of a

sequential *t*-test analysis to determine the minimum number of measurements needed to estimate the average percolation rate within a puddled rice field with a specified degree of precision. Pedotransfer functions relate available soil data to parameters needed for simulation. A specific type of pedotransfer function uses soil horizons as 'carriers' of data. This approach is illustrated for both a large scale (Chapter 4) and a small scale soil survey (Chapter 11) conducted in the Philippines. Measurements of soil hydraulic conductivity and water retention functions that are needed to run soil water balance and/or crop growth simulation models are expensive and time consuming. In Chapter 5, three methods to derive soil hydraulic conductivity data are compared. The number of such measurements can be reduced considerably if 'classical' soil horizons that are to be sampled can be merged into broader, hydraulic-functional horizons. A hydraulic-functional horizon comprises one or more soil horizons that are similar in terms of soil hydraulic functions. A detailed soil survey was carried out in a 50 ha dryland rice area to test the concept of hydraulic-functional horizons (Chapters 4 and 5).

Geostatistics provides quantitative techniques to interpolate point data to areas of land and to design efficient sampling schemes, which base the number of observations on spatial heterogeneity and not on the scale of the map to be made. The use of geostatistics to determine the spatial variability of rice-soil physical properties and rice yield and to interpolate to areas of land is discussed in Chapter 6. The impact of cracking of a previously puddled rice soil in the dry season on the soil-water balance and the benefits of a pre-tillage practice prior to reflooding a field for the next rice crop are outlined in Chapter 7. The water use efficiency of flooded rice fields was also studied (Chapter 9).

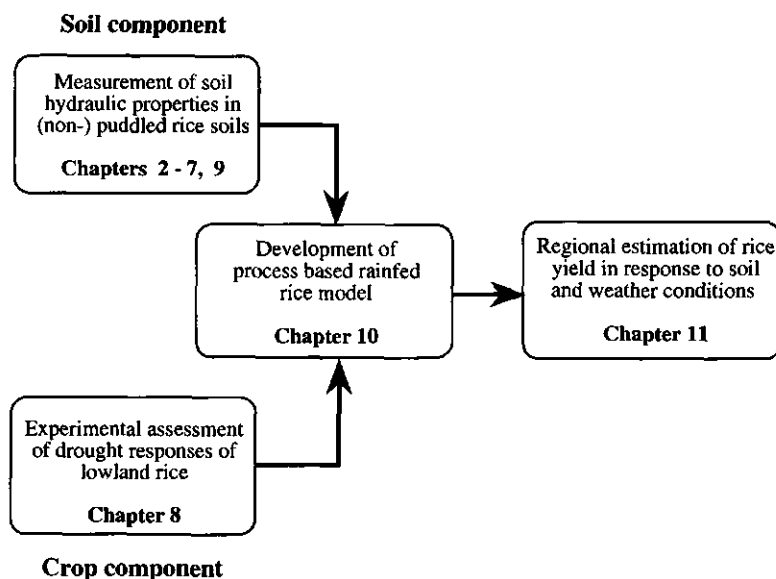


Fig. 1.4 Outline of the thesis.

In Chapter 8, the 'crop component' of the rainfed rice ecosystem is discussed. The responses of two lowland rice cultivars to temporary drought at different growth stages were studied.

Based on the findings presented in Chapters 2 - 9, a rainfed rice model was developed (Chapter 10). In Chapter 11, this model was coupled to a Geographic Information System (GIS) and used to assess regional rice yield losses due to drought within the province of Tarlac in the Philippines.

Chapter 2

Hydraulic resistance in puddled rice soils: measurement and effects on water movement

Abstract A technique is presented to measure *in situ* infiltration rate and pressure head gradients within a puddled rice soil. Measurements at 33 sites within a small 0.1 ha plot indicated unsaturated flow conditions in the non-puddled subsoil. The least permeable layer within the profile, as determined by the greatest gradient in pressure head, was found to be at the interface of puddled topsoil (0 - 15 cm) and non-puddled subsoil. Average thickness of this layer was about 5 cm. Hydraulic resistance of the least permeable layer at all measurement sites was log normally distributed with an average value of 209 days, and 95% confidence limits at 156 and 262 days. Corresponding average hydraulic conductivity was 0.36 mm d^{-1} with 95% confidence limits at 0.27 and 0.45 mm d^{-1} . Measured pressure heads in the subsoil showed good agreement with values predicted from comparison of measured hydraulic resistance in the puddled surface soil and non-puddled subsoil. Puddling reduced infiltration rate by a factor of 500.

Introduction and objectives

There is concern in much of south and south-east Asia that rice-irrigation schemes (constructed often at high cost) are not able to supply water sufficient to support rice production over the whole area that the schemes were designed to service (e.g. Sattar and Bhuiyan, 1985; Kanwar, 1986; Bhuiyan, 1987; Ghani, 1987). In part, this failure of supply occurs because rates of water infiltration and percolation in individual farm fields may be higher than expected - particularly for those fields where water-percolation rate is not controlled by the shallowness and slow drainage of groundwater. In such fields, farmers seek to lessen water requirement by manipulating the soil (usually by puddling, but sometimes by compaction using rollers or tracked vehicles) to create a zone of low hydraulic conductance. The puddling procedure also assists weed control, and the puddled zone has low mechanical strength that allows easy transplanting of rice seedlings and effective extension of rice roots. Most rice in Asia, whether irrigated or rainfed, is grown on puddled soils; but not all rice on puddled soils is established by transplanting, some is direct-seeded onto the wet soil surface (De Datta, 1986).

In the initial phase of the puddling process, the soil is submerged under standing water for 2 - 10 days to promote soil chemical reduction and lessen soil mechanical strength and hence the draft force and energy needed for the puddling tillage. The puddling tillage usually comprises one or two plowings to 0.15 m depth and two or more harrowings and a final levelling, all using animal power or two-wheeled, gasoline-

powered hand-tractors (Painuli et al., 1988) or may involve gasoline-powered rotovation using low ground-pressure equipment (Villaruz, 1986). In animal-powered puddling there is soil compression beneath the animal hooves that creates a compact zone (sometimes called a plow or traffic pan) in the upper layer of the non-puddled subsoil (e.g. Moormann and van Breemen, 1978). In addition settling and consolidation of dispersed clay particles may occur (Sharma and De Datta, 1985a). Both compaction and clay translocation will create a zone of low hydraulic conductivity. The non-puddled subsoil beneath this less permeable layer usually has a higher hydraulic conductivity and consequently there can be non-saturated subsoil flow (and negative soil-water pressure potentials) in conjunction with saturated flow in the puddled and compacted layers (Tagaki, 1960; Prihar et al., 1985; Adachi, 1990). Hundal and De Datta (1984) reported a different field situation in which the subsoil layer restricted percolation rate to a greater degree than the puddled topsoil.

Quantitative understanding of this puddled-soil system, and of the influence that soil management can have on water percolation and water conservation, would be advanced if the effect of puddling on the hydraulic conductivity of the various soil layers was better defined. Similarly, in the simulation of rice production, as in rice production itself, crop-water relations and soil-water transmission are crucial components. Many soil-water simulations assume one-dimensional (vertical) water flow through a succession of soil layers, and the hydraulic conductivities of such layers are needed as parameters in the simulation.

In this present study we investigated the use of miniature tensiometers to monitor *in situ* the soil-water pressure at closely-spaced depths in each of several columns of puddled submerged rice soil. The columns were encapsulated but maintained hydraulic continuity with the underlying strata, and water was infiltrated into them at measured constant rates. The effect of puddling on the hydraulic resistance of the various soil layers, the variability of those resistances, and the determinant of water infiltration through the plow layer were studied within a 0.1 ha experimental field.

Materials and methods

The experiment was sited on a 50 m x 20 m field at the International Rice Research Institute, Philippines (14°30' N, 121°15' E) that had not previously been puddled and, therefore, had no puddling-induced compact layer. The soil was mixed, isohyperthermic Typic Tropudalf; Ap and Bt horizons respectively comprised 38%, 44%, 18% and 48%, 39%, 13% of clay, silt, and sand. The field was divided into 36 plots of 5.0 m x 4.0 m, each hydraulically isolated by double walls (bunds) of soil 0.25 m high and 0.25 m wide. All plots were submerged for 10 days, then plowed four times and harrowed four times using water-buffalo power, and maintained submerged. The field-water table was sufficiently deep that unsaturated subsoil conditions could prevail. Measurements were started 10 days after the last harrowing.

In situ measurement of infiltration rate and pressure heads

Centrally within each plot, a metal ring with a diameter of 80 cm and a height of 40 cm was pushed into the soil to a depth of approximately 30 cm. A steel cylinder with a diameter of 20 cm and a height of 25 cm was placed in the centre of this ring and pushed downwards to 1 cm below the upper rim, while continuously removing soil around the outside of this inner cylinder. At the bottom end of the cylinder, an additional 10 cm depth of soil was exposed and covered with a gypsum/cement mixture to prevent lateral seepage of water and to allow one-dimensional flow in the soil. A perspex cover with a water inlet and air outlet was screwed on top of the cylinder and connected to a mariotte burette. Finally ten small pressure-transducer tensiometers (5 cm long, 6 mm outside diameter) were inserted into each column at 2 cm intervals from a depth of 4 to 22 cm in a spiral configuration (Fig. 2.1).

At each site the depth of the puddled layer was recorded as the depth of easily removed soft mud. The rate of infiltration into each column was monitored throughout a 24-h period, at the end of which the soil-water pressure potentials were measured in the various soil columns.

For comparison, infiltration rates were also measured at nine non-puddled sites (adjacent to the 36 puddled plots), following the procedures described above.

Hydraulic conductivity of subsoil

At two sites within the experimental field the hydraulic conductivity curve of the subsoil Bt horizon was determined using a combination of two methods:

- the column method (Bouma, 1982) for the vertical saturated hydraulic conductivity using steel cylinders of 25 cm height and 20 cm diameter;
- the crust method (Bouma et al., 1983) for unsaturated conductivities at pressure heads between 0 and -5 kPa using the same cylinders; unsaturated flow is induced by applying artificial crusts of sand and quick-setting cement on top of the samples.

An equation of the form:

$$k(h) = k_s |h|^n \quad (2.1)$$

was fitted to the data, where k_s is the saturated hydraulic conductivity (cm d^{-1}), h is the pressure head (cm), and n is a dimensionless soil constant.

Calculation of hydraulic resistance

The flux q (cm d^{-1}) through a soil layer with thickness z_L (cm) can be described by Darcy's law:

$$q = -k_L[(h_T - h_B + z_L) / z_L] \quad (2.2)$$

where k_L is the hydraulic conductivity of the soil layer (cm d^{-1}), and h_T and h_B pressure

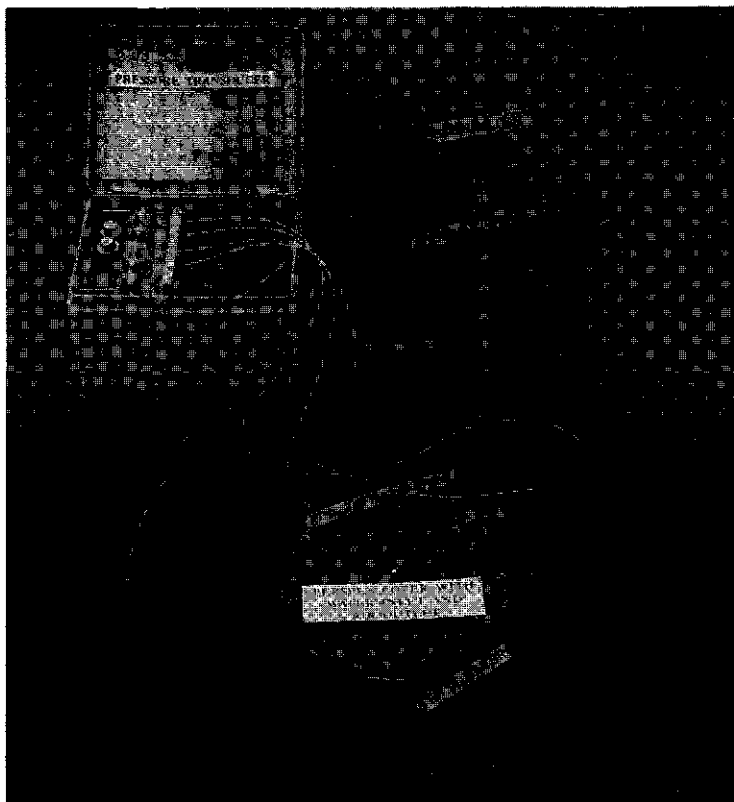


Fig. 2.1 Equipment used to measure *in situ* infiltration rate and pressure head gradients in a submerged puddled clay soil.

head (cm) at top and bottom respectively (e.g. Falayi and Bouma, 1975).

Water flow through a soil will be restricted by the least permeable layer, i.e. the layer with the greatest hydraulic gradient $h_T - h_B$, if the flow rate is constant. In puddled soil, as the non-puddled subsoil usually will have a higher conductivity than the puddled topsoil, negative pressure heads will develop in the subsoil. Under steady-state downflow of water, the negative pressure head that is developed can remain constant over a considerable depth and usually starts at the interface of both layers (Takagi, 1960).

In the absence of a pressure head gradient in the subsoil (gravity flow) the unsaturated hydraulic conductivity $k(h_B)$ of the subsoil (Hillel and Gardner, 1969) will equal flux q .

The hydraulic resistance R_L of a specific layer (in days) is the ratio of the thickness of a soil layer to its hydraulic conductivity:

$$R_L = z_L / k_L = -(h_T - h_B + z_L) / q \quad (2.3)$$

Assuming gravity flow in the subsoil flux q can be written as:

$$q = -k(h_B) = -(h_T - h_B + z_L) / R_L \quad (2.4)$$

From Eqn 2.4 it can be seen that the infiltration rate through the puddled layer is affected by both the characteristics of the non-puddled subsoil, through its $k(h_B)$ conductivity curve, and by the physical properties (hydraulic resistance, R_L) of the least permeable layer (Hillel and Gardner, 1969 and 1970).

As the thickness of the puddled layer is not constant the depth to the least permeable layer will vary. For each of the 36 monitoring sites graphs were, therefore, prepared of pressure head vs depth. Curves were eye-fitted through the data and the hydraulic resistance of the layer with the greatest gradient in pressure head was calculated.

Average resistance and conductivity values and associated 95% confidence intervals were determined. 'Resistance curves', according to Eqn 2.3, were derived assuming average values for h_T and Z_L . These curves were compared with measured hydraulic conductivity curves $k(h_B)$ of the subsoil Bt horizon.

Results and discussion

Infiltration rates measured in the 36 puddled subplots ranged from 0.2 to 5.2 mm d⁻¹. The geometric average infiltration rate was 1.8 mm d⁻¹. Infiltration rates measured at the non-puddled sites ranged from 20 cm d⁻¹ to 233 cm d⁻¹ with an average infiltration rate of 96 cm d⁻¹, indicating a decrease of infiltration rate through puddling by a factor of 500. Similarly large differences between puddled and non-puddled soils were reported by Sanchez (1973).

Average depth of puddling as determined by the thickness of easily removed soft mud, was 15 cm. The shallowest puddled layer was 9 cm, the deepest 18 cm.

Fig. 2.2 shows pressure heads that were measured at a depth of 10 and 22 cm. The pressure head at 10 cm tends to be positive, whereas the pressure at 22 cm in all cases is negative, indicating unsaturated flow conditions in the subsoil. Similar observations were made by Sur et al. (1981), Tabuchi et al. (1990) and Adachi (1990). Mean value of the pressure head at a depth of 10 cm was 7.8 cm, and at 22 cm was -11.3 cm. Pressure heads measured at three of the 36 sites are not included because of rainfall during the measurements causing ponding water in the outer cylinder.

Average pressure heads and standard errors of the means are presented in Fig. 2.3. In the upper part of the puddled layer pressure head increases almost linearly with increasing distance from the water/atmosphere interface. At greater depth the puddled layer becomes less permeable, inducing unsaturated conditions in the subsoil. For most of the 33 sites a constant pressure head was reached at greater depth ($= h_B$). In case of a deep puddled layer h_B was taken as the pressure head measured at 22 cm.

For reasons of brevity only four of the 33 graphs of change of pressure head with depth are shown in Fig. 2.4. For these sites, puddled layer depth varied from 11 to 18 cm. The interval with the greatest pressure head gradient is indicated. Comparison with puddled layer depths shows that the location of the least permeable layer is found at the interface of puddled topsoil and non-puddled subsoil (Fig. 2.4). This result is consistent

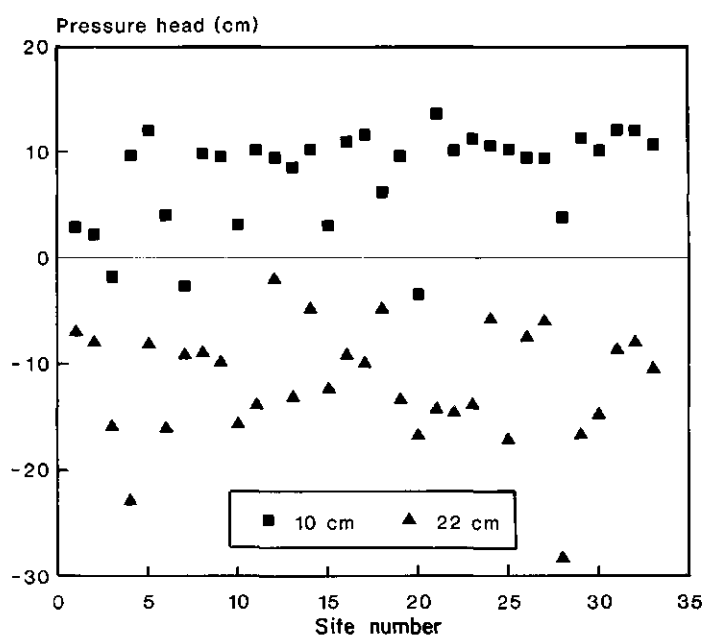


Fig. 2.2 Pressure heads measured at a depth of 10 and 22 cm at 33 measurement sites.

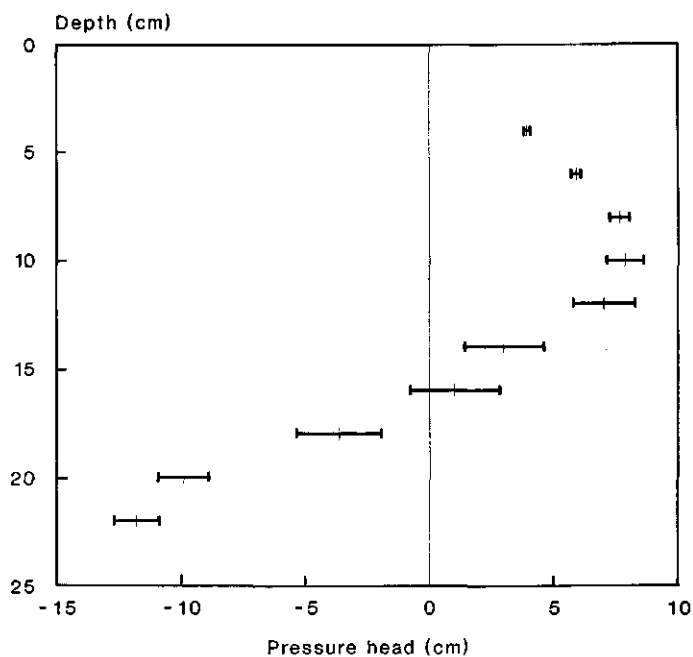


Fig. 2.3 Change in mean pressure heads with depth at 33 measurement sites. The bars represent the standard errors of the means.

with laboratory experiments of Adachi (1990). Compaction by animal hooves and blocking of macropores through clay translocation may have caused the formation of this layer.

Hydraulic resistance of the least permeable layer was calculated for the 33 sites that were not affected by rain. Resistance was log normally distributed. Mean and variance were estimated using transformed data. Geometric average was 209 days. Lower and upper 95% confidence limits were 156 and 262 days. Corresponding average hydraulic conductivity (calculated using Eqn 2.3) was 0.36 mm d^{-1} with 95% confidence limits at 0.27 and 0.45 mm d^{-1} .

The average thickness of the least permeable layer Z_L was 5.3 cm. Average pressure head at the top of this layer, h_T , was 10.1 cm. Using these values 'resistance curves' were prepared for both upper and lower confidence limits of R_L according to Eqn 2.4.

Hydraulic conductivity data for the subsoil Bt horizon obtained for two sites within the experimental field were parameterized using the power function model (Eqn 2.1). Good fits between measured and modelled data were obtained ($R^2 > 0.95$). Values for k_s and n were 134 cm d^{-1} , -2.49 and 95 cm d^{-1} , -2.63 , respectively.

Results are plotted in Fig. 2.5. It can be seen that infiltration rate and pressure head in the subsoil decrease as the resistance of the puddled layer increases. Hydraulic conductivity curves and resistance curves intersect at pressure heads between -10 and -20 cm. These values are in good agreement with the average pressure head measured in the field at a depth of 22 cm (-11.7 cm, see Fig. 2.3). Flow rate and pressure head that are developed in the subsoil are, therefore, a function of both non-puddled subsoil

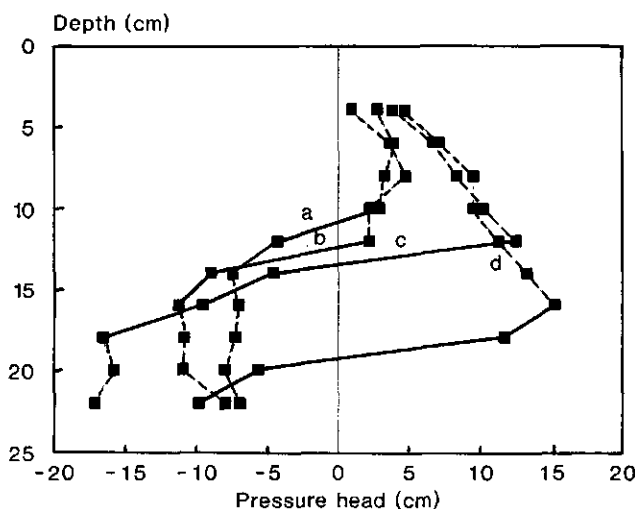


Fig. 2.4 Pressure heads measured in situ at 4 measurement sites (a, b, c, d) with different puddled layer depths (a: 11 cm, b: 13 cm, c: 15 cm, and d: 18 cm). Greatest pressure head gradients are indicated with bold lines.

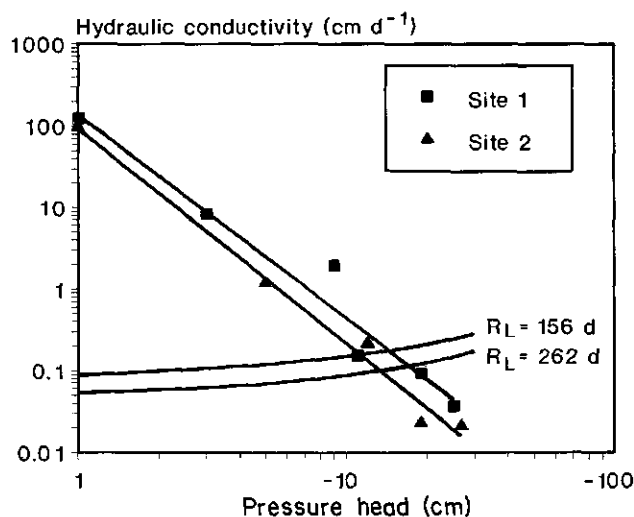


Fig. 2.5 'Resistance curves' (see text) of the least permeable layer in the puddled topsoil (95% confidence limits) and hydraulic conductivity of the non-puddled subsoil as a function of pressure head measured at two sites.

(through its hydraulic conductivity curve) and the resistance of a less permeable layer in the lower part of the puddled topsoil.

Conclusions

The results of this experiment indicate that the zone at the base of the puddled layer is an important determinant of water economy and rice production in puddled-soil systems. Supporting observations showed that puddling decreased percolation by a factor of 500, and that measured values of soil-water pressure in the unsaturated subsoil were consistent with predictions made from measured values of hydraulic resistance in the puddled surface soil and non-puddled subsoil.

Chapter 3

Sampling number and design for measurements of infiltration rates into puddled rice fields

Abstract Fifty-six infiltration rate (IR) measurements were made in puddled clay soil in a 0.05 ha experimental rice field consisting of 16 subplots, following a standard stratified sampling scheme. Log-transformed IR measurements were approximately normally distributed. Analysis of stationarity revealed the absence of a trend, whereas estimating the coefficients of the covariance function revealed a pure nugget effect, indicating spatial independence.

A sequential *t*-test was used to determine the number of measurements that is sufficient to characterize the average rate of infiltration in the experimental plot under study. Results showed that eight measurements yielded mean estimates that were not significantly different with 95% confidence from results obtained using all 56 measurements. Application of the test thus resulted in an 85% saving of measurement effort as compared with the original sampling scheme.

The question of the design of the measurement scheme, i.e. which of the eight measurements to select is addressed by means of selecting all possible combinations of the eight observations among the 16 subplot centres, and calculating the mean squared error (MSE) and the mean variance of the prediction error (MVP) in a test set consisting of the 40 other measurements. The risk of taking an inappropriate configuration is relatively small as compared to the actual mean value to be obtained.

Introduction

In rice fields that are rainfed or imperfectly irrigated and where water tables are deeper than rice-rooting depth, the rate of infiltration (IR) of impounded water partly determines whether and how long the soil can be maintained submerged. Without such submergence, weed growth increases and rice may suffer water shortage, each causing a decrease in rice-yield. Rice farmers lessen infiltration by various land preparation methods, of which the most common is puddling which uses animal, human, or gasoline-engine power to plow, harrow, and level soil that is saturated or submerged with water deriving either from irrigation or initial monsoon rains (Greenland, 1985; Painuli et al., 1988). This procedure lessens soil aggregation and macroporosity in a layer of 0.1 to 0.3 m depth (depending on puddling implement and soil type). Below this layer, a compact layer of low hydraulic conductance is created, especially in case of animal-powered puddling (Moormann and van Breemen, 1978; IRRI, 1987; Sharma and De Datta, 1985a).

Preferred rates for infiltration are 1 - 3 mm d⁻¹ in rainfed or inadequately irrigated

lands (usually in the tropics) and 5 - 15 mm d⁻¹ in irrigated temperate lands where higher infiltration may be needed to leach organic toxins that can persist from year to year in cooler climates but which in the tropics are destroyed in the hot dry soil of the post-monsoon season. Similarly, deliberate or unavoidable drying of a previously submerged puddled rice soil creates cracks that may extend through the puddled layer (and that often persist even after resubmergence) and hence cause substantial increase in infiltration rate and major change in the seasonal water balance because of preferential flow that bypasses the bulk soil (Moormann and van Breemen, 1978; Wickham and Singh, 1978; Tabuchi, 1985). Thus, measured rates of infiltration into puddled rice soils range from 0.1 mm d⁻¹ to several hundred mm d⁻¹, and may vary widely within a single field (Greenland, 1985; Hasegawa et al., 1987).

Notwithstanding such variability, infiltration values that are representative of a whole field or a farming region are needed to support the planning and operation of rice-irrigation systems and the management and simulation of rice production. Measurements of vertical infiltration of water into submerged soil are made essentially at a set of points within one or more fields (a typical infiltrometer has an inner-tube diameter of 0.20 m). Besides, the total of vertical infiltration plus horizontal peripheral seepage can be determined for the whole area of a field bounded by its surrounding soil walls or bunds (0.3 m high and wide).

A methodology to determine the minimum number of such point measurements as well as their spatial distributions needed to determine representative infiltration values to specified degrees of precision is the intended output of this present study. Such methodology can help soil- and water-management researchers in rice-growing countries to develop measuring procedures that are economic of scarce resources.

Sampling and interpolation are based on the stationarity of the underlying stochastic field. If this field obeys the intrinsic hypothesis, the range, slope and nugget variance parameters of the semivariogram are used, whereas in cases of the fields for which only the increments are stationary use is made of the pseudo-covariance function (Gajem et al., 1981). However, Webster (1985) recommends that as many as 60 point measurements may be needed to define the semivariogram for an area and variable not previously measured. Such a series of measurements (as for water-infiltration rate) is likely to be expensive, and for any variable that has only slight spatial dependence would be wasteful of effort and equipment. Moreover, if a soil variable does not show clear spatial structure, e.g., a large nugget effect as compared to the sill value, little or no gain in precision is obtained from the use of kriging or cokriging as compared to simple trend surfaces (Matheron, 1989; Stein et al., 1989).

Our methodology seeks to determine the degree of spatial variation of infiltration. Additionally, we evaluate an iterative statistical procedure (that could be adopted for other rice soils) to identify measuring strategies appropriate to specific requirements for precision for area-representative infiltration estimates.

Methods and procedures

Site and soil management

In 1989 experiments were conducted in a 41.0 m x 12.0 m field at the International Rice Research Institute, Los Baños, Philippines (14°30' N, 121°15' E). Walls of soil, 0.25 m high and wide (bunds) divided the field into 16 plots of 4.5 x 5.5 m, each of which was puddled and kept submerged throughout the experiment. Puddling comprised one plowing and two harrowings that each used water-buffalo power and traditional implements. The soil was classified according to Soil Taxonomy (Soil Survey Staff, 1975) as a clayey, mixed, non-acid, isohyperthermic, Vertic Tropaquept.

Physical and morphological measurements

Infiltration rates through puddled rice soils are commonly measured using double-ring infiltrometers (FAO, 1979). In this study, infiltration was measured using infiltrometers of a non-standard design (Fig. 3.1) that minimized evaporation and allowed insertion of small soil-water-pressure tensiometers at various depths within the enclosed columns of soil into which infiltration was measured (Chapter 2). Each infiltrometer had one outer cylinder of 0.8 m diameter, and 0.4 m height, which was pushed into the puddled and underlying soil to a depth of approximately 0.3 m. A second cylinder of 0.2 m diameter and 0.25 m length was placed in the centre of this ring and pushed downwards to 0.01 m below its upper ring while continuously removing soil around the outside of this inner cylinder. At the bottom end of the cylinder, an additional 0.10 m depth of soil was ex-

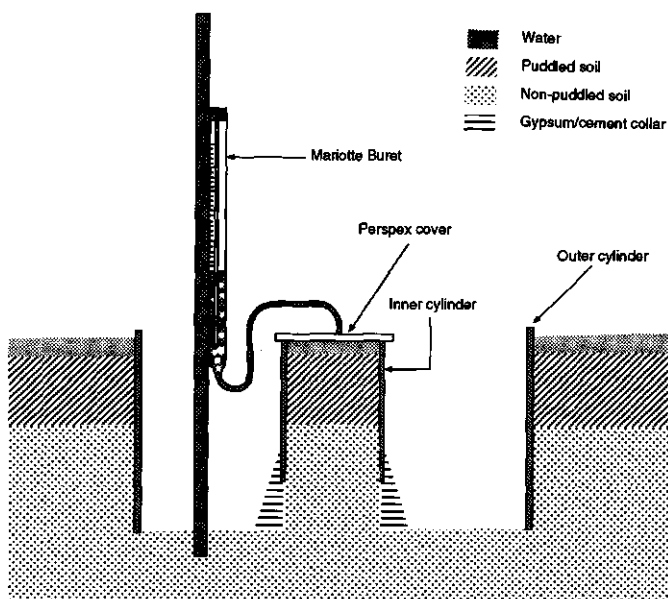


Fig. 3.1 Schematic diagram of equipment used to measure *in situ* infiltration rate in a submerged puddled clay soil.

posed and covered with a gypsum/cement mixture to prevent lateral seepage of water and to allow one-dimensional flow in the soil. The inner cylinder was capped with a transparent plastic cover to minimize evaporation and remained attached to the underlying soil. Water for infiltration through the column was fed through an inlet in the plastic cover from a mariotte burette. Infiltrimeters were monitored until each achieved a constant infiltration rate. A depth-to-water table was monitored using piezometers and was consistently of such a magnitude (0.8 - 1.0 m) that infiltrated water could readily drain beyond infiltrimeter depth.

Infiltrimeter rates were measured at 56 sites, using the technique explained above, where the infiltrimeter column remains attached to the underlying soil. In addition, for each of eight randomly selected plots, one enclosed infiltrimeter column was detached to determine the infiltration rate when no underlying soil presented a hydraulic resistance to water flow. Dominant pathways of water flow through these same eight columns were visualized by adding methylene blue dye to the infiltrating water, cutting the soil columns to expose horizontal cross sections, and identifying on these cross sections the channels of preferential flow by tracing their dye stainings onto transparent plastic sheets.

Statistical methods

(a) Sampling scheme and spatial dependence When observations are to be collected in a newly visited area, it is recommended to collect at least 50 - 60 observations, a number which is necessary to estimate semivariograms (Webster, 1985). In many studies, however, taking this many observations is a time-consuming and costly activity and, if the semivariogram turns out to be a pure nugget effect, not worth the effort. In this study we followed the current standard practice by making a total of 56 measurements in the puddled soil following a predetermined stratified sampling scheme. Stratification was imposed by the presence of the bunds, possibly yielding different conditions for every subplot due to differences in puddling. The sampling scheme was determined such that variation and spatial dependence structure of the IR measurements could be quantified. One measurement was carried out in the centre of each of the 16 subplots. In every subplot, one additional measurement was carried out at a randomly located point. In order to have sufficient observations to estimate semivariogram parameters, three additional measurements were carried out in eight subplots at randomly selected locations (Fig. 3.2).

Log-transformation of the original data set was needed to obtain symmetrically distributed data. To investigate whether the log-transformed data were normally distributed the Lilliefors test for normality was carried out, which is essentially a modification of the Kolmogorov test (Lilliefors, 1967).

The spatial dependence structure of the log(IR) data was described with a polynomial pseudo-covariance function depending upon the distance $|h|$ between observations (Starks and Fang, 1982; Stein, 1991):

$$c(h) = \alpha_0 \cdot \delta(|h|) + \alpha_1 \cdot |h| + \alpha_3 \cdot |h|^3 + \alpha_5 \cdot |h|^5 \quad (3.1)$$

(b) *Sequential sampling* A feature commonly encountered when studying infiltration rates is the lack of a clear spatial structure (Stein et al., 1989; Haraguchi, 1990). Besides, the number of observations taken (56) was unnecessarily large to study the infiltration rate in a 0.05 ha field; it heavily disturbs the soil and may not be worth the effort. Since the main objective of the study concerns the prediction of IR-values in a small area, the mean value was considered to be adequate. The total of 56 observations served as a reference, and was considered to be a sample closely associated with the IR-population.

When observations are hypothesized to be independent, the area is considered to be homogeneous, and hence the study of spatial variation is of relatively little importance. Stein et al. (1989) recommended to start with a stratification of the area. Observation densities within strata are then increased step by step. After every measurement the mean and the standard deviation of the observations may be calculated. When relevant changes occur sampling is continued, otherwise it stops. This rather descriptive procedure may be extended by sequential *t*-testing.

A procedure to test whether the mean IR value is equal to some pre-defined value is given by the sequential *t*-test (Wald, 1947; Wetherill and Glazebrook, 1986; Stein et al., 1989; Finke et al., 1992). With the sequential *t*-test a hypothesis H_0 is formulated and tested that the mean value μ of the $\log(\text{IR})$ values is equal to some predetermined value μ_0 against the alternative hypothesis H_a that $\mu \neq \mu_0$. H_0 is rejected if $\text{abs}(\mu - \mu_0) > \delta_1 \cdot s$, where δ_1 is the allowed tolerance and s is the observed standard deviation. A choice for δ_1 has a large impact on the performance of the test (Finke et al., 1992). In this study δ_1 was set to 0.7, which means that a mean infiltration rate of 1 mm d⁻¹ ($\log(\text{IR}) = 0$) is considered to be significantly different from an infiltration rate of 5 mm d⁻¹ ($\log(\text{IR}) = 0.7$). By means of this test the H_0 hypothesis based on a mean value calculated for a small set of two observations, which is minimum to estimate s , is tested on newly arrived observations.

In this study, a sequential *t*-test was used to investigate how many observations were necessary to properly estimate the mean. Starting with two observations in the study area, the number was successively increased to 32 observations following the sampling scheme of the original 56 observations as follows:

- 2: One measurement in the centres of 2 subplots, at $(x, y) = (18.35, 3.05)$ and at $(x, y) = (23.15, 8.85)$, see Fig. 3.2;
- 8: One measurement at the centres of alternate subplots;
- 16: One measurement at each subplot centre;
- 32: Two measurements in each subplot, one central, the other randomly located.

The total of 56 observations served as a reference, and was considered to be a sample closely associated with the IR-population.

Seven hypotheses concerning the mean of $\log(\text{IR})$ were tested with error probability $\alpha = 5\%$: $\mu_0 = \text{mean}(\log(\text{IR})) = 0, 0.3, 0.5, 0.7, 1.0, 1.5, 2.0$, respectively. Observations evenly distributed over the area are taken, until the H_0 hypothesis is either confirmed or rejected. If the H_0 hypothesis is rejected, a new H_0 hypothesis may be

formulated and sampling is continued. Sampling may be stopped when the H_0 hypothesis is accepted. This procedure yields the number of observations that is sufficient to estimate the mean value with a prescribed precision in terms of a factor times the observed standard deviation.

(c) *Selection of the subplots* An important question concerns the quantification of the error which is likely to occur when only a few observations are collected, due to a subjective selection of the data configuration. A general procedure may run as follows. Suppose that the sequential t -test yields a number of n_1 observations being sufficient to characterize the mean value with given precision. The remaining n_2 observations, or any well defined subset thereof, are used as a test set. Kriging, which in the case of a pure nugget effect and the absence of a trend is equivalent to using the average value, was used to predict infiltration rates to this test set. The quality of the predictions is then evaluated by means of calculation of the mean squared error (MSE) and the mean variance of the prediction error (MVP). The MSE value is given by:

$$\text{MSE} = \frac{1}{n_2} \sum_{i=1}^{n_2} (y_i - t_i)^2 \quad (3.3)$$

where t_i ($i = 1, \dots, n_2$) is the prediction carried out in the i th location of the test set and y_i is the observed value in this test point. The MVP value is given by:

$$\text{MVP} = \frac{1}{n_2} \sum_{i=1}^{n_2} \text{Var} (T_i - Y_i) \quad (3.4)$$

where T_i is the (stochastic) predictor for the (also stochastic) variable Y_i in the i th test point and $\text{Var} (T_i - Y_i)$ for $i = 1, \dots, n_2$ is the prediction error variance obtained in this point. Although T_i and Y_i may not be available themselves, the variance of their difference is given by common prediction procedures (Stein, 1991).

Every subset of n_1 observations yields one MSE value and one MVP value. The effect of the choice for any configuration is studied by calculating the mean values for every possible configuration consisting of the n_1 points obtained as a result of the sequential sampling procedure. By means of defining different classes the mean values obtained for any configuration of n_1 points was assigned to any of these classes. In this way, the risk of taking any configuration is investigated by considering the mean values which fall into different classes.

For comparison the overall mean of $\log(\text{IR})$, computed for all the 56 measurement sites, was used as a prediction for the values in the n_2 test points. An MSE-value was calculated.

Results and discussion

Infiltration rates

Infiltration rates, ranging from a low 0.1 mm d^{-1} to 130 mm d^{-1} , showed a highly skewed frequency distribution. A few extreme values may have been caused by the proximity of a drainage pipe, possibly creating large hydraulic gradients. Log transformation of the data resulted in approximately Gaussian distributed log-infiltration values ($\log(\text{IR})$), as confirmed by the Lilliefors test. The mean value for $\log(\text{IR})$ was 0.31, with a standard deviation equal to 0.86. This value corresponds to a geometric mean value of the infiltration rate equal to 2 mm d^{-1} , whereas the arithmetic mean equals 12 mm d^{-1} . These values agree with those found by Adachi and Ishiguro (1987), Greenland (1985), and Sharma and De Datta (1985a and 1985b).

Results for detached and attached cylinders (Fig. 3.1) were very similar: mean infiltration rates for the 8 cylinders were 20 mm d^{-1} and 15 mm d^{-1} , respectively. Lauren et al. (1988) reported large differences between saturated hydraulic conductivities (k_s) measured using detached cylinders and k_s values determined *in situ*. They explained this phenomena by preferential flow through macropores that were continuous throughout the detached cylinder and discontinuous in the attached ones. This implies that in our study continuous macropores did not occur.

Methylene blue procedures were effective only at high infiltration rate. At low infiltration, the dye was filtered out within a few centimeters. Tracing of methylene blue indicated that high infiltration was caused by preferential flow along roots of weeds in the puddled layer that were not destructed by plowing. In the non-puddled subsoil, flow partly continued through biopores, but no traces of methylene blue were found at the bottom of the cylinder, again indicating the absence of continuous macropores.

Spatial structure and sample size

(a) *Identification of the stochastic field* Since the hypothesis of log-normality of the increments was not rejected, trend parameters were determined for every degree of the trend by means of Restricted Maximum Likelihood (Table 3.1). Also, the corrected Akaike's Information Criterion was determined, yielding values equal to 23.8 for both the 0th and the 1st order trend and 24.2 for the 2nd order trend. No distinction between a 0th and a 1st order trend could be made when identifying the stationary field on the basis of the lowest AIC_c value, whereas a 2nd degree trend is unlikely.

For reasons of convenience we applied a trend of degree 0; a stochastic field in which the $\log(\text{IR})$ variable showed no trend. The fact that a linear trend was equally suitable is possibly due to a few outlying observations. Also, the (asymptotic) standard deviation of the α_1 was equal to 0.04, which does not corroborate the hypothesis that $\alpha_1 \neq 0$. The corresponding semivariogram (Fig. 3.3), although slightly increasing, could be interpreted as a pure nugget effect as well (0.69, in units of the squared log infiltration rate), yielding sufficient confidence to treat the observations as being independent.

Table 3.1 Estimated coefficients of the pseudo-covariance function and Akaike's Corrected Information Criterion (AIC_c) for different degrees of the trend.

Degree trend	α_0	α_1	α_3	α_5	AIC _c
0	0.652	-0.0046			23.6
1	0.269	-0.2027	0.00003		23.8
2	0.146	-0.5640	0.00051	-0.00000	24.2

(b) *Sequential testing* The impact of increasing the number of observations on the mean log(IR) values and the standard deviations indicates that after sampling the centre points in 8 of the 16 subplots, no substantial changes are encountered. Only a slight decrease in the mean is observed, as well as a small decrease in the standard deviation (Fig. 3.4). Therefore, the number of $n_1 = 8$ observations was judged to be sufficient to define the mean value of the IR measurements with sufficient precision. A test set to calculate mean MSE and MVP values was defined as the collection of the 40 off-centre observations in the subplots.

The mean MSE and MVP values estimated in the 40 test sites are illustrated in Fig. 3.5. Mean MSE values range between 0.6 and 0.8. Mean MVP values decrease steadily

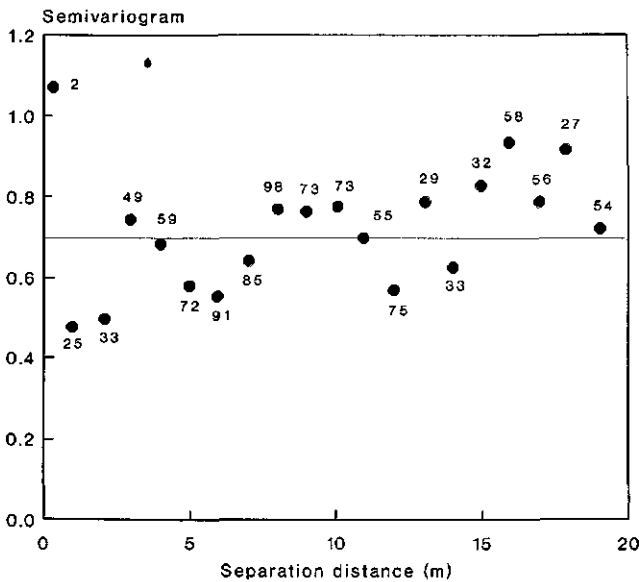


Fig. 3.3 Semivariogram and fitted pure nugget model of log-transformed infiltration rates. Included are the numbers of pairs of observation points for each semivariogram value.

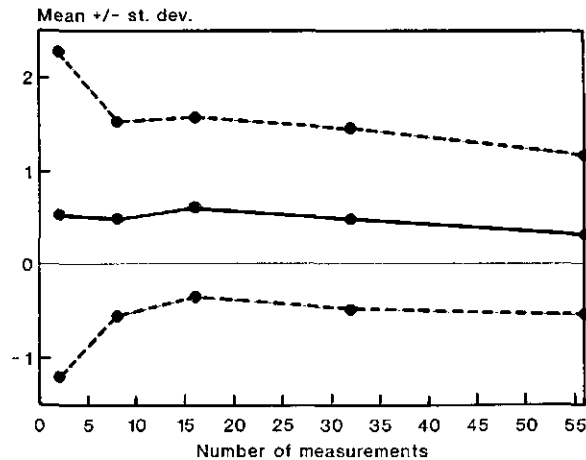


Fig. 3.4 Changes in mean and standard deviation of $\log(\text{IR})$ as a function of the number of measurements.

while increasing the number of measurements. Using the overall mean of the $\log(\text{IR})$ observations as a prediction for the 40 test sites yields an MSE of 0.80. Only a slight gain in precision is therefore obtained using kriging, which in this study is close to taking 'local averages' as may be noticed from the small value of the coefficient α_1 of the pseudo-covariance function.

By means of sequential testing, seven different H_0 hypotheses were tested (Fig. 3.6) with error probability levels 0.05. Starting with two measurements, the number of obser-

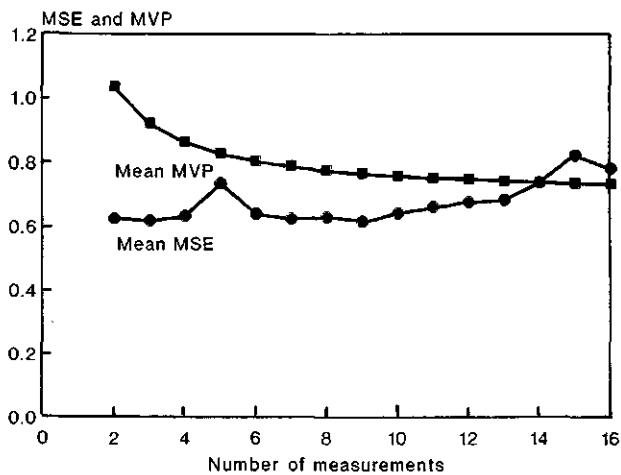


Fig. 3.5 Mean MSE and mean MVP values as a function of the number of observations used to predict $\log(\text{IR})$ values at the 40 test sites.

vations was increased to 8, 16 and finally 32. From the sequential t -test it followed that the hypotheses $H_0: \mu = 2$ and $H_0: \mu = 1.5$ are rejected after, respectively, 8 and 16 observations. Two hypotheses $H_0: \mu = 0.3$, and $H_0: \mu = 0.5$ are accepted after 8 measurements; the hypothesis $H_0: \mu = 0.7$ is accepted after 16 measurements. The hypotheses $H_0: \mu = 0$ and $H_0: \mu = 1.0$ remain indecisive, even after 32 measurements, indicating that extra effort is needed to verify these hypotheses. The fact that the test does not distinguish between the hypotheses $H_0: \mu = 0.3$, $H_0: \mu = 0.5$ and $H_0: \mu = 0.7$ is not alarming since this corresponds to infiltration rates between 2 mm d⁻¹ and 5 mm d⁻¹. Eight measurements were, therefore, sufficient to characterize the average infiltration rate in the experimental plot under study, thus reducing costs by an estimated 85% as compared with the standard geostatistical procedures.

In order to investigate the question concerning the sampling configuration, mean values of log(IR) obtained by any of the 12870 possible configurations of 8 observations within the 16 measured subplot centres were classified into 13 classes according to Table 3.2. It is noted that taking different configurations can result in different mean values. However, differences are minor, when the calculated value is considered: in 95% of all the possible configurations, the estimated mean value is between 0 and 1, and in 62% of all possible configurations between 0.30 and 0.75. We conclude, that the risk of taking

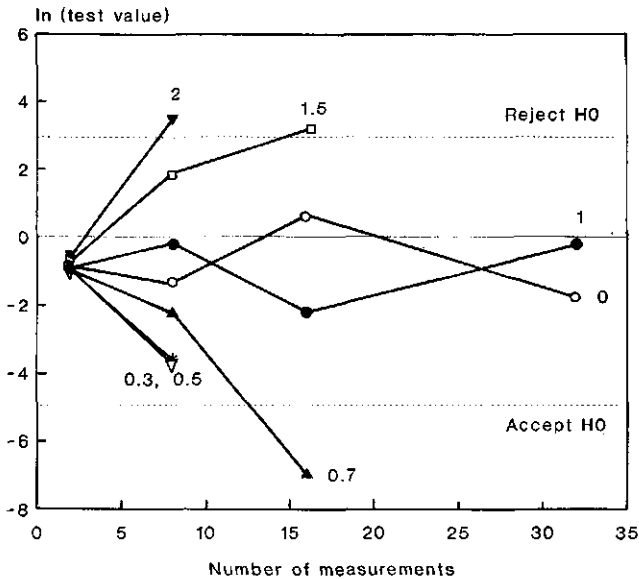


Fig. 3.6 Sequential t -test values as a function of the number of log(IR) measurements. Seven H_0 hypotheses are tested for the mean value of log(IR): $\mu = 0$, $\mu = 0.3$, $\mu = 0.5$, $\mu = 0.7$, $\mu = 1.0$, $\mu = 1.5$ and $\mu = 2.0$. The H_0 -acceptance and the H_0 -rejecting lines, based on a $1-\alpha = 0.95$ confidence level, apply to all hypotheses. Between these two lines is an indifference zone.

Table 3.2 Frequencies of occurrence for the mean value (μ) of $\log(\text{IR})$ in various chosen ranges, as obtained by all possible configurations of eight centre points to estimate μ .

Class	Range for μ	Frequency of occurrence
1	$\mu < -1.00$	0.00
2	$-1.00 < \mu < -0.75$	0.00
3	$-0.75 < \mu < -0.50$	0.00
4	$-0.50 < \mu < -0.30$	0.00
5	$-0.30 < \mu < 0.00$	0.00
6	$0.00 < \mu < 0.30$	0.10
7	$0.30 < \mu < 0.50$	0.23
8	$0.50 < \mu < 0.75$	0.39
9	$0.75 < \mu < 1.00$	0.23
10	$1.00 < \mu < 1.25$	0.05
11	$1.25 < \mu < 1.50$	0.00
12	$1.50 < \mu < 2.00$	0.00
13	$2.00 < \mu$	0.00

an inappropriate sampling design is relatively small as compared to the actual mean value which applies to $\log(\text{IR})$ values in this study.

The sequential sampling procedure requires selection of measurement locations in advance, e.g. at random, on a grid or along transects. It is recommended to work from a low to a high observation density, reducing the distances between observations step by step. After each new observation the test value of the sequential test is calculated. As soon as the pre-defined limits based on confidence levels are reached, measurements are stopped, otherwise measurements are continued.

This study shows that appropriately designed sampling and measurement strategies, such as sequential t -testing, can allow substantial savings when compared with standard nested sampling procedures, which implicitly assume presence of spatial data structure. Expert knowledge is necessary to estimate internal variability trends in the land units to be characterized.

Chapter 4

Sampling strategies for measurement of soil hydraulic properties to predict rice yield using simulation models

Abstract Measurements of soil hydraulic conductivity and water retention functions that are needed to run soil water balance and/or crop growth simulation models are expensive and time consuming. The number of such measurements can be reduced considerably if 'classical' soil horizons that are to be sampled can be merged into broader, hydraulic functional horizons. A hydraulic functional horizon comprises of one or more soil horizons that are similar in terms of soil hydraulic functions.

A detailed soil survey was carried out in a 50 ha dryland rice area to test the concept of hydraulic-functional horizons and to obtain soil hydraulic input data for a crop growth simulation model. The feasibility of identifying hydraulic-functional horizons from visual appraisal of texture and structure during the field survey was demonstrated. Soil water retention and conductivity data determined for the functional horizons and weather data from a nearby weather station were used to simulate potential and rainfed rice yield for 25 years.

A variability analysis showed that the effect of variation in soil hydraulic properties on simulated rice yield was relatively small compared to the effect of variation in year to year weather conditions.

It was concluded that sampling strategies for soil hydraulic functions should be based on a first rough comparison of the impact of weather variability and soil heterogeneity on yield variability using simulation and sensitivity analyses.

Introduction

Simulation of the crop-water balance for rainfed rice (or any other crop) within a given area requires, among others, representative values for soil hydraulic functions and representative profile descriptions for the various soil types present. Soil hydraulic functions are here the soil water retention curve, which defines the volumetric water content (θ) as a function of soil water pressure (h), and the hydraulic conductivity curve, which relates the hydraulic conductivity (k) to water content or pressure head.

Sampling activities for the measurement of soil hydraulic functions usually will concentrate on soil horizons (see e.g. Peck et al., 1977; Wösten et al., 1985; Feddes et al., 1988). The reasons for this are twofold. First, different soil horizons may have different hydraulic functions which need to be characterized as distinct input in soil water balance simulation models. Secondly, the 'linking' of hydraulic functions to soil horizons allows extrapolation of these functions to other sites where no sampling has been carried out, through simple knowledge of the soil profile.

The linking of soil hydraulic functions to soil horizons is an example of a class-pedotransfer function (Bouma and van Lanen, 1987; Finke et al., 1992). Examples of continuous pedotransfer functions, relating easily measured soil properties like bulk density, texture and organic matter to both water retention and hydraulic conductivity are given by e.g. Bloemen (1980), Ahuja et al. (1985), Haverkamp and Parlange (1986), Wösten et al. (1986), Wösten and van Genuchten (1988) and Daamen et al. (1990).

For class-pedotransfer functions, the major issue is the confrontation between classical ways of soil horizon identification and the relationship between these horizons and the hydraulic properties of interest. In soil surveys, soil horizons are generally identified on the basis of differences in texture, structure, colour, presence of mottles and many other, mainly visual, characteristics. Soil hydraulic functions, however, are very much related to texture and structure, but do generally not have relationships with aspects such as colour or mottling. Therefore, for our purposes, soil horizons can be better defined on the basis of properties that are clearly related to soil hydraulic functions only.

In a study by Wösten et al. (1985), soil hydraulic properties were determined for, what they called 'major soil horizons' occurring in an area of 650 ha. In this chapter the term 'functional horizon' is used. A functional horizon comprises one or more 'classical' soil horizons that are similar in the properties of interest. In our case the properties of interest are the soil hydraulic functions. It has further been suggested that 'hydraulic-functional' soil horizons can be identified in the field on the basis of visual appraisal of textural and structural properties (Wösten et al. 1985, 1986; Woodhead et al. 1991). Because hydraulic-functional horizons are identified using a limited number of criteria compared to classical soil horizons, the number of identified functional horizons will generally be less than that of classical soil horizons. This saves time in sampling procedures for hydraulic measurements, and, if simulations are needed for a large number of sites, can reduce the number of simulation runs considerably.

In this study, the concept of hydraulic-functional horizons, and their identification from visual appraisal of texture and structure in the field was evaluated for a 50 ha area of dryland rice in the Philippines. The hydraulic characteristics of the functional horizons were used as input for a combined crop growth-water balance simulation model. The model was used to simulate rainfed rice yield for 25 years of historical weather data for two contrasting soil types within the study area. The effect of spatial variability in the measured soil hydraulic functions within functional horizons, and in thickness of the uppermost functional horizon on simulated rice yield was studied. A comparison was made with the impact of variability in weather conditions on simulated yield. Such variability analyses are helpful in determining sampling strategies for hydraulic functions that minimize the number of expensive and time-consuming measurements.

Materials and methods

Study area and soil survey

The 50 ha study area is part of the experimental farm of the International Rice Research Institute (IRRI), Philippines (14°30' N, 121°15' E). The climate is characterized by two pronounced seasons; dry from December to May and wet from June to November. Heavy monsoon rains occur in the months of August and September. The total annual rainfall is about 2200 mm; total annual rainy days averaged over a 15 year period, is 66.

The area lies between two creeks that have deposited alluvial material derived from pleistocene and more recent volcanic activity. The alluvial deposits are underlain by weathering volcanic tuff. Going from the elevated north-south central part of the area towards the creeks, the alluvial fraction of the profile becomes more and more pronounced. The depth to the volcanic tuff layer in the central part varies strongly over small distances and ranges from close to the surface to more than 2.2 m depth.

A detailed soil survey was made at a scale 1 : 6000 on a regular grid with a separation distance of 40 m between a total number of 144 auger borings. The presence of tuff fragments in the subsoil and the depth to the paralithic tuff layer were expected to be important for soil hydraulic characterization of the study area. Auger borings extended to a maximum depth of 2.2 m or to the upper surface of the unweathered volcanic tuff layer. The occurrence of tuff fragments in the subsoil was recorded.

The point information derived from the 144 auger borings was transformed in areal information by combining similar auger boring descriptions into soil units on a soil map. Soil classification was based on Soil Taxonomy (Soil Survey Staff, 1975). Additional mapping criteria included presence of tuff fragments in the subsoil and depth to the paralithic tuff layer. Tuff fragments were considered to be present if they occupied more than 10% of the soil volume. Three classes of depth to the tuff layer were considered: 0 - 50 cm, 50 - 100 cm and > 100 cm.

Based on the 144 auger borings, a representative site for every mapping unit was selected. At this site a pit was dug and a detailed representative profile description (RPD) was made. A RPD contains the sequence of (classical) soil horizons, the depths and thicknesses of these horizons and a range of properties of each horizon.

Hydraulic functional horizons

Soil-textural and soil-structural features of soil horizons that were distinguished during the soil survey were used to identify hydraulic-functional horizons in each RPD. For example, soil horizons that were distinguished because of color differences only, were merged into one hydraulic-functional horizon.

The validity of the concept of hydraulic-functional horizons was tested using two different approaches. First, at two representative sites for two contrasting mapping units, soil hydraulic properties were not only measured for the identified hydraulic-functional horizons (see above) but also for all soil horizons occurring within the profile. The measurements were used to evaluate whether the identified hydraulic-functional horizons

(derived by merging comparable soil horizons) were indeed similar in their hydraulic properties. Also, these measurements could indicate whether further merging into even larger hydraulic-functional horizons was feasible. For practical reasons, the measurements of the hydraulic properties only involved the soil moisture contents at saturation, at $h = -100$ cm, at $h \approx -1,000$ cm and at $h = -3,000$ cm.

In the second approach, other hydraulic criteria were defined to test the effectiveness of the identified hydraulic-functional horizons. They were selected based on their relevance for simulation of rainfed rice yield. In this study, three criteria were used:

- (i) Critical water depth: the depth of water table which can sustain a given upward flux of water of 2 mm d^{-1} to the bottom of the root zone, assuming that this root zone is dried out to wilting point ($h = -15,000$ cm). As shown by Gardner (1958), this depth may be obtained by integrating Darcy's law.
- (ii) Water content at field capacity ($h = -100$ cm).
- (iii) Percentage available water between field capacity ($h = -100$ cm) and wilting point ($h = -15,000$ cm).

During the monsoon season, the groundwater table level in the study area is usually shallow, and capillary rise to the root zone might be an important contributor to crop water supply. Criterion (i) gives an indication of the possibilities of capillary rise.

A *t*-test for two or three means (Steel and Torrie, 1980) was used at the 1% significance level to investigate the similarities and differences between the functional horizons in values calculated for the three criteria described above. This approach was especially chosen to evaluate whether the hydraulic-functional horizons identified previously could be merged into larger hydraulic-functional horizons.

Measurement of soil hydraulic functions

Hydraulic-functional horizons were sampled in duplicate at representative sites for every soil unit that was distinguished on the soil map. For horizons that only occurred in one soil unit, additional samples at other sites within the same soil unit were taken.

The saturated and unsaturated hydraulic conductivity k was measured as a function of soil water pressure h using a combination of 3 or 4 methods:

- (i) The column method (Bouma, 1982) for vertical saturated conductivity (k_s) using encased soil columns 0.25 m high and 0.20 m diameter;
- (ii) The crust method (Booltink et al., 1991) for h between 0 and -50 cm, using the soil cylinders of Method (i);
- (iii) The hot air method (Arya et al., 1975) for $h < -50$ cm, using encased soil cylinders 0.10 m high and 0.050 m diameter; and
- (iv) The cube method (Bouma and de Laat, 1981) for $h > -800$ cm, to estimate the reduction of hydraulic conductivity due to horizontal crack formation.

For Method (iv), at each sampling site three 0.3 m cubes were encased in gypsum and left to dry in the laboratory to approximately -250 , -500 and -750 cm pressure (one

separate cube for each pressure). Each cube was turned on its side and diluted white paint was poured into the cube to stain the airfilled cracks. The surface area of the stained cracks was drawn on plastic sheets after returning the cube to its upright position and after removal of the peds. The resulting white pattern was digitized and the percentage stained area of each cube was calculated. Reduced k values, for each pressure head were then calculated using the following equation (see Bouma and de Laat, 1981):

$$k_{\text{reduced}} = k_{\text{measured}} (100 - x)/100 \quad (4.1)$$

where x is the percentage stained area.

Results obtained with the hot air and cube methods were compared at two sites for two hydraulic-functional horizons using the Wind-evaporation method with 80 mm high, 100 mm diameter undisturbed cores (Wind, 1968; Boels et al., 1978). The Wind-method can be used for pressure heads within the range of a tensiometer (i.e. > -800 cm) and accounts for the effect of horizontal cracks on unsaturated hydraulic conductivity (Bronswijk, 1988a).

The water retention characteristics were measured as a function of soil water pressure h using a combination of the following two methods:

- (i) The hanging water column method for $-150 \text{ cm} < h < 0 \text{ cm}$ using 300 cm^3 samples (Richards, 1965); and
- (ii) The evaporation method for $-800 \text{ cm} < h < -150 \text{ cm}$ (Bouma et al., 1983).

For Method (ii), pressure potentials were periodically measured in the soil samples previously used for both column and crust method, while at the same time subsamples were taken to determine water contents.

For each hydraulic-functional horizon, geometric-mean $k(h)$ and $h(\theta)$ curves were determined and parameterized using the following empirical equations presented by van Genuchten (1980):

$$S = (\theta - \theta_r) / (\theta_s - \theta_r) = [1 + |\alpha h|^n]^{-m} \quad (4.2)$$

$$k(S) = k_s S^l [1 - (1 - S^{1/m})^m]^2 \quad (4.3)$$

The parameter S is the degree of saturation; θ_r and θ_s refer to the residual and saturated values of the volumetric water content θ ; k_s is the saturated hydraulic conductivity; α , n , m and l are parameters which determine the shape of the functions and $m = 1 - 1/n$.

Values for θ_s and k_s were fixed at their independently measured averages. Residual moisture content was set to 0.01. As a result only three model parameters: α , n and l were optimized using the RETC program (van Genuchten et al., 1991).

The variability in the hydraulic functions was expressed by the upper measured extremes (i.e. highest conductivity and moisture content at a given pressure potential) and the lower measured extremes (i.e. lowest conductivity and moisture content at a given

pressure potential). The number of hydraulic functions per hydraulic functional horizon was too small to express this variability using other techniques such as scaling (Miller and Miller, 1955, 1956; Warrick et al., 1977; Russo and Bresler, 1980; Hopmans and Stricker, 1989; Wösten, 1991).

Simulation modelling

The combined crop growth-water balance simulation model used in this study was the model MACROS (Penning de Vries et al., 1989). The MACROS-L2C module for water limited crop production was combined with the soil-water balance module SAWAH (ten Berge et al., 1992; Woodhead et al., 1991) to simulate the production of rainfed rice. SAWAH is a one dimensional water balance model, especially developed for rainfed rice environments. It can simulate water movement in submerged and non-submerged rice soils. The flow equation is numerically solved under given boundary conditions. Ten soil compartments can be distinguished for which hydraulic parameters can be specified. As a reference, fully irrigated, potential production was also simulated using the MACROS module LID.

Simulations were conducted using weather data from 25 consecutive wet seasons (1960 - 1984), obtained from records from a weather station located within the 50 ha study area. Weather data included daily solar radiation, maximum and minimum air temperature, windspeed, vapor pressure and rainfall. Seeding of rice was assumed to start when cumulative rainfall exceeded 75 mm during seven consecutive days after 1 June.

The effect of spatial variability in the measured soil hydraulic functions within functional horizons, and in thickness of the uppermost functional horizon on simulated rice yield was studied for two contrasting representative profiles.

Thickness of the top functional horizon was set to the RPD value and to the minimum and maximum thickness encountered in the 50 ha riceland area. To account for changes in thickness of the top functional horizon, the thickness of the second functional horizon was decreased or increased accordingly. In the simulations, average hydraulic functions were used as input for each functional horizon.

The impact of variability in hydraulic functions was investigated by simulating rice yield for all possible combinations of average, upper and lower extremes of the measured hydraulic functions of all functional horizons. Both representative profiles contained four functional horizons (see below), resulting in $3^4 = 81$ simulation runs per profile per year.

An analysis of variance was used to compare the impact of temporal variability in weather and spatial variability in above-mentioned properties of hydraulic functional horizons on simulated rice yield.

Results and discussion

Soil map and hydraulic-functional horizons

The soils in the study area were mainly classified as Typic Tropudalfs (Soil Taxonomy,

Soil Survey Staff, 1975). The soil map (Fig. 4.1) contains 22 delineated areas. Six major soil units were distinguished (Table 4.1). The C1 and C2 horizons in mapping units 1 and 2 only differed in color and showed no textural or structural differences. These horizons were, therefore, merged into one hydraulic-functional horizon (FH3). A slight increase in tuff fragments was apparent with depth for mapping unit 4 for horizons B1, B2 and B3, although the percentage remained very low (< 10%). B1, B2 and B3 horizons were therefore merged into one hydraulic-functional horizon (FH2). In mapping unit 6, Bg1, Bg2 and Bg3 horizons were differentiated because of an increase in mottling intensity with depth. There were no structural or textural differences, however, and the horizons were merged into one hydraulic-functional horizon (FH5). The transition horizon CR that was found in mapping units 1 and 2 was, because of its high content of sand, considered to be part of the tuff layer and merged with the R horizon (FH4).

In total, five hydraulic-functional soil horizons were distinguished (FH1 - FH5) and described in terms of organic matter content, texture and bulk density (Table 4.2, Fig. 4.2).

Soil hydraulic functions

Measured $\theta(h)$ and $k(h)$ data sets, and fitted van Genuchten curves are presented in Figs 4.3 and 4.4 for all five identified hydraulic-functional horizons. Results obtained with the Wind-evaporation method agreed well with results derived from the combined use of

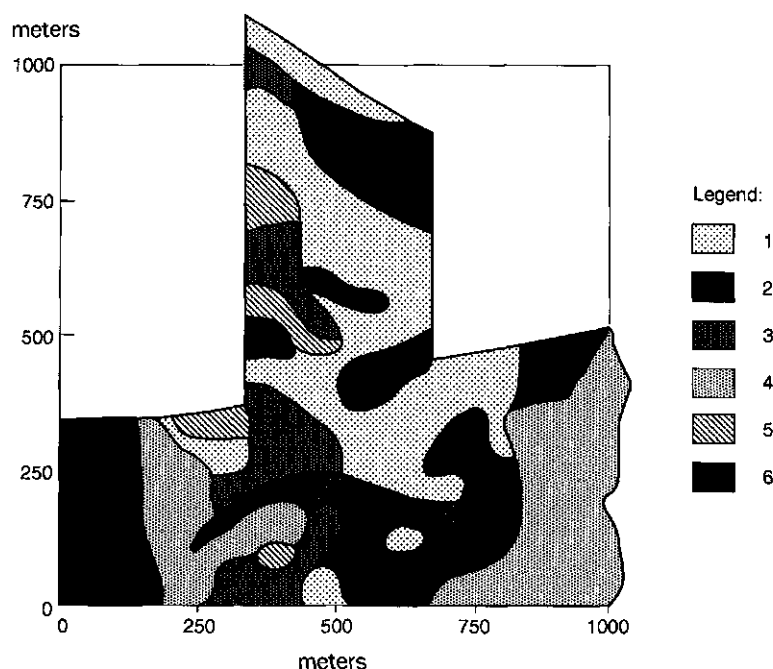


Fig. 4.1 Soil map of the 50 ha dryland rice area. The legend is explained in Table 4.1.

Table 4.1 Mapping units of the soil map and their classification according to Soil Taxonomy (Soil Survey Staff, 1975).

Mapping unit	Classification	Tuff fragments in subsoil	Paralithic contact
1	Isohyperthermic, mixed typic Tropudalf	yes	0.5 - 1.0 m
2	Isohyperthermic, mixed typic Tropudalf	yes	> 1 m
3	Isohyperthermic, mixed typic Tropudalf	no	0.5 - 1.0 m
4	Isohyperthermic, mixed typic Tropudalf	no	> 1 m
5	Isohyperthermic, paralithic Tropaquept	yes	< 0.5 m
6	Isohyperthermic, mixed vertic Tropaquept	no	> 1 m

the hot air and the cube methods (see hydraulic conductivity curves in Fig. 4.4 for FH1 and FH2). For all hydraulic-functional horizons (except for FH5) a sharp drop in hydraulic conductivity occurs in the range from saturation to $h = -10$ cm. This indicates the presence of soil macropores which drain and, therefore, no longer contribute to the conductivity as soon as the soil becomes unsaturated. Water retention curves clearly shift to higher moisture contents at greater depth (see also Table 4.3). The highest soil moisture content at saturation is obtained for hydraulic-functional horizon 4 (tuff layer). Hydraulic parameters for the average curves of each hydraulic-functional horizon are presented in Table 4.4.

Table 4.2 Soil characteristics of hydraulic-functional horizons (FH1 - FH5).

Horizon	% clay	% silt	% sand	% C _{org}	bulk density (g cm ⁻³)
FH1 (Ap)	39 ± 2*	43 ± 2	18 ± 2	1.16 ± 0.30	1.17 ± 0.05
FH2 (B)	51 ± 4	36 ± 3	13 ± 2	0.74 ± 0.18	1.11 ± 0.04
FH3 (C)	44 ± 6	30 ± 4	26 ± 8	0.42 ± 0.14	0.92 ± 0.06
FH4 (R)	20 ± 5	25 ± 6	55 ± 9	0.20 ± 0.13	0.89 ± 0.03
FH5 (Bg)	53 ± 9	37 ± 5	10 ± 5	0.52 ± 0.17	1.08 ± 0.05

* standard deviation

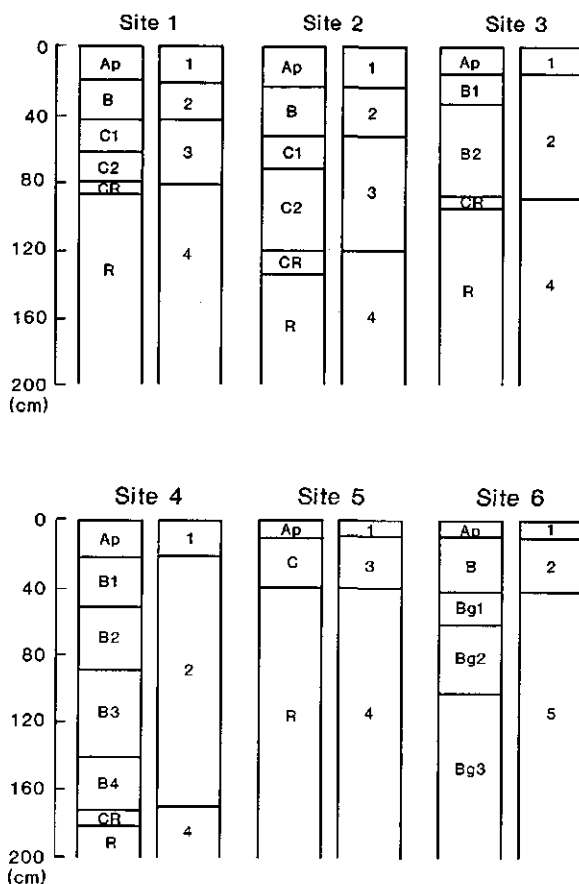


Fig. 4.2 Soil horizons and hydraulic-functional soil horizons occurring at six representative sites within the 50 ha dryland rice area.

Testing the concept of hydraulic-functional horizons

At two representative sites, located in mapping units 1 and 6, all soil horizons were sampled to determine soil moisture content at saturation and at negative pressures h of -100 , -1000 and -3000 cm (Table 4.3). Results indicate that merging of soil horizons C1 and C2 and of horizons CR and R within mapping unit 1, and merging of horizons Bg1, Bg2, Bg3 within mapping unit 6 into hydraulic-functional soil horizons is legitimate. Differences in moisture content are small and within the range found for the corresponding hydraulic-functional horizon.

The critical water depth of hydraulic-functional horizons 1 and 4 differed significantly from that of hydraulic-functional horizons 2, 3 and 5. This is caused by the horizontal cracking that was observed for hydraulic-functional horizons 2, 3 and 5 which reduced possibilities for capillary rise. Hydraulic-functional horizon 5 is significantly different from all other hydraulic-functional horizons (Table 4.5).

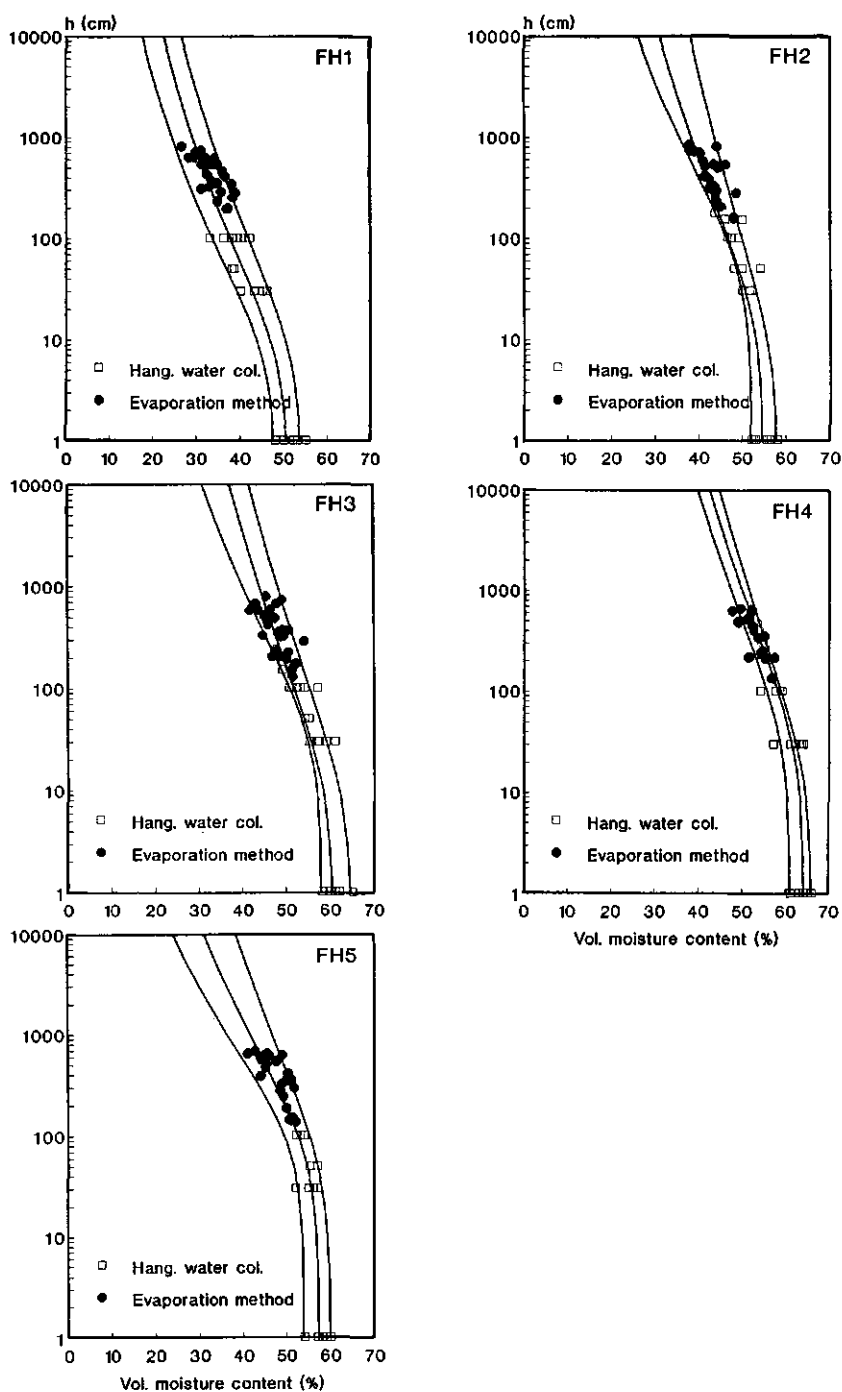


Fig. 4.3 Experimental soil water retention data (symbols) and calculated curves (average, and upper and lower extremes) using the van Genuchten model for the five hydraulic-functional soil horizons (FH1 - FH5).

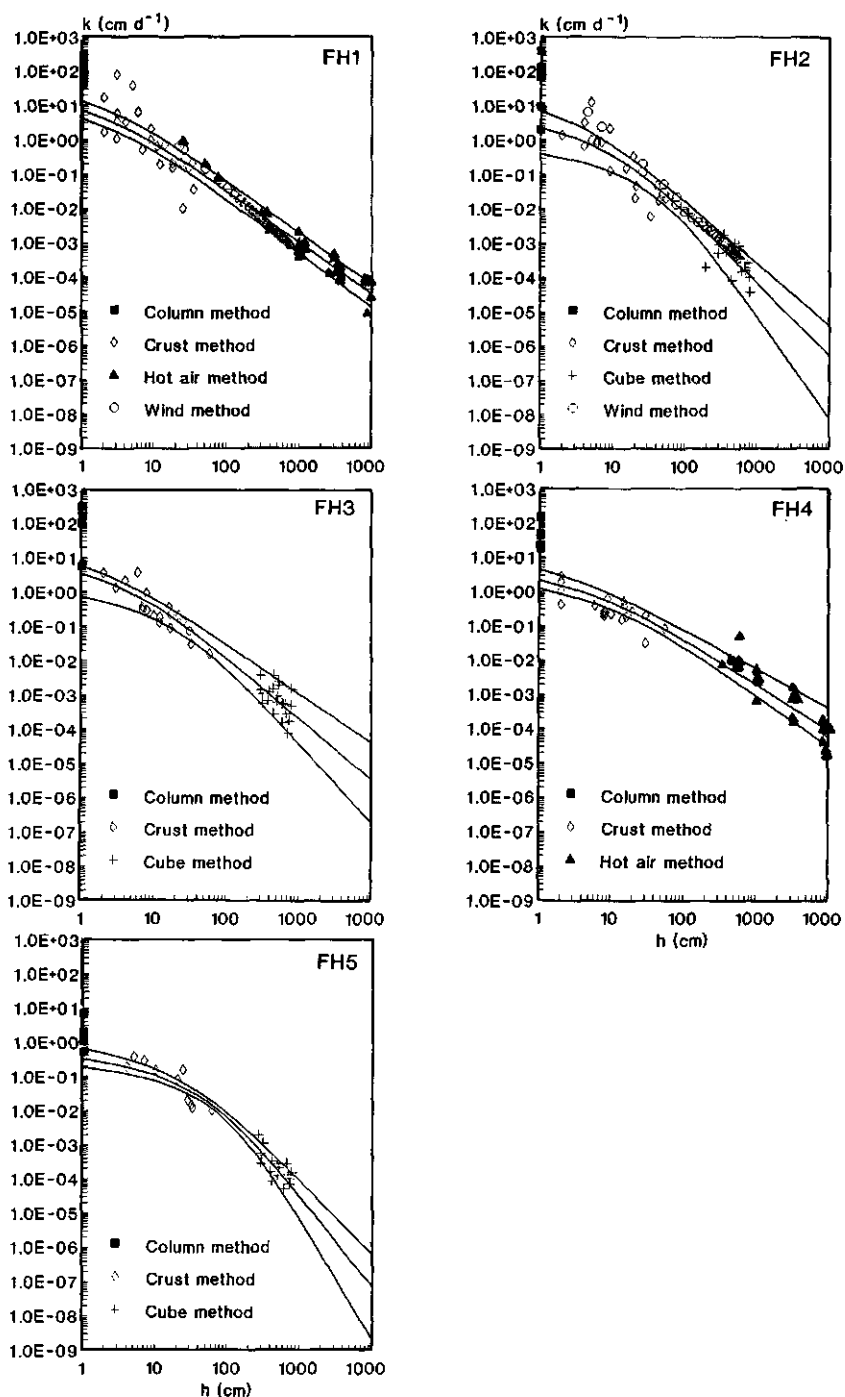


Fig. 4.4 Experimental hydraulic conductivity data (symbols) and calculated curves (average, and upper and lower extremes) using the van Genuchten model for the five hydraulic-functional soil horizons (FH1 - FH5).

Table 4.3 Volumetric soil moisture contents measured at saturation θ_s , at $h = -100$ cm (θ_1), at $h = -1000$ cm (θ_2) and at $h = -3000$ cm (θ_3) for individual soil horizons occurring at two sites in the 50 ha upland rice area. Corresponding hydraulic-functional horizons (FH1 - FH5) are indicated.

Site 2						Site 6					
Hor	θ_s (%)	θ_1 (%)	θ_2 (%)	θ_3 (%)	FH	Hor	θ_s (%)	θ_1 (%)	θ_2 (%)	θ_3 (%)	FH
Ap	52	39	34	24	1	Ap	49	37	32	29	1
B	56	51	42	30	2	B	54	50	43	33	2
C1	62	59	48	38	3	Bg1	59	53	46	41	5
C2	61	58	45	41	3	Bg2	59	51	48	42	5
CR	64	59	55	44	4	Bg3	61	55	49	40	5
R	66	59	53	46	4						

Table 4.4 Parameters for van Genuchten's soil-hydraulic functions as calculated for the 5 hydraulic-functional soil horizons identified for a 50 ha area of the IRRI farm. k_s is the saturated hydraulic conductivity; θ_s is the volumetric water content at saturation; and θ_r the residual volumetric water content (set to 0.01); α , n and l are parameters estimated with the RETC program.

Functional horizon	k_s (cm d ⁻¹)	θ_s (cm ³ cm ⁻³)	α (cm ⁻¹)	n (-)	l (-)	θ_r (cm ³ cm ⁻³)
FH1 (Ap)	127.0	0.51	0.127	1.119	-6.2	0.01
FH2 (B)	35.0	0.55	0.047	1.095	-0.6	0.01
FH3 (C)	103.0	0.61	0.078	1.076	-4.9	0.01
FH4 (R)	42.0	0.64	0.032	1.073	-11.1	0.01
FH5 (Bg)	2.0	0.57	0.011	1.133	3.2	0.01

Table 4.5 Average values and standard deviations of three hydraulic criteria calculated for hydraulic functions measured for all 5 hydraulic-functional horizons. FC is moisture content at field capacity (pF = 2), AW is available soil water between field capacity and wilting point (pF = 4.2), WT is depth of the water table (see text). Values that are significantly different are denoted by different symbols (a, b, c, d).

Hydraulic criteria	FH1		FH2		FH3		FH4		FH5	
	avg	st.d.	avg	st.d.	avg	st.d.	avg	st.d.	avg	st.d.
FC (cm ³ cm ⁻³)	0.38 ^a	0.03	0.47 ^b	0.03	0.52 ^c	0.02	0.58 ^d	0.02	0.53 ^c	0.02
AW (cm ³ cm ⁻³)	0.17 ^a	0.02	0.17 ^a	0.04	0.16 ^a	0.04	0.17 ^a	0.03	0.23 ^a	0.07
WT (cm)	69 ^a	11	31 ^b	7	40 ^b	13	93 ^a	27	18 ^c	3

The moisture contents at field capacity of all hydraulic-functional horizons are significantly different from each other, except for those of hydraulic-functional horizons 3 and 5. The available water of none of the hydraulic-functional horizons is significantly different (Table 4.5).

Using as a criterion that hydraulic-functional horizons can only be combined when they are significantly similar in all three criterion-values, none of the distinguished hydraulic-functional horizons could be combined into larger groups.

It was concluded that the identification of hydraulic-functional horizons on the basis of visual appraisal of textural and structural soil properties in the field was successful. Measured water retention characteristics of individual soil horizons agreed well with water retention characteristics determined for corresponding functional horizons. Identified functional horizons could not be further merged on the basis of hydraulic criteria relevant to rainfed rice modelling.

Simulated rice yields

Average simulated potential rice yield for the 25-yr period was 6.4 t ha^{-1} , ranging from 5.6 to 7.1 t ha^{-1} (Figs 4.5 and 4.6). These yields are determined by variation in solar radiation and temperature only and agree well with field experimental data obtained recently at IRRI.

Average simulated rainfed rice yield for soil unit 1 using average hydraulic functions and the RPD thickness of the top functional horizon was 5.2 t ha^{-1} , ranging from 2.8 to 6.5 t ha^{-1} . For soil unit 6 an average of 5.8 t ha^{-1} was found with a range from 3.9 to 7.0 t ha^{-1} .

Simulated rainfed rice yields for the two soil units are shown in Figs 4.5 and 4.6. Potential yields are plotted as well. Fig. 4.5 shows the results of the simulations conducted with variable thickness of the top functional horizon. From the graphs it can be seen that variability in thickness of the top functional horizon has a negligible effect on simulated rice yield. An analysis of variance showed that for both soil units 98% of the variability in simulated rice yield is explained by weather variability only. For both soil units, the differences between simulated potential and simulated water-limited rice yield are generally not very large. This indicates that both natural rainfall and hydraulic properties of the soils favour rice growth. The soils in this area are characterized by a relatively high water availability between field capacity and wilting point (Table 4.5). Especially for soil unit 6, simulated rainfed yields were close to potential yield. This is caused by the presence of FH5 in the soil profile (see Fig. 4.2), which has a low saturated hydraulic conductivity (see Table 4.4). This hydraulic-functional horizon limits deep drainage and assures effective water use.

The variability in hydraulic functions had much more impact on rainfed rice yield in case of soil unit 1 than in case of soil unit 6 (Fig. 4.6). For soil unit 1, 65% of the variability in simulated rice yield is explained by weather variability. For soil unit 6, 91% of the variability in simulated rice yield is due to changing weather conditions.

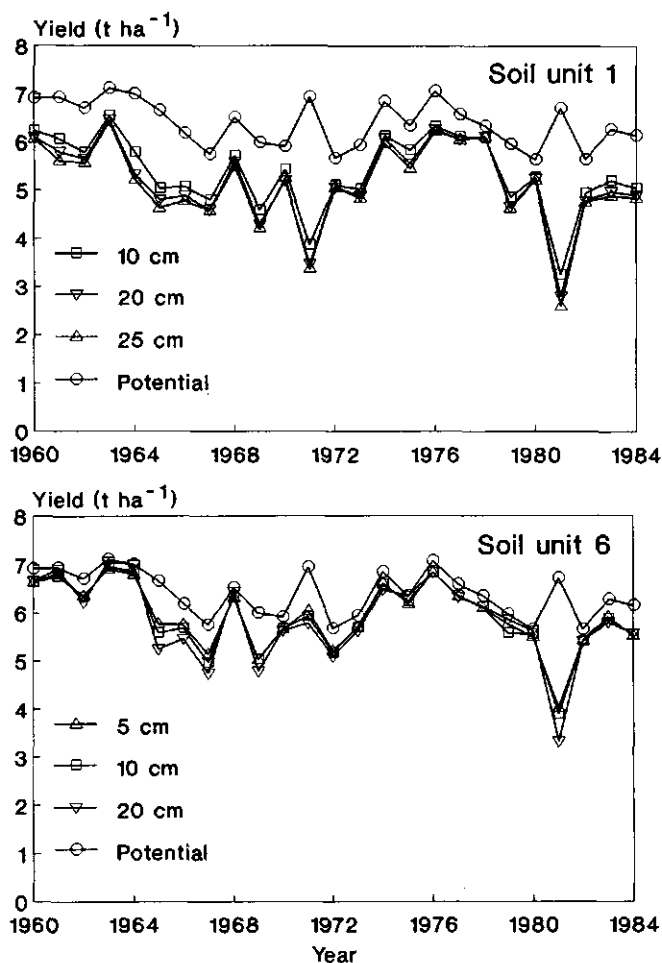


Fig. 4.5 Rainfed rice yield calculated for 25 consecutive wet seasons (1960 - 1984) for soil units 1 and 6, varying the thickness of hydraulic-functional soil horizon 1. Average hydraulic functions were used for all 4 hydraulic-functional soil horizons occurring in both soil units. For comparison potential rice yields are plotted as well.

Conclusions

Merging of soil horizons into a smaller number of hydraulic-functional horizons before labour intensive sampling is accomplished, can save considerable time and effort. Measurements of soil hydraulic properties are time consuming and expensive and should be kept to an absolute minimum if possible. In this case study, the feasibility of identifying hydraulic-functional horizons from visual appraisal of texture and structure during field surveys was demonstrated.

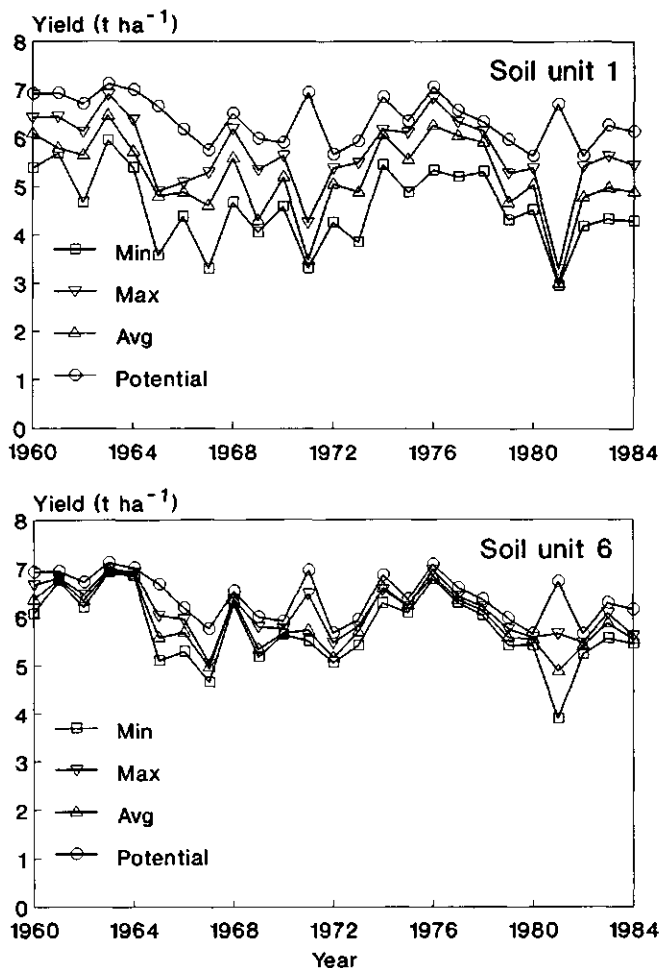


Fig. 4.6 Minimum, maximum and average simulated rainfed rice yields resulting from spatial variability in soil hydraulic functions for soil units 1 and 6, and simulated potential rice yield calculated for 25 consecutive wet seasons (1960 - 1984).

The effect of spatial variability in soil (hydraulic) properties on simulated crop yield depends on the relative sensitivity of the model to those properties, and the relative magnitude of the variation in the area of interest, compared to variability in other yield determining factors. In this case study, the impact of temporal variation in weather was much larger than that of spatial variation in thickness of the uppermost hydraulic-functional horizon. In one soil unit, it was also much larger than that of spatial variability in soil hydraulic functions of hydraulic functional horizons. In any other situation, however, these results may be totally different. Therefore, before embarking on an expensive

measurement program to collect soil (hydraulic) information that is to be used as input in soil water and/or crop growth simulation models, careful attention should be paid to the desired level of accuracy of these data.

A combination of simulation and sensitivity analyses can be used to design decision schemes for soil sampling. A first general survey, followed by a limited number of measurements, can give a first impression of the values of soil properties of interest and their spatial variability in a given area. These data may then be used to perform a sensitivity analysis with a simulation model in the range (or somewhat larger) of the collected data values, and for a number of clearly different years (e.g. years with relatively low and high rainfall). The results of such sensitivity analyses would indicate the desired level of accuracy and detail (e.g. measurement procedure, number of measurements, sampling distance, number of soil horizons to sample) with which soil (hydraulic) data need to be collected. If from the sensitivity analysis follows that the model is relatively insensitive to variability in an input parameter, costly measurements may not be needed and a suitable pedotransfer function may be used instead. In other cases, pedotransfer functions will not give accurate information, and detailed in-field measurements will be necessary.

For this case study for instance, sensitivity analyses and model exercises that were conducted later revealed that simulated rainfed rice yield was hardly sensitive to hydraulic conductivity in the ranges encountered in the various identified hydraulic-functional horizons (Chapter 5). Simulated rice yield was more sensitive to the shape of the water retention curve. Therefore, in this study area, the number of measurements needed to determine soil hydraulic conductivity characteristics of hydraulic functional horizons could have been much smaller than the number of measurements needed to determine the water retention characteristics.

Soil-plant-weather interactions are complex and general guidelines for soil sampling are not easy to define. Therefore, a first analysis using simulation models can be very helpful to optimize soil sampling strategies.

Chapter 5

Comparing the performance of a soil-water balance model using measured and calibrated hydraulic conductivity data: a case study for dryland rice

Abstract Simulation of the water balance of a small 0.05 ha field of dryland rice (grown on non-submerged soil) requires knowledge of the soil's hydraulic conductivity functions. We compared three methods to generate such functions: direct measurement in the laboratory on samples from soil horizons occurring within the field (Method 1); use of average hydraulic conductivity functions measured in a 50 ha dryland rice region surrounding the field (Method 2); and deriving the hydraulic conductivity function through model calibration (Method 3).

Differences in hydraulic conductivity functions obtained by the three methods were large. The impact of these differences on simulation results using a soil-water balance model was evaluated. Simulated and observed water contents in 0 - 0.4 m depth were compared for two representative 0.05 ha fields within the 50 ha dryland rice area, during three monsoon seasons and one dry (non-monsoon) season. Good agreement between observed and simulated soil water contents was obtained with input derived from either of the three methods. Best results were obtained with Method 1 but differences in model performance were small because simulation results were relatively insensitive to hydraulic conductivity input data. Implications for sampling strategies are discussed.

Introduction

About 13% of the world's riceland is dryland - that is non-submerged, often referred to as upland (IRRI, 1991a; Khush and Garrity, 1984). Such land is prepared, and the rice seeded, under non-submerged conditions; this is in contrast to wetland rice, where soils are maintained submerged, and the rice often transplanted. Thus for dryland rice, crop-water availability and production depend on storage of rainfall in the soil profile, possibly supplemented by capillary rise from a groundwater table.

Simulation of the crop-water balance for dryland rice requires knowledge of the soil water retention curve, which defines the volumetric water content (θ) as a function of the soil water pressure head (h), and the hydraulic conductivity curve, which relates the hydraulic conductivity (k) to water content or pressure head. For large area simulations, representative soil hydraulic functions that can be determined cost-effectively are needed. If possible, they should be derivable from observations and measurements made during routine soil surveys (Wösten and van Genuchten, 1988).

Representative water-retention data are measured relatively easily; the relation of hydraulic conductivity to water content or potential is more difficult. In this study we compared three methods to derive soil hydraulic conductivity functions for two 0.05 ha test sites within a 1.0 ha field used for dryland rice. Direct measurement on samples taken from soil horizons occurring at the test sites (Method 1) is expected to be the most accurate method to determine values for soil hydraulic conductivity; however, data cannot easily be extrapolated to other fields (Wösten et al., 1990).

For extensive regions (several ha) comprising many fields, hydraulic functions for a particular field might be estimated from the average hydraulic functions for *hydraulic-functional horizons* (FHs) occurring in the area if such functions have been determined (Method 2). FHs usually comprise a grouping of two or more soil horizons distinguished from a soil survey map or through a specially undertaken program of auger borings. If average hydraulic properties are known for each FH, soil hydraulic properties can be interpolated to fields that were not specifically measured during the survey (Chapter 4).

Alternatively, the hydraulic conductivity curve can be estimated using a combined soil-water and crop growth simulation model and an optimization procedure to fit a time series of simulated soil-water contents to a series of measured values at various positions and depths in the 1.0 ha field (Method 3) (Woodhead et al., 1991). As with Method 1, results cannot easily be extrapolated to other fields. Another drawback of the method is that many time series are needed.

The objective of this study was to evaluate and compare Methods 1, 2 and 3 in a 50 ha dryland rice area. This has been done by using the hydraulic functions derived from the three methods as input for a soil-water balance model and subsequent comparison of simulated with observed soil water contents.

Materials and methods

Study area

The study was conducted on a 50 ha area of the experimental farm of the International Rice Research Institute (IRRI) at Los Baños, Philippines (14°30' N, 121°15' E). The climate has two distinct seasons: dry from December to May, and wet from June to November. Heavy precipitations occur during August and September; total annual rainfall (15 year average) is about 2200 mm from 66 rainy days. The study area lies between two creeks that have deposited alluvial material deriving from Pleistocene and more recent volcanic activity. The alluvial deposits are underlain by weathering volcanic tuff. The depth to the upper surface of the volcanic tuff varies strongly over small distances, ranging from almost zero to more than 2.2 m. Six soil-mapping units were used to characterize the area (Chapter 4).

Two test sites of 0.05 ha were identified within a gently sloping 1.0 ha field used during several preceding years for dryland rice. The sites were considered to be repre-

sentative for two of the six mapping units, covering 51% of the study area. The field represented a toposequence with a slope of 1 - 2%, with shallow groundwater at the lower end, and deeper water tables upslope. The test sites are coded 1A and 3B in IRRRI (1988) and Woodhead et al. (1991) and were located along the contour lines. Site 1A was located at the lower end of the field, whereas Site 3B was located upslope. The difference in elevation between both test sites was 0.97 m. In each of the test sites, thickness and depth to the upper surface of each soil horizon was determined by auger borings. The soil at each site was classified as a fine mixed, isohyperthermic Typic Tropudalf (Soil Survey Staff, 1975).

Soil-water retention

Water-retention characteristics were determined for four locations within the 1.0 ha field. Characteristics were determined for duplicate samples for each 0.1 m increment of depth through 0 - 0.6 m at each location. Measuring techniques involved sand table for soil-water pressure h of 0, -1, and -10 kPa, sand-kaolin table for $h = -50$ kPa, and pressure plate for $h = -100$ and -1,500 kPa (Klute, 1986).

Hydraulic conductivity

Estimates for the relation $k(h)$ of hydraulic conductivity (saturated and unsaturated) to soil-water pressure h were determined by the before mentioned Methods 1, 2, and 3. These methods are described in detail below.

Method 1: Direct measurement of hydraulic conductivity of soil horizons at each test site

Two samples were taken at Sites 1A and 3B from each soil horizon and for each of three measuring techniques:

- (i) The column method (Bouma, 1982) for vertical saturated conductivity (k_s) using encased soil columns 0.25 m high and 0.20 m in diameter;
- (ii) The crust method (by the version of Booltink et al., 1991) for h between 0 and -5 kPa, using the soil cylinders of technique (i);
- (iii) The hot air method (Arya et al., 1975) for $h < -5$ kPa, using encased soil cylinders 0.10 m high and 0.050 m in diameter; additionally, the hot air method was augmented by the cube method (Bouma and de Laat, 1981) to estimate the effect of horizontal cracks in lessening $k(h)$: cubes were of 0.30 m dimensions and measurements (one replicate cube each) were made at -30, -60 and -90 kPa.

Resulting hydraulic conductivity curves were parameterized using a simple power function expression:

$$k(h) = k_s |h|^n \quad (5.1)$$

where k_s is the saturated hydraulic conductivity, h is the pressure head, and n is a soil-specific dimensionless constant.

Table 5.1 Physical properties and fitted k_s and n parameters for four hydraulic-functional horizons (FH1 - FH4) occurring in the 50 ha survey area and at both test sites (k_s is saturated hydraulic conductivity; n is a dimensionless soil constant).

Horizon	k_s (cm d ⁻¹)	n (-)	clay (%)	silt (%)	sand (%)	$C_{org.}$ (%)	bulk density (g cm ⁻³)
FH1 (Ap)	55	-1.58	39 ± 2*	43 ± 2	18 ± 2	1.16 ± 0.30	1.17 ± 0.05
FH2 (B)	24	-1.82	51 ± 4	36 ± 3	13 ± 2	0.74 ± 0.18	1.11 ± 0.04
FH3 (C)	42	-1.78	44 ± 6	30 ± 4	26 ± 8	0.42 ± 0.14	0.92 ± 0.06
FH4 (R)	17	-1.36	20 ± 5	25 ± 6	55 ± 9	0.20 ± 0.13	0.89 ± 0.03

* standard deviation

Method 2: Use of average hydraulic conductivity functions determined for hydraulic-functional horizons

In a preceding study (Chapter 4), the hydraulic functions of all five hydraulic-functional horizons occurring in the 50 ha study area were measured at least six times. For each FH, six to eight well-distributed sampling locations were selected. Replicate measurements for each hydraulic-functional horizon were used to calculate the geometric average hydraulic functions for every hydraulic-functional horizon. These geometric hydraulic conductivity functions were parameterized using Eqn 5.1 and were used in Method 2 to simulate soil water contents at test Sites 1A and 3B. Physical properties and fitted k_s and n parameters for the hydraulic-functional horizons occurring at the test sites are given in Table 5.1.

Method 3: Deriving hydraulic conductivity through model calibration

The parameters k_s and n expressing the $k(h)$ function were also calculated by model calibration. The procedure involved minimizing an objective function C :

$$C = \frac{1}{NM} \sum_{j=1}^M \sum_{i=1}^N (\theta_{obs}(z_i, t_j) - \theta_{sim}(z_i, t_j))^2 \quad (5.2)$$

where N is the number of depth intervals considered, M is the number of observation dates, and $\theta_{obs}(z_i, t_j)$ and $\theta_{sim}(z_i, t_j)$ are observed and simulated volumetric water contents at depth z_i and time t_j , respectively.

A numerical optimization procedure - a controlled random search procedure (Price, 1979) - was used to obtain the hydraulic conductivity function. A simple expression for $k(h)$ was chosen to facilitate calibration, see Eqn 5.1. The method consists of two steps. First a determined initial number of parameter sets (NPS, i.e., combinations of k_s and n) are randomly generated. Values for k_s were allowed to vary between 0 and 400 cm d⁻¹ and n from -1.0 to -5.0. For each parameter set the criterion value C is calculated. In the

second step, new parameter sets are generated and replace existing ones if they have a criterion value C lower than any of the current sets. A new parameter set is obtained by choosing at random $q + 1$ different parameter sets from the existing NPS. A new parameter $P'(i)$ is obtained from the following equation:

$$P'(i) = 2 \cdot g(i) - P(i, q + 1) \quad (5.3)$$

where $g(i)$ is the average value of parameter i from the first q randomly chosen parameter sets. The value of C is calculated for $P'(i)$ and compared with the largest C . If the new combination is better, it replaces the worst of stored parameter combinations. The ranges of each parameter will narrow after several iterations.

The parameters k_s and n were assumed to be constant throughout the profile. Nine time series of soil-water contents in 0 to 0.8 m depth were used for calibration of the $k(h)$ curve. They were derived from several years of field experiments conducted at various elevations within the 1.0 ha experimental field. These data sets were not included in the ones used for methodology evaluation purposes in this study.

Crop, soil and weather measurements

Direct seeded dryland rice (*Oryza sativa*, cv IR36) was grown at both Sites 1A and 3B during the dry season (DS) of 1987 - 1988 and the three wet seasons (WS) of 1986, 1987 and 1988. Measurements were made during each season of plant height, leaf area index, above-ground dry matter, and root depth (each at 2 - 3 week intervals). No harvest was obtained for DS1987 - 1988 because of severe drought stress.

Groundwater level was monitored daily, using piezometers. Soil water contents were measured approximately weekly by core sampling at 0.10 m depth intervals down to 0.80 m depth or to a shallower water table (five replicates per sampling occasion and test site).

Weather variables - including rainfall, global radiation, air temperature and humidity, and wind speed - were recorded at a meteorological station 0.5 km distant from the test sites.

Simulation of soil-water contents

The soil hydraulic conductivity functions derived through Methods 1, 2, and 3 were used as input for a soil-water balance model. The methods were then evaluated by comparing soil-water contents predicted by the model with the water contents actually measured at Sites 1A and 3B.

The simulation model used was Simulation Algorithm for Water flow in Aquic Habitats (SAWAH) (ten Berge et al., 1992), which is a one-dimensional soil-water sub-routine developed for rainfed rice environments. It numerically solves equations of soil-water flow (saturated and unsaturated) through a profile comprising up to 10 layers, for each of which the hydraulic-conductivity functions can be specified by k_s and n .

Crop growth was not simulated. Instead, crop model components were used to

determine daily values of the potential transpiration rate, the water extraction rates from the distinct soil layers, and the potential soil evaporation below the canopy. These rates were calculated on the basis of the *big leaf concept*, from measured leaf area index and measured standard meteorological variables at screen height: global radiation, wind speed, minimum and maximum air temperature and air humidity. Daily values of leaf area index and root depth were obtained by linear interpolation between measured data and were used as forcing inputs (see for details Penning de Vries et al., 1989).

In climates with high air humidity and radiation, as was prevalent on the test sites, the potential transpiration may be underestimated by 15 - 30% when calculated from daily averages (FAO, 1977). To correct for this phenomenon, daily values of potential transpiration were multiplied by a factor 1.3.

For all three methods of generating hydraulic conductivity functions, the derived $k(h)$ were used through SAWAH to predict soil-water contents (θ) at various depths (z) and times (t). Method 1 used the k_s and n derived specifically for the test site soil horizons, while Method 2 used average k_s and n values appropriate to those four hydraulic-functional horizons (FHs) occurring at the test sites. For Method 3, k_s and n were assumed constant throughout the test site profiles, and their values were optimized to match measured $\theta(z, t)$.

To compare the performance of SAWAH over a range of depth, simulated and observed total water contents in the upper 0.4 m of the profile (roughly coinciding with rice rooting depth) were calculated as well.

Statistical analysis

Predicted and measured θ for both 0.1 m and 0.4 m layers were compared graphically and by regression. Comparisons were also made in terms of the Mean Error of Prediction (MEP):

$$\text{MEP} = \frac{1}{n} \sum_{i=1}^n (x_i - y_i) \quad (5.4)$$

and the Mean Squared Error of Prediction (MSEP):

$$\text{MSEP} = \frac{1}{n} \sum_{i=1}^n (x_i - y_i)^2 \quad (5.5)$$

where n is the number of data points of measured and calculated total water content, x_i the measured water content, and y_i the calculated water content.

The MEP is a measure for the bias in the simulation results. Values close to zero indicate that measured and calculated water storages do not differ systematically from each other. Values that differ greatly from zero indicate the presence of a systematic deviation or bias.

The MSEP is a measure for the scatter of the data point around the 1 : 1 line. Low MSEP values indicate little scatter, whereas high MSEP values indicate large scatter.

With the assumption of normal distribution and independence of differences between measured and calculated water content, the half width of the 95% confidence interval for MEP (W) can be calculated as (Wösten et al., 1990):

$$W = t_{\text{stat}} ((\text{MSEP} - \text{MEP}^2) / (n - 1))^{0.5} \quad (5.6)$$

where n is the number of observations (simulations), and t_{stat} is Student's t -statistic for $\alpha = 0.05$ and $n - 1$ degrees of freedom. The evaluations were each made for six data sets, comprising two replications (Sites 1A, 3B) and the three methods.

Results and interpretation

Soil horizons and hydraulic conductivities

Five soil horizons were distinguished at both Sites 1A and 3B. There were slight differences between the sites in the depths and thicknesses of these horizons. Depth to the volcanic tuff layer R, was 0.8 m at site 1A and 1.0 m at Site 3B. The soil horizons C1 and C2 differed only in color and could be merged into one hydraulic-functional horizon (FH3) as outlined in Chapter 4. The Ap, B and R soil horizons were equivalent to hydraulic-functional horizons FH1, FH2 and FH4 in Chapter 4:

- Site 1A: Ap (FH1) 0 - 0.20 m; B (FH2) 0.20 - 0.40 m;
 C1 (FH3) 0.40 - 0.65 m; C2 (FH3) 0.65 - 0.80 m; R (FH4) > 0.80 m
- Site 3B: Ap (FH1) 0 - 0.20 m; B (FH2) 0.20 - 0.40 m;
 C1 (FH3) 0.40 - 0.75 m; C2 (FH3) 0.75 - 1.05 m; R (FH4) > 1.05 m

Average textural properties and bulk densities for the four hydraulic-functional horizons FH1 - FH4 occurring at the test sites are presented in Table 5.1.

Values for k_s and n fitted to hydraulic conductivity data determined for samples taken from the five soil horizons at both test sites (Method 1) are presented in Table 5.2. Good fits between measured and fitted data were obtained ($r^2 > 0.95$). Average k_s and n values for the four hydraulic-functional horizons as derived for the 50 ha survey area are listed in Table 5.1 (Method 2). For k_s , values are of order 0.2 to 0.5 m d⁻¹, and 50 ha survey values are acceptably consistent with Sites 1A and 3B values (i.e. within a factor of 2).

In Method 3, minimization of the objective function $C(k_s, n)$ continued until seasonal totals of each water balance term (i.e. runoff, drainage, transpiration, and evaporation) differed by no more than 1 mm among parameter combinations. This resulted in a distribution of k_s and n for each of the nine data sets used in the calibration. All combinations of k_s and n were then merged. They covered a wide range, with averages of 2.0 m d⁻¹ and -2.2, respectively, and standard deviations of 1.1 m d⁻¹ and 0.7. Parameters k_s and n were significantly correlated at 0.1% level ($r = -0.39$). The average values of k_s and n were used as input for the SAWAH simulations.

Table 5.2. Fitted k_s and n parameters obtained for the five soil horizons occurring at the test sites (Method 1). Corresponding hydraulic-functional horizons (FH1 - FH4) are indicated as well (k_s is saturated hydraulic conductivity; n is dimensionless soil constant).

Horizon	Site 1A		Site 3B	
	k_s (cm d ⁻¹)	n (-)	k_s (cm d ⁻¹)	n (-)
Ap (FH1)	42	-1.54	26	-1.42
B (FH2)	26	-1.74	41	-1.51
C1 (FH3)	5	-1.40	29	-1.79
C2 (FH3)	29	-1.80	64	-1.75
R (FH4)	13	-1.37	17	-1.42

Prediction of soil-water contents

Predictions of soil-water content via SAWAH and the k_s - n combinations determined through Methods 1, 2, 3 are compared with measured soil-water contents in Fig. 5.1. Each data point corresponds to one simulated value - at one test site, time, and depth - and to the mean of the five corresponding replicate field samples. (Depth intervals were 0 - 0.1 m, 0.1 - 0.2 m, 0.2 - 0.3 m and 0.3 - 0.4 m). Fig. 5.1 represents model performance for the two conductivity parameters k_s and n , measured by each of the three methods. Each graph includes a 1 : 1 line. Simulated water contents agreed well with observed water contents at all depths. High r^2 coefficients were obtained: 0.82 (Method 1), 0.79 (Method 2), and 0.75 (Method 3) for Site 1A and 0.79 (Method 1), 0.75 (Method 2) and 0.73 (Method 3) for Site 3B. From the graphs and the high r^2 coefficients obtained for each method, it follows that the best results were obtained with Method 1 but that differences in model performance with input derived from either of the three methods were minimal.

Fig. 5.2 compares measured and simulated total water content in the 0 - 0.4 m rice-rooting layer, at both test sites and for each of the three methods. For reasons of brevity results are given for two distinctly different seasons only: the wet season of 1986 (WS86) and the dry season of 1987 - 1988 (DS87 - 88). Again it is apparent that model performance is not influenced much by input derived from either of the three methods. Predicted totals are all within 25 mm of corresponding measured totals, and most are within 10 mm; under very dry conditions (end of DS87 - 88) predictions are less reliable.

Statistical analyses for the predictions of total water content in 0 to 0.4 m depth for both Sites 1A and 3B are summarized in Table 5.3 for each of the three methods. Values for the MEP are very low in all cases and well within the 95% confidence limit for MEP, indicating zero-bias predictions. MEP and MSEP values in Table 5.3 indicate that predictions are slightly more accurate using input derived with Method 1, compared with

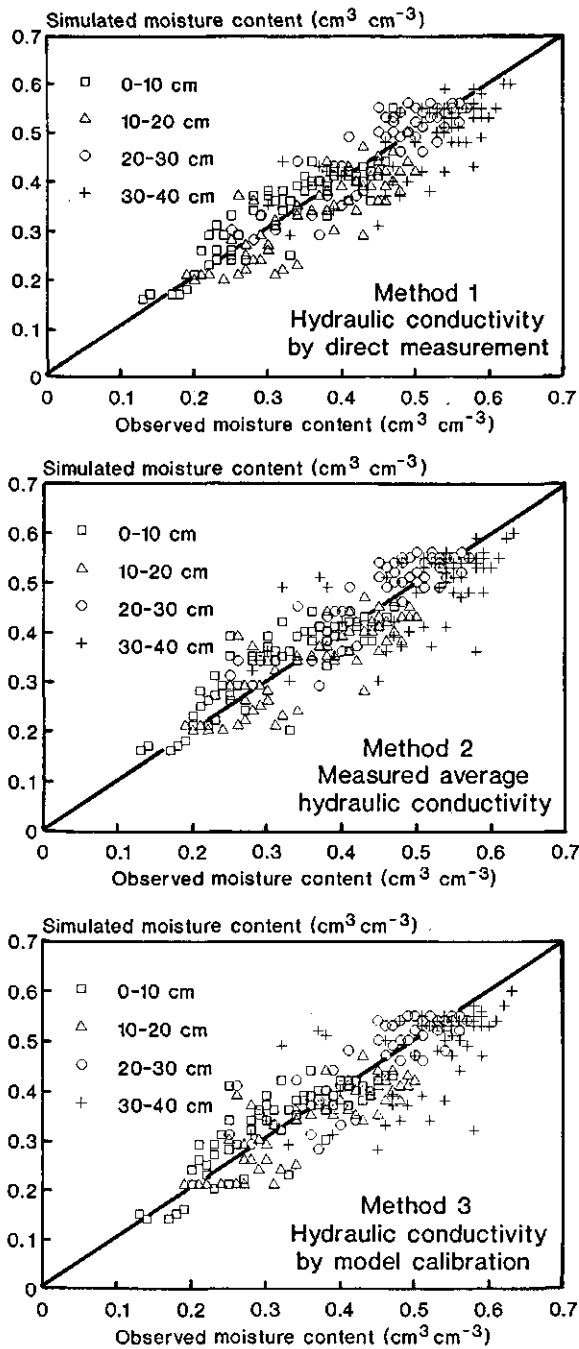


Fig. 5.1 Measured and simulated volumetric soil-water content in 0.1 m thick layers at various depths and at both test sites during three wet seasons and one dry season using measured (Methods 1 and 2) and calibrated (Method 3) hydraulic conductivity data.

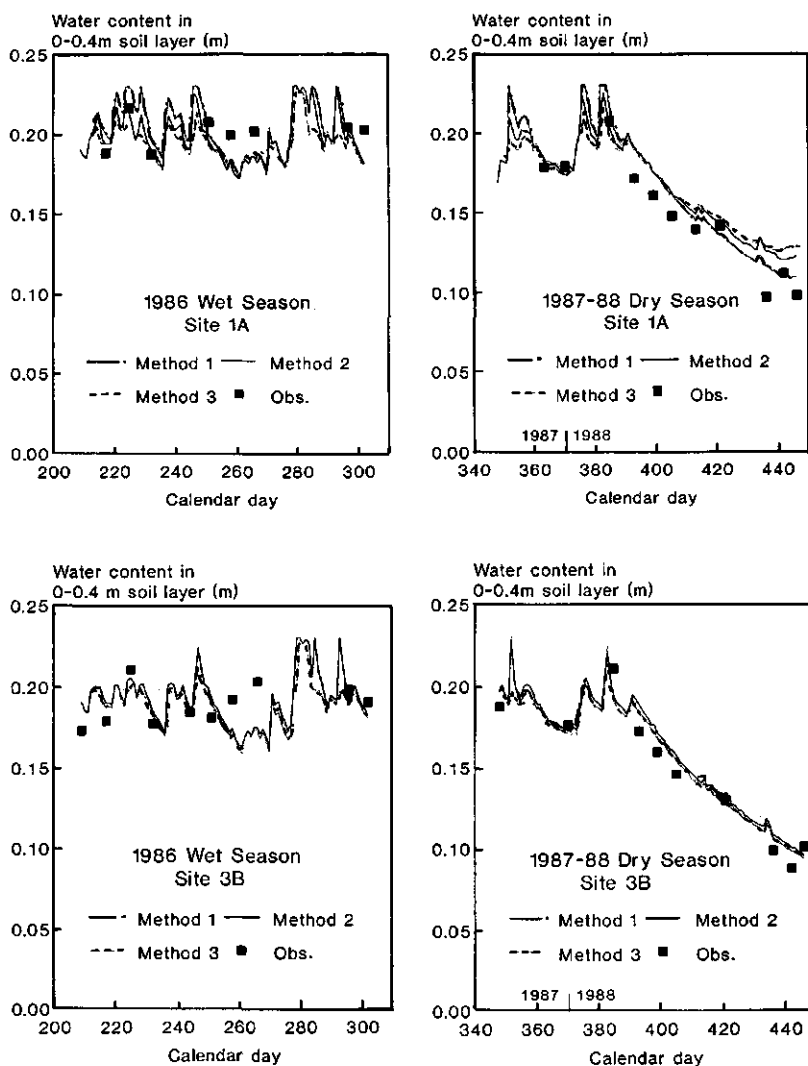


Fig. 5.2 Simulated and observed total water content (equivalent m depth) in 0 to 0.4 m soil layer using measured (Methods 1 and 2) and calibrated (Method 3) hydraulic conductivity data for one wet season (1986) and one dry season (1987 - 1988) and for the Sites 1A and 3B.

the other two methods, but these differences have little practical significance.

It is striking to see that considerable variation in k_s and n as determined by Methods 1, 2 and 3 does not really affect the simulations. This also follows from the wide range of k_s and n that was obtained from deriving the hydraulic conductivity function through model calibration (Method 3). The lack of sensitivity to k_s and n for these particular soils and seasons can be explained by the large values of k_s . Under the prevailing conditions,

Table 5.3 Mean error of prediction (MEP), mean squared error of prediction (MSEP) and half-width of 95% confidence interval (W95) for the mean error of predicted water content in 0 - 0.4 m depth at Sites 1A and 3B using Methods 1, 2 and 3. N-obs is number of observations.

Site	Method	N-obs (-)	MEP (mm)	MSEP (mm ²)	W95 (mm)
1A	1	44	0.1	146	3.7
	2	44	0.8	161	3.9
	3	44	2.3	205	4.3
3B	1	46	0.7	210	4.4
	2	46	-1.7	228	4.5
	3	46	0.7	210	4.4

where water tables are usually deeper than 0.7 m (Site 1A) and 1.0 m (Site 3B), large quantities of daily rainfall will pass through the 0 to 0.4 m layer within one day. Moreover, because the 0.4 m layer rarely dried to beyond -100 kPa in the 1986, 1987 and 1988 wet seasons, the effect of differences among *n*-values was constrained. Upward flow through capillary rise was of importance only during dry spells and in case of a shallow groundwater table.

This study shows that simulation models can be very helpful to optimize sampling strategies for soil hydraulic conductivity functions. For the type of relatively permeable soils with an often deep groundwater table at the two test sites, considerable variation in hydraulic conductivity has only a minor impact on simulation results. Detailed measurements of hydraulic conductivity are, therefore, not useful. In wetland rice soils, however, where farmers try to reduce water losses to the subsoil by manipulating the soil (usually by puddling) completely different results may be obtained (Chapter 2).

A sampling strategy for soil hydraulic conductivity should be based on a first analysis of the effect of soil heterogeneity on a response variable (e.g. soil water content in the topsoil or rice yield) using simulation models. The impact of variability in soil hydraulic conductivity can be simulated if some preliminary measurements are made at representative sites within the area, or if data for soil horizons, similar to the ones occurring at the representative sites, are available. A first analysis of the impact of variability in soil hydraulic conductivity on a response variable using simulation models may save considerable sampling effort.

Conclusions

Three methods to derive soil hydraulic functions needed to simulate the soil-water

balance of two 0.05 ha dryland rice fields were compared: direct measurement in the laboratory on samples from soil horizons occurring within the fields (Method 1); use of average hydraulic conductivity functions measured in a 50 ha dryland rice region surrounding the fields (Method 2); and calculating the hydraulic conductivity function by model calibration (Method 3). All methods showed good agreement between observed and simulated soil water contents within 0 to 0.4 m depth for three wet (monsoon) seasons and one dry season. Best results were obtained with Method 1, but differences were small. Closer analysis revealed that for this type of permeable soils, simulation results were relatively insensitive to soil hydraulic conductivity.

Sampling strategies for soil hydraulic conductivity should be based on a first analysis of the impact of soil heterogeneity on a response variable (e.g. rice yield, water content in the topsoil) using simulation models. This can be done by some preliminary measurements at representative sites within the area or by using average soil hydraulic conductivity functions for hydraulic-functional horizons occurring in the area, while assuming a certain variability in hydraulic conductivity. If simulation results are very sensitive to variation in hydraulic conductivity, more sampling effort will be needed and vice versa.

Chapter 6

Spatial interpolation of soil hydraulic properties and simulated rice yield

Abstract Non-submerged rice yield was simulated for a 50 ha dryland rice area in two different ways. In Procedure 1, simulations were conducted for six sites, representative for the six soil units distinguished within the area. In Procedure 2, simulations were conducted for 133 auger borings and results were interpolated to management units of three different sizes using block kriging. Differences between both procedures in predictions of rainfed rice yield for the total area and for 22 extra sites were small.

A combination of a Geographic Information System (GIS) and Procedure 1 was used to identify areas with highest potential for rainfed dryland rice. Statistical analysis showed that the six soil units could be grouped into three yield classes. The highest yields were obtained for 11% of the survey area and were associated with the presence of a Bg soil horizon in the soil profile.

It was concluded that the best procedure for spatial interpolation of simulated rice yield should follow from preliminary simulation and sensitivity analyses of the impact of weather variability and soil heterogeneity on yield variability and associated cost-benefit calculations.

Introduction

Crop simulation models are widely used to predict crop yields under a range of weather conditions and for different soil types (e.g. van Keulen et al., 1987; Feyen, 1987; Feddes et al., 1988; van Lanen et al., 1992). For rainfed conditions, the soil hydraulic properties (i.e. water retention and hydraulic conductivity) are important input data for simulation models that predict crop yield.

Sampling for the measurement of soil hydraulic properties is often carried out at regular depth intervals. This might be acceptable for homogenous soils with a weakly developed soil profile. If clear pedological horizons exist, however, it is advisable to sample per horizon. In doing so, soil physical information at any site within the area under study can be derived from the soil profile by linking physical data to horizons observed in the soil, based on measurements in similar horizons elsewhere (Wösten et al., 1985).

Measurement of soil hydraulic properties is time consuming and costly. For large areas of land, hydraulic properties can be estimated efficiently after identification of hydraulic-functional horizons, comprising one or more 'classical' soil horizons that are similar in soil hydraulic functions, as shown in Chapter 4. Hydraulic-functional horizons can be sampled at a number of sites and average water retention and hydraulic

conductivity functions can be derived. Applying these functions at unsampled locations is possible if the spatial pattern of depths to hydraulic-functional horizons as well as their thicknesses in the study area are known. This information can be derived either by interpolation of point data using statistical methods, such as kriging (e.g. Journel and Huijbregts, 1978; Webster, 1985; Di et al., 1989), or from a soil map (e.g. Wösten et al., 1985). Crop simulation models can then be used to predict yields for any location or field if adequate data on weather, crop and groundwater depth are available.

For each mapping unit on a soil map, a soil surveyor compiles landscape characteristics and auger data into a representative profile description (RPD). This RPD can be used to relate soil horizons to soil hydrological characteristics that can serve as input for crop simulation models (e.g. Wösten et al., 1985). This approach relies on expert knowledge to interpolate point information to areas of land. It is also possible to run a crop simulation model using data from profile descriptions at every single boring and interpolate the results to areas of land using a statistical method like kriging (de Wit and van Keulen, 1987; Stein et al., 1992).

In this paper predictions of non-submerged rice yield derived from a soil map (Procedure 1) were compared with predictions obtained from block kriging point data (Procedure 2) for a 50 ha dryland rice region and for specific locations within this area. Block kriging was carried out for management units of three different sizes. Comparison of both procedures focused on simulated yields, using a validated simulation model, and not on measured yields.

Another objective was to design sampling strategies to derive areal estimates, with known precision, of depth to hydraulic-functional horizons and of simulated rainfed rice yield within the 50 ha survey area.

Materials and methods

Study area

The 50 ha study area was located at the experimental farm of the International Rice Research Institute (IRRI) in Los Baños, Philippines (14°30' N, 121°15' E). The area is embedded between two creeks that have deposited alluvial material originating from Pleistocene and more recent volcanic activity. The alluvial portion of the profile becomes thicker from the elevated north-south central part of the area towards the creeks.

Depth to a volcanic tuff layer in the central part varies strongly over small distances and ranges from close to the surface to a depth beyond the reach of an auger (2.2 m). The study area is gently sloping and consists of moderately well drained clay soils.

The climate is characterized by two pronounced seasons: a dry season from December to May and a wet season from June to November. Heavy monsoon rains occur during the months of August and September. Total annual rainfall is about 2200 mm while rainfall occurs during 66 days of the year, as averaged for a 15 year period.

Management units of three different sizes (MU1, MU2, MU3; Fig. 6.1), with

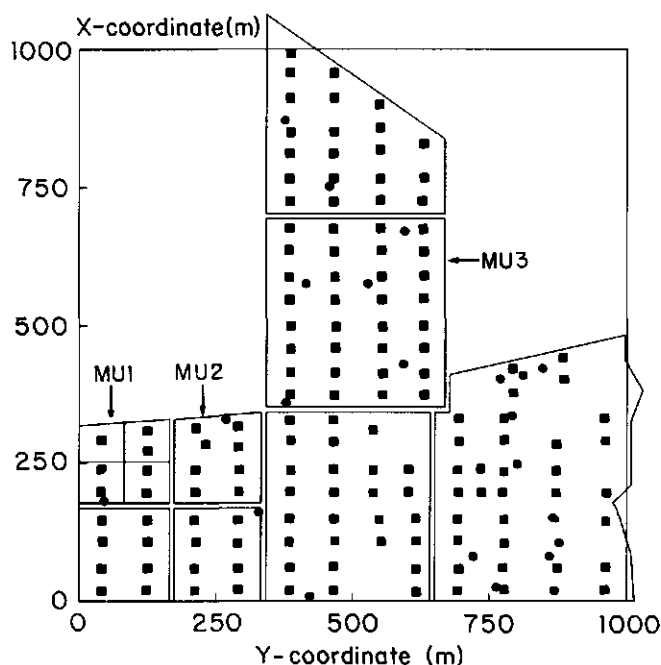


Fig. 6.1 Map of the 50 ha dryland rice area and locations of the auger borings. The area can be subdivided into five large management units (MU3), 20 medium size management units (MU2), and 80 small management units (MU1). Data points used in the block kriging procedure (squares) and test points (dots) are included.

approximate dimensions of 80 m x 80 m (MU1); 160 m x 160 m (MU2); and 350 m x 350 m (MU3) are being used within the area.

Soil survey

After discussion with a soil surveyor familiar with the area (P. Agustin, pers. comm.) and a half day reconnaissance survey, six soil units (SU1 - SU6) were distinguished (Table 6.1). Soil classification was based on Soil Taxonomy (Soil Survey Staff, 1975). Additional mapping criteria included presence of tuff fragments in the subsoil and depth to the paralithic tuff layer. Tuff fragments were considered to be present if they occupied more than 10% of the soil volume. Three classes of depth to the tuff layer were considered: 0 - 50 cm (SU5), 50 - 100 cm (SU1, SU3) and > 100 cm (SU2, SU4, SU6).

The soil survey was made at a scale of 1 : 6000 on a regular 40 m x 80 m grid. A total of 144 auger observations were made to a maximum depth of 2.2 m or to the upper surface of the volcanic tuff layer. An additional test set of 22 auger borings was collected at randomly selected locations, independent from the original survey (Fig. 6.1).

The point information derived from the 144 auger boring descriptions was trans

Table 6.1 Mapping units of the soil map, their classification according to Soil Taxonomy (Soil Survey Staff, 1975), depth of the tuff layer (average \pm standard deviation) and simulated rainfed rice yield (average \pm standard deviation). Nr. obs. is number of observations.

Soil unit	Classification	Tuff fragm. in subsoil	Nr. obs.	Depth tuff layer (m)	Yield (t ha ⁻¹)
SU1	Isohyperthermic, mixed typic Tropudalf	yes	44	0.81 \pm 0.13	5.2 \pm 0.9
SU2	Isohyperthermic, mixed typic Tropudalf	yes	38	1.33 \pm 0.29	4.7 \pm 0.7
SU3	Isohyperthermic, mixed typic Tropudalf	no	17	0.81 \pm 0.17	5.4 \pm 0.8
SU4	Isohyperthermic, mixed typic Tropudalf	no	23*	1.59 \pm 0.38	4.8 \pm 0.8
SU5	Isohyperthermic, paralithic Tropudalf	yes	6	0.31 \pm 0.09	5.5 \pm 0.8
SU6	Isohyperthermic, mixed vertic Tropaquept	no	16**	1.69 \pm 0.16	5.8 \pm 0.8

* No tuff layer present within 2.2 m for 10 observations.

** No tuff layer present within 2.2 m for 8 observations.

formed in areal information by combining similar auger boring descriptions into soil units on a soil map (Fig. 6.2, Table 6.1). The delineation of the soil boundaries was partly based on terrain features. If this was not possible, each observation point was compared with neighbouring observation points. If neighbouring observations points did not belong to the same soil unit a boundary was drawn half-way in between both points.

Table 6.2 Soil characteristics of hydraulic-functional horizons (FH1 - FH5).

Horizon	C _{org.} (g kg ⁻¹)	clay (kg kg ⁻¹)	silt (kg kg ⁻¹)	sand (kg kg ⁻¹)	bulk density (g cm ⁻³)
FH1	11.6 \pm 3.0*	0.39 \pm 0.02	0.43 \pm 0.02	0.18 \pm 0.02	1.17 \pm 0.05
FH2	7.4 \pm 1.8	0.51 \pm 0.04	0.36 \pm 0.03	0.13 \pm 0.02	1.11 \pm 0.04
FH3	4.2 \pm 1.4	0.44 \pm 0.06	0.30 \pm 0.04	0.26 \pm 0.08	0.92 \pm 0.06
FH4	2.0 \pm 1.3	0.20 \pm 0.05	0.25 \pm 0.06	0.55 \pm 0.09	0.89 \pm 0.03
FH5	5.2 \pm 1.7	0.53 \pm 0.09	0.37 \pm 0.05	0.10 \pm 0.05	1.08 \pm 0.05

* standard deviation

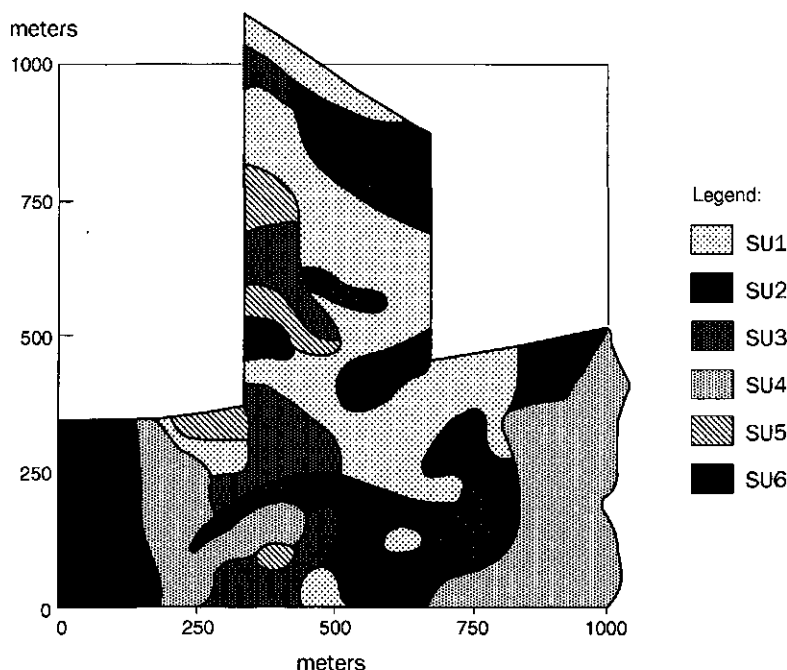


Fig. 6.2 Soil map of the 50 ha dryland rice area. The legend is given in Table 6.1.

Based on the 144 auger borings, a representative site for every soil unit was selected. At this site a pit was dug and a detailed representative profile description (RPD) was made. A RPD contains the sequence of (classical) soil horizons in a particular mapping unit, the depths and thicknesses of these horizons and a range of properties of each horizon.

Soil horizons described within each profile description were translated into five hydraulic-functional horizons (FH1 - FH5) using the methodology outlined in Chapter 4 (Table 6.2).

Measurement of soil hydraulic functions

Hydraulic-functional horizons were sampled at representative sites for every soil unit that was distinguished on the soil map. Six to eight replicate measurements were made for each of the five hydraulic-functional horizons.

Average water retention and hydraulic conductivity characteristics of the five hydraulic-functional horizons were determined (Chapter 4) and specified in terms of van Genuchten parameters (van Genuchten, 1980), see Table 6.3.

Crop simulation modelling

Simulations for direct seeded, medium duration upland rice were carried out for 133 out of the 144 auger locations (eliminating disturbed profiles), for the 22 test points and for

each RPD. Saturated and unsaturated water flow was calculated using the one-dimensional water balance model SAWAH (ten Berge et al., 1992).

The SAWAH model requires knowledge of soil water retention and hydraulic conductivity functions for each hydraulic-functional horizon. External boundary conditions (irrigation, rainfall, evaporation, transpiration, groundwater table depth) need to be specified daily. In this study, the groundwater level was set to 1.0 m depth throughout the growing season, which was considered as a reasonable average value. SAWAH is very suitable for rice soils because it can handle partly saturated (i.e. because of a perched water table) and partly unsaturated profiles.

Crop growth was simulated using the MACROS-L1D model (Penning de Vries et al., 1989). Input requirements are: geographical latitude; daily data on solar radiation, minimum and maximum temperature, windspeed and relative humidity; plant density; date of crop emergence and parameters that describe the morphological and physiological characteristics of the crop.

In MACROS-L1D it is assumed that the ratio between actual (T_a) and potential transpiration (T_p) decreases linearly from 1 to 0 if the root zone water content predicted by the SAWAH model drops from field capacity ($h = -10$ kPa) to wilting point level ($h = -1.5$ MPa). The reduction in growth rate due to water shortage is more or less proportional to the reduction in transpiration rate (van Keulen and Wolf, 1986). In MACROS-L1D, the actual growth rate G_a , limited by soil moisture in the root zone, is obtained by multiplying the potential growth rate G_p by the factor T_a / T_p .

Simulations were conducted for 25 consecutive wet seasons (1960 - 1984). Seeding of rice was assumed to start when cumulative rainfall exceeded 75 mm of rain during seven consecutive days after 1 June.

Potential (fully irrigated) and water-limited (rainfed) crop yields were simulated for all 25 seasons. For the sake of brevity, we refer to the average values over 25 seasons as *potential rice yield* and *rainfed rice yield*, respectively. To get a rough impression of the

Table 6.3 Parameters for van Genuchten's soil-hydraulic functions as calculated for the five hydraulic-functional horizons identified for a 50 ha area of the IRRI farm (k_s is the saturated hydraulic conductivity, θ_s the volumetric water content at saturation, and θ_r the residual volumetric water content (set to 0.01)).

Horizon	k_s m d ⁻¹	θ_s cm ³ cm ⁻³	α cm ⁻¹	n -	l -	θ_r cm ³ cm ⁻³
FH1 (Ap)	1.27	0.51	0.127	1.119	-6.2	0.01
FH2 (B)	0.35	0.55	0.047	1.095	-0.6	0.01
FH3 (C)	1.03	0.61	0.078	1.076	-4.9	0.01
FH4 (R)	0.42	0.64	0.032	1.073	-11.1	0.01
FH5 (Bg)	0.02	0.57	0.011	1.133	3.2	0.01

importance of total rainfall during the growing season, yields were also simulated for situations with 25% higher or lower rainfall. This was done by simply multiplying daily values of rainfall in all 25 years by 1.25 and 0.75, respectively.

Results are expressed as average yields per hectare over 25 years for each rainfall regime and for the fully irrigated situation.

Statistical procedures

The theory of geostatistics provides a means to deal quantitatively with spatial variability and an optimal prediction technique: kriging. Kriging has the advantage that it provides both an unbiased predictor and a minimum prediction error variance. Block kriging is a general form of kriging in which average values are predicted over an area.

In this study, the spatial dependence structure of every hydraulic-functional horizon and of rainfed rice yield was determined using the package AKRIP (Kafritsas and Bras, 1981; Bregt et al., 1991). For block kriging, the approach of Stein et al. (1991) was followed, which allows for optimal areal predictions for irregular shaped areas. Depth to hydraulic-functional horizons and rainfed rice yield was predicted for block sizes of 50 m x 50 m, 100 m x 100 m and 300 m x 300 m (corresponding roughly to field or rice-farm scale) for a location in the centre of the study area (x-coordinate = 500, y-coordinate = 500; see Fig. 6.1).

The effect of reducing the number of auger borings on prediction error variance was investigated by reducing the original data set of 144 augerings with steps of 10 auger borings to a minimal set of 20 auger borings. Reduction of the data set was done in such a way that the remaining observations remained distributed more or less uniformly over the study area, to maintain a grid configuration. This information can be used to design optimal sampling densities, on regular grids for future surveys in neighbouring areas.

An optimal sampling strategy should seek to minimize the maximum prediction error variance. If variation is isotropic this can be achieved by sampling on a regular equilateral triangular grid. A square grid is however more convenient and will only result in slightly larger kriging variances (Webster, 1985).

The quality of representative profile descriptions (Procedure 1) and of block kriged values (Procedure 2) for estimating an average value for the total study area was investigated. Values for a mapping or management unit were compared with values for the individual borings in that mapping or management unit by calculating the mean error of prediction (MEP) (Bregt and Beemster, 1989):

$$MEP = \frac{1}{n} \sum_{u=1}^m \sum_{i=1}^k (t_u - z_{ui}) \quad (6.1)$$

where

MEP is the mean error of prediction,

t_u the value of RPD of u th mapping unit in soil map or block kriged value of u th management unit,

z_{ui} the value of i th boring in the u th mapping unit or management unit,

- n the total number of borings,
- m the number of mapping or management units, and
- k the number of borings in the u th mapping or management unit.

The quality of the predictions for specific locations was investigated by means of a test set of 22 additional auger borings, which was sampled independently of the 144 original observations. Use was made of two different measures: the Mean of Squared Errors of Predictions ($MSEP_t$) and the Mean of Errors of Predictions (MEP_t). The $MSEP_t$ and MEP_t are defined by the following expressions, in which n is the number of observations in the test set:

$$MSEP_t = \frac{1}{n} \sum_{i=1}^n (t_i - zt_i)^2 \quad (6.2)$$

$$MEP_t = \frac{1}{n} \sum_{i=1}^n (t_i - zt_i) \quad (6.3)$$

where zt_i is the observation in the i th *test* point and t_i is the prediction obtained either by block kriging for management units of different sizes or by using mapping units in case of the soil map.

The Root Mean Squared Error of Prediction, $RMSEP_t$, allows comparison with MEP_t in the same units and is obtained by simply taking the square root of $MSEP_t$. For block kriging, MEP_t must theoretically be zero since kriging provides an unbiased estimator. When predictions agree well with observations, $MSEP_t$ will be small, whereas in the case that large deviations occur, $MSEP_t$ will be large. The quality of predictions was investigated for depth and thicknesses of hydraulic-functional horizons and for rainfed rice yield.

Results and discussion

Rice yields

The seeding date which was dependent on the amount of rainfall after June 1, was quite variable. Earliest seeding date was day (day of year) 152, latest seeding date was 205, with an average date over 25 years of 164.

Average potential rice yield for the 25-yr period was 6.4 t ha^{-1} , ranging from 5.6 to 7.1 t ha^{-1} (Fig. 6.3). These yields agree well with field experimental data obtained recently at IRRI. Simulated rainfed rice yields obtained for the 133 auger borings ranged from 3.5 to 6.5 t ha^{-1} and were very similar for the three weather scenario's that were considered (Fig. 6.3). Closer analysis revealed that this similarity was caused by inefficient use of water, due to deep drainage. Rain is not distributed regularly over the seasons but comes in heavy showers and typhoons. In this type of relatively permeable soils with high saturated conductivity values (Table 6.3, except for FH5) large quantities

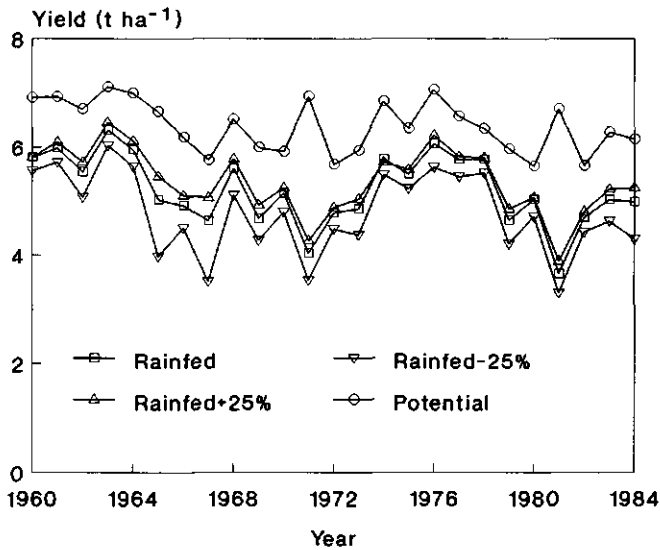


Fig. 6.3 Average potential rice yield for 25 years and average rainfed rice yield calculated for 133 auger borings for the same 25 years and for three weather scenario's (historic rainfall, historic rainfall +25% rain and historic rainfall -25% rain, see text).

of daily rainfall quickly drain to the subsoil.

Largest yields were obtained for soil unit 6 (5.8 t ha⁻¹, see Table 6.1), which can be explained by the presence of FH5 in the soil profile. FH5 is comprised of Bg horizons, close to the surface. These horizons have a low saturated conductivity (Table 6.3). Water losses due to deep drainage in this soil unit are therefore small. Simulated yields probably would have been even greater (although the average of 5.8 t ha⁻¹ is already very close to the average potential yield of 6.4 t ha⁻¹) if adequate data on groundwater table depth would have been available. At shallow depth mottling occurs within this mapping unit, indicating fluctuation of groundwater close to the surface, whereas in the simulations a constant water table of 1.0 m depth was assumed.

Spatial dependence and sampling strategies

Descriptive statistics of thicknesses and depth to functional soil horizons within the 50 ha study area are given in Table 6.4. Block kriging was carried out for different block sizes (50 m x 50 m, 100 m x 100 m and 300 m x 300 m) for one location in the centre of the study area. The effect of reducing the original number of 144 augerings for FH3 and rainfed rice yield is shown in Figs. 6.4a and b. The standard deviation of the prediction errors does not change much even if the number of observations is reduced to 60. The other soil horizons displayed similar patterns, except for depth to FH4. This variable showed no spatial dependence structure and the standard deviation of the prediction error as, therefore, not affected by block size. Graphs like Fig. 6.4a can be used in future sur-

Table 6.4 Descriptive statistics for depth to all hydraulic functional horizons, FH (cm) and for simulated rainfed rice yield over 25 wet seasons (kg ha^{-1}).

Variable	Number of observations	Mean	Standard deviation
Thickness of FH1	133	13	5
Depth to FH2	107	12	4
Depth to FH3	83	57	33
Depth to FH4	126	108	43
Depth to FH5	27	61	45
Rainfed rice yield	133	5198	398

veys in nearby areas to optimize sampling schemes if only a limited number of observations can be afforded. Fig. 6.4b shows the effect on the prediction error for rainfed rice yield. From the graphs it can be seen that the sampling scheme that was used in this survey was unnecessarily detailed. Instead of the original 144 observations less than 60 would have been sufficient. Figs 6.4a and b indicate the appropriate number of observations needed in accordance with the minimum standard deviation of the prediction errors. Uncertainties about the block mean of a regionalized variable decrease as the block size increases.

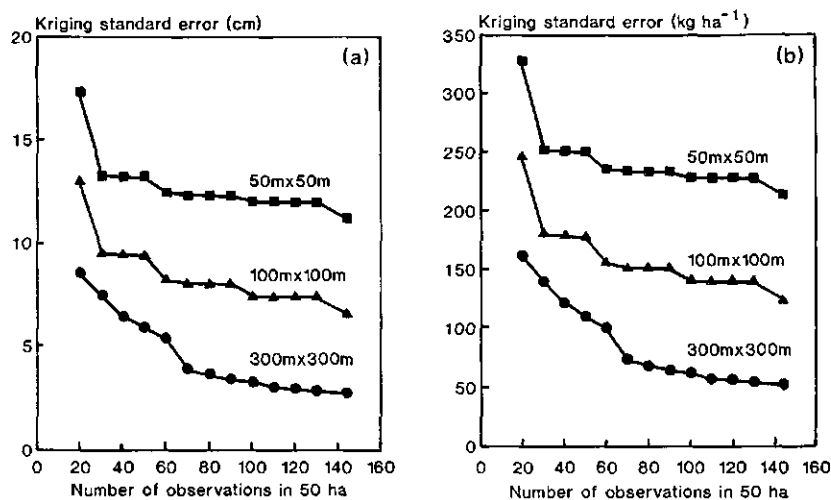


Fig. 6.4 Kriging standard error in relation to the number of observations for depth to hydraulic functional horizon 3 (a) and rainfed rice yield (b) over 50 m by 50 m, 100 m by 100 m and 300 m by 300 m blocks.

Comparing Procedures 1 and 2

Simulated rainfed yield calculated for the 133 borings and 25 years ranged from 3.5 to 6.5 t ha⁻¹. The average rainfed yield of 5.2 t ha⁻¹ was considered to be the best possible prediction of the average rice yield in the 50 ha survey area. The variation in simulated yield (Fig. 6.3) is caused by variability in soil hydraulic properties and weather only. In reality, other factors, like the spatial variability of soil nutrients and possible incidence of pest and diseases will play a role as well. In a study on spatial variation of soil properties and upland rice yield in West Sumatra, Indonesia, Trangmar et al. (1987) reported average yields of about 2.0 t ha⁻¹ with a standard deviation of 0.9 t ha⁻¹ for a 0.1 ha rice field. Dobermann (1993) also found considerable spatial variability for irrigated direct-seeded rice yield in a 3.6 ha field in Russia. Rice yields in this study ranged from 0.7 to 7.9 t ha⁻¹, with an average yield of 3.8 t ha⁻¹.

The MEP_t gives an indication of the quality of prediction of the average value from the block kriged data. The MEP_t ranged from -3 (MU1) to 24 kg ha⁻¹ (MU3) indicating a very good prediction quality for all three management units. Management unit size therefore hardly affects the prediction of average rainfed rice yield of the whole area. The MEP_t obtained when using the soil map was -88 kg ha⁻¹, indicating only minor differences between both interpolation procedures.

In Table 6.5, MEP_t and RMSEP_t values are given for depth to and thicknesses of FHs. MEP_t values are generally low and predictions are, therefore, unbiased. RMSEP_t values increase with management unit size for the thickness of FH1 and depth to FH2, FH3, FH4 which is caused by loss of information due to generalization. Depth to FH5 is not included in Table 6.5 because this horizon was observed at only a few test sites. RMSEP_t values are especially large for FH4, indicating a large short range variability. Measurement errors do not contribute significantly to this short range variability as auger boring data can be taken with a precision of about 5 cm.

For rainfed rice yield, lowest MEP_t and RMSEP_t were also obtained with Procedure 2, using kriging for smallest management unit sizes. Prediction by interpolation of point data seems therefore slightly more accurate than by use of the soil map. Comparing Table 6.5 with Fig. 6.4 shows that the errors made when predicting for a point location are larger than when predicting for a field. An explanation for this is the averaging of soil spatial variability within a block, causing smaller errors when predicting for fields than for points.

Combining Procedure 1 and GIS to derive areal estimates for yield classes

A *t*-test for two or more means (Steel and Torrie, 1980) revealed that simulated rice yields for soil unit 6 were significantly different from the rice yields for soil units 2 and 4 (Student's *t*-statistic > 4). The soil map can, therefore, be simplified in a map showing only three classes: low (soil units 2 and 4), medium (soil units 1, 3 and 5) and high yield (soil unit 6). A Geographic Information System (GIS) was used to translate the soil map into a yield class map and to determine relative areas per class. Highest yields were obtained for 11% of the 50 ha survey area.

Table 6.5 Mean error (MEP_t) and root mean square error (RMSEP_t) for block kriged predictions and soil map predictions at test points of thickness of FH1 (cm), depth to FH2 - FH5 (cm) and rainfed rice yield (kg ha⁻¹). Block kriging was carried out for three different management unit sizes (MU1, MU2, MU3, see text); *n* is the number of test points.

Variable	<i>n</i>	MU1		MU2		MU3		Soil map	
		MEP _t	RMSEP _t	MEP _t	RMSEP _t	MEP _t	RMSEP _t	MEP _t	RMSEP _t
FH1	22	2	4	1	4	2	4	-	-
FH2	22	2	3	2	3	3	5	-	-
FH3	21	5	25	3	32	1	37	-	-
FH4	21	-2	41	-3	45	-1	58	-	-
Yield	22	31	261	-47	288	-10	269	-87	343

The presence of the Bg soil horizon in parts of the 50 ha survey area assured efficient water use. Sampling strategies for future surveys in neighbouring areas should be guided by the spatial covariance structure of this soil horizon.

Conclusions

Hydrological data derived for six representative sites on a soil map were used as input in a crop simulation model (Procedure 1). Results were compared with an alternative approach in which rice yields were simulated for point observations and interpolated to management units of different sizes using block kriging (Procedure 2). Both procedures yielded similar results for the total area. When specific point locations were considered best results were obtained using Procedure 2 but differences were only minor. Increase or decrease of seasonal rainfall by 25% had little effect on rice yields over the whole survey area due to large deep drainage losses to the subsoil. A combination of a GIS and Procedure 1 revealed the importance of the presence of a Bg soil horizon in the soil profile for efficient water use.

In this study, predictions of simulated rice yield to areas of land by interpolation of 133 auger boring observations using kriging and by interpolation of six representative profiles using a soil map gave similar results. In any other environment this may be quite different. Simulation models can be used to determine if the use of a soil map for interpolation purposes is adequate. For this purpose, expert knowledge is necessary on the variability of depth to hydraulic-functional horizons within each soil unit. This information can be used to conduct a sensitivity analysis with a simulation model for a number of clearly different years (e.g. years with relatively low and high rainfall). If the model is sensitive to the variability within the soil unit, use of the soil map for prediction purposes

for specific sites can not be recommended.

If the soil map cannot be used, or if it can be used for part of the survey area only, additional auger data are needed to characterize the spatial variability within soil units. Often such data will be readily available, as soil maps are not only based on representative profiles, but on auger borings as well. Kriging can be used to interpolate such point observations to areas of land. For the study reported here, graphs of the standard deviation of the prediction errors of depth to hydraulic-functional horizons versus sampling density for different management unit sizes can help to optimize future soil surveys in neighbouring areas.

An excellent example of the importance of scale was given in a study by Wösten et al. (1987b). They used a crop-soil simulation model to investigate grass yield losses incurred by farmers in the east of the Netherlands. In this area (1435 ha) water tables were being lowered by extraction for drinking water. Three different soil maps (1:10,000, 1:50,000 and 1:250,000) were used as a basis for the soil water balance module. Damage estimates for the area as a whole could be obtained using all maps. However, yield loss predictions for a particular farmer's field were only possible if the detailed 1:10,000 soil map was used as an input. Reliable output at this scale depends on more detailed soil input information, which demands more sampling effort and higher cost.

The best procedure for spatial interpolation of simulated rice yield should therefore follow from preliminary simulation and sensitivity analyses of the impact of weather variability and soil heterogeneity on yield variability and associated cost-benefit calculations.

Chapter 7

Reducing bypass flow through a dry, cracked and previously puddled rice soil

Abstract Reducing water losses through bypass flow is important in rice growing areas (rainfed and irrigated) where water losses during land preparation for rice are high due to soil cracking on the surface and a relatively permeable subsoil. Bypass flow processes were studied in a cracked, previously puddled rice soil.

Vertical continuity of soil cracks (10 - 30 mm wide) was determined in the field using a morphological staining technique. Cracks reached a depth of 0.65 m. An infiltration experiment showed that water was mainly absorbed in the subsoil between 0.2 and 0.5 m depth.

In a laboratory experiment, simulated rainfall was applied to large undisturbed soil columns taken from the field. High bypassing ratios (> 0.9) were obtained for low (10 mm h^{-1}) and high rain intensities (30 mm h^{-1}).

Shallow surface tillage (0 - 5 cm) in the field reduced bypass flow and laboratory experiments showed 45 - 60% water savings as a result of making the cracks discontinuous. For rainfed rice areas, introduction of this tillage practice may lead to earlier transplanting and, therefore, reduced risk for late drought. In some areas this may broaden the scope for a second crop. In irrigated rice systems, water savings during land preparation may enable an increase in the command area of an irrigation system.

Introduction

Water flow through vertically continuous macropores (cracks, worm channels) bypassing an unsaturated surrounding soil matrix is known as *bypass flow* or *short circuiting* (Bouma and Dekker, 1978; Beven and Germann, 1982). A field measurement technique to quantify bypass flow was introduced by Bouma et al. (1981) and used by e.g. Kneale and White (1984).

Bypass flow water may be partly absorbed laterally along crack faces or at the bottom of a crack or macropore, a process that has been termed *internal catchment* (van Stiphout et al., 1987). Flow processes including vertical and lateral infiltration and internal catchment were studied in detail in a well-structured clay soil by Booltink and Bouma (1991). Recently Radulovich et al. (1992) showed that for micro-aggregated soils, flow along preferential paths may govern water movement. Wild (1972) reported water flow through cracks in unsaturated soils. Studies on bypass flow through macropores surrounded by a soil matrix near saturation were conducted by Bouma and Wösten (1979) and Steenhuis and Muck (1988).

The bypassing ratio (i.e. the ratio of the rate with which water bypasses the soil matrix to the application rate) usually increases as soil moisture content increases (e.g. van Stiphout et al., 1987). If the soil is very dry however, bypassing ratios can be also very high, due to water repellency (L.W. Dekker, pers. comm.). In a heavy clay soil, bypassing ratios may again become zero near saturation if swelling causes crack closure.

Bypass flow may be of importance if a cracked soil is rewetted for the next rice crop. Rice farmers need to mix water and soil in their fields to create a soft medium for transplanting, a process that is called puddling. Puddling limits water and nutrient losses through reduced percolation and assists weed control. The puddling tillage usually comprises one or two plowings to a depth of 0.15 m and two or more harrowings and a final levelling, using animal power or two-wheeled, gasoline-powered hand tractors. For effective puddling, the moisture content of the topsoil will have to be between field capacity and saturation (Sharma and De Datta, 1985a). If water is not absorbed well by the topsoil large amounts of water can be lost as a result of bypass flow through the rooted zone which for rice is only between 0.3 and 0.4 m deep.

Bypass flow can also have an important impact on the growth of an upland crop after rice. Water may infiltrate to beyond the reach of roots. However, if roots can use the water that has bypassed the topsoil, the phenomenon is beneficial for the crop because surface evaporation losses are minimized (van Stiphout et al., 1987).

In this study, bypassing ratios were determined for a dry, cracked, previously puddled rice soil, at the onset of the monsoon season in the Philippines. The possibility of using shallow surface tillage to reduce water losses due to bypass flow was investigated.

Materials and methods

The field experiments were sited on a 40 m x 20 m field at the International Rice Research Institute (IRRI) in Los Baños, Philippines (14°30' N, 121°15' E). The climate at the study area has two pronounced seasons: dry from December to May and wet from June to November. The soil was classified as mixed, isohyperthermic Typic Tropudalf (Soil Survey Staff, 1975). Ap and Bt horizons respectively comprised 39%, 42%, 19% and 49%, 36%, 15% of clay ($< 2 \mu$), silt (2 - 50 μ) and sand (50 - 2000 μ).

The field was previously puddled and flooded for rice. Just before harvesting the rice crop, at the end of February 1990, the bund surrounding the field was breached, to allow lateral drainage of remaining ponded water. No further crop was grown and soil cracking started soon after drainage. Two field experiments and one laboratory experiment were carried out in April 1990, before the onset of the monsoon season. Moisture content of the previously puddled topsoil was in the range 0.20 - 0.24 m³ m⁻³, corresponding approximately to wilting point (a matric potential of -1.5 MPa). Large cracks of 1 to 3 cm width and an average spacing of 0.2 m were visible at the soil surface. The soil had a total porosity of 0.57 - 0.60 m³ m⁻³, and a moisture content at field capacity (matric potential of -10 kPa) of 0.55 - 0.57 m³ m⁻³.

A second laboratory experiment was conducted on cores removed from the field in June 1990, after the first rains of the monsoon season, when moisture content of the topsoil had increased to $0.31 - 0.35 \text{ m}^3 \text{ m}^{-3}$.

Field experiment 1

Macropore continuity in the experimental field was studied by pouring approximately 30 liters of water-soluble white paint (diluted 20 times with water) over two small subplots of 1 m^2 of cracked soil. After three hours, these subplots were carefully dug out and horizontal planes were prepared at several depths. Drawings were then made of dominant pathways of water flow by tracing the walls of stained cracks and macropores onto transparent plastic sheets.

Field experiment 2

A second field experiment was carried out to determine the pattern of absorption of the bypass water with depth. Two small plots of 1 m^2 (sites A and B) were used. Soil moisture contents were determined at 50 mm intervals down to 0.5 m depth just outside each plot. Samples were taken in the centre of clods ('clod sampling') and near and directly below cracks ('crack sampling'), as illustrated in Fig. 7.1. For clod sampling, 50 mm high, 50 mm diameter cylinders were used. For crack sampling in the topsoil, 2 - 3 mm of soil was scraped from the outside of the clod (i.e. the crack face) at three depths: 25 - 75, 75 - 125 and 125 - 175 mm. At greater depth the same cylinders used for clod sampling were used, placed directly under a crack, after removing the overlying soil.

Both plots were flooded during a few minutes, applying 30 mm of water to each plot only. One hour later soil moisture profiles inside each plot were determined. Again samples were taken in the centre of clods and near cracks, using the procedure described above. All moisture content determinations were based on four replicate samples.

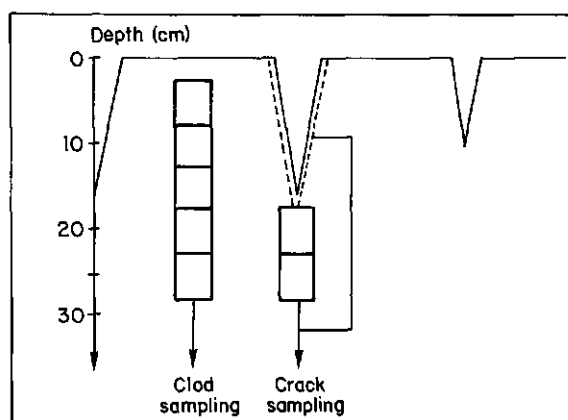


Fig. 7.1 Sampling procedures for field experiment 2.

Laboratory experiment 1

Six soil cores, 0.21 m in diameter and 0.25 m long, were collected from the same field in which both field experiments were conducted, in April 1990. Sampling sites were chosen in such a way that all cores contained one major crack of about 1 cm width that extended to the bottom of the core. The crack was filled with air dry fine sand prior to sampling to avoid sample disturbance while excavating the cylinders. The enclosed soil cores were removed to the laboratory and sand was removed from the cracks. Any space between soil and cylinder wall was filled with grease to avoid boundary flow between soil and cylinder. Initial moisture content of all cores was in the range of 0.20 - 0.24 m³ m⁻³.

A needle array (comprising 48 needles), connected to a mariotte buret, timer and a pulsating pump, was used to apply rain to the surface of the soil cores at a constant rate. Three showers were applied to each core. For three cores, they had an intensity of approximately 10 mm h⁻¹ and lasted three hours each. The period between the showers was 1.5 hours. For the remaining three cores the intensity was 30 mm h⁻¹ and showers lasted only one hour. The period between these showers was 30 minutes. All cores thus received 90 mm water in total. Before each third rain shower, methylene blue powder was applied to the surface of some of the cores, to colour pathways of water flow. Outflow at the bottom of each core was collected and weighed at 5 min. intervals. "Bypassing ratios" (BR) were calculated as outflow rate / application rate.

Laboratory experiment 2

A second laboratory experiment was conducted in June 1990, after the first monsoon rains, to investigate the possibility of reducing bypass flow by using shallow surface tillage. Simulated rainfall was applied to four newly sampled undisturbed soil cores of 0.21 m diameter and 0.25 m height using the same procedure as in laboratory experiment 1. All cores again contained one major crack that extended through the full cylinder height. Bypassing ratios were determined for low (5 mm h⁻¹) and high (15 mm h⁻¹) rain intensities. Two showers were applied to each core. For two cores, they had an intensity of approximately 5 mm h⁻¹ and lasted six hours each. For the remaining two cores the intensity was approximately 15 mm h⁻¹ and each shower lasted two hours. The period between showers was 24 hours.

Shallow surface tillage (0 - 50 mm) was then applied to the cracked rice field using a rototiller (two passes). Tillage resulted in a topsoil consisting of clods with an average diameter of about 20 mm. These clods were collected from the field and placed on top of another set of four cracked soil cores from which the top 5 cm had been removed. Initial weight of this second set of four cores was 10 - 15% less than the first set of four soil cores due to loose stacking of the clods. Simulated rainfall was also applied to these cores, at both low (5 mm h⁻¹) and high (15 mm h⁻¹) intensities. The volume of water absorbed in the tilled cores, at the start of outflow, was compared with the volume absorbed in the non-tilled cores.

Results and discussion

Field experiment 1

The field sheets of stained cracks (Fig. 7.2) and additional field observations showed that cracks reached a depth of 65 cm. Cracks therefore extended well beyond the root zone of the previously grown rice crop. Strong horizontal cracking was observed at the interface between the puddled and non-puddled layers. Under puddled, flooded conditions the zone at the base of the puddled layer has the greatest hydraulic resistance for water flow (Chapter 2). Cracking breaks this hydraulic resistance and water can then easily reach the subsoil.

Field experiment 2

Two different moisture profiles were obtained from clod and crack sampling for both site A and B (Fig. 7.3). The initial moisture content of samples taken near cracks was less in the top 20 cm but greater in the subsoil than for samples taken from the centre of soil

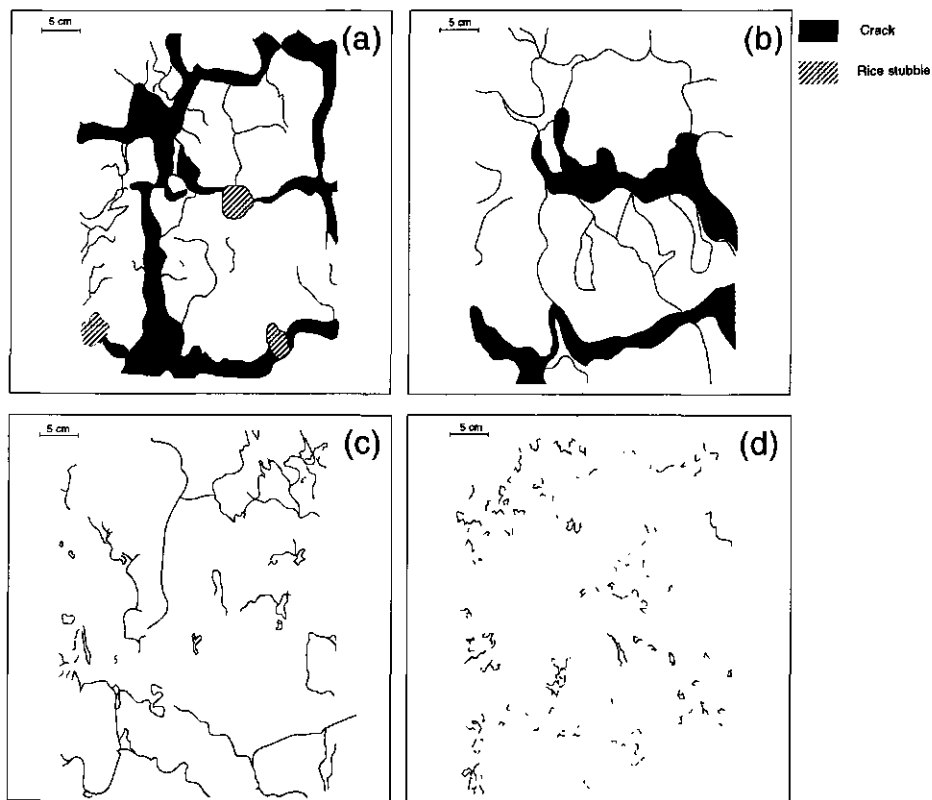


Fig. 7.2 Stained walls of cracks and macropores at horizontal sections taken at the soil surface (a), and at depths of 0.1 m (b), 0.25 m (c), and 0.5 m (d).

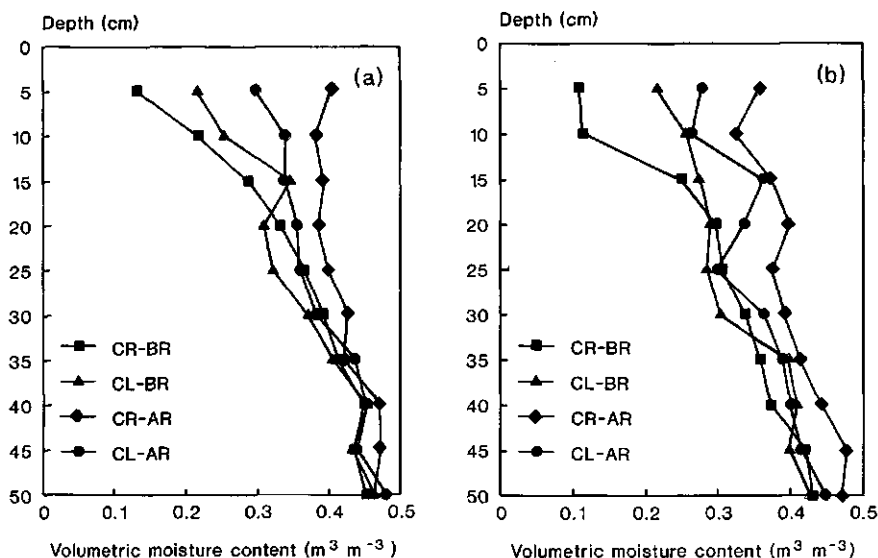


Fig. 7.3 Soil moisture profiles before and after water application to a cracked soil (site A and site B). CR is crack sampling; CL is clod sampling; BR is before water application; AR is after water application. Average standard error of the mean of four replicate moisture contents: $0.02 \text{ m}^3 \text{m}^{-3}$.

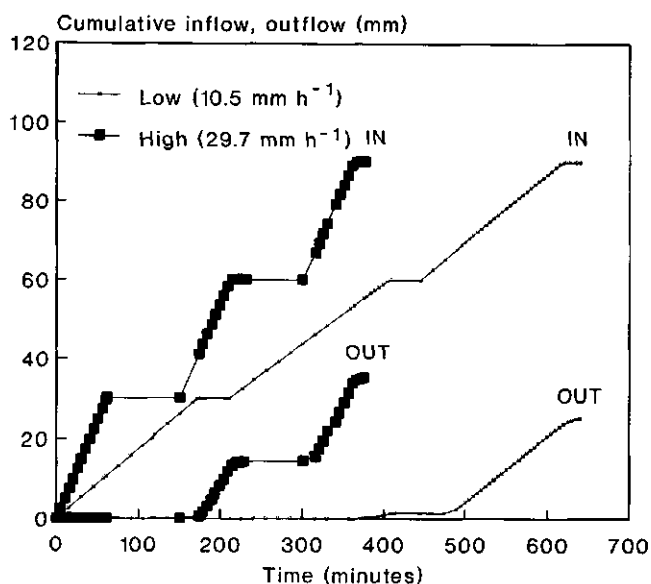


Fig. 7.4 Cumulative outflow (OUT) and inflow (IN) with time during application of two rain showers of different intensities to 0.25 m soil cores.

Table 7.1 Bypassing ratios, absorption rates, cumulative outflow and standard deviation of cumulative outflow for 25 cm cores after applying different rain intensities. Bypassing ratios and absorption rates were calculated from the steady state outflow reached in the third shower. Cumulative outflow is calculated for each core at the end of all three showers (laboratory experiment 1).

Applied intensity (mm h ⁻¹)	Bypass ratio (%)	Absorption rate (mm h ⁻¹)	Cumulative outflow (mm)	Standard deviation (mm)
10.5	92	0.8	25.2	2.3
29.7	94	1.7	35.1	4.1

clods. Crack closure because of swelling processes did not occur. Fig. 7.3 suggests that water flow occurred mainly through the cracks, as the greatest moisture contents were obtained from the crack samples. Water infiltrated to at least 0.45 m on site A and more than 0.5 m on site B (Fig. 7.3). This supports the results obtained in field experiment 1 and has important consequences for water management during land preparation for the next rice crop. Water applied to the plots did not follow Darcy type flow, a result that has been observed by many others (Bouma and Dekker, 1978; van Stiphout et al., 1987; Bronswijk, 1991).

Laboratory experiment 1

The results of the bypass flow experiments in the laboratory with rain intensities of 10 and 30 mm h⁻¹ are shown in Fig. 7.4. Once outflow had started, it reached a steady rate almost immediately, for both rain intensities. Bypassing ratios and absorption rates were calculated and averaged over three cores.

Table 7.1 shows that the bypassing ratios at steady state outflow during the third shower were high (> 0.9) and very similar for both rain intensities. This resulted in low absorption rates of 1 to 2 mm h⁻¹. Measurements of soil moisture content at different depths in some of the cores indicated that the cores remained unsaturated (moisture contents were in the range of 0.44 - 0.48 m³ m⁻³). The analysis of methylene blue stains, after application of the tracer showed that cracks carried water through the cores and that no flow along the cylinder wall occurred.

Results indicate that bypass flow in these cracked, previously puddled clay soils occurs under unsaturated conditions. As soon as the application rate exceeds the infiltration rate of the soil matrix, water will start flowing downwards along the walls of the cracks. These walls will gradually become saturated and further downward flow will occur until the end of the crack is reached ('internal catchment'). Rainfall in the Philippines usually will have a higher intensity than the lowest application rate used in this study (5 mm h⁻¹ in laboratory experiment 2). Typhoon rains can reach intensities of 50 mm h⁻¹ (IRRI,

1991b). It is, therefore, likely that bypass flow contributes significantly to water flow in such cracked clay soils at the onset of the monsoon season.

If the soil at the depth of internal catchment is relatively permeable, water will quickly drain downwards and will be lost from the topsoil. If the subsoil is resistant to water flow, water will start ponding in the cracks which will lead to slow lateral infiltration into the soil matrix.

After the non-monsoon season, rice farmers will try to rewet a field to a moisture content between field capacity and saturation. The results indicate that this may require a large amount of water due to the high bypass flow losses and low absorption rates.

Laboratory experiment 2

Outflow from the cylinders started earlier in the second laboratory experiment than in the first laboratory experiment because of a greater initial moisture content. Initial weight of the tilled set of four cores was 10 - 15% less than the non-tilled cores due to loose stacking of clods. Nevertheless, the effect of the tilled surface was that 45% (at 15 mm h⁻¹) to 60% (at 5 mm h⁻¹) more water was saved (Table 7.2). Some of the smallest clods entered and blocked the cracks. Slaking of the clods did not occur. This shallow pre-tillage at the onset of the monsoon season makes cracks discontinuous, and water is therefore better retained in the topsoil.

Practical applications

Pre-tillage will be especially promising in rice growing areas where water losses during the land preparation for rice are high due to a relatively permeable subsoil. Introduction of pre-tillage may then result in considerable water savings. In Bangladesh this practice has been successful in the Kahalu Upzila region, where it enabled an expansion of the command area of the irrigation system from 50 to 80% (M.A. Sattar, pers. comm.). The pre-tillage should be carried out after the first monsoon rains to facilitate breaking of the soil clods. The mechanism discussed here may also be responsible for the water savings

Table 7.2 Time to first outflow, and absorbed water at the start of outflow from tilled (T) and non-tilled (NT) 25 cm soil cores at two rain intensities (laboratory experiment 2).

Treatment	Rain intensity (mm h ⁻¹)	Time before start outflow (min)	Absorbed water at start outflow (mm)
NT	4.4	282	21
T	4.7	435	34
NT	17.1	47	13
T	15.3	74	19

of 300 - 400 mm that were recently reported in the Philippines, by dry seeding instead of transplanting of rice (IRRI, 1992 and S.I. Bhuiyan, pers. comm.).

For rainfed rice areas, introduction of a pre-tillage may result in a reduced risk of late drought because rice can be transplanted earlier as a result of water savings. In some areas this may broaden the scope for a second crop. In irrigated rice systems, water savings during land preparation may enable an increase in the command area of the irrigation system.

Consequences for modelling of water flow in cracked soils

Simulation models are increasingly being used to predict plant-soil-weather interactions. The processes described here do not follow the classical concept of Darcy water flow used in most simulation models (e.g. Belmans et al., 1983; ten Berge et al., 1992).

Modelling of water flow in cracked soils can be done following an empirical approach or a mechanistic approach. Van Stiphout et al. (1987) used an empirical approach in which a depth of infiltration of bypass water was introduced and the percentage of bypass flow was defined as a function of soil pressure head in the topsoil. Bronswijk (1988b) presented the simulation model FLOCR, in which shrinkage characteristics of soils are included as hydraulic parameters that can be specified for each soil layer. FLOCR can simulate the soil water balance of swelling and shrinking soils by calculating water transport through the soil matrix and through cracks.

Conclusions

The processes of bypass flow and subsurface infiltration differ from the classical concept of surface infiltration. Relatively simple techniques can be used to quantify bypass flow, macropore continuity and depth of infiltration.

High bypassing ratios were found in dry, cracked, previously puddled rice soils. Low rain intensities and shallow surface tillage reduced water losses due to bypass flow. Surface tillage makes cracks discontinuous, and water is therefore better retained in the topsoil. This practice can be important in areas where water losses during land preparation for rice are high due to the relatively permeable subsoil. In rainfed areas introduction of shallow surface tillage before the onset of the monsoon season may avoid the risk of a late drought due to earlier transplanting. In irrigated rice systems, irrigation systems may be able to support rice production over a larger area.

Chapter 8

Drought stress responses of two lowland rice cultivars

Abstract The response of two lowland rice cultivars, IR20 and IR72, to temporary drought in a puddled clay soil was studied in a greenhouse experiment. Drought in both vegetative and reproductive stages strongly affected plant morphology, causing reduced leaf area production, leaf rolling, and early leaf senescence. Relative transpiration rate per unit of leaf area remained equal to that of well-watered plants, even if soil water status dropped by nearly 50%. As soil-water content declined further, a decrease in relative transpiration rate was observed. Yield differences between plants that were temporarily stressed in the vegetative phase and well-watered plants were not significant for both cultivars. However, flowering and maturity were strongly delayed. Severe drought in the reproductive phase resulted in large yield reductions. The following morphological and physiological plant responses to soil moisture content were quantified for different growth stages: (1) rate of new leaf production; (2) rate of leaf rolling; (3) rate of senescence and (4) relative transpiration rate.

Introduction

Quantification of physiological and morphological responses of rice to drought stress is essential for predicting the impact of soil and weather conditions on rice production using process based crop simulation models. It is well known that drought delays phenological development (Turner et al., 1986; Puckridge and O'Toole, 1981; Inthapan and Fukai, 1988), and affects physiological processes like closing of stomata, and reduction of photosynthesis, respiration and translocation of assimilates to the grains (e.g. Fukai et al., 1985; Turner, 1986). Drought strongly affects the morphology of the rice plant. Leaf area development may be hampered, and tillering and panicle development may be reduced (e.g. O'Toole and Cruz, 1980; O'Toole and Baldia, 1982). On the other hand, drought may induce more rapid root growth (e.g. O'Toole and Chang, 1979; O'Toole and Moya, 1981).

Recently it was suggested, on basis of interpretation of experimental data with simulation models, that upland rice crops continue to transpire at high rates during severe drought periods (Woodhead et al., 1991). This could be due to lack of stomatal control. However, Fukai (pers. comm.) found a reduction of transpiration of upland rice plants, even at soil moisture contents close to saturation. For lowland rice, grown in puddled soils, hardly any information on physiological and morphological responses of lowland rice is available. As a result, existing models use standard relationships that have been derived for other crops (Penning de Vries et al., 1989).

A greenhouse experiment was therefore conducted to study the physiological and morphological responses of two lowland rice varieties to temporary drought at five different growth stages: transplanting, two weeks after transplanting, mid-tillering, panicle initiation and flowering. Both the response during the drought period itself and the ability to recover from drought stress were investigated.

Materials and methods

Plant and soil material and growing conditions

The experiment was conducted in a greenhouse of the International Rice Research Institute, Philippines (14°30' N, 121°15' E), from 30 January to 6 June 1992. The climate at the study area is characterized by two pronounced seasons: a dry season from December to May and a wet season from June to November.

Two cultivars of rice, IR20 and IR72 were grown in pvc pots (20 cm diameter and 25 cm height). Three 21 days old seedlings were planted in the centre of each pot. The pots were filled with saturated puddled soil material from the IRRI Experimental Farm (saturated volumetric moisture content $\theta_s = 0.73 \text{ cm}^3 \text{ water cm}^{-3} \text{ soil}$) from a submerged field that was plowed and harrowed 5 days before. The soil was classified as a mixed isohyperthermic Typic Tropudalf (Soil Survey Staff, 1975) and comprised 13% sand, 39% silt and 48% clay. Each pot contained one 1 cm diameter hole at 5 cm from the bottom to allow for adequate drainage at the onset of drought.

Temperature and relative humidity were monitored throughout the experiment. High fertilizer inputs were imposed to ensure that reduced growth of droughted plants was caused by drought stress only. A basal application equivalent to 100 kg N ha⁻¹, 40 kg P ha⁻¹ and 40 kg K ha⁻¹, was mixed with the puddled soil material in each pot. Additional ammonium sulphate was added between mid-tillering and panicle initiation (60 kg N ha⁻¹) and at flowering (40 kg N ha⁻¹); the exact timing depending on drought treatment. During the experiment, occasional spraying of insecticides was needed.

Experimental layout

All pots of a particular treatment were placed side by side on a wooden tray of 10 cm height, to simulate a 20 x 20 cm planting density. Blocks were rotated weekly to avoid any influence of placing of the trays on plant growth. A large number of pots was needed for every treatment because of periodical harvests for plant and soil data. Every block was surrounded by one row of border pots (Fig. 8.1). Border pots received the same treatment as the centre pots within a block but were not used for any measurement. The total number of pots used in this experiment was about 650.

Timing of drought stress and recovery

All plants were watered daily, unless otherwise specified. Soil and water evaporation losses were minimized by covering the pots with round plastic sheets, with an adjustable

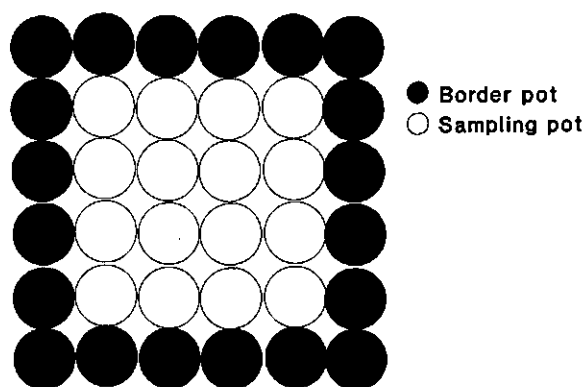


Fig. 8.1 Experimental lay-out.

hole in the centre to allow for optimal tillering of the rice plant.

Drought was induced at transplanting (A), two weeks after transplanting (B), mid-tillering (C), panicle initiation (D) and flowering (E). Panicle initiation was defined as the first day when a white feathery cone was present inside the leaf sheath of the rice plant. Flowering was defined as the moment when 90% of the plants subjected to a certain treatment had at least one flowering panicle. Drought stress was started by simply withholding the daily water application, by syphoning any ponded water from the soil surface and by draining percolation water accumulated at the bottom of the cylinder. For the drought treatments at an early growth stage (A, B), the plastic cover was removed to impose water deficits through soil evaporation as it was anticipated that transpiration losses at an early growth stage would be insufficient to induce any drought stress.

The droughted plants were watered again after a relatively short (Early Recovery, ER) or a longer period (Late Recovery, LR). For drought at flowering only one, short period of drought was imposed (Early Recovery, ER only). For comparison, a number of pots for each variety was kept well-watered, and a number of pots was left to dry out completely.

A visual judgement of the degree of leaf rolling was made daily at midday using a 1 to 5 leaf rolling scale. A leaf rolling score of 1 indicates a first sign of leaf rolling, whereas score 5 means that the leaf has completely rolled up (O'Toole and Cruz, 1980; see Fig. 8.2).

For all treatments, the ability of the rice plant to recover from drought stress was investigated. Recovery (by simply submerging the droughted plants in water) was started when plants clearly suffered from drought, i.e. leaf rolling score 5 (Early Recovery, ER) and when plants were close to dying, i.e. leaf rolling score 5 and 50% dead leaves (Late Recovery, LR). After the onset of the recovery period, plants were kept well-watered until maturity. A schedule of the drought-recovery treatments is given in Table 8.1.






Score	Shape of leaf
1	
2	
3	
4	
5	

Fig. 8.2 Leaf rolling scores (after O'Toole and Cruz, 1980).

Plant and soil sampling

Plants from four pots per treatment were sampled periodically to determine Leaf Area Index (LAI), and dry matter weight and nitrogen content of stem, leaves, and panicles. For the well-watered plants, seven periodical harvests were carried out; i.e., one, two, and four weeks after transplanting, at mid-tillering, at panicle initiation, at flowering and at maturity. The plants in the other treatments were sampled at the onset of the drought period, at the start of early and late recovery and at final harvest for every treatment. Plant components (i.e. green and dead leaves, stem, roots, panicles and grains) were detached and fresh weight of each component was taken. For samples taken from the

Table 8.1 Duration of drought stress (days) for rice cultivars IR20 and IR72 at different growth stages.

Onset drought	Recovery	Code	IR20	IR72
Transplanting	early	AER	39	39
	late	ALR	42	42
Two weeks after transplanting	early	BER	23	23
	late	BLR	26	26
Mid-tillering	early	CER	13	15
	late	CLR	17	20
Panicle initiation	early	DER	12	14
	late	DLR	14	16
Flowering	early	EER	8	12

droughted pots, leaves were soaked for a few minutes in an acid solution to unfold the leaves. Leaf area was determined using a Delta-T meter. Samples were oven-dried for one week at 80 °C.

Plant height was measured daily during the early stage of growth and weekly at the later stages. Plant height was measured from the ground level to the tip of the tallest leaf, and for mature plants from ground level to the tip of the tallest panicle. Leaf scores were given daily to droughted plants only.

At each sampling for the droughted pots, soil moisture content was determined gravimetrically at three depths within each of the four pots (0 - 5, 5 - 10 and 10 - 15 cm) using 5 cm height and 5 cm diameter cylinders. Using fresh weight and oven-dry weight (48 h at 105 °C) of each sample, volumetric moisture content and bulk density were calculated.

Transpiration rate

The well watered pots were weighed daily to estimate transpiration losses. At the start of a drought treatment, pots were weighed to determine initial weight. Subsequently, all droughted plants were weighed in the early morning on a balance with a resolution of 1 g. Transpiration rate was calculated as the difference in pot weight between successive days.

Sinclair and Ludlow (1986) compared actual transpiration rates of droughted pots with well-watered pots by calculating relative transpiration rates. They defined relative transpiration rate as the ratio between weight loss of droughted pots and weight loss of well-watered pots. However, if drought stress results in a reduced LAI, potential transpiration of the well-watered plants will overestimate the potential transpiration of the droughted plants.

The relative transpiration rate of crops with a different LAI can be estimated by the relative amount of absorbed radiation (Kropff and Spitters, 1992). Therefore, the potential transpiration of the stressed plants was calculated from the transpiration of the well-watered plants by:

$$T_p(D) = T_p(WW) \cdot \frac{1 - e^{-0.4 \cdot LAI(D)}}{1 - e^{-0.4 \cdot LAI(WW)}} \quad (8.1)$$

where

$T_p(D)$ is the potential transpiration rate droughted plant,

$T_p(WW)$ the potential transpiration rate well-watered plant,

$LAI(D)$ the LAI of the droughted plant, and

$LAI(WW)$ the LAI of the well-watered plant.

The factor 0.4 used in Eqn 8.1 is the extinction coefficient for global radiation in rice plants (Kropff, 1993).

Soil moisture ratio

The puddled soil that was used in this experiment shrunk considerably upon water release. Soil-water status was therefore expressed as a ratio of the volume of the solid phase, instead of as a ratio of soil volume. The soil moisture ratio (SMR) was defined as the ratio of the volume of water and the volume of the solid phase:

$$\text{SMR} = (\theta_s \cdot V - W) / (1 - \theta_{\text{sat}}) \cdot V \quad (8.2)$$

where

θ_s is the saturated moisture content ($\text{cm}^3 \text{ cm}^{-3}$),

W the weight loss of the pot (g), and

V the pot volume (cm^3).

The soil moisture ratio of the saturated puddled soil material used in this study was as high as 2.7, because of its large θ_s value (0.73). Soil moisture ratios can be easily converted into volumetric soil moisture contents and/or soil pressure heads, provided the soil shrinkage characteristic of the soil material is known (Bronswijk, 1989). For the soil material used in this study, a soil moisture ratio of 1.5 roughly corresponded to a volumetric soil moisture content of 0.5 or a soil pressure head of -100 kPa , and a soil moisture ratio of 0.5 to a volumetric soil moisture content of 0.25 or a soil pressure head of -1.5 MPa .

Results and discussion

Impact of drought on yield and yield components

Yield data of IR20 and IR72 are summarized in Table 8.2. For IR20, yields of droughted and well-watered plants did not differ significantly if drought was imposed at transplanting or two weeks after transplanting. The same was true for IR72, except if drought was induced two weeks after transplanting with late recovery. Drought at mid-tillering, panicle initiation and flowering strongly reduced yields to below 200 g m^{-2} (Table 8.2).

The low yields obtained if drought was induced at panicle initiation or flowering were caused by a large percentage of unfilled grains. Drought at tillering did not result in an increase in the percentage of unfilled grains compared with the well-watered control plants, but yield reduction was caused by a lower number of panicles and a lower number of grains per hill. The 1000 grain-weight remained fairly constant among treatments, except if drought was induced at panicle initiation (Table 8.3).

Results indicate that in this greenhouse experiment, rice plants were very forgiving for drought stress in the vegetative phase, i.e. if drought was induced before mid-tillering. This may be due to the desynchronized tillering that is typical for rice.

Impact of drought on development rate

Drought in the vegetative phase of the crop postponed flowering and maturity by about two weeks. Drought in the reproductive stage had no effect on development rate.

Table 8.2 Mean grain yield of the nine drought treatments and well-watered control for rice cultivars IR20 and IR72. Data are averages of four replicates. Means followed by a common letter are not significantly different at the 5% confidence level.

Onset of drought	Recovery	Yield IR20 (g m ⁻²)	Yield IR72 (g m ⁻²)
Transplanting	early	744 ^a	830 ^a
	late	686 ^{ab}	793 ^a
Two weeks after transplanting	early	684 ^{ab}	724 ^{ab}
	late	701 ^{ab}	561 ^{bc}
Mid-tillering	early	555 ^{bc}	666 ^{abc}
	late	492 ^c	504 ^c
Panicle initiation	early	255 ^d	223 ^d
	late	148 ^d	91 ^d
Flowering	early	110 ^d	152 ^d
Well-watered	n. a.	827 ^a	723 ^{ab}

Impact of drought on physiological processes

Daily weight losses of droughted and well watered pots were compared for all treatments and for both varieties. Using Eqn 8.1, the potential transpiration rate of the droughted plants was calculated. For reasons of brevity, only the results of one treatment (AER) are given here (Fig. 8.3). The moment pots were covered (indicated with the letter S in Fig. 8.3), droughted and well-watered plants were still of similar size and transpiration rates therefore of similar magnitude. As drought continued, leaf production of the droughted plants stopped, and transpiration rates remained constant, whereas the transpiration rate of the well-watered pots increased rapidly. Only after 15 days, the transpiration rate of the droughted plants started to deviate from the potential transpiration rate calculated using Eqn 8.1. This means that even at low soil moisture contents, droughted plants still transpired at potential rate, i.e. stomata remained open. At 39 days after transplanting, plants were rewatered (R, see Fig. 8.3) and leaf production started soon afterwards. Flowering and maturity of the droughted plants were postponed by about 10 days. Plants that were not recovered showed 100% dead leaves at 50 DAT (D, see Fig. 8.3).

For drought at the remaining four growth stages similar results were obtained, i.e. transpiration rate of droughted plants remained close to the potential transpiration rate even at relatively low soil moisture ratios.

Relationships between leaf morphology and soil moisture ratio

For drought at transplanting, drought two weeks after transplanting, and drought at mid-tillering, leaf expansion stopped when soil moisture ratios dropped below 1.7 (Fig. 8.4a).

Table 8.3 Yield components of the nine drought treatments and the well-watered control for both rice cultivars IR20 and IR72. Data are average of four replicates.

	Number of panicles per hill		Number of filled grains per panicle		Unfilled % of grains per hill		1000 grain weight (g)	
	IR20	IR72	IR20	IR72	IR20	IR72	IR20	IR72
Drought at transplanting								
early recovery	24	24	81	64	16	16	15.5	22.7
late recovery	28	21	64	75	15	20	15.6	20.8
Drought two weeks after transplanting								
early recovery	29	21	65	67	20	19	15.8	20.9
late recovery	27	20	67	55	14	24	15.7	20.9
Drought at mid-tillering								
early recovery	21	31	62	52	9	12	17.2	21.6
late recovery	18	18	67	54	14	18	17.1	21.9
Drought at panicle initiation								
early recovery	30	31	24	17	62	71	14.2	17.0
late recovery	28	26	13	7	76	87	14.8	16.7
Drought at flowering								
early recovery	19	28	21	8	73	89	11.5	22.1
Well-watered control	19	24	114	58	6	19	16.6	21.5

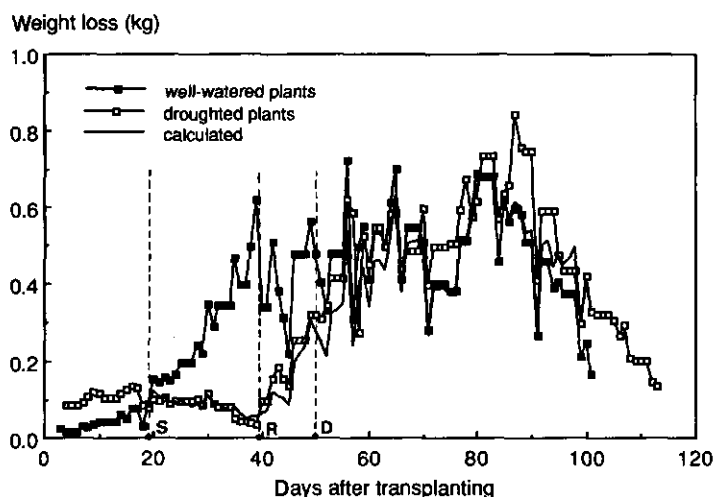


Fig. 8.3 Average daily weight losses (kg) of pots transplanted with IR72 for drought at transplanting (early recovery) and for well-watered plants. S: start of drought R: start of recovery, D: 100% dead leaves (in case of continued drought). The solid line is calculated with Eqn 8.1.

At lower soil moisture contents, leaf rolling started. Increase in leaf rolling score from 1 to 5 occurred within a relatively narrow range of soil moisture ratios. As drought progressed, the percentage of dead leaves increased rapidly as well. Both leaf rolling score and percentage of dead leaves were linearly related with soil moisture ratio.

The response of leaf morphology to drought could be separated into three more or less sequential phases:

- Leaf production stops (vegetative phase only),
- Leaf rolling starts, and
- Leaf senescence starts.

For most treatments, phases 2 and 3 showed some overlap, i.e. dead leaves appeared at leaf rolling scores below 5. Results for drought at transplanting (AER, ALR) and drought at mid-tillering (DER, DLR) are shown in Figs 8.4b and 8.5b (leaf rolling score) and Figs 8.4c and 8.5c (percentage dead leaves).

Relationship between transpiration rate and soil moisture ratio

Graphs of soil moisture ratio and relative transpiration rate (i.e. actual transpiration rate of droughted plants / potential transpiration rate of droughted plants) are shown in Figs 8.4d and 8.5d for drought at transplanting (AER, ALR) and drought at mid-tillering (DER, DLR) respectively. For drought at transplanting and two weeks after transplanting, plants transpired at a potential rate until soil moisture ratios dropped below 1 (Fig. 8.4d). At soil moisture ratios below 1, transpiration rates declined rapidly. Transpiration rates of droughted plants at later growth stages started to deviate from potential rates at soil moisture ratios below 1.2 (Fig. 8.5d). Transpiration rates declined linearly with soil moisture ratio and no major differences between the two varieties were observed.

Impact for modelling of rainfed rice production

The soil-water - drought response relationships presented above may be used in models that predict rice growth and yield in rainfed environments. Both well-tested soil water balance models, like the SAWAH module (ten Berge et al., 1992) and crop simulation models that simulate potential yield under well-watered conditions, like the model ORYZA1 (Kropff et al., 1993a) are available. The relationships obtained in this study may be used to couple both type of models. Soil moisture ratios, obtained via SAWAH, may be translated into changes in leaf morphology and relative transpiration. If such drought responses were used as an input for ORYZA1, predictions of grain yield under water-limited conditions could be made.

Conclusions

The response of two lowland rice cultivars, IR20 and IR72, to temporary drought in a puddled clay soil was studied in a greenhouse experiment. Plant morphology was

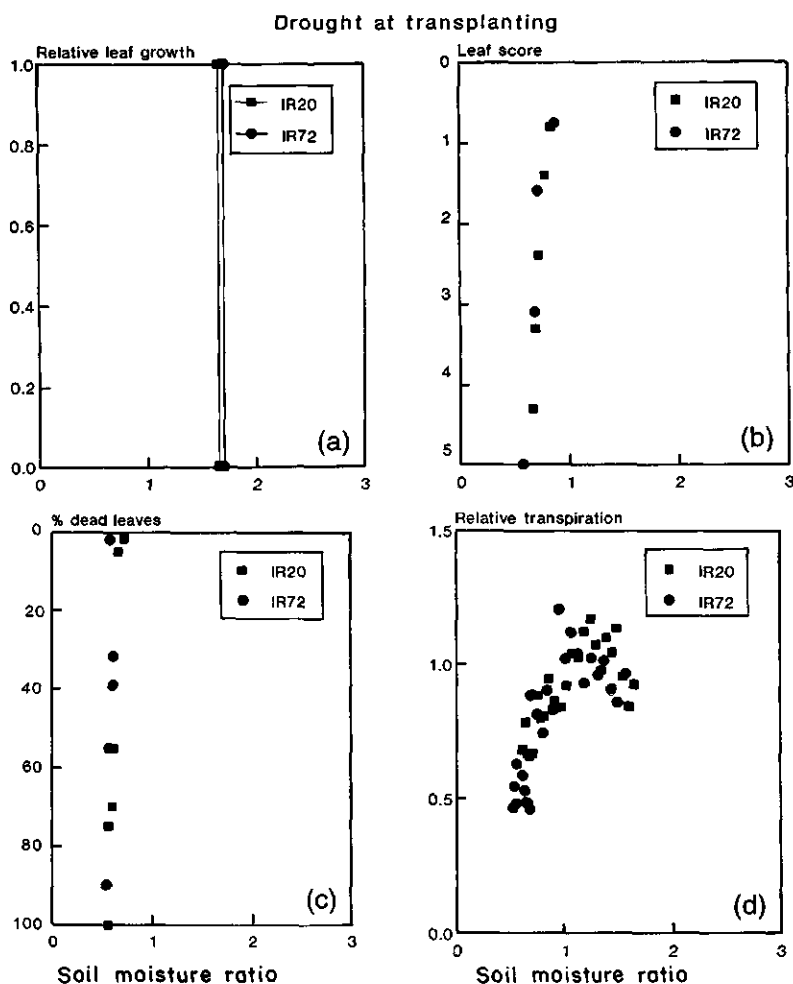


Fig. 8.4 Relationships of soil moisture ratio ($\text{cm}^3 \text{cm}^{-3}$) with (a) relative leaf growth, (b) leaf score, (c) % dead leaves and (d) relative transpiration rate for drought at transplanting for rice cultivars IR20 and IR72.

strongly affected, causing reduced leaf area production, leaf rolling and early leaf senescence. Potential transpiration of droughted plants was derived from the transpiration of well-watered plants after correcting for differences in LAI. The relative transpiration per unit of leaf area remained equal to that of well-watered plants, even if the soil water ratio dropped from 2.7 to 1.2, i.e. by 50%. As soil water content dropped further, a decrease in relative transpiration was observed. The following morphological and physiological responses to soil moisture content were quantified for different growth stages: (1) rate of new leaf production, (2) rate of leaf rolling, (3) rate of senescence, and (4) relative transpiration rate.

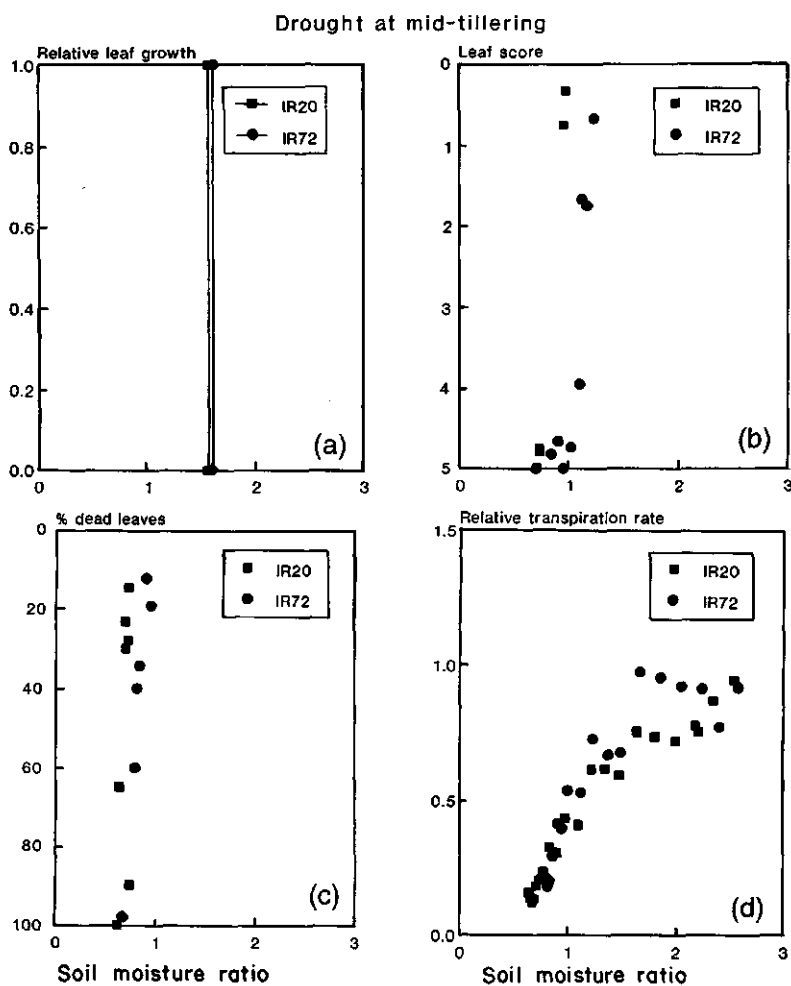


Fig. 8.5 Relationships of soil moisture ratio ($\text{cm}^3 \text{cm}^{-3}$) with (a) relative leaf growth, (b) leaf score, (c) % dead leaves and (d) relative transpiration rate for drought at mid-tillering for rice cultivars IR20 and IR72.

Yield differences between plants that were temporarily stressed in the vegetative phase and well-watered plants were not significant for both IR20 and IR72. However, flowering and maturity were strongly delayed. Drought in the reproductive phase caused large yield reductions.

Chapter 9

Understanding the water use efficiency of flooded rice fields

Abstract The water use efficiency of a flooded puddled rice field was studied through analysis of the components of the water balance in the field and through simulation modelling. Seepage and percolation (SP) losses were the main determinants of water use efficiency in a field experiment conducted in the Philippines. Seepage through and underneath bunds can greatly increase total water loss. SP rates in well-puddled soil varied between 0.4 cm d⁻¹ without seepage to 3.62 cm d⁻¹ with seepage, and cumulative SP losses varied between 88 and 350 cm per crop cycle, respectively.

The vertical profile of puddled rice soil can schematically be described by a layer of ponded water, a muddy layer with little resistance to water flow, a compacted layer with large resistance to water flow, and the non-puddled subsoil. Using this concept, the one-dimensional flow model SAWAH accurately simulated ponded water depth and pressure head gradients within the soil profile for the test field without seepage, using measured soil-hydraulic input data. SAWAH is suitable for in-depth analyses of the water balance of puddled rice fields and for extrapolation of empirical research findings. However, for practical applications in rainfed lowland rice-ecosystems, a simplified way of calculating the soil water balance is preferred, which is introduced in the next chapter.

Introduction

More than 75% of global rice production is harvested in irrigated rice ecosystems which constitute 55% of total harvested rice area. About 25% of total rice acreage is under rainfed lowland cultivation, and produces 17% of global rice production (IRRI, 1993). In rainfed ecosystems, water is the major factor that determines rice production. In irrigated rice ecosystems, the availability of water for agriculture is threatened in many places by increasing urban and industrial demand. In view of projected increases in rice production demands from a growing world population (65% increase from 1992 to 2020; IRRI, 1993), efficient use of water in rice-ecosystems is of crucial importance. Water use efficiency of rice fields can be analyzed by studying the components of the water balance (Fig. 9.1).

In Asia, contributing 90 - 95% of world production (Pathak and Gomez, 1991), rice in irrigated and rainfed lowland environments is mostly grown under flooded conditions. To achieve this, fields are bunded and soils are puddled by plowing at water-saturated conditions, followed by harrowing and levelling. Puddling leads to destruction of soil aggregates and macropore volume, and to a large increase in micropore space (Moor-

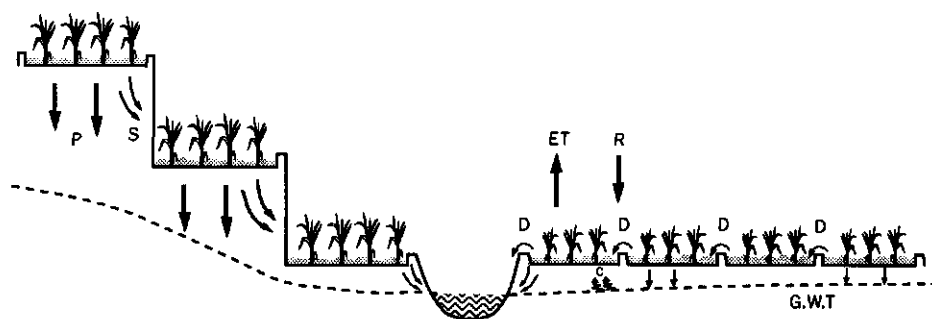


Fig. 9.1 Schematic representation of a toposequence of rice fields; ET = evapotranspiration; R = rainfall; D = runoff; C = capillary rise; P = percolation; S = seepage; GWT = groundwater table.

mann and van Breemen, 1978). Consequently, the hydraulic conductivity and percolation rate are reduced.

The water balance of a puddled rice field is determined by the following components: irrigation supply, rainfall, evaporation, transpiration, runoff, seepage and percolation. Rainfall in excess of bund height leaves the system as surface runoff. This surface runoff can be input in a neighbouring field, but in a sequence of fields, neighbouring fields will pass-on the surface runoff until it is lost in a drain, creek or ditch. Transpiration by the rice crop withdraws water from the puddled layer (which is replenished with ponded water) and from the non-puddled subsoil, if rice roots are growing sufficiently deep.

Percolation is the vertical movement of water beyond the root zone to the water table, while seepage is the lateral movement of subsurface water (IRRI, 1965). In practice, the two are often inseparable (Wickham and Singh, 1978). The amount of seepage is determined by piezometer head differences between fields. The difference in piezometer head is large near drains, ditches or creeks and in terraced rice-fields with considerable difference in elevation. Seepage loss from rice terraces in the middle of a toposequence to lower lying fields may be offset by incoming seepage from higher fields. Top-end terraces will experience net seepage-loss; bottom-end terraces net seepage gain.

The amount of seepage is further affected by the soil-physical characteristics of the field and bunds, the state of maintenance, the relative length of the bunds compared with the surface area of the field, and by the depth of the water table in the field and in the drain, ditch or creek (Wickham and Singh, 1978). The percolation rate of puddled rice fields is affected by a variety of soil factors (Wickham and Singh, 1978): structure, texture, bulk density, mineralogy, organic matter content and concentration of salts in soil solution. In general, a heavy texture, montmorillonitic clay mineralogy, high sodium content of irrigation water and a high bulk density are favorable for effective puddling and low percolation rates. The percolation rate is further influenced by the water regime in and around the field. Increased depths of ponded water increase percolation due to the

larger gradient in hydraulic head imposed (Sanchez, 1973; Ferguson, 1970; Wickham and Singh, 1978). In a field survey in the Philippines, Kampen (1970) found, for the same reason, that percolation rates were larger in fields with deep water tables (> 2 m depth) than in fields with shallow water tables (0.5 - 2 m).

Though water loss and water-use efficiency of puddled rice fields have been extensively monitored, most studies so far have been empirical by nature. In this study, water-use efficiency of puddled rice fields was related to soil hydraulic properties through simulation modelling. The one-dimensional soil water balance model SAWAH (Simulation Algorithm for Water flow in Aquic Habitats, ten Berge et al., 1992) was used to explore the dynamics of the water balance of puddled soil. SAWAH was validated using data from a field experiment conducted in the Philippines. The application of a one-dimensional flow model to simulate the water balance on a field scale is discussed. Overall conclusions are drawn on the water-use efficiency of puddled rice fields based on analyses with SAWAH and the result of the field experiment.

Materials and methods

The soil water balance model SAWAH

The one-dimensional soil water flow model SAWAH solves the general flow equation numerically under given boundary conditions. The model requires knowledge of the soil water retention curve, which relates the volumetric water content (θ) to soil water pressure head (h), and the hydraulic conductivity curve, which relates the hydraulic conductivity (k) to water content or pressure head. Soil hydraulic properties have to be specified for all identified soil layers in the profile up to a maximum of 10. External boundary conditions (irrigation, rainfall, evaporation, transpiration, water table depth) need to be specified daily. Because the water table is a boundary condition, capillary rise and percolating soil water do not affect its depth (complete lateral recharge and discharge). Runoff occurs when ponded water depth is higher than bund height.

SAWAH can accurately simulate the soil water balance of rainfed, non-puddled rice fields (Chapter 5). In Chapter 2 it was shown that a typical puddled topsoil consists of a 'muddy' layer of low density in the top that gradually changes into a relatively compacted poorly permeable layer at the bottom (Fig. 9.2). The top of the puddled layer contains normally only about 20 - 30% soil particles by volume. Bulk density increases gradually with depth. The virtually hydrostatic pressure head profile found in these muddy topsoils, even under steady state percolation (Chapter 2), indicate that either the resistance of this layer is negligible, or that the solid soil particles form no rigid soil matrix. The largest resistance is found in the compacted layer at the bottom of the puddled layer. Therefore, in SAWAH, the compacted layer was considered as the top layer of the soil. The pressure head at the top of this layer was the summation of the depth of the muddy layer and the depth of the ponded water layer. Because of the low concentration of soil particles in the muddy layer, its higher mass-density with respect to water was neglected.

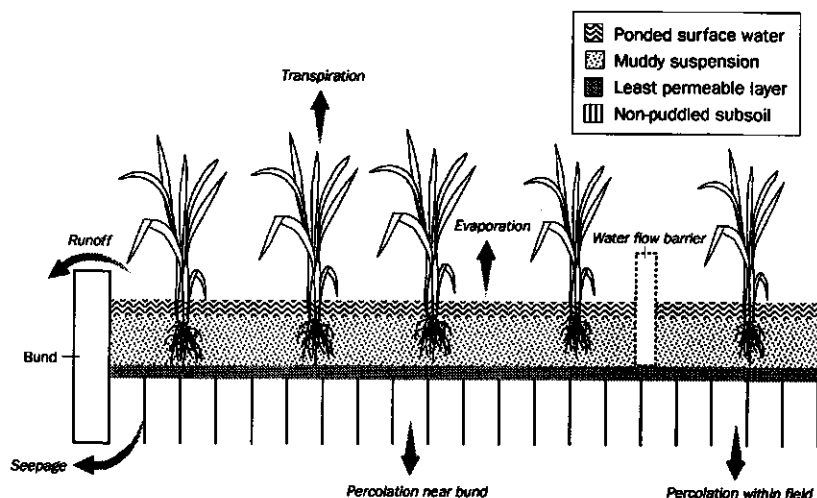


Fig. 9.2 Lay-out field experiment, and functional soil layers used in SAWAH. The 'muddy suspension' gradually increases in bulk density with depth but is treated as a uniform layer in SAWAH.

Field experiment

The experiment was conducted in the dry season of 1991 on a 30 m x 15 m experimental field not previously used for rice, at the International Rice Research Institute, Philippines (14°30' N, 121°15' E). The soil was classified as a mixed, isohyperthermic Typic Tropudalf (Soil Survey Staff, 1975). At the start of land preparation, the field was submerged for 15 days, then plowed two times and harrowed four times with a water-buffalo. Throughout the experiment the fields remained submerged. The soil horizon just below the puddled layer contained 49% clay, 37% silt and 14% sand (hydraulic-functional horizon 2, in Chapter 4).

Rice cultivar IR64 was transplanted on 2 February 1991, at a planting density of 20 x 20 cm. Measurements of the water balance components started 6 days after transplanting (6 DAT). On 18 February (16 DAT) a plastic sheet was installed at one meter from the bund, reaching down to the bottom of the puddled zone to reduce water losses near the bunds (Fig. 9.2). A hand weeding was carried out half-way the growing season, on 16 March (42 DAT). On 13 April (70 DAT), the field was divided into two subplots by placing a plastic sheet in the middle of the field. One plot remained submerged, while the other was left to dry out.

Measurements

Ponded water depth was measured daily and before and after each irrigation, using sloping gauges (Wickham and Singh, 1978). Water table depth was measured daily using piezometers. Percolation rate was determined using double ring infiltrometers

(FAO, 1979). Twelve sets in the area within the plastic sheets, and six sets between the sheets and the bunds were monitored daily.

Irrigation supply was controlled through a calibrated pump. Rainfall and evaporation (class A pan) were measured daily at a meteorological station within 200 m distance of the experimental field.

Crop evapotranspiration was measured from pots with plants placed in the field. Twenty pots (20 cm diameter, 25 cm height) were distributed regularly over the field in pairs of two: one pot with plant, one pot without plant. Each pot was weighed almost daily, between 7 and 8 a.m. in the morning. Losses due to evaporation (pots without plant) and evapotranspiration (pots with plant) were calculated as the difference in pot weight between successive days. Pots were kept well-watered throughout the experiment. To ensure minimal disturbance to the rice plants, the pots were filled as follows: a metal cylinder (32 cm diameter; 45 cm height) was pushed in the puddled soil to a depth of approximately 40 cm. A smaller cylinder (20 cm diameter; 25 cm height) was placed in the center of this cylinder, and pushed downward to 5 cm below the upper rim. Soil material between inner and outer cylinder was removed. The inner cylinder, containing one hill or bare soil only, was taken out and the bottom was closed. These pots were re-installed in plastic bags (to prevent possible leakage) in the outer cylinders in the field. Evapotranspiration and evaporation rates were calculated from the weight losses of the pots with and without plant respectively. Weighing of the pots started on 8 March 1991 (34 DAT).

Hydraulic conductivities were measured of both the compacted layer in the puddled soil and of the underlying subsoil. For the compacted layer, in-situ saturated hydraulic conductivities were measured at 12 sites distributed regularly over the field, using the method presented in Chapter 2.

The saturated hydraulic conductivity of the subsoil horizon was measured for one site within the field, using the column method (Bouma, 1982), and the unsaturated conductivity for soil water pressures h between 0 and -2 kPa, using the crust method (Booltink et al., 1991). Sample cylinders were 0.25 m high and 0.20 m in diameter. The data were compared with measurements conducted for the same soil horizon within a 50 ha area surrounding the test field (Chapter 4). All conductivity data were parameterized using the equation:

$$k(h) = k_s |h|^p \quad (9.1)$$

where

k_s is the saturated hydraulic conductivity (cm d^{-1}),

h the pressure head (cm), and

p a soil-specific dimensionless constant.

Samples for measurement of water retention of the subsoil were taken at the same measurement site as used for measurement of hydraulic conductivity. Water retention

data were determined as a function of soil water pressure h , using the hanging water column method (Richards, 1965) for $-15 \text{ kPa} < h < 0 \text{ kPa}$ (300 cm^3 samples), and the evaporation method for $-80 \text{ kPa} < h < -15 \text{ kPa}$ (Bouma et al., 1983). For the evaporation method, pressure potentials were periodically measured in the soil samples, previously used for both column and crust method, while at the same time subsamples were taken to determine water contents. The data were compared with measurements conducted for the same soil horizon within a 50 ha area surrounding the test field (Chapter 4).

All water retention data were parameterized using the following equation presented by van Genuchten (1980):

$$\theta = \theta_r + (\theta_s - \theta_r) / (1 + |\alpha h|^n)^m \quad (\text{with } m = 1 - 1/n) \quad (9.2)$$

where θ_r and θ_s are the residual and saturated water contents (cm^3 water cm^{-3} soil) respectively, and α (cm^{-1}) and n (-) and m (-) are soil-specific shape factors.

Simulations

SAWAH was used to simulate the depth of ponded water and pressure head gradients within the profile as dynamic variables. The measured daily values for rainfall, irrigation supply and evapotranspiration were used as driving variables, and the measured water table depths served as boundary conditions. The measured hydraulic conductivity and water retention curves were input data. Simulated values of ponded water depth and pressure head were compared with observed values.

Results and discussion

Measurements

The field experiment was divided into four stages. Stage I was the period after transplanting and before plastic sheets were installed to stop seepage near the bunds of the field. Stage II occurred between the installment of the sheets and the disturbance of the soil by weeding. Stage III was after the disturbance of the soil, and stage IV started after the field had been divided by a plastic sheet into two subplots at the end of the season (the test plot still being irrigated, the other plot drying out).

Percolation rates were determined from the double-rings within the field, and for the area near the bunds (Table 9.1). For each stage, the combined field-average seepage and percolation rate (SP) was derived from sloping-gauge readings at the beginning of the stage (Table 9.1). The percolation rate within the field (P') was comparable with the percolation rate measured near the bunds (P'') during stage I, indicating that the puddling of the soil was as effective in the middle of the field as close to the bunds (Table 9.1). During stage II, the average percolation rate determined from the double-rings was of similar magnitude as the field-average percolation rate determined from the sloping-gauge

Table 9.1 Measured field-average seepage and percolation (SP), percolation (P' within field; P'' near bund), and saturated hydraulic conductivity of the compacted layer (k_s) for the four stages distinguished in the field experiment. All values are in cm d^{-1} .

Stage	SP	P'	P''	k_s^*
I	3.62	0.41	0.46	0.082 (0.030, 0.122)
II	0.40	0.43	0.53	0.082 (0.030, 0.122)
III	1.46	-	-	-
IV	3.26	-	-	-

*Values between brackets are minimum and maximum values.

readings. Between stage II and III, the compacted layer in the puddled topsoil was disturbed by hand-weeding, and measured field-average SP rates nearly tripled. The difference in field-average SP rates between stages I and II, and between stages III and IV illustrate the large effect of seepage on total water loss. In stage II the blocking of seepage through and underneath the bunds reduced the SP rate 10-fold. The drying of the neighbouring plot in stage IV induced seepage from the test plot underneath the plastic barrier through the (permeable) subsoil, thus increasing the field-average SP rate 2.2-fold. In stage I, the ratio of bund length over surface area was 0.20, and in stage IV, the ratio of plastic barrier over surface area was 0.07.

Evaporation measured with the class A pan (E_{pan}), and evaporation (E) and evapotranspiration (ET), derived from the pots are plotted in Fig. 9.3. E derived from the pots without plant became gradually lower than E_{pan} , due to shading effects of the growing rice plants surrounding the pots. ET was consistently higher than E_{pan} . Because ET measurements started 34 DAT and continued 25 days, this holds for a closed canopy situation. The following equation related ET to E_{pan} :

$$ET = 1.44 E_{\text{pan}}, \quad r^2 = 0.56 \quad (9.4)$$

Total water consumption from the beginning of stage I to the end of stage IV is presented in Table 9.2. Calculations were also made of water losses for the hypothetical situations where the four different stages would have lasted for the whole duration of the experiment. The values in Table 9.2 correspond well with the ranges found in experimental field studies in the Philippines by Tabal et al. (1992). They measured irrigation needs, rainfall and drainage and estimated evaporation and transpiration to derive water losses over a cropping season for a large number of rice fields. Water requirements ranged from 1000 to 4000 mm per rice crop.

The saturated hydraulic conductivity of the compacted layer varied between 0.03 and 0.12 cm d^{-1} (Table 9.1). Water retention and hydraulic conductivity data of the non-

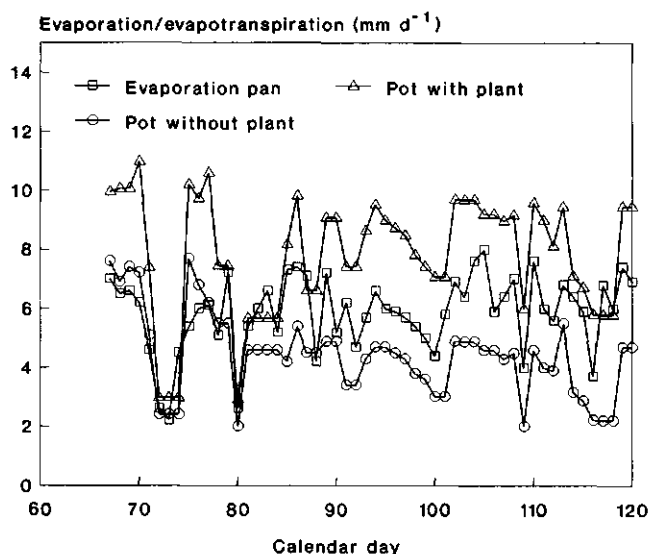


Fig. 9.3 ET (pot with plant), E (pot without plant) and E_{pan} measured in the field experiment (see text).

Table 9.2 Measured cumulative water use for the field experiment, and calculated values for four hypothetical situations based on SP rates of the four individual stages (see text). ET_{cum} is the cumulative evapotranspiration, SP_{cum} the cumulative seepage and percolation, and SUM the cumulative water use for one crop cycle.

	ET_{cum} (cm)	SP_{cum} (cm)	SUM (cm)
Measured	55.5	74.9	130.4
Calculated			
- Situation 1	55.5	296.8	352.3
- Situation 2	55.5	32.8	88.3
- Situation 3	55.5	119.7	175.2
- Situation 4	55.5	267.3	322.8

puddled subsoil determined for one site within the field fell within the range of extremes reported in Chapter 4 for the same soil horizon (Table 9.3).

Simulations

Ponded water depth was simulated using the measured hydraulic properties of puddled top- and non-puddled subsoil as input parameters. For k_s of the compacted layer, the

Table 9.3 Fitted parameter values k_s and p of the hydraulic conductivity curve (Eqn 9.1); and θ_r , θ_s , α and n determined for the water retention curve (Eqn 9.2) of the subsoil horizon. Average, upper and lower extreme values are taken from Chapter 4.

	k_s (m d ⁻¹)	p (-)	θ_r (m ³ m ⁻³)	θ_s (m ³ m ⁻³)	α (cm ⁻¹)	n (-)
On-site	0.60	-2.41	0.01	0.56	0.0554	1.1121
Upper extreme	4.82	-2.49	0.01	0.58	0.1099	1.0623
Average	0.77	-2.32	0.01	0.55	0.0468	1.0954
Lower extreme	0.08	-2.00	0.01	0.52	0.0152	1.1429

average value and the lowest and highest values were used (Table 9.1). For the hydraulic conductivity and water retention data of the subsoil, average, lower and upper extremes reported in Chapter 4 were used (Table 9.3).

Simulated and observed pressure head distributions in the puddled layer of the profile are shown in Fig. 9.4. Simulations agree well with observed data. The shape of the curve is similar to observations made by Iwata et al. (1988), Adachi (1990), Tabuchi et al. (1990) and observations reported in Chapter 2.

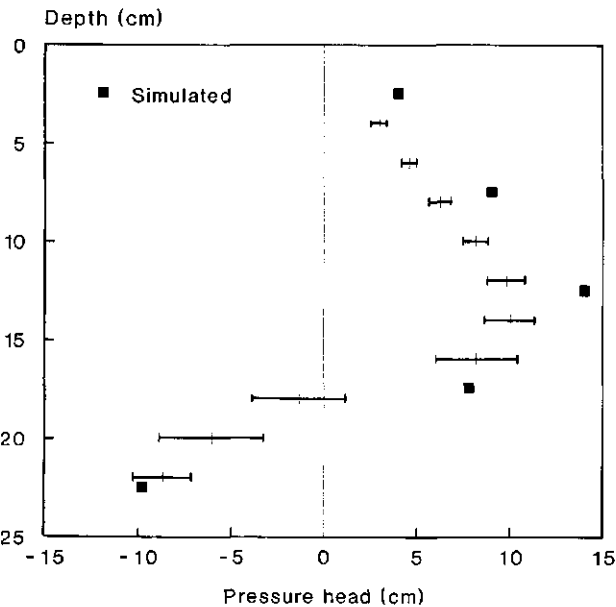


Fig. 9.4 Measured and simulated pressure head distribution in the field experiment. The bars represent the standard errors of the means.

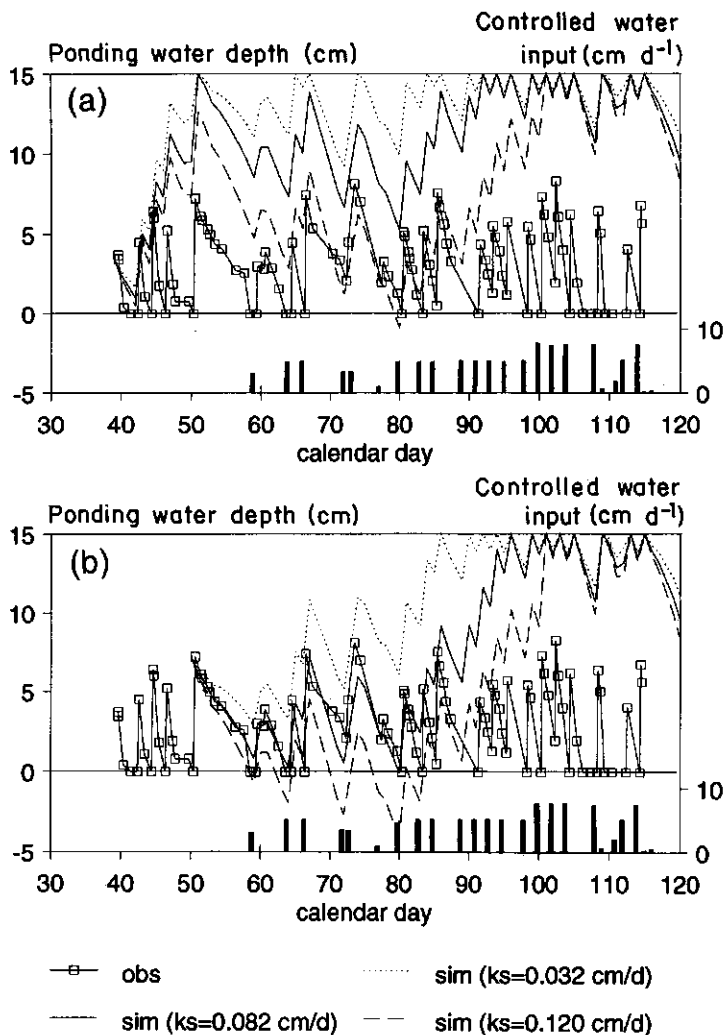


Fig. 9.5 Observed and simulated ponded water depths in the field experiment. (a) Start of simulation is first day of experiment. (b) Start of simulation is first day of stage II (see text).

Simulated values of ponded water depth were very much affected by the differences in k_s of the compacted layer, whereas the variation in measured hydraulic properties of the subsoil had no effect. When simulation was started at the beginning of stage I, water losses were underestimated and simulated ponded water depth were much higher than observed (Fig. 9.5a). This was caused by the fact that SAWAH is a one-dimensional flow model that does not account for seepage. When simulation was started in stage II, simulated ponded water depths using the average k_s of the compacted layer were in good agreement with observed values during that stage (Fig. 9.5b). With the damaging of the compacted layer in stage III, however, the effective, field-average k_s of this layer

increased and water losses were again underestimated.

Conclusions

Water-use efficiency of puddled rice fields is determined by seepage and percolation (SP) losses. Seepage through and underneath bunds can have a dramatic impact on total SP losses. In our field experiment, SP in a well-puddled soil varied from 0.4 cm d⁻¹ without seepage to 3.62 cm d⁻¹ with seepage through and underneath all four bunds (bund length/surface area ratio of 0.20). Extended over a complete growing season, cumulative SP losses varied between 88 and 350 cm, compared to 55 cm cumulative evapotranspiration. These values agree well with observations in the Philippines by Tabal et al. (1992). Proper maintenance of bunds may greatly improve water-use efficiency, especially if a rice field is next to a drain or a creek, or if neighbouring fields are not flooded.

The vertical profile of puddled rice soil can schematically be described by a layer of ponded water, a muddy layer with no resistance to water flow, a compacted layer with large resistance to water flow, and the non-puddled subsoil. Using this concept, the one-dimensional flow model SAWAH accurately simulated the water balance of a test field without seepage using measured input data for the hydraulic properties of the compacted layer and the underlying subsoil. In this experiment, water loss by percolation was determined by the saturated conductivity of the compacted layer. It was not affected by the hydraulic characteristics of the (permeable) subsoil.

Because of its high degree of detail, SAWAH is very suitable for in-depth analyses of the water balance of puddled rice fields. Using SAWAH for regional simulation studies may be less attractive as it will be often difficult to fulfill the data needs of the model. In Chapter 10, a simpler way of calculating the soil water balance of flooded rice fields is introduced.

Chapter 10

Modelling the soil-plant water balance of rainfed lowland rice

Abstract A soil-water balance module (PADDY) and a module predicting the response of rice to drought (DSTRESS) were developed and coupled to a crop growth simulation model (ORYZA1) to simulate rice growth and production in rainfed lowland rice ecosystems. PADDY predicts changes in ponded water depth and root zone water content and accounts for root zone volume changes due to soil shrinkage. DSTRESS uses linear functions to describe the following physiological and morphological responses of the rice crop to drought: (1) rate of new leaf production, (2) rate of senescence, (3) rate of leaf rolling, and (4) relative transpiration rate. ORYZA1 is a well documented and validated general crop simulation model parameterized for rice.

The combined PADDY-DSTRESS-ORYZA1 model was validated using two field experiments in the Philippines. Measured and simulated changes in ponded water depth under flooded soil conditions were in good agreement. In one of the field experiments, temporary drought was induced at different growth stages. The model satisfactorily predicted changes in root zone water content, leaf area index, total above ground dry matter and panicle dry weight across drought treatments over time.

Introduction

In Asia, rainfed and irrigated rice soils are mostly puddled prior to direct-seeding practices or transplanting of rice seedlings. Puddling usually comprises one or two plowings, one or two harrowings and a final levelling under water-logged soil conditions. After harvesting of the rice crop, sometimes an upland crop is grown, profiting from residual soil water and sometimes capillary rise from a groundwater table. Puddling reduces percolation rate, hampers weed growth and provides a soft medium for roots. In rainfed ecosystems, drying will cause a puddled soil to transfer from a muddy layer to a compact soil, a process that can be called 'ripening'.

Because of the variability and the complexity of rainfed lowland rice ecosystems, process based simulation models can be used as a tool for quantitative understanding of the system and for prediction of rice growth and production. Such models enable e.g. detailed analysis of experimental data, or extrapolation of research findings to other environments.

Kropff et al. (1993a) recently introduced ORYZA1, an improved model for irrigated rice production. The model was validated with a large number of field experiments, and yields can be predicted accurately for a range of environments. To use the model

ORYZA1 in rainfed rice environments, the model needs to be coupled to a soil-water balance module via an 'interface' that translates the soil-water status into a crop response.

This chapter presents a new soil-water balance module (PADDY), especially developed for rainfed rice soils and upland crops after rice, and a 'drought stress module' (DSTRESS) that acts as an interface between PADDY and ORYZA1. Both modules are written in FORTRAN and make use of the Fortran Simulation Environment (FSE, van Kraalingen, 1991). The ORYZA1-DSTRESS-PADDY simulation model was validated using two experiments conducted in the Philippines in 1991 and 1992.

Materials and methods

The crop simulation model ORYZA1 is documented elsewhere (Kropff et al., 1993a). Only the main characteristics of the model are given here.

Light and temperature are the main factors determining the crop growth rate in ORYZA1. Using the measured or simulated Leaf Area Index (LAI) and the vertical distribution of leaf area, the light profile in the canopy is calculated. Based on single leaf photosynthesis, the photosynthesis profile in the full canopy is obtained. The daily assimilation rate is obtained by integrating over the height of the canopy and over the day. Subtracting respiration requirements and losses due to the conversion of carbohydrates into structural dry matter, gives the net daily growth rate in $\text{kg ha}^{-1} \text{d}^{-1}$. The dry matter produced is partitioned among the various plant organs based on a partitioning coefficient that depends on the stage of phenological development.

In the model, phenological development rate is a function of ambient mean daily air temperature. If the canopy is not yet closed, leaf area development is calculated from mean daily temperature. When the canopy closes, the increase in leaf area is obtained from the increase in leaf weight. Time step of integration is one day. Input requirements for the crop simulation model are:

- Geographical latitude,
- Daily data on solar radiation and minimum and maximum temperature,
- Plant density,
- Date of crop emergence or transplanting, and
- Parameters that describe the morphological and physiological characteristics of the crop species.

Morphological characteristics are leaf area development and the light extinction coefficient. Physiological characteristics include the assimilation-light response curve parameters, dry matter partitioning functions, maintenance respiration coefficients, and growth respiration coefficients.

In water-limited environments, water availability, light and temperature are determining the crop growth rate (provided no nutrient limitations occur). In Chapter 8, functions were derived that can be used to describe a number of physiological and morphological

responses of the rice crop to soil-water content of the root zone. These functions were incorporated in the module DSTRESS. The module PADDY was developed to predict the soil-water status of a puddled root zone. Both modules are described in more detail below. The linkage between ORYZA1, PADDY and DSTRESS is shown in Fig. 10.1.

Description of PADDY

A puddled rice soil profile consists of a muddy layer with little resistance to water flow, a compacted layer with large resistance to water flow and the non-puddled subsoil (Chapter 9). The muddy layer gradually increases in bulk density with depth but is treated here as a uniform layer. In PADDY, it is assumed that the first two layers of the soil profile comprise the muddy and compacted layers, respectively. Maximum number of soil layers is 10. Time step of integration in PADDY is one day.

The soil water balance of a rice crop in puddled soil with standing water, without seepage, can be summarized as:

$$dW_p = I + R + C - E - P - T - D \quad (10.1)$$

where

dW_p is the change in ponded water depth (mm d^{-1}),

I irrigation supply (mm d^{-1}),

R rainfall (mm d^{-1}),

C capillary rise (mm d^{-1}),

E evaporation (mm d^{-1}),

T transpiration (mm d^{-1}),

P percolation (mm d^{-1}), and

D bund overflow / surface runoff (mm d^{-1}).

If there is ponded water on the soil surface, it is assumed that water requirements for transpiration and evaporation result in a reduction of the ponded water level.

In PADDY, percolation rate can be either assumed to be constant or can be calculated. In Chapters 2 and 9, it was shown that the percolation rate through a puddled soil is affected by both the characteristics of the non-puddled subsoil, through its hydraulic conductivity curve, and by the physical properties (i.e. hydraulic resistance) of the least permeable layer in the puddled topsoil. Using an iterative Newton-Raphson procedure (Wolfram, 1991) fluxes through this least permeable layer, and non-puddled subsoil are calculated and compared until the difference between both fluxes become negligible. The procedure is illustrated in Fig. 10.2. PADDY starts with taking a random value for the pressure head h in the non-puddled subsoil (1). The difference between the flux through the puddled topsoil (f_t) and the non-puddled subsoil (f_s) at that pressure head is then calculated (2). If this difference is too large, the intersection of the tangent line with the x -axis is calculated, which yields a new value for h (3). A new difference between fluxes f_t and f_s is calculated (4) etc. The calculations continue until the difference between f_t and f_s becomes close to zero.

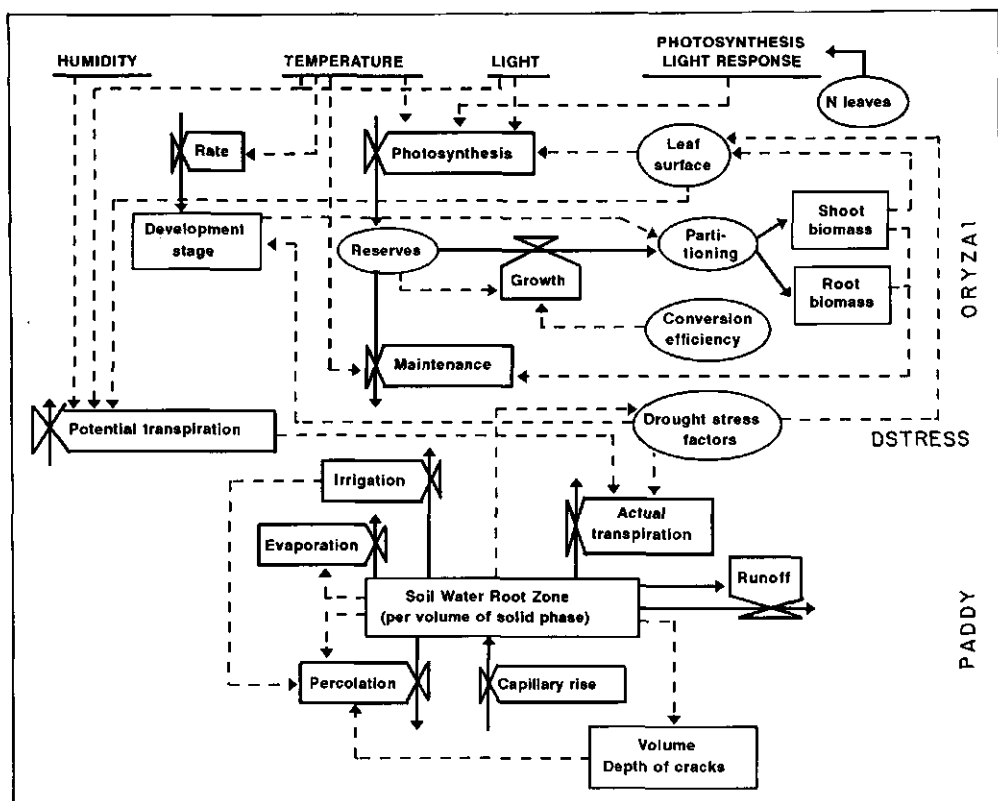


Fig. 10.1 Linkage between the modules ORYZA1, PADDY and DSTRESS.

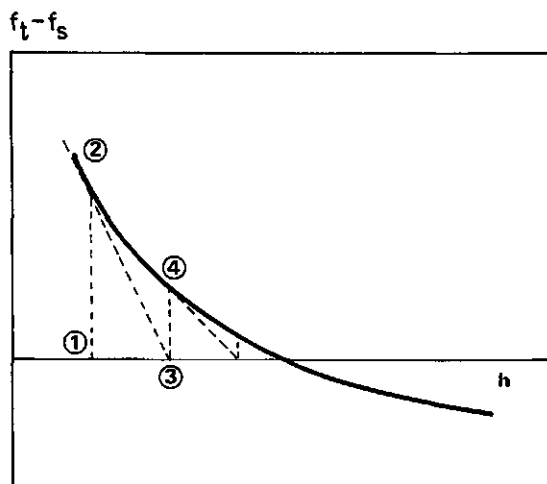


Fig. 10.2 Iterative procedure used in the soil-water balance module PADDY to calculate percolation rates for a puddled soil by minimizing the difference between the fluxes through the puddled topsoil (f_t) and non-puddled subsoil (f_s).

It is assumed in the model that the percolation rate is zero if there is no standing water. After calculation of the percolation rate, the change in ponded water depth is recalculated. The amount of water in excess of bund height is lost from the soil profile as runoff. The soil water balance of a puddled soil without standing water can be summarized as:

$$dW_R = I + R + C - T_a - E \quad (10.2)$$

where

dW_R is the daily change in soil water content of the root zone (mm d^{-1}),

I irrigation (mm d^{-1}),

R rainfall (mm d^{-1}),

C capillary rise (mm d^{-1}),

T_a actual transpiration by the vegetation (mm d^{-1}), and

E soil evaporation (mm d^{-1}).

In PADDY, capillary rise from the water table to a soil compartment occurs if its water content is below field capacity. Capillary rise does not contribute to the soil water content of compartments 1 and 2. This means that the rice crop will profit from capillary rise only if roots penetrate deeper than the two top compartments. Capillary rise is calculated using the SUBSOL subroutine from the WOFOST simulation model (van Diepen et al., 1988), which is based on integration of the Darcy equation for steady, upward, vertical flow (Gardner, 1958).

The potential rates of soil and water evaporation and crop transpiration with soil or water background are calculated from the Penman reference evapotranspiration. This reference evapotranspiration is calculated from daily weather data (vapour pressure, temperature wind speed) using a Penman type equation (Penman, 1948).

The actual transpiration rate (T_a) is derived from the potential transpiration rate and a drought stress factor calculated by DSTRESS (Fig. 10.1).

The actual soil evaporation rate is calculated assuming that cumulative evaporation is proportional to the square root of time (Stroosnijder, 1982). The rate on the first day is assumed to be 60% of potential soil evaporation. In reality, puddled clay soils will probably dry out faster because of the rapid appearance of shrinkage cracks. Fujioka and Sato (1986) reported that cracks increased the evaporation surface more than twice in a puddled clay soil.

Continued drying of a puddled clay soil results in the formation of soil shrinkage cracks and subsidence of the soil surface. To simulate cracking of the puddled root zone, knowledge of the soil's shrinkage characteristic is needed (Bronswijk, 1988a). An example of a soil shrinkage characteristic is shown in Fig. 10.3. The shrinkage characteristic relates soil volume to soil water content and is often expressed as the relation between moisture ratio and void ratio of soil aggregates.

The moisture ratio v is defined as the volume of water V_w over the volume of the

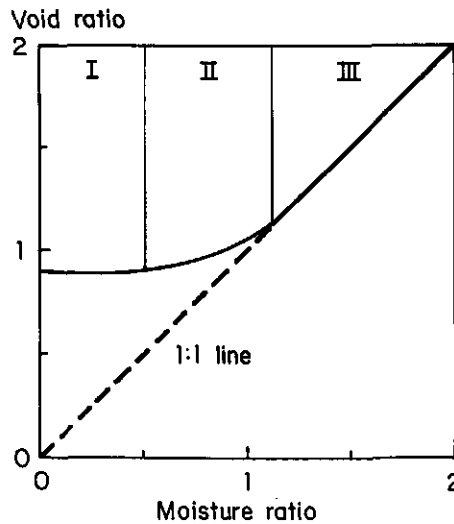


Fig. 10.3 Soil shrinkage characteristics: (I) zero-shrinkage phase, (II) residual shrinkage phase, (III) normal shrinkage phase (after: Bronswijk and Evers-Vermeer, 1990).

solid phase V_s (Bronswijk, 1988a):

$$v = V_w / V_s \quad (10.3)$$

The void ratio e is defined as the volume of pores V_p over the volume of the solid phase (Bronswijk, 1988a):

$$e = V_p / V_s \quad (10.4)$$

The sum of V_p and V_s is equal to the volume of the soil matrix.

The shrinkage characteristic includes three phases (Bronswijk, 1988a; Ishiguro, 1992):

- Normal shrinkage: volume decrease of soil aggregates is equal to water loss;
- Residual shrinkage: volume of soil aggregates decreases upon drying, but water loss is greater than volume decrease (air enters soil); and
- Zero shrinkage: volume of soil aggregates remains constant upon drying.

The shrinkage characteristic is used in PADDY to calculate the volume of pores per volume of soil (ε , $\text{m}^3 \text{m}^{-3}$) and the volume of water per volume of soil (θ , $\text{m}^3 \text{m}^{-3}$):

$$\varepsilon = e / (1 + e) \quad (10.5)$$

$$\theta = v / (1 + e) \quad (10.6)$$

The relation between soil volume and void ratio of soil aggregates is:

$$V = V_s (1 + e) \quad (10.7)$$

where

V is the volume of soil aggregates (m^3), and

V_s the volume of solid phase (m^3).

If there is no ponded water, the soil moisture ratio of the root zone is calculated. Using the shrinkage characteristic, the void ratio is derived (Eqn 10.4). Total porosity and volumetric water content are then calculated with Eqns 10.5 and 10.6, respectively. The volume change of soil aggregates occurs as subsidence and cracking. A dimensionless geometry factor determines the partitioning of total volume change over change in layer thickness and change in crack volume. It can be shown (Bronswijk, 1988a) that:

$$dZ = Z_1 - (V_2 / V_1)^{1/rs} Z_1 \quad (10.8)$$

and

$$dCR = (V_1 - V_2) - Z_1^2 (Z_1 - Z_2) \quad (10.9)$$

where

dZ is the change in layer thickness (m),

dCR change in crack volume (m^3),

V_1, V_2 volume of soil matrix before and after shrinkage (m^3),

Z_1, Z_2 layer thickness before and after shrinkage (m), and

rs the geometry factor (set to 3).

It is assumed that shrinkage is irreversible (ripening). This means that the porosity can only decline upon drying and will not increase if the water content of the root zone increases. Field experiments conducted at International Rice Research Institute (IRRI) showed that cracks penetrated through the compacted layer if the pressure head in the topsoil dropped below -100 kPa (IRRI, 1992). In PADDY, cracks are assumed to have penetrated through the compacted layer if its simulated moisture ratio drops below 1.2, which for IRRI soils is equivalent to a soil pressure head of -100 kPa.

If the soil cracks have not yet reached the compacted layer it is assumed that all incoming water is used to replenish the first soil compartment but that cracks will not close. During this phase the percolation rate is zero. As soon as the water content of the top compartment has reached saturation, water starts ponding again and the percolation rate will increase. The amount of water that can be stored in the top compartment is calculated taking into account the changes in volume and porosity of the top compartment due to cracking. If cracks are deep enough to reach the compacted layer (i.e. soil pressure head < -100 kPa), all water in excess of field capacity will be drained from the

top compartment. For the cracked topsoil, field capacity water content is defined as 95% of total porosity. For the non-puddled subsoil, field capacity is defined as the water content for which the soil pressure head equals -10 kPa. Water that drains from the cracked root zone will fill up soil layers below the root zone up to field capacity. Any excess water will be drained at a maximum rate equal to the saturated hydraulic conductivity of the subsoil horizon. The water content of soil compartments below the groundwater table depth is reset to saturation.

Description of DSTRESS

The module DSTRESS is the link between the rice growth simulation model ORYZA1 and PADDY. Input for DSTRESS is the soil water content of the root zone, predicted by PADDY. In DSTRESS, rooting depth at transplanting is set to 0.05 m, and increases to 0.2 m with a constant growth rate of 0.02 m d^{-1} , if the rice crop reaches the mid-tillering growth stage.

The water content predicted by PADDY is calibrated between the saturated moisture content of the ripened, previously puddled soil and the moisture content at pressure head $h = -1.5$ MPa. This relative water content is translated by DSTRESS into the following physiological and morphological crop responses to drought stress (Chapter 8):

- Inhibition of new leaf production,
- Leaf rolling,
- Senescence,
- Decrease in relative transpiration, and
- Decrease in development rate in the vegetative stage.

These responses were defined as linear functions of soil water content of the root zone. This concept is illustrated in Fig. 10.4. A similar approach was taken by Sinclair (1986) and McCree and Fernandez (1989).

The first response of the rice crop to drought is an inhibition of new leaf production. In DSTRESS, it is assumed that if drought continues, roots will grow deeper with a constant 'exploration rate' of 0.02 m d^{-1} to a maximum of 0.4 m. If drought occurs in the vegetative stage, the development rate will be affected as well, i.e. the development rate will be slowed down and flowering and maturity will be postponed. In DSTRESS this is represented as a relation between the stress level and a multiplication factor for the development rate. This multiplication factor increases from 0 to 1 between transplanting and flowering. This means that the closer the development stage to flowering, the smaller the postponement effect.

If the soil moisture content of the root zone drops further, leaves will start to roll. The extent of leaf rolling scale is expressed on a 1 to 5 scale (O'Toole and Cruz, 1980). Maximum leaf rolling (leaf score 5) decreases the leaf area index of the rice crop by 50%. Continued drought will result in senescence of leaves. The simulation stops if all leaves have died. Stomatal closure will occur at relatively low soil moisture contents in the vegetative phase, and at higher soil moisture contents in the reproductive phase.

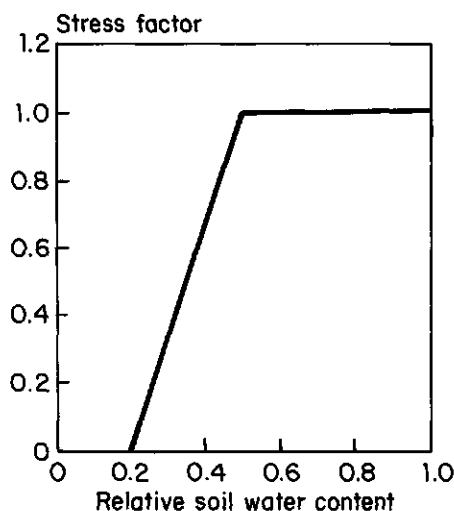


Fig. 10.4 Relationship between relative root zone water content and drought stress factors (see text).

DSTRESS calculates the actual transpiration rate from the soil water content of the root zone and the potential transpiration rate.

The relationships between stress factors and root zone water content were obtained from a greenhouse study presented in Chapter 8. In that study it was concluded that new leaf production was more strongly inhibited than relative transpiration per unit leaf area during drought periods. This means that CO_2 assimilation continues, but the C produced cannot be used for leaf production. In DSTRESS, excess C is stored in a pool and released for leaf production as soon as drought stress is released.

Field experiments

The field experiments were conducted at the International Rice Research Institute (IRRI), Los Baños, Philippines ($14^{\circ}30' \text{ N}$, $121^{\circ}15' \text{ E}$). The soil was classified as a mixed, isohyperthermic Typic Tropudalf (Soil Survey Staff, 1975). Ap and Bt horizons respectively comprised 38%, 44%, 18% and 48%, 39%, 13% of clay, silt, and sand. At the start of land preparation, the fields were submerged for 15 days, then plowed two times and harrowed four times using a water-buffalo.

The first experiment was conducted in the dry season of 1991 on a 30 m x 15 m field, not previously used for rice and is described in detail in Chapter 9.

The second experiment was conducted in the dry season of 1992 on a 2000 m^2 field. An improved semi-dwarf Indica rice cultivar (IR72) was transplanted (15 x 15 cm spacing, 30 day old seedlings) on 26 February 1992. Fertilizer was applied 3 days before transplanting (60 kg N ha^{-1} , 40 kg P ha^{-1} and 40 kg K ha^{-1}) and at major phenological stages: 60 kg N ha^{-1} at mid-tillering and at panicle initiation and another 40 kg N ha^{-1} at flowering.

Four drought treatments in four replications were tested in a randomized complete block design in 10 by 5 m subplots. These subplots were separated by bunds and hydraulically isolated by plastic sheets dug into the soil down to 0.6 m. Prior to the start of the experiment, all plots were submerged for 10 days, then plowed three times and harrowed three times using a water-buffalo.

Drought treatments

Drought was initiated at transplanting (T1), at mid-tillering (T2) at panicle initiation (T3) or during the grain filling stage (T4) by simply draining the ponded water from the plots. Two different durations of drought were imposed:

D1: Plants were recovered early (leaf score 1), and

D2: Plants were recovered late (leaf score 3).

An overview of the treatments is given in Table 10.1. After recovery, plots were kept well-watered throughout the experiment.

Crop, soil and weather measurements

For the well-watered plots plant sampling was done approximately every two weeks. For the droughted plots, this was done at the time of recovery, at flowering and at physiological maturity. For drought at transplanting, one additional sampling was carried out in between the time of recovery and the time of flowering. At each sampling, 12 hills were sampled to determine LAI, dry weight and N content of leaves, stem and panicle. Plants were dried at 70 °C.

Groundwater level was monitored daily, using piezometers. Soil water contents were measured approximately two times a week by core sampling at 0.10 m intervals down to 0.5 m depth.

Weather variables (i.e. rainfall, global radiation, air temperature, humidity, wind speed) were recorded at a meteorological station located within 200 m from the experimental field.

The soil shrinkage curve of the puddled topsoil was determined as follows. Four 0.2 m diameter and 0.2 m height pots were filled with puddled soil material from the experimental field. Three rice seedlings were transplanted in each plot and pots were watered daily until 40 days after transplanting. From that moment onward, pots were covered with a round plastic sheet with an adjustable hole in the centre to allow for optimum growth of the rice plant. This sheet minimized soil and water evaporation losses and drying of the pots was therefore due to water losses via transpiration of the rice plant only. Four tensiometers were installed at 5 cm depth intervals. Tensiometers and decrease in pot weight were monitored approximately four times a day. Volumetric soil moisture contents were determined at several depths within the soil columns using 100 cm³ cylinders, after the air entry value of the tensiometers was exceeded. Soil shrinkage was determined by calculating moisture ratios and void ratios from the volumetric moisture contents assuming a density of the solid phase of 2.5 g cm⁻³.

Table 10.1 Drought-recovery schedule imposed during field experiment 2. Drought at transplanting (T1); drought at mid-tillering (T2); drought at panicle initiation (T3); drought during grain filling stage (T4); well-watered (T0). D1, D2 indicate different durations of drought.

Treatment	Start of drought	Start of recovery	Duration (days)
T1D1	26 February	17 March	21
T1D2	26 February	21 March	25
T2D1	28 March	15 April	19
T2D2	28 March	20 April	24
T3D1	20 April	6 May	16
T3D2	20 April	15 May	25
T4D1	1 May	18 May	18
T4D2	1 May	no recovery	25
T0	n.a.	n.a.	0

Model validation

The soil water balance module PADDY was tested using the data obtained from field experiment 1 (described in detail in Chapter 9). Input variables were rainfall, irrigation, evapotranspiration rates from daily weighing of pots installed in the field and groundwater table depths measured using piezometers. Average and upper and lower extreme values for measured hydraulic properties of the puddled topsoil and the non-puddled subsoil were used (Table 9.3). Simulated and observed changes in ponded water depth were compared.

The ORYZA1-DSTRESS-PADDY model was evaluated using physiological and morphological parameters of IR72, obtained from a dry season experiment conducted at IRRI in 1992 (Kropff et al., 1993a). To evaluate the different components of the model, a series of runs was conducted prior to the final run with all variables simulated. In the first series of runs (Simulation series 1), no water balance was added, and the following measured values were input in the model for every treatment separately, besides transplanting date, and weather data:

- Leaf Area Index (LAI) as a function of time,
- Leaf N concentration as a function of time,
- Specific Leaf Area (SLA) as a function of time,
- Development rate coefficients in vegetative (DVRV), and reproductive phase (DVRR).

In the next four series of runs (Simulation series 2 - 5), the DSTRESS and PADDY modules were added to ORYZA1. No specific measured values of the various treatments was used. All parameters used were obtained from the dry season experiment reported by Kropff et al. (1993a), except for DVRV, DVRR and leaf N concentration as a function of time, which were derived from the well-watered plots. LAI and soil-water content were either simulated or measured values were used:

- 2 - Simulations using ORYZA1-DSTRESS-PADDY with measured LAI and measured 0 to 10 cm water content,
- 3 - Simulations using ORYZA1-DSTRESS-PADDY with measured LAI and simulated 0 to 10 cm water content,
- 4 - Simulations using ORYZA1-DSTRESS-PADDY with simulated LAI and measured 0 to 10 cm water content,
- 5 - Simulations using ORYZA1-DSTRESS-PADDY with simulated LAI and simulated 0 to 10 cm water content.

Such an analysis helps to determine if the water balance component and the LAI component are simulated accurately.

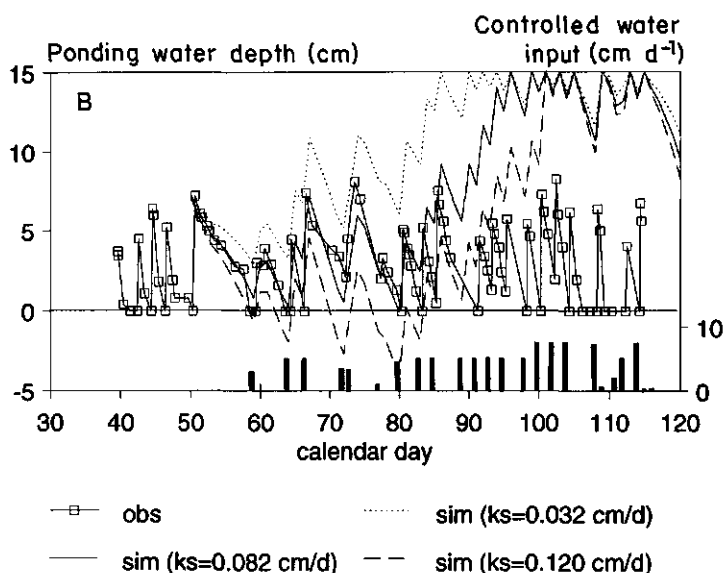


Fig. 10.5 Simulated and observed changes in ponded water depth for field experiment 1 using soil water balance module PADDY.

Results and discussion

PADDY accurately predicted changes in ponded water depth for field experiment 1 (Fig. 10.5). In Chapter 9, the more complicated SAWAH soil water balance model (ten Berge et al., 1992) was tested using the same field data. Results from this study show that the iteration procedure used in PADDY to calculate the flux through the soil profile under flooded soil conditions was as effective as the small time step calculations used in SAWAH.

The results of field experiment 2 in terms of yields are summarized in Table 10.2. All drought treatments resulted in yield losses compared with the well-watered plots. Drought at transplanting resulted in yield losses of 3 - 4 t ha⁻¹. Drought during grain filling did not affect yield significantly. Field observations during plant sampling showed that in case of drought, roots penetrated as deep as 30 - 40 cm. Well-watered plants did not grow deeper than puddled layer depth (i.e. 15 - 20 cm).

The dry matter distribution functions hardly varied among treatments (Fig. 10.6) and

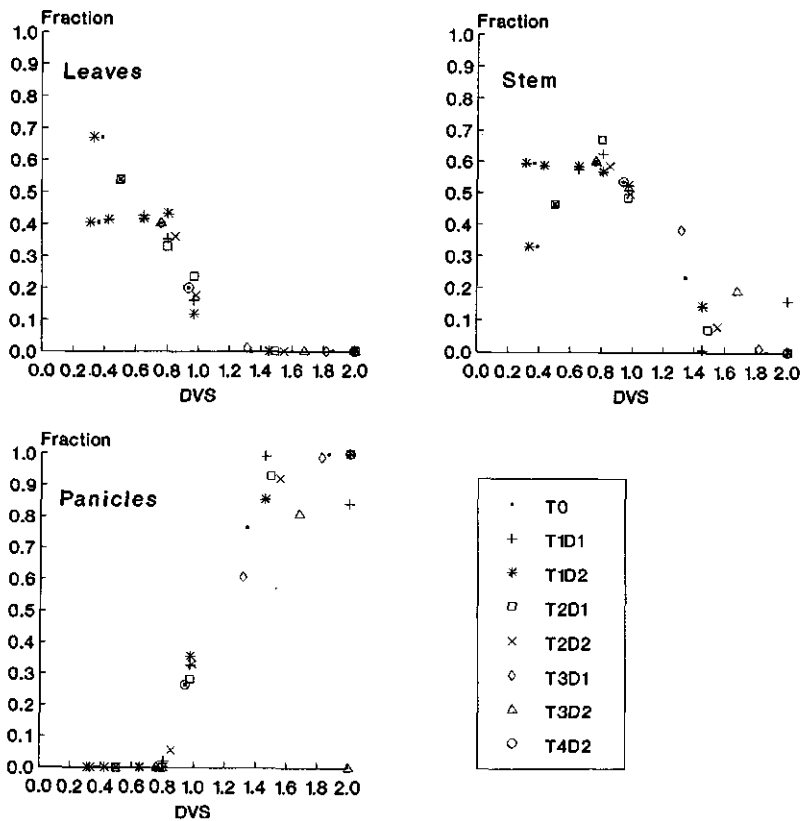


Fig. 10.6 Distribution pattern of dry matter over leaves, stems and panicles as a function of development stage (DVS) for cv. IR72 in field experiment 2. Codes are explained in Tables 10.1 and 10.2.

Table 10.2 Observed and simulated grain yield for field experiment 2 and Simulation series 1 to 5 (Sim1 to Sim5). Drought at transplanting (T1); at mid-tillering (T2); at panicle initiation (T3); and during grain filling stage (T4); well-watered (T0). D1, D2 indicate different durations of drought, see Table 10.1.

Treatment	Observed yield (t ha ⁻¹)	Simulated yields (t ha ⁻¹)				
		Sim 1	Sim 2	Sim 3	Sim 4	Sim 5
T1D1	5.9	5.9	6.8	6.7	5.4	6.0
T1D2	5.0	5.2	5.8	5.8	5.2	5.8
T2D1	7.9	7.7	7.6	7.8	7.7	7.9
T2D2	7.0	7.4	6.6	6.7	7.4	7.6
T3D1	6.1	7.3	6.3	6.0	6.7	6.8
T3D2	5.3	5.9	5.0	5.0	5.0	5.7
T4D1	8.2	7.8	7.7	7.8	7.6	7.7
T4D2	6.9	7.5	6.7	7.0	6.2	6.9
T0	8.4	8.4	8.4	8.4	8.3	8.3

Table 10.3 Observed and simulated grain yield (Simulation series 5) and crop growth duration of cv. IR72 as affected by drought stress at various physiological growth stages during field experiment 2. Treatments are explained in Tables 10.1 and 10.2.

Treatment	Observed		Simulated	
	Yield (t ha ⁻¹)	Growth duration (d)	Yield (t ha ⁻¹)	Growth duration (d)
T1D1	5.9	154	6.0	150
T1D2	5.0	154	5.8	152
T2D1	7.9	147	7.9	147
T2D2	7.0	149	7.6	148
T3D1	6.1	144	6.8	144
T3D2	5.3	144	5.7	144
T4D1	8.2	144	7.7	144
T4D2	6.9	144	7.7	144
T0	8.4	144	8.3	144

were very similar to results obtained by Kropff et al. (1993a). The use of one dry matter distribution function for all treatments was, therefore, justified.

The simulation results for all five simulation series were compared with observed data. For reasons of brevity, results here only show a comparison of simulated and

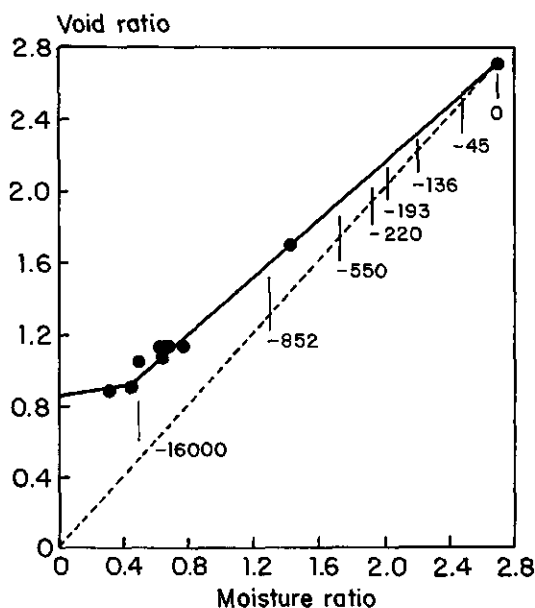


Fig. 10.7 Soil shrinkage characteristic of a puddled clay soil. Values in diagram indicate soil pressure heads (cm).

observed yield (Table 10.2). Simulated and observed data are presented in more detail for Simulation series 5 in Table 10.3. The length of the growth period was predicted well by the model, except for drought at transplanting, where the model underestimated the length of the growing period. The use of ORYZA1 without a soil-water balance module resulted generally in over-estimation of yield, indicating that yield losses could not be solely attributed to changes in leaf morphology. Adding the soil-water balance and the drought stress modules resulted in better predictions, regardless of whether simulated or measured LAI and soil-water contents were used. R^2 values ranged from 0.84 to 0.92.

The soil shrinkage curve determined for the puddled topsoil in field experiment 2 is shown in Fig. 10.7. Total shrinkage is very high. The normal shrinkage phase is almost non-existent as air entry occurs almost directly below saturation. Similar observations were made by Bronswijk and Evers-Vermeer (1990) for a half ripe subsoil in the Netherlands. Treatment effects on root zone water content were simulated reasonably well (Fig. 10.8).

Simulated (Simulation series 5) and observed LAI, total biomass, and panicle dry weight are shown in Figs 10.9 to 10.11. If drought occurred at transplanting, recovery did not result in fast re-growth of leaves, and LAI remained below 3.0 (Figs 10.9a and 10.9b). This effect was not observed in the greenhouse study (Chapter 8) and might be due to the fact that the field dried out faster than the pots, probably aggravating the transplanting shock. In the model ORYZA1 (Kropff et al., 1993a) it is assumed that when LAI is less than 1, plants grow exponentially as a function of temperature sum.

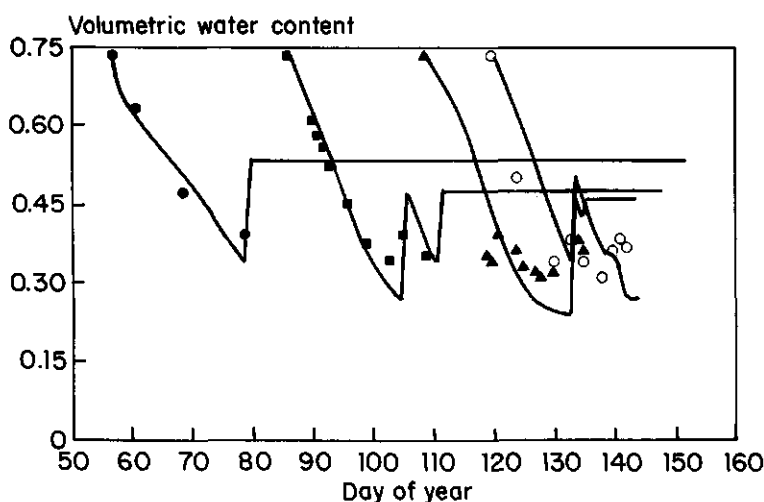


Fig. 10.8 Simulated (lines) and observed (symbols) soil water content ($\text{m}^3 \text{m}^{-3}$) for cv. IR72 in field experiment 2 for drought at transplanting (0 - 5 cm, late recovery, closed circles), drought at mid-tillering (0 - 10 cm, late recovery, squares) drought at panicle initiation (0 - 10 cm, late recovery, triangles), and drought at flowering (0 - 10 cm, no recovery, open circles).

When LAI exceeds 1, the SLA concept is used. In the ORYZA-DSTRESS-PADDY model it is assumed that if drought occurs at LAI values lower than 1, LAI is no longer simulated with an exponential function, but using the SLA concept. Using this concept, LAI was simulated accurately (Figs 10.9a and 10.9b).

Results indicate that the model could satisfactorily explain differences in biomass production and yield across drought treatments, given the inputs mentioned above.

Conclusions

A new rainfed rice model suitable for puddled soils was developed and tested using two field experiments conducted in the Philippines. The model consists of a well-tested rice growth model ORYZA1, the soil water balance module PADDY, and a drought stress module DSTRESS. The combined ORYZA1-DSTRESS-PADDY model can be used to investigate yield losses due to drought in rainfed environments and may be used to quantify the benefits of improved irrigation facilities. It is also a starting point for simulation studies on rice-upland crop rotations.

The current version of ORYZA1-DSTRESS-PADDY is completely source driven, i.e. sink size limitations are not taken into account. Further model development should focus on predicting the number of spikelets and the number of filled and unfilled grains under irrigated and water-limited conditions.

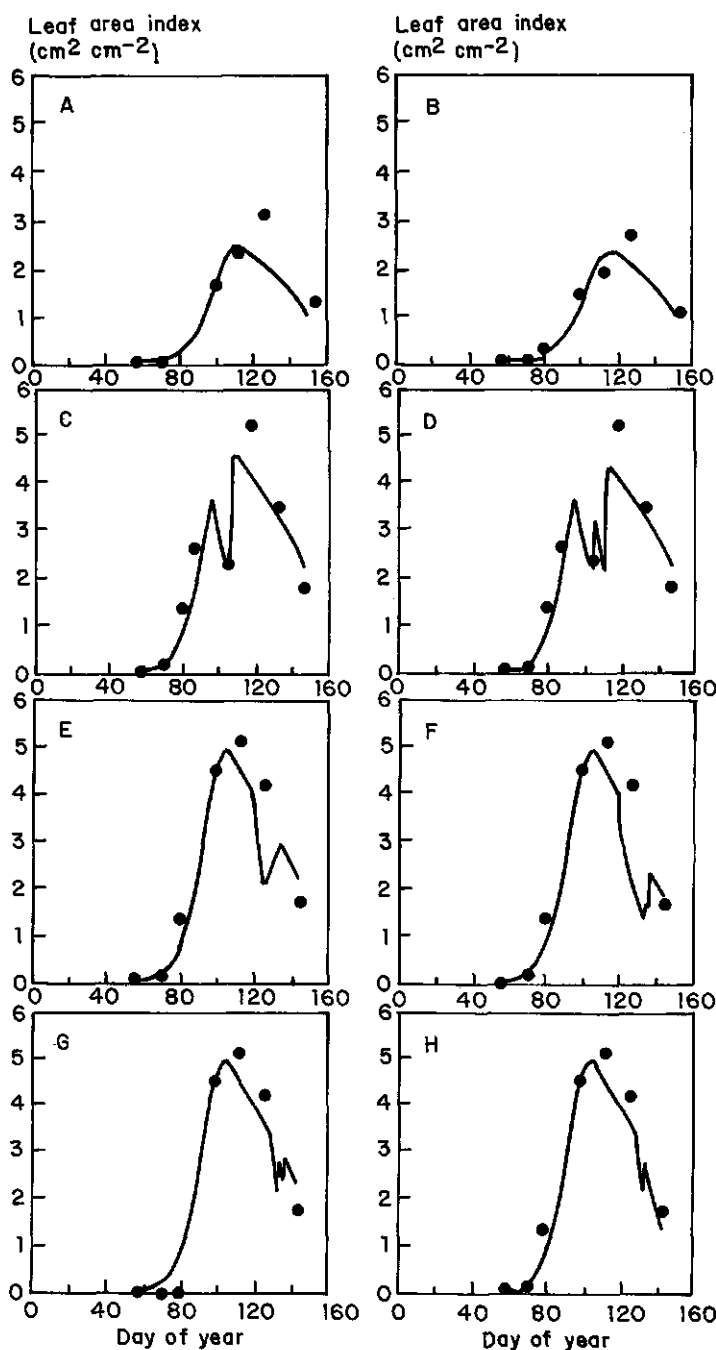


Fig. 10.9 Simulated (lines) and observed (symbols) Leaf Area Index (LAI, $\text{m}^2 \text{m}^{-2}$ soil) for cv. IR72 in field experiment 2 for all drought treatments: A is drought at transplanting, early recovery; B at transplanting, late recovery; C at mid-tillering, early recovery; D at mid-tillering, late recovery; E at panicle initiation, early recovery; F at panicle initiation, late recovery; G at flowering, early recovery; H at flowering, late recovery.

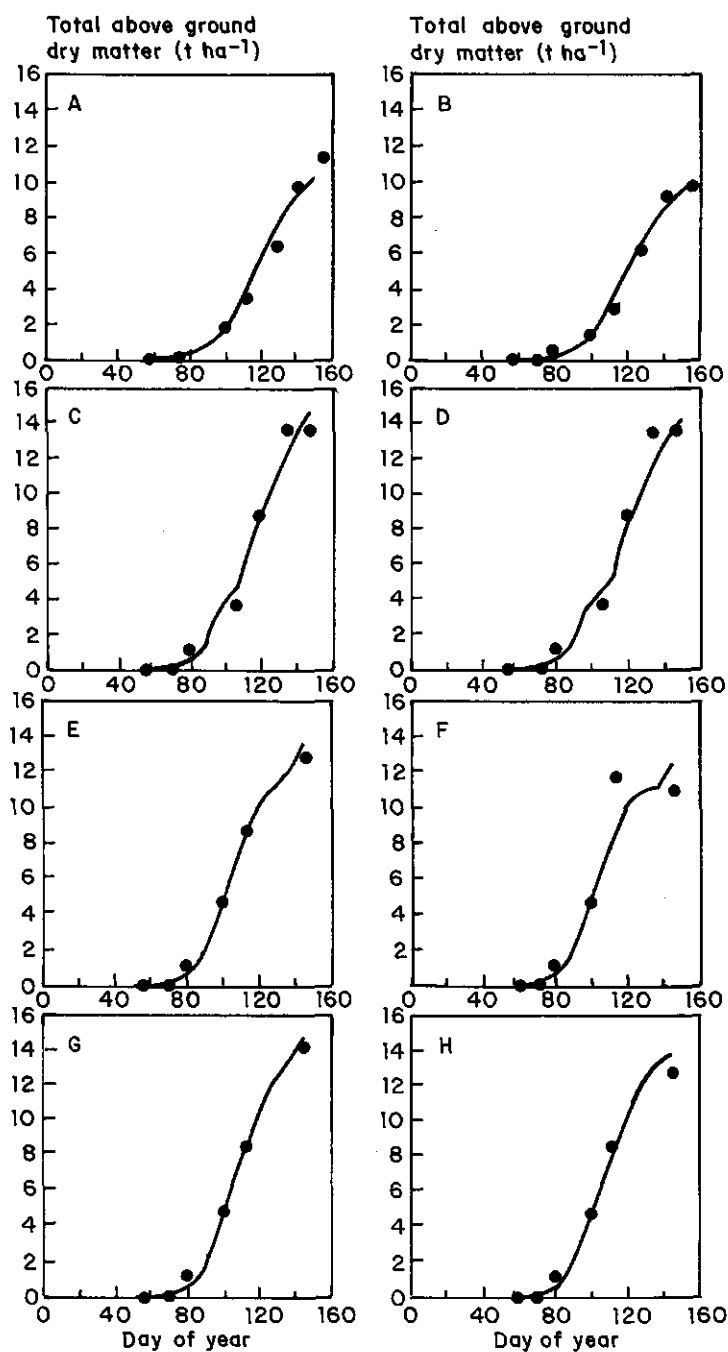


Fig. 10.10 Simulated (lines) and observed (symbols) total dry matter weights (t ha^{-1}) for cv. IR72 in field experiment 2 for all drought treatments: A is drought at transplanting, early recovery; B at transplanting, late recovery; C at mid-tillering, early recovery; D at mid-tillering, late recovery; E at panicle initiation, early recovery; F at panicle initiation, late recovery; G at flowering, early recovery; H at flowering, late recovery.

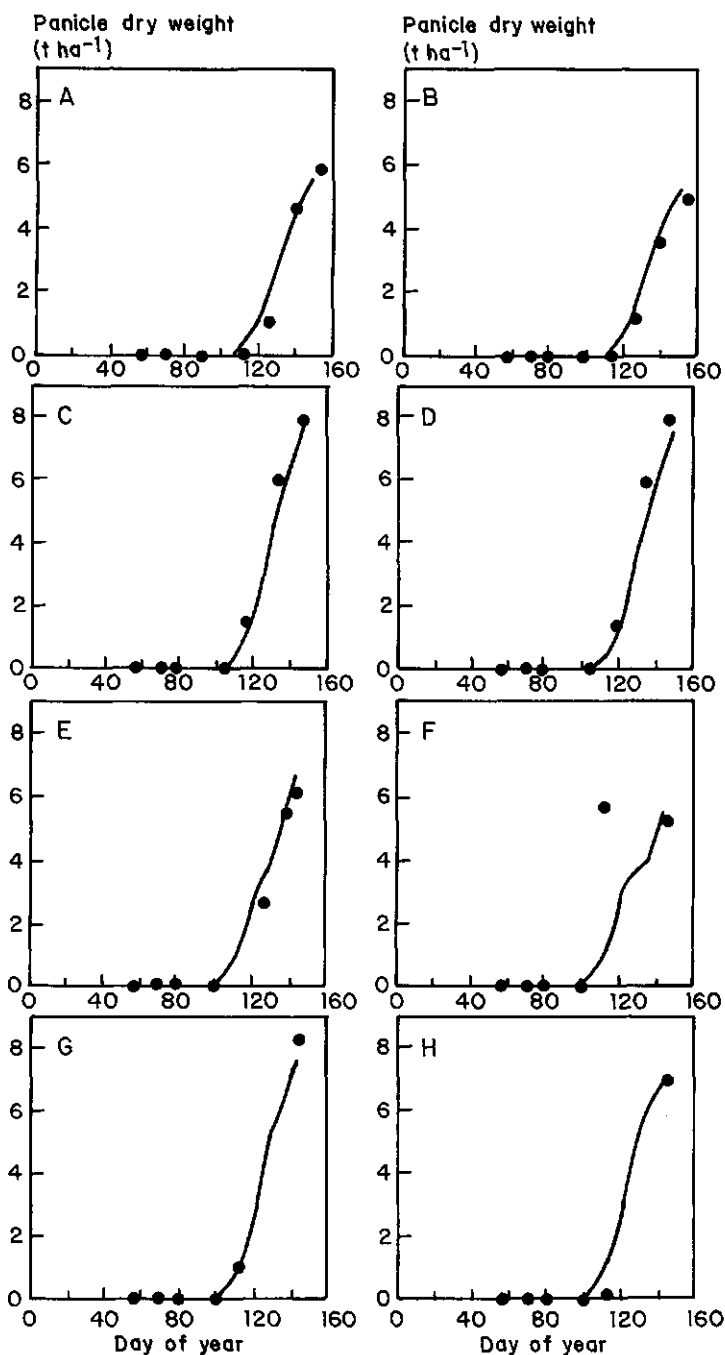


Fig. 10.11 Simulated (lines) and observed (symbols) panicle dry weights (t ha^{-1}) for cv. IR72 in field experiment 2 for all drought treatments: A is drought at transplanting, early recovery; B at transplanting, late recovery; C at mid-tillering, early recovery; D at mid-tillering, late recovery; E at panicle initiation, early recovery; F at panicle initiation, late recovery; G at flowering, early recovery; H at flowering, late recovery.

In PADDY, soil cracking is treated in an empirical way. If the soil moisture ratio in the root zone drops below a critical value, cracks are assumed to break through the least permeable layer in the puddled topsoil. The volume of soil cracks can be predicted by PADDY, provided the soil shrinkage characteristic of the puddled topsoil is known. Evaporation through cracks may accelerate the drying of a puddled soil. In PADDY this not taken into account. More research is needed on ripening of puddled soils of different texture and soil cracking upon drying.

In case of drought stress, roots will grow deeper with a fixed 'exploration rate'. The impact of drought on rooting depth and root growth needs to be studied in more detail as well.

Chapter 11

Case study on regional application of crop growth simulation models to predict rainfed rice yields: Tarlac province, Philippines

Abstract Paddy rice is the major crop grown during the monsoon season (June - November) in the Philippines. Under non-irrigated growing conditions, rice yield losses may occur due to drought. In this study the potential of crop simulation models to quantify such risk on a regional level, based on soil hydrological and climatic data was investigated. For this purpose, soil hydraulic properties were determined for 7 major soil types under rice cropping occurring within the province of Tarlac in the Philippines. The crop growth model ORYZA1-DSTRESS-PADDY, introduced in Chapter 10, was used to predict rainfed rice yield as a function of these soil characteristics and long-term weather information (25 years).

Potential (irrigated) rice yield varied from 5.4 to 6.7 t ha⁻¹. The impact of groundwater table depth on capillary rise and rainfed rice yield was investigated for each of the 7 major soil types. The importance of puddling intensity on water use efficiency and rice yield was studied by varying the saturated hydraulic conductivity of the least permeable layer in the puddled topsoil. Water-limited (rainfed) rice yield ranged from 0 to 6.7 t ha⁻¹. Risk involved in growing rainfed rice was quantified by calculating yield probability distributions for each soil type. Spatial variability of simulated rainfed rice yield within the province was analysed using a Geographic Information System.

Introduction

One of the major limitations to rice production in the Philippines is water supply and availability. A large part of the total Philippine rice production is from rainfed areas where rice is grown only once a year during the wet season (June to November). For the rest of the year these areas are usually left fallow. Erratic rainfall results in yield variability. In some areas, due to increasing urban and industrial demand for water, irrigation schemes can support only part of the area they were designed to service. In addition, poor management and eroding infrastructure contribute to unsatisfactory performance of irrigation systems (Bhuiyan, 1987), thus increasing the amount of rice grown under rainfed conditions.

In both irrigated and rainfed rice areas there is a need to optimize water use efficiency at the regional level. This can be done through: (i) improvement of irrigation facilities, (ii) introduction of water-saving techniques, (iii) adjustment of choice of crop and/or planting time. For any of these approaches, a thorough systems analysis is needed to

evaluate different solutions for different environments.

A systems analysis, in this case, can not rely on traditional agronomic field station or farmer's field experiments. This would be too costly and time consuming, given the need to conduct such experiments over a number of years, cropping seasons, and across different environmental conditions. Especially in rainfed environments, experiments must be conducted over a large number of years, to allow for climatic variability.

To overcome such limitations, crop growth simulation models (provided adequate data on soil, weather and crop and soil management procedures are available) can be used to determine potential (fully irrigated) and water-limited (rainfed) yields for a target area. Efforts are currently underway to evaluate different cropping systems in centuries old tank irrigation systems in Tamil Nadu, South India, using simulation models to minimize risk of crop failure. Poor maintenance of these tank irrigation systems cause declining command areas and reduced rice yields due to water scarcity in November - December, at the end of the growing season (Palanisami, 1993). The potential of water-saving techniques in different environments, like puddling (Chapters 2 and 3), or the introduction of a pre-tillage before re-flooding a dry cracked field for the next rice crop (Chapter 7) are best evaluated using simulation models as well, provided long-term weather data and reliable soil data are available.

An economic evaluation of strategies to optimize water use efficiency requires an accurate estimate of the probability distribution of production (Anderson, 1991). Simulation models can provide such probability distributions using long-term weather data. For a spatial analysis of drought risk, models need to be linked with a Geographic Information System (GIS) containing soil and long-term weather data of the target area (Nix, 1987).

In this study, the potential of crop simulation models to quantify drought risk in rainfed rice environments based on soil hydrological and climatic data was investigated. A methodology is presented to obtain soil hydraulic input data on a regional scale. A case study was conducted for a province in central Luzon, one of the major Philippine islands.

Materials and methods

Simulation models should be validated for environmental conditions prevailing in their target area. Recently, Kropff et al. (1993a) introduced ORYZA1, an improved model for irrigated rice production. The model was validated with a large number of field experiments, and yields can be predicted accurately for a range of environments. Input requirements for yield prediction using the model ORYZA1 are:

- Geographical latitude,
- Plant density,
- Date of crop emergence and transplanting, and
- Daily weather data (radiation, temperature).

In rainfed rice environments, the model ORYZA1 needs to be coupled to a soil-water balance via an 'interface' that translates the soil-water status in a crop response.

For this study, a soil-water balance module (PADDY) was developed that can be used for puddled soils (Chapter 10). Greenhouse studies were conducted to investigate the impact of temporary drought, induced at different growth stages, on rice growth and yield (Chapter 8). This experimental work resulted in a 'drought stress' module (DSTRESS). DSTRESS translates the soil moisture status predicted by PADDY in a crop response predicted by ORYZA1. The soil and crop components of the combined ORYZA1-DSTRESS-PADDY model were validated using field experimental data (Chapter 10).

In addition to the data needs of ORYZA1 specified above, use of the ORYZA1-DSTRESS-PADDY model requires (Chapter 10):

- Daily weather data (wind speed, relative humidity, rainfall),
- Soil hydraulic properties (i.e. hydraulic conductivity and water retention characteristics and saturated moisture content of the puddled topsoil), and
- Daily data on groundwater table depth.

Study area

The province of Tarlac is located in the northern part of the Philippines on the island Luzon (Fig. 11.1). The province covers an area of approximately 300,000 ha. It is composed of 17 municipalities with a total population of about 740,000 people (BSWM, 1992).

Three major landscapes can be identified in the province: an alluvial flood plain in the north-east, a hilly area in the centre of the province and a mountainous area in the west (Fig. 11.2). The alluvial flood plain occupies about one third of the province area and is dissected by rivers and creeks. The hilly landscape is slightly undulating to strongly rolling terrain and is mainly composed of shale and sandstone. The mountainous landscape is of volcanic origin and is highly dissected with steep to very steep ridges. Pyroclastic hills border the province in the south. Due to the 1991 eruption of Mt. Pinatubo, part of this area is again covered with a thick layer of 'lahar', i.e. mud flow.

Crop and soil management

The area used for crop production in Tarlac is about 140,000 ha, and is mainly situated in the alluvial flood plain. The five major crops grown are rice (111,000 ha), sugarcane (20,500 ha), sweet potato (5,000 ha), corn (1,500 ha) and vegetables (500 ha). Of the area used for rice, 59,000 ha is irrigated, and 52,000 ha is rainfed (BSWM, 1992). Areas with adequate irrigation can be harvested twice a year; areas without irrigation can be harvested only once. Sugarcane and vegetable crops are grown on loamy to sandy soils.

Farmers use the first monsoon rains in May for rainfall collection. Soils are plowed and harrowed under near water saturated conditions using animal power or small hand tractors. Land preparation may require over one-third of the total water used for irrigated

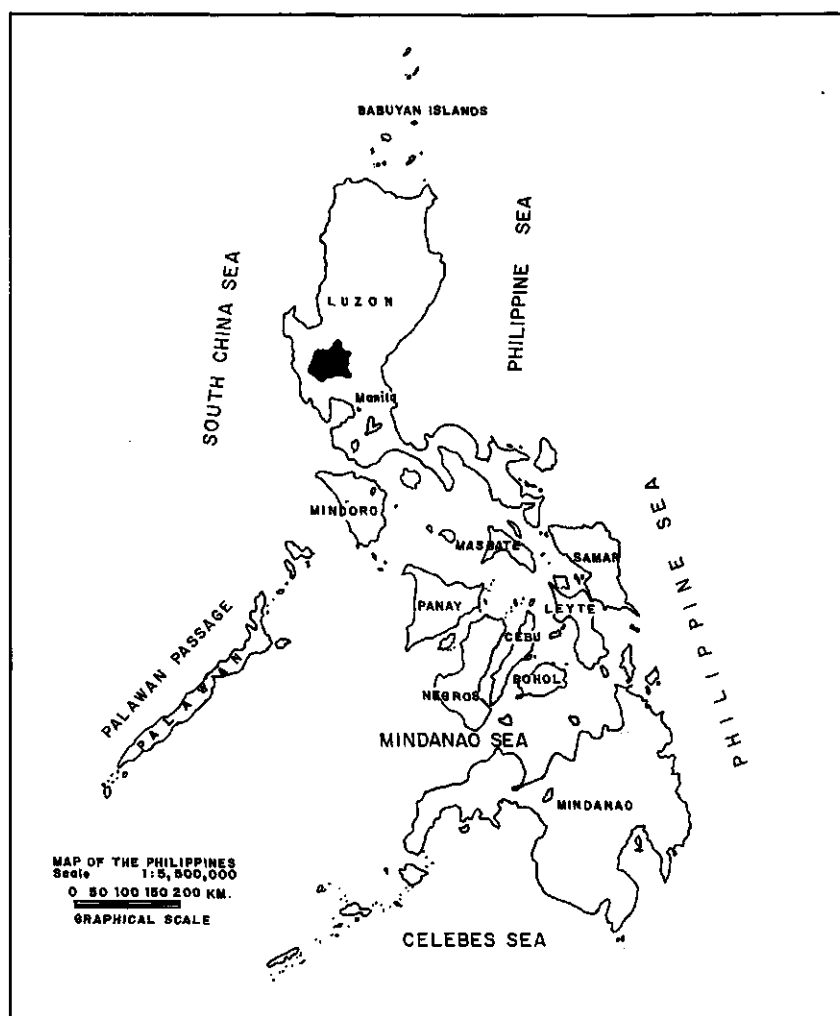


Fig. 11.1 Location of the province of Tarlac in the Philippines.

rice production (IRRI, 1978). Rice is usually transplanted between 15 and 30 June, although direct seeding is also practiced. Harvesting is normally done in October. In case of adequate irrigation facilities a second crop may be grown from November to April.

The average size of a rice farm in Tarlac is 1.7 ha. Farmers mainly apply inorganic fertilizer, often in two splits: one 7 - 30 days after transplanting and one around panicle initiation. Basal application is seldom used. Weed control measures are especially needed under rainfed conditions (BSWM, 1992).

Climate data

The province has two pronounced seasons: wet during the months of June to November

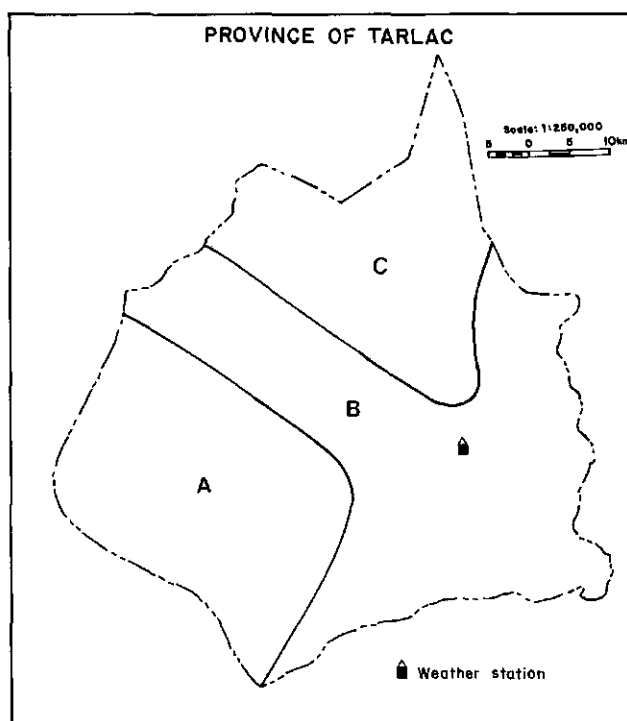


Fig. 11.2 Location of major landscapes and weather station Hacienda Luisita in the province of Tarlac. A: High altitude volcanic mountains (above 500 m) and andesitic hills (2200 - 2900 mm rain yr^{-1}); B: Low altitude areas which are andesitic hills, terraces footslopes and alluvial plains (1700 - 2200 mm rain yr^{-1}); C: alluvial plains (1300 - 1700 mm rain yr^{-1}). Source: BSWM, 1992.

and dry from December to May. Most precipitation is due to monsoon rains that reach Luzon from the south west and west. There is only one fully equipped meteorological station in the province, Hacienda Luisita (Fig. 11.2). At the time of this study only five years of complete daily weather data were available from this station. This included daily observations of rainfall, relative humidity, maximum and minimum temperature and sunshine hours.

Highest maximum temperatures in Tarlac occur in April (36 °C). Lowest minimum temperatures are reached in January (19 °C). Rainfall is highest in the mountainous range with annual rainfall varying between 2200 and 2900 mm yr^{-1} . The alluvial plains receive about 1700 - 2200 mm yr^{-1} (BSWM, 1992; Fig. 11.2). Because of the paucity of weather data, additional data on rainfall were obtained from the Philippine weather bureau PAGASA for 12 rainfall stations within the province. Although for some stations rainfall data were available for a large number of years, measurement series overlapped during only three years for 10 out of the 12 stations. No conclusions on geographical

distribution of rainfall could be derived from these data. Total solar radiation in the monsoon season (June - November) for Hacienda Luisita was compared with four meteorological stations outside Tarlac. Again, only three years within each time series of measurements overlapped for all stations. Total solar radiation was quite similar for all four stations (Table 11.1).

The set of five years of complete daily weather data was considered insufficient to get an idea of yield variability within the province. The weather generator program SIMWTH (Supit, 1986) was, therefore, used to generate 25 years of weather from the available 5 years.

Soil survey data

A soil map of Tarlac province (1:50,000) was provided by the Bureau of Soils and Water Management, Quezon City, Philippines. The map contains 67 different mapping units. Each of these mapping units is characterized by a representative profile description and by laboratory data like texture and organic matter content for every soil horizon, distinguished within the profile. The detailed soil map was digitized using the GIS package PC-ARC/INFO (ESRI, 1987).

The total number of mapping units was reduced by generalization, taking into account similarity in soil properties and importance of the unit in terms of surface area. Soil mapping units belonging to the same soil series, were merged, which reduced the original number of mapping units from 67 to 25. Soil units that occupied less than 1% of the total province were merged with other similar units. A representative profile was selected for every generalized mapping unit, except for the mountainous area. This simplification of the original soil map was done by an experienced soil surveyor with a good knowledge of the diversity of soils in the Tarlac province.

Guided by the detailed soil map, representative soil profiles were located for each of the generalized soil units. Soil horizons within each of these representative profiles were grouped into hydraulic-functional horizons according to texture and a simple depth criterion (topsoil or subsoil). A similar approach was followed in Chapter 4.

Table 11.1 Total solar radiation (averaged over three years) in the monsoon season for Hacienda Luisita and three of the nearest meteorological stations, outside Tarlac province.

Station	Years	Total solar radiation (MJ m ⁻²)
Dagupan	1978-1980	2518
Cabanatuan	1978-1980	2652
Manila	1978-1980	2582
Hacienda Luisita	1978-1980	2555

Soil physical data

Sampling activities for the measurement of the soil hydraulic functions (i.e. water retention and hydraulic conductivity) were concentrated on hydraulic-functional horizons in every representative profile. Sampling was carried out in the dry season of 1991 (two replicate samples per hydraulic-functional horizon).

Procedures used for estimating the water retention curve, relating soil water content θ to soil water pressure h were:

- The hanging water column method (Richards, 1965) for $-15 \text{ kPa} < h < 0 \text{ kPa}$ using 71 mm diameter, 70 mm height undisturbed cores, and
- The pressure cell method (Klute, 1986) for $h < -100 \text{ kPa}$, using 51 mm diameter, 20 mm height disturbed cores.

The saturated and unsaturated hydraulic conductivity k was measured as a function of soil water pressure h using a combination of three methods:

- 1 The constant head method of Klute (1986) for vertical saturated conductivity (k_s) using 0.25 m high and 0.2 m diameter soil cores,
- 2 The crust method (Booltink et al., 1991) for $-2 \text{ kPa} < h < 0 \text{ kPa}$, using the soil samples of Method 1, and
- 3 The one-step outflow method (Kool et al., 1985) using 70 mm high and 70 mm diameter soil cores for $-50 \text{ kPa} < h < 3 \text{ kPa}$. Saturated samples were subjected to a pressure of 50 kPa, after equilibrium at a pressure of 3 kPa was reached (Booltink, unpubl. data).

Soil hydraulic properties were assumed to be represented by van Genuchten's closed-form equation (van Genuchten, 1980) involving four unknown parameters: coefficients a , n , l and residual moisture content θ_r . Two other parameters, i.e. the saturated moisture content (θ_s) and the saturated hydraulic conductivity (k_s) were set equal to their measured values. Values for the four unknown parameters were determined by nonlinear least-squares fitting using the program MULSTP (van Dam et al., 1990) of measured time series of cumulative outflow and measured water-retention data. Crust method data were used to validate the fitted hydraulic conductivity curve for soil-water pressures near saturation.

For three heavy clay soils an alternative way to determine the conductivity curve $k(h)$ was needed because of very low outflow volumes ($< 5 \text{ ml}$) from the one-step outflow experiments. For these sites, $k(h)$ characteristics were derived using the Wind method (Wind, 1968) and 80 mm high, 100 mm diameter undisturbed cores. Experimental data were analysed using the WIND program (Halbertsma, unpublished) and parameterized in terms of van Genuchten's unsaturated functions using the RETC program (van Genuchten et al., 1991). In total, hydraulic conductivity and water-retention characteristics were determined for 30 hydraulic-functional soil horizons.

To mimic puddled soil conditions, the top 10 cm of large 0.25 m height and 0.2 m diameter undisturbed soil cores were hand stirred during one minute in the laboratory

using large quantities of water. Saturated volumetric moisture content of the puddled soil material was determined after one week (to allow for settling of the soil particles) using 100 cc cores. The hydraulic conductivity of the least permeable layer in the puddled topsoil was determined for two samples per soil type using the method outlined in Chapter 2.

Simulation of rice production

As a first qualitative step, soils unsuitable for rice growth were eliminated from the analysis. This included the mountainous area and light-textured soils, except for soils that were classified on the soil map as 'severely flooded' because of their proximity to a river. It was assumed that rice grown on such soils does not suffer from drought stress. Simulations were only conducted for potentially suitable soils.

Potential (irrigated) rice yield was simulated using the model ORYZA1. Water-limited (rainfed) rice yield was simulated using the ORYZA1-DSTRESS-PADDY model. Crop parameters for rice cultivar IR72 were derived from a wet season experiment conducted at IRRI in 1991 (Kropff et al., 1993a). Simulations started at transplanting, assuming 30 days old seedlings. Initial LAI, temperature sum and development stage of the seedlings were taken from the study presented in Chapter 10. Initial rooting depth was assumed to be 0.05 m.

After discussion with an expert from the Bureau of Soils and Water Management, Quezon City, Philippines (Sanidad, pers. comm.), transplanting of rice was assumed to start when cumulative rainfall exceeded 75 mm during seven consecutive days after 1 June.

Thickness of the puddled topsoil was set to 0.2 m, with the least permeable layer occurring between 0.15 and 0.20 m depth. At transplanting, the puddled topsoil was assumed to be saturated with an initial ponded water depth of 0.05 m. Subsoil horizons were assumed to be at field capacity level ($h = -10$ kPa). Measured hydraulic conductivity functions for each soil horizon were input in the model.

The impact of groundwater table depth and thoroughness of puddling on rainfed rice yield was investigated for each of the major soil types under rice cropping. Groundwater table depth was varied between 0.5 and 1.0 m.

The saturated hydraulic conductivity of the least permeable layer in the top 0.2 m of a puddled clay soil at the experimental farm of the International Rice Research Institute in the Philippines was determined in Chapter 2. Average value was 0.036 cm d^{-1} with 95% confidence limits at 0.027 and 0.045 cm d^{-1} . In this study, two classes of puddling (poorly puddled and well puddled) were considered and expressed in terms of the hydraulic conductivity k_s of the puddled topsoil:

well puddled: k_s (least permeable layer) = 0.01 cm d^{-1}

poorly puddled: k_s (least permeable layer) = 0.10 cm d^{-1}

Combined with the two groundwater table depths, four simulation series were created:

Series 1: k_s puddled topsoil = 0.01 cm d⁻¹; groundwater table depth = 0.5 m
Series 2: k_s puddled topsoil = 0.01 cm d⁻¹; groundwater table depth = 1.0 m
Series 3: k_s puddled topsoil = 0.10 cm d⁻¹; groundwater table depth = 0.5 m
Series 4: k_s puddled topsoil = 0.10 cm d⁻¹; groundwater table depth = 1.0 m

The approach outlined above can only result in a broad overview of yield losses due to drought in Tarlac. Soil types were characterized by measurements conducted at one representative site only. Spatial variability of soil hydraulic properties or depth to soil horizons is not taken into account. Sensitivity analyses can be conducted to investigate the importance of variability in model input parameters.

Validation

Simulated rice yields were compared with data reported by the Philippine Bureau of Soils and Water Management obtained during a survey in Tarlac in 1990. Some of the representative sites were revisited during the wet season of 1991 and sampled for grain yield. Most of these fields had received additional irrigation during the growing season, often through small gasoline driven pumps. An estimate of grain yield at the various sites was obtained by counting the number of hills in one m² and by determining grain yield for twelve hills. Six additional hills were analysed for N-content in stem, leaves and grains.

Results and discussion

Soil data

The digitized, generalized soil map of the Tarlac province is shown in Fig. 11.3. The total number of mapping units was reduced from 67 to 14. Excluding the mountainous areas, 11 mapping units could be distinguished (Table 11.2). Generalization reduced the number of delineated areas (polygons) from 369 to 219. Van Genuchten parameters, determined for the representative profiles are listed in Table 11.3. Saturated moisture content and hydraulic conductivity refer to soil conditions prevailing in the dry season. Puddled volumetric soil moisture content for each soil type under rice cropping was in general 0.1 to 0.2 cm³ cm⁻³ higher than the values indicated in Table 11.3.

Soil series 27, 28, and 52 (Tables 11.2 and 11.3) were considered unsuitable for rice growth because of their light texture. No simulations were conducted for soil series 46 as this soil type only occurs in the area devastated by the Mt. Pinatubo eruption.

Simulation results

Potential yields in the province varied from 5.4 to 6.7 t ha⁻¹. These yields are considerably higher than irrigated rice yields reported by BSWM (1992), which varied between 2.5 and 3.5 t ha⁻¹. This discrepancy may be due to a large number of factors, e.g. lack of fertilizer, incidence of pest and diseases etc., which are not taken into account by the ORYZA1-DSTRESS-PADDY model. Harvest data from the survey conducted for

Table 11.2 Major soil types occurring in Tarlac province and relative surface area (expressed as a percentage of the total surface area of the province).

Code	Soil series	Surface area (%)
10*	Rugao clay loam	3.9
12*	Alaminos clay loam	2.9
18*	Padapada, Peneranda clay	5.6
25*	San Manuel silt loam	5.0
26*	Moncada clay loam	4.3
27, 28	La Paz, Banga, Pawing loamy sand	4.3
30*	Zaragosa clay loam	12.0
46 ¹	Barang, Cabetican, Quingua silt loam	3.7
52	Ramos, Luisita, Angeles silt loam	7.1
59*	Tarlac clay loam	4.7
-	Villar fine sandy loam (hilly area)	5.2
-	Mountainous area, miscellaneous	41.3

* Soils under rice cropping.

¹ Soil series is mostly covered by mud flow (lahar) due to the 1991 Mt. Pinatubo eruption.

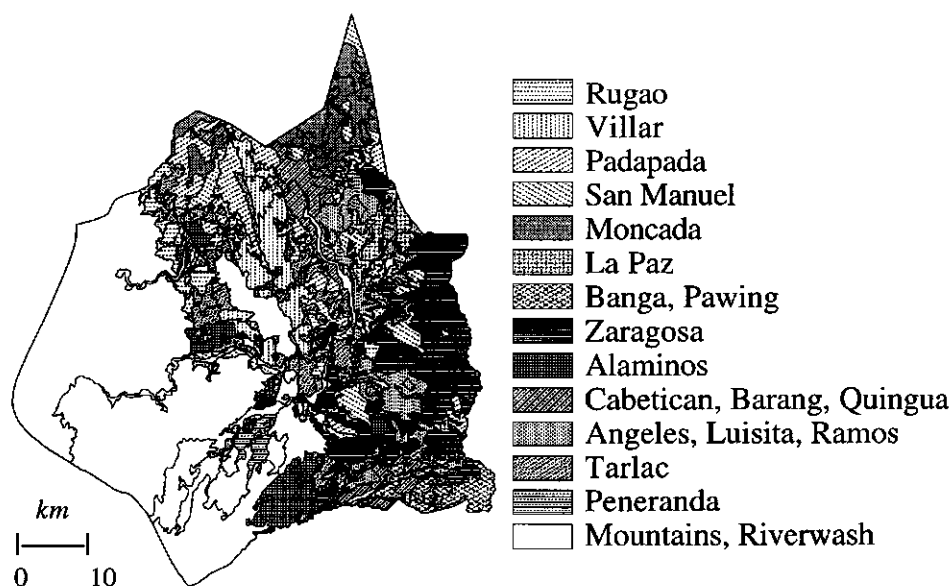


Fig. 11.3 Generalized soil map of Tarlac province.

Table 11.3 Textural properties and van Genuchten's parameters as estimated for hydraulic-functional horizons (code 1, 2, 3) occurring in representative profiles (e.g. code 25) of the Tarlac province.

Hor. code	Depth (cm)	Sand (%)	Silt (%)	Clay (%)	k_s (m d ⁻¹)	θ_s (-)	α (cm ⁻¹)	n (-)	l (-)	θ_r (-)
10-1	0-19	27.0	28.0	45.0	0.092	0.52	0.0171	1.114	-6.95	0.001
10-2	19-46	54.5	13.5	32.0	0.038	0.44	0.0176	1.261	0.15	0.001
10-3	>46	63.0	13.0	24.0	0.002	0.50	0.0009	1.397	5.77	0.001
12-1	0-16	33.0	24.0	43.0	0.41	0.65	0.0074	1.098	14.22	0.001
12-2	>16	24.0	27.7	48.3	0.02	0.49	0.0251	1.106	8.13	0.001
18-1	0-29	23.0	23.0	54.0	0.02	0.55	0.0036	1.233	-5.86	0.001
18-2	>29	19.0	17.5	63.5	0.015	0.57	0.0027	1.210	-5.17	0.001
25-1	0-23	2.4	43.2	54.4	0.05	0.44	0.0124	1.150	-4.96	0.005
25-2	>23	48.6	18.4	33.0	0.91	0.41	0.0283	1.175	18.89	0.193
26-1	0-31	9.4	26.6	64.0	0.03	0.45	0.0155	1.148	8.97	0.060
26-2	31-90	15.6	47.9	36.5	0.041	0.47	0.0031	1.256	29.82	0.004
26-3	>90	1.4	33.6	65.0	0.005	0.47	0.0034	1.235	-0.47	0.155
27-1	0-27	54.6	26.4	19.0	1.16	0.47	0.0097	1.618	3.34	0.044
27-2	27-58	81.6	6.4	12.0	5.43	0.48	0.0096	2.035	1.40	0.047
27-3	>58	86.8	3.7	9.5	6.20	0.48	0.0082	1.904	4.39	0.014
28-1	0-23	82.6	6.4	11.0	0.32	0.50	0.0056	1.639	5.04	0.028
28-2	>23	89.6	0.4	10.0	5.77	0.40	0.0133	2.963	1.82	0.052
30-1	0-17	36.0	37.0	27.0	0.07	0.47	0.0088	1.128	-1.91	0.011
30-2	17-32	34.0	27.0	39.0	0.21	0.46	0.0091	1.082	13.14	0.031
30-3	>32	32.5	25.0	42.5	0.09	0.52	0.0121	1.122	31.98	0.001
46-1	0-29	33.2	41.0	25.8	0.08	0.43	0.0154	1.286	12.07	0.001
46-2	>29	38.8	29.5	31.7	0.14	0.46	0.0116	1.145	6.80	0.133
52-1	0-22	69.0	16.0	15.0	0.18	0.43	0.0165	1.293	-0.93	0.001
52-2	22-82	80.0	4.5	15.5	1.08	0.41	0.0654	1.175	-1.15	0.071
52-3	>82	87.5	1.0	11.5	2.46	0.46	0.0317	1.434	7.07	0.105
59-1	0-18	74.4	2.6	23.0	0.05	0.49	0.0088	1.205	11.57	0.001
59-2	18-39	40.0	20.6	39.0	0.44	0.44	0.0204	1.107	17.57	0.001
59-3	>39	10.4	20.6	69.0	0.009	0.44	0.0630	1.120	-2.69	0.156

this study show much higher yields, which are more in agreement with model predictions (Table 11.4), which may be attributed to the fact that most farmers included in the survey used shallow gasoline-driven irrigation pumps to overcome dry spells.

Simulated rainfed rice yields for all soil types and simulation series are given in Table 11.5. For reasons of brevity, the variability of rainfed rice yield over 25 years for the four simulation series is shown in Figs 11.4 and 11.5 for two distinctly different soil

Table 11.4 Percentage filled grains, grain yield, plant density and N-content in stem, leaves and grains for several representative sites in the Tarlac province. (I = irrigated, R = rainfed; at site 28, two varieties were sampled: 28A = IR64 and 28B = IR72).

Profile Code	I/R	Filled grains (%)	Grain yield (t ha ⁻¹)	Plant density (hills m ⁻²)	Nitrogen content		
					Stem (%)	Leaves (%)	Grains (%)
10A	I	81.0	5.0	34	0.42	0.86	0.95
10B	R	63.2	3.0	27	0.44	0.95	1.17
18	I	73.7	4.2	40	0.37	0.42	0.99
25	I	66.8	4.5	35	0.56	1.51	1.25
26	R	57.1	1.7	35	0.63	0.28	1.27
27	I	89.0	4.6	27	0.29	0.49	0.91
28A	I	83.7	3.6	20	0.32	0.75	0.82
28B	I	78.7	5.3	20	0.44	0.87	0.95
30	I	72.0	6.6	46	0.41	0.60	1.07
52	I	81.3	4.9	38	0.55	0.68	1.04

Table 11.5 Average rainfed rice yields (t ha⁻¹) per soil type (see Table 11.2), calculated for Scenarios 1 - 4 (see text).

Soil type	Scenario 1	Scenario 2	Scenario 3	Scenario 4
10	5.3	5.2	4.1	3.8
12	4.6	4.6	2.8	2.8
18	5.3	5.3	4.3	4.3
25	5.5	5.3	4.2	3.7
26	4.9	4.8	3.8	3.8
30	4.7	4.4	3.5	3.1
59	5.5	5.4	4.2	3.9

types only (Zaragoza soil series and Padapada soil series). For comparison potential yields are also shown. From the graphs it follows that without additional irrigation facilities, growing rice under rainfed conditions is risky.

Comparison of rainfed yield with potential yields quantifies the yield gap between fully irrigated and rainfed production. This information indicates the yield losses farmers experience due to lack of irrigation water, under otherwise optimal growing conditions. Production risk was quantified by calculating cumulative probability functions for rainfed

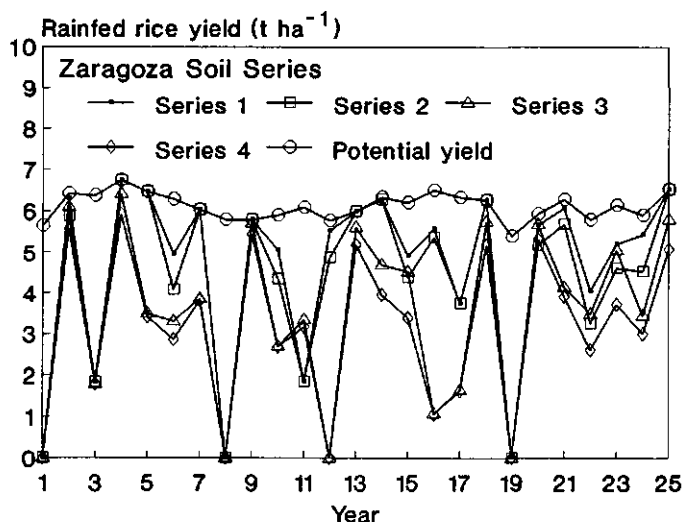


Fig. 11.4 Potential and rainfed rice yield calculated for 25 consecutive wet seasons and four simulation scenarios on Zaragoza soil.

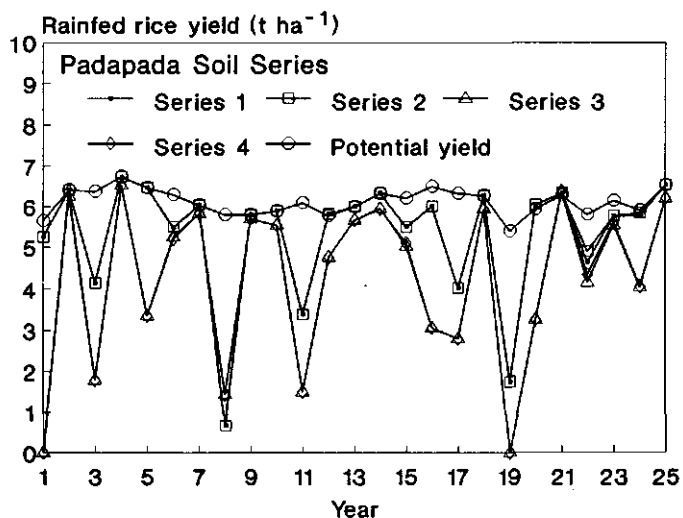


Fig. 11.5 Potential and rainfed rice yield calculated for 25 consecutive wet seasons and four simulation scenarios on Padapada soil.

rice yield for each soil type. Results are shown for Zaragoza and Padapada in Figs 11.6 and 11.7. For Zaragoza, a shallow groundwater table had a positive effect on grain yield due to increased capillary rise to the root zone. For Padapada this effect was almost non-existent. Poorly puddling resulted in yield losses for both soils, but yield losses were especially high for Zaragoza. These results can be attributed to the relatively permeable

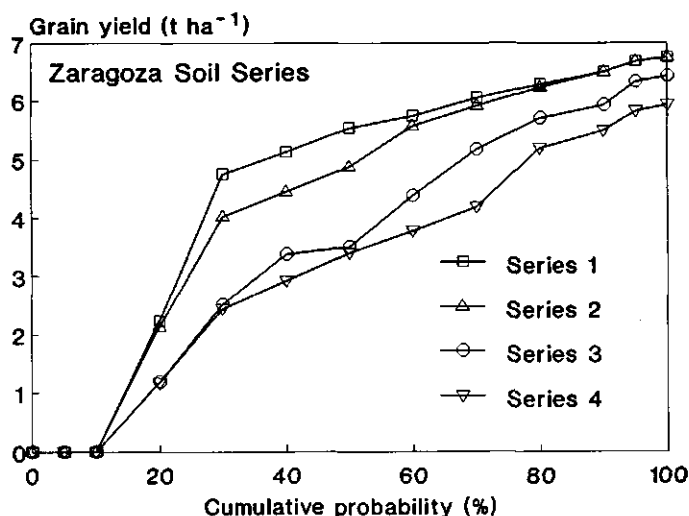


Fig. 11.6 Cumulative distribution function for rainfed rice yield on Zaragoza soil.

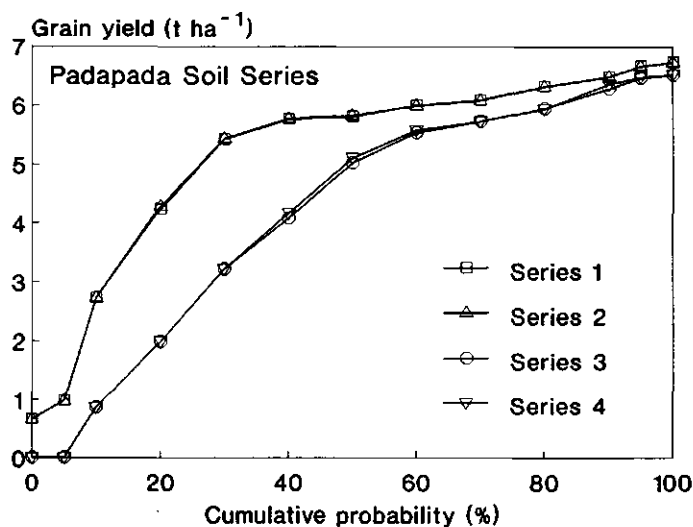


Fig. 11.7 Cumulative distribution function for rainfed rice yield on Padapada soil.

subsoil of Zaragoza soil series compared with the Padapada soil series, which makes the hydraulic resistance of the puddled topsoil less effective. If cracks penetrate through the puddled topsoil, water distribution within the soil profile as simulated by the PADDY water balance module, is determined by the hydraulic conductivity of the subsoil (Chapter 10). For Padapada, water may start ponding on the soil surface even if deep cracks are present due to the low hydraulic conductivity of the non-puddled subsoil. For Zaragoza, a substantial amount of rainfall may be lost due to deep drainage if cracks have

Table 11.6 Hydraulic conductivity of the least permeable layer in the puddled topsoil (k_s) determined for the major soil types under rice cropping in Tarlac province. Measurements were conducted in the laboratory on two samples per soil series.

Soil type	Sample 1 k_s (cm d ⁻¹)	Sample 2 k_s (cm d ⁻¹)
10	0.090	0.161
12	0.015	0.025
18	0.014	0.0036
25	0.096	0.464
26	0.045	0.069
30	0.074	0.123
55	0.075	0.044
59	0.049	0.167

penetrated through the least permeable layer in the puddled topsoil.

The saturated hydraulic conductivity of the least permeable layer in the puddled topsoil of the Padapada clay determined in the laboratory, was about 0.01 cm d⁻¹, compared with 0.1 cm d⁻¹ for Zaragoza clay loam (Table 11.6). Scenarios 1 and 2 seem therefore appropriate for Padapada, whereas scenarios 3 and 4 are more applicable to Zaragoza. This means that yield differences between Padapada and Zaragoza under rainfed conditions without any additional irrigation are large (Table 11.5).

The spatial distribution of risk due to temporary drought in the monsoon season in Tarlac can be mapped by assigning yield levels at different risk levels using a GIS. In this study, only one weather station was used, and a yield map therefore follows the boundaries delineated on the soil map.

Simulated rainfed rice yield was mapped at the 10 and 90% cumulative probability levels (Fig. 11.8). Simulations were conducted assuming average k_s values determined in the laboratory (Table 11.6) and a groundwater table depth of 1.0 m. The Zaragoza soil series occupies a large part of the province (Fig. 11.3, Table 11.2) and growing rice under rainfed conditions in the province is, therefore, risky.

For all soil types more effective puddling increased grain yields. Puddling may however create a zone of large resistance to root penetration at greater depth in the soil profile (plow pan). If this zone impedes exploration of the water reserves in the subsoil by the rice roots, puddling may have adverse effects on yield. This aspect was not investigated because of lack of good data on penetration resistance of the various soil types and its effect on root growth.

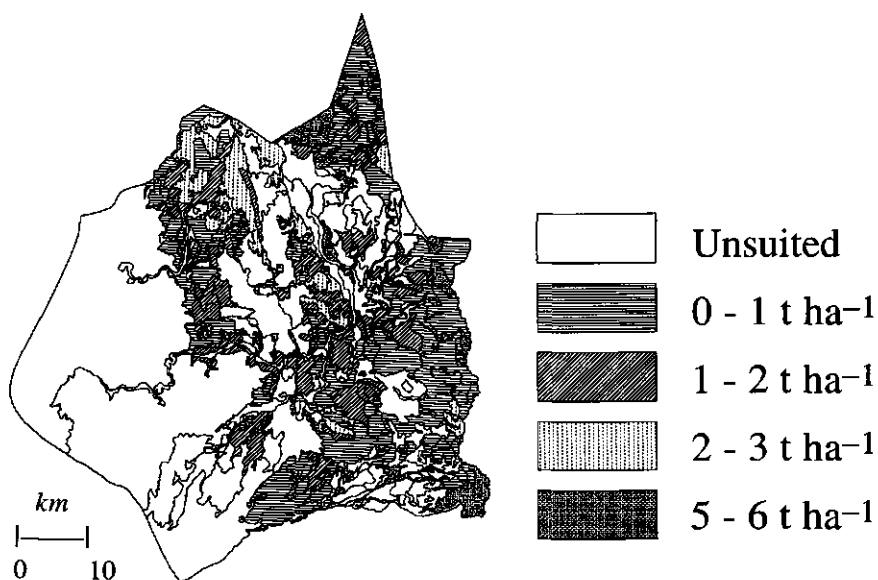


Fig. 11.8a Map of simulated rainfed rice yield (t ha^{-1}) at 10% cumulative probability.

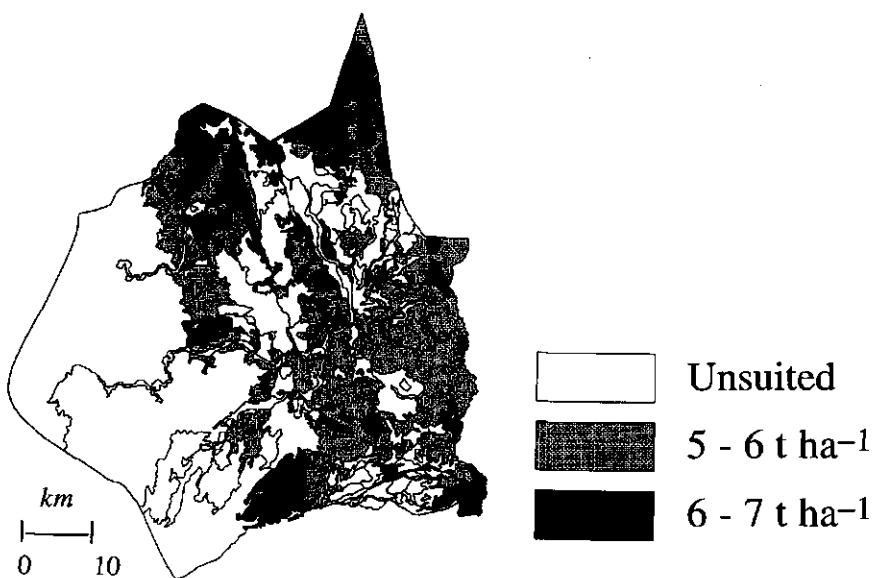


Fig. 11.8b Map of simulated rainfed rice yield (t ha^{-1}) at 90% cumulative probability.

Conclusions and implications

A methodology was presented to quantify rice yield losses due to drought at a regional level. This involves the following steps:

1 Collection of weather data

- Acquire long-term weather data from meteorological stations within the target area or within its immediate surroundings; assign zones to every meteorological station and create a weather map.

2 Inventarization of soil data

- Acquire an up-to-date detailed soil map (e.g. from the national soil survey institute).
 - If more soil units are distinguished on the soil map than can be sampled: reduce the total number of soil units by generalization, taking into account similarity in soil properties and importance of the unit in terms of surface area.
 - Select a representative profile for every (generalized) soil unit.
 - Locate every representative profile in the field, guided by the soil map.
 - Group soil horizons into hydraulic-functional horizons based on similarity in soil texture and soil structure.
 - Sample every hydraulic-functional horizon at each representative site.
 - Determine hydraulic properties of every hydraulic-functional horizon in the laboratory.
 - Interpolate to non-sampled areas using the (generalized) soil map.
 - Estimate course of groundwater table depth throughout the growing season per soil unit.
- 3 Identification of crop and soil management practices.
- 4 Identification of soil types that are unsuitable for rice.
- 5 Estimation of probability distributions of potential (irrigated) and water-limited (rainfed) rice yield for all combinations of suitable soil types and weather zones that occur within the target area using a validated crop-soil model.
- 6 Display of maps or tables of unsuitable land, irrigated and rainfed crop yields and yield gaps using the GIS software.

The methodology was illustrated with a case study conducted for the Philippine province of Tarlac. Only one weather zone could be distinguished for this province due to paucity of weather data. A sensitivity analysis on the impact of variability in input parameters on simulated rice yields was limited to two important soil parameters: groundwater table depth and saturated hydraulic conductivity of the least permeable layer in the soil profile. Risk involved in growing wet-season rice was quantified for seven major soil types. Production risk was relatively high for large parts of the province. Socio-economic analyses combined with crop modelling are needed to show if alternative land uses (e.g. growing sugarcane instead of rice) can be considered.

Groundwater table depth affected rice yield for some soil types due to capillary rise to the root zone. Long-term data on groundwater table depth are rare. For regional applica-

tion of models, an estimate of groundwater table depth must be made. Sometimes motting features in the soil profile can help to identify groundwater fluctuations during the growing season (Moormann and van Breemen, 1978).

The hydraulic conductivity of the least permeable layer in the puddled topsoil was an important determinant of rainfed rice yield for light-textured soils with a relatively permeable subsoil. If no information on this soil parameter is available, a constant percolation rate determined for the various soil types may be used as an input for the PADDY soil water balance module. Recent experimental results obtained at IRRI (Tuong and Wopereis, unpublished data) showed that lateral percolation losses toward and into bunds, and the effect of poorly puddled spots may be of importance in areas with a relatively permeable subsoil (see also Chapter 12). More complex numerical models that allow for lateral flow into the bunds (e.g. Walker and Rushton, 1984) are needed under these circumstances. On a regional scale, one-dimensional models, like the PADDY soil water balance module can still be used, provided a constant percolation rate is assumed, incorporating both vertical and lateral percolation losses.

Rainfall variability had a very strong impact on yield variability. Field experiments conducted for one or two years in such environments may give misleading results. Long-term weather data are needed to determine probability distributions of crop yield to perform an economic evaluation (Anderson, 1991). Unfortunately in many rice growing countries in Asia there is a lack of long-term weather data as was also the case in this study in Tarlac.

Supplementary irrigation increased wet season rainfed rice yields and reduced yield variability. Irrigation may also increase the potential for a dry-season crop (e.g. mung-bean) which would boost total crop production and income per year relative to rainfed conditions. The scope for a dry season crop after rice could be investigated using the PADDY soil-water balance module and a good descriptive model for the dry season crop.

In order to cope with climatic and soil variability, development of well-tested crop growth models and data bases on soil, climate and soil and crop management procedures is required. Coupling such models to a GIS allows spatial analysis of risks. If combined with socio-economic analyses this can be a very powerful tool for policy makers, which may ultimately benefit the farmer.

Chapter 12

General discussion

Rainfed rice is grown under lowland and upland conditions. Rainfed lowland rice comprises approximately 37 million hectares of land (harvested area) or 25% of total world rice area. With a total of 92 million t yr⁻¹ it produces 17% of global rice supply. Upland rice covers about 19 million hectares, and contributes 4% to world production, with average yields of 1 t ha⁻¹ or less (IRRI, 1993). Uncertainty and risk characterize rainfed environments. Farmers have to deal with drought spells, floods, typhoons, incidence of pests, diseases and weeds, rat and bird damage, adverse soil conditions and poverty, and have to make decisions on crop and soil management procedures, like timing of transplanting or fertilizer application.

Despite these problems most research has been focused on irrigated rice (IRRI, 1989) and relatively little attention has been paid to quantitative interpretation of experimental data using process-based simulation models. Especially in rainfed environments, such models can be very helpful in getting a better understanding of the system, as has been shown for many crops other than rice (e.g. Muchow et al., 1991; van Keulen et al., 1987). Drought screening or fertilizer trials may yield completely different results from one season to another. Such laborious field experiments must be conducted over a series of years and planting dates and on the relevant soil types to obtain results that can be used for recommendations. Moreover, extrapolation of the research findings to other areas is difficult. Simulation modelling facilitates the understanding of complex agricultural systems. It is a powerful tool in agricultural research, which can be used to focus field experimental work, which is often restricted because of time and expenses involved.

First objective of this thesis was to identify, adapt, and develop methods to characterize soil properties in rainfed rice ecosystems. Ultimate goal was to quantify the impact of soil and climate variability on rainfed rice yield using 'yield gap analysis' at a regional level. The concept of yield gaps is illustrated in Fig. 12.1. With optimal crop and soil management at both sites 1 and 2, yields may still differ due to differences in weather (i.e. solar radiation and temperature) and rice variety grown (yield gap 1). The maximum attainable yield at site 2 may be lower than its potential yield (yield gap 2) due to other yield limiting factors (e.g. availability of water and/or nutrients) and yield reducing factors (incidence of pests, diseases and weeds). In this thesis attention was focused on yield gaps due to water limitations only.

To estimate the spatial distribution of rainfed rice yield in a given target area, knowledge about the soil-crop-weather system and its variability in space and time is needed. For interpretation of spatial and temporal changes in the system, crop-soil simulation

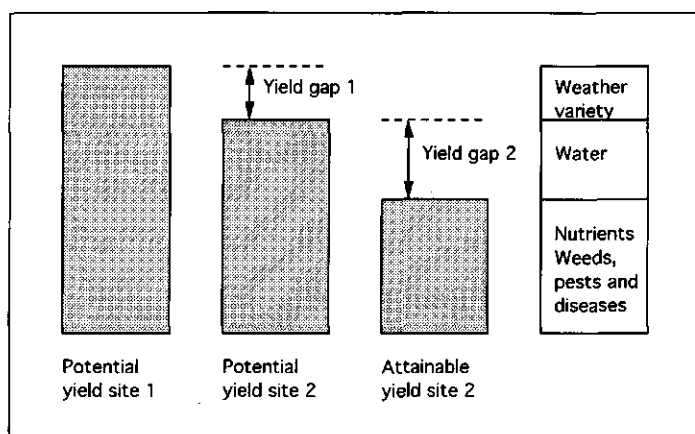


Fig. 12.1 Yield gap analysis.

models or expert knowledge may be used. To extrapolate the resulting information geostatistical techniques or Geographic Information Systems (GIS) are available. For this study, a new rainfed rice simulation model, suitable for puddled soils, was developed and coupled to a GIS to estimate rainfed rice production at a regional level. Greenhouse and field experiments intended for model development were conducted under optimal nutrient conditions and strict pest and diseases control.

Environmental characterization of rainfed rice ecosystems

An overview of procedures and tools that can be used in environmental characterization for yield gap analysis is given in Fig. 12.2. First of all a decision is needed on what systems approach to take. Bouma et al. (1993) distinguished five levels of systems approaches for soil environmental characterization. The required minimum data set for these levels increases proceeding from level 1 to 5 (Chapter 1). Crop models also differ in level of detail, ranging from simple equations like:

$$Y = S + G \times D \quad (12.1)$$

where, Y is the grain yield, S the net amount of allocated stem reserves, G the average growth rate per day in the grain-filling period, and D the length of the grain filling period (Kropff et al., 1992), to relatively complex models like ORYZA1 (Kropff et al., 1993a, Chapter 10).

The next step is to check if all data requirements can be fulfilled, i.e. if the minimum data set required is readily available (Fig. 12.2). If this is not the case additional measurements may be considered. Availability of appropriate measurement techniques

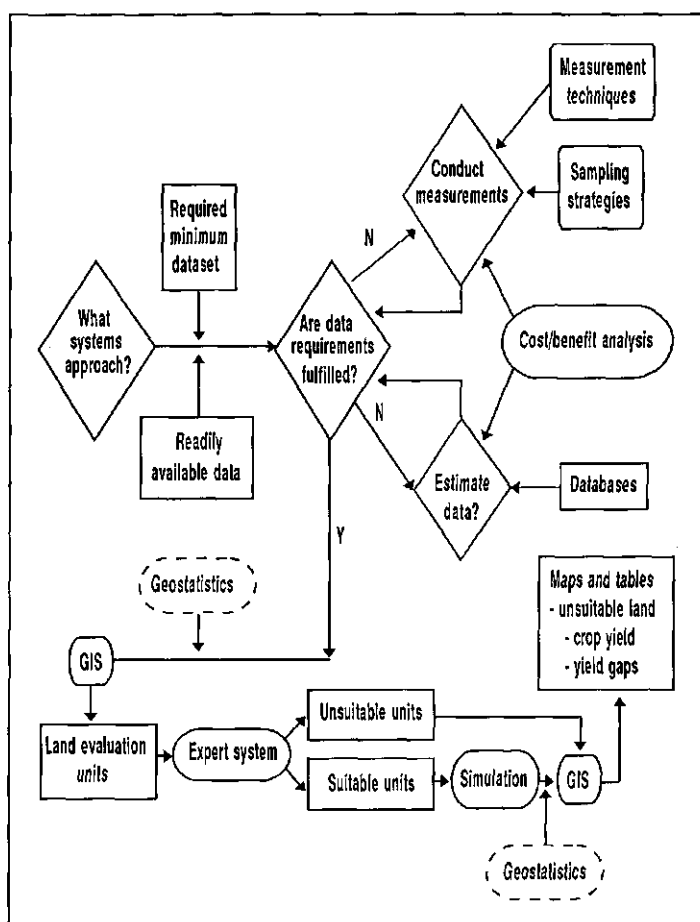


Fig. 12.2 Flow diagram for environmental characterization and regional yield gap analysis. Shown are tools, input - output data and decisions needed.

and sampling strategies and a cost/benefit analysis determine if measurements are conducted. If not, model input parameters may be estimated using databases. If this is also not an option, a more general systems approach should be adopted (Fig. 12.2).

After fulfilling all data requirements, spatial data can be stored in a GIS. Input data will usually include the geographical distribution of soil, climate and administrative units and associated attribute data (e.g. soil texture, rainfall, actual crop yield). Interpolation from point to areas of land may be done before or after model analysis; geostatistical interpolation techniques may be used for this purpose. An overlay of input data results in maps of Land Evaluation Units (LEUs). Each LEU is a unique combination of a soil, climate and administrative unit. An expert system is used to determine the suitability of each LEU for a specific land use. Crop simulation models are then applied to potentially

suitable LEUs to evaluate production constraints. Finally, the GIS software is used to display maps or tables of unsuitable land units, crop yields or yield gaps.

Various aspects of Fig. 12.2 were treated in detail in Chapters 2 - 11 and will be discussed below.

Minimum data sets

Weather data required for simulation models under fully irrigated conditions (Production Situation 1, PS1) are minimum and maximum temperature and solar radiation. For rainfed conditions (Production Situation 2, PS2), daily information on wind speed, relative humidity and rainfall is required as well (Chapter 1). A major problem for the use of simulation modelling techniques in rice growing countries in Asia is the paucity of long-term daily weather data, as was also observed in the case study presented in Chapter 11.

Crop parameters needed for PS1 were summarized in Chapter 1 for the ORYZA1 model. For water-limited environments, in addition 'drought stress factors' are needed that relate crop response to root zone water content (Chapter 10).

Soil information is only needed in PS2. An overview of the minimum data sets needed to use integral and differential soil-water balance modules is given in Chapter 1. An integral model especially developed for wetland soils (PADDY) was introduced in Chapter 10. Important additional data needs for this model include the moisture content of the puddled topsoil at saturation and a constant percolation rate in case of ponded water on the soil surface. PADDY can also simulate the impact of ponded water depth on percolation rate provided the saturated hydraulic conductivity of the least permeable layer in the puddled topsoil and the hydraulic conductivity characteristics of the subsoil are known (Chapter 10). In that case it can also deal with capillary rise from the groundwater table to the root zone.

Soil hydraulic functions (i.e. soil water retention and hydraulic conductivity) are difficult to measure, and it is, therefore, extremely helpful that they can be derived from more easily obtained soil characteristics, determined during routine soil surveys, using 'pedotransfer functions'. Class pedotransfer functions relate physical data to soil horizons. A standard series of 360 conductivity/retention curves for surface- and subsoils of some 150 soil profiles is used in the Netherlands (Wösten et al., 1987; Wösten et al., 1990). Such data sets can be used for studies carried out over large areas, like in zonation studies. Much work has been done to derive continuous pedo-transfer functions, i.e. to relate soil hydraulic characteristics to simple soil characteristics such as texture, bulk density, and organic matter content. At IRRI, efforts are underway to produce a data base for soils under rice cropping in Asia, together with soil scientists of National Agricultural Research Centres collaborating in research networks in Asia.

Environmental data on crop and soil management practices (e.g. is rice transplanted or direct-seeded, amount of fertilizer used, rainfed/irrigated) requires expert knowledge of the target area.

Measurement techniques

Standard techniques developed for upland soils (e.g. Klute, 1986) cannot be used in submerged freshly puddled soils as undisturbed samples are impossible to take. Measurements of puddled soil conductivity reported in literature usually refer to soil material that has not been continuously submerged. Upon drying, the soft puddled muddy layer gradually changes into a stiff paste and shrinkage cracks will form at the soil surface. This causes an irreversible change in soil structure ('ripening'). Reporting on the hydraulic conductivity of puddled soils is, therefore, only useful if soil conditions are clearly defined. In Chapter 2, an *in situ* method was introduced for the measurement of the hydraulic conductivity of continuously submerged puddled soils.

A clear definition of soil conditions is also of crucial importance when sampling for bypass flow measurements. Especially in heavily cracked, previously puddled clay soils, placement of the sample cylinder will largely determine the outcome of the measurements. Volume and depth of cracks and initial moisture content of the sample should be known before conducting any measurement (Chapter 7).

Differential models require knowledge of soil hydraulic conductivity and water retention functions. For this study, a large number of measurements were conducted using a range of techniques that were described elsewhere (Wopereis et al., 1993). Although a thorough comparison between all methods was beyond the scope of this study, it was concluded that for heavy textured soils the Wind method (Wind, 1968) should be preferred. The method yields both water retention and hydraulic conductivity data and results can be obtained within a few days. For lighter textured soils the Wind method is relatively time consuming. In that case the one-step outflow method (Kool et al., 1985) and modified by Booltink (pers. comm.) can be a good alternative.

Sampling strategies

Measurements should be conducted in soil horizons to provide a means for extrapolating soil physical information from point data to areas of land. The number of measurements can be reduced by focusing on 'hydraulic-functional horizons' that can be derived by merging individual soil horizons on basis of similarity of soil structure and soil texture (Chapter 4). Geostatistical techniques can be very helpful in designing sampling strategies to minimize the number of point observations needed to estimate the spatial variability of depth and thicknesses of soil horizons (Chapter 6).

Before embarking on an expensive measurement program, simulation models can be used to investigate the relative importance of model input parameters. In Chapter 4, it was concluded that sampling strategies for soil hydraulic functions should be based on a first rough comparison of the impact of weather variability and soil heterogeneity on yield variability using simulation and sensitivity analyses. In practice this means that for a new area a reconnaissance survey should be made to determine which major soil types occur within the area. For these major soil types some preliminary measurements are made of hydraulic conductivity and water retention. Sensitivity analyses using a simulation model are then conducted to reveal if additional measurements are needed.

The scale of spatial variation is important when defining sampling procedures. Three levels are distinguished in this thesis: field level (around 0.1 ha, Chapter 3), village level (around 100 ha, Chapter 6) and regional level (around 100,000 ha, Chapter 11). Intermediate forms occur between these levels.

Spatial sampling strategy at field level (Chapter 3)

Expert knowledge may sometimes indicate that soil variability in a certain area is likely to be low. In such cases appropriately designed sampling and measurement strategies, such as sequential *t*-testing, can allow substantial savings when compared with standard geostatistical sampling procedures, which implicitly assume presence of spatial data structure and require the estimation of a semivariogram based on at least 50 measurements. Sequential *t*-testing of infiltration rates in a puddled rice field was illustrated in Chapter 3.

Derivation of a semivariogram may be impractical for many studies, especially if measurements are laborious and expensive. Moreover, a small 0.1 ha field may have insufficient space for 50 - 60 measurements of a certain soil property, and simple averaging may be sufficient to make areal statements from point observations.

Spatial sampling strategy at village level (Chapter 6)

A village is defined here as an area comprising about 100 ha. At such scale, site specific recommendations for individual fields (or parts thereof) are often needed, rather than uniform recommendations for the 100 ha.

Geostatistical techniques can be used to estimate the spatial variability of a soil property using semivariograms and to make predictions for unvisited locations. Some 50 - 60 observations are needed to estimate a semivariogram. The decision where to locate these observations is governed by two conflicting considerations: the area should be covered as evenly as possible to minimize spatial uncertainty; on the other hand, some observations need to be close to each other to estimate short-range variability. The first consideration requires a regular grid pattern, the second requires additional observations at short distances. Sampling schemes to estimate a semivariogram were proposed by e.g. Russo (1984) and Warrick and Meyers (1987).

Sampling schemes for interpolation from point data to areas of land were discussed by McBratney et al. (1981) and McBratney and Webster (1981). They concluded that, if variation is isotropic (i.e. equal in all directions) a regular equilateral triangular sampling grid should be used. A square grid is however more convenient and will only result in slightly higher kriging variances.

In many studies prior information is available. This can be a soil map, or a number of point observations collected previously. If a soil map is available, it is recommended to sample separately within distinctly different soil units. This is called stratified sampling. Interpolation to areas of land should also be carried out separately for the various strata, i.e. stratified sampling, followed by stratified kriging.

Spatial sampling at regional level (Chapter 11)

In this thesis, a region is set to around 100,000 ha, or province size. At this level, statistical sampling is unaffordable. At the regional level, prior information may be available in the form of a small scale soil map. To characterize the different soil units, every property may be measured at representative sites (Chapter 11). One step further is to include spatial variability within units. Auger boring descriptions that were made during a soil survey are often shelved in national soil survey institutes. Such data can e.g. be used to assess the spatial variability of depth and thicknesses of soil horizons in soil units and their impact on the outcome of regional crop simulation studies.

Simulating rainfed rice production

Model development

Part of this study focused on the development of a new simulation model suitable for rainfed lowland rice grown in puddled soils (Chapter 10). The model was used to estimate rice yield losses due to drought at a regional level (Chapter 11). The importance of puddling intensity and groundwater table depth on yield was demonstrated.

Soil cracking in the soil-water balance module PADDY is treated in an empirical way. The moment cracks break through the least permeable layer in the puddled topsoil is related to a critical value of the soil moisture ratio in the root zone, derived from field experiments conducted at IRRI (Chapter 10). Volume of soil cracks can be predicted by PADDY provided the soil shrinkage characteristic of the puddled topsoil is known. More research is needed on ripening of puddled soils of different texture and soil cracking upon drying, with and without a rice crop. Increase in evaporation through cracks may accelerate the drying of a puddled bare soil, which is not taken into account in the current model version of PADDY. However, if a rice crop is grown, this effect will be small.

Under well-watered conditions PADDY assumes that rice roots will not grow deeper than 0.2 m. In case of drought stress, roots will grow deeper with a fixed exploration rate, e.g. 1 or 2 cm d⁻¹. More research is needed to investigate the impact of drought on rooting depth and root growth.

Drought stress responses of lowland rice were investigated through experiments (Chapters 8 and 10) and model development (Chapter 10). Changes in leaf morphology and relative transpiration resulting from temporary drought were related to soil-water status of the root zone. Relative transpiration rate per unit leaf area remained at a potential level, even at relatively severe stress levels (i.e. at soil pressure potentials clearly below -100 kPa). A similar observation was made by O'Toole and Cruz (1980). They gave as a possible explanation that a semi-aquatic species such as rice, may not respond in the same manner as a well adapted upland species. Drought stress responses were mathematically described in the module DSTRESS. The model ORYZA1 and the DSTRESS module do not yet account for sink limitations. Further model development could focus on this aspect, i.e. predicting the number of spikelets and number of filled and unfilled

grains under irrigated and water-limited conditions.

Extrapolation

Simulation modelling is a suitable tool for extrapolating research findings over regions, since it accounts for crop-environment interactions. It requires however a means to extend point-information over wider geographic areas and to combine data sets from different disciplines. Geostatistical techniques can be used for this purpose (Chapter 6) or a Geographical Information System (GIS), as was shown in Chapter 11.

As indicated by Burrough (1992) the quality of GIS-modelling studies would greatly improve by providing information on:

- Data collection, level of resolution and quality;
- The use of the basic analytical functions of the GIS, and
- Data requirements, sensitivity and error propagation in the models.

Burrough (1992) introduced the idea of an intelligent geographical information system that would confront the user with major sources of error in various data operations and would present a set of options with which better results could be achieved.

For rice, first concern is still the lack of data. Ready-to-use environmental data bases on soil, weather, and crop and soil management procedures at a range of scales are badly needed. Improvement and parameterization of models for the various Production Situations (Chapter 1) is another important issue. The errors that result from inaccuracies in the model, model parameters and soil and weather data input will determine for a large extent the quality of GIS-modelling studies on rice.

Increasing water use efficiency

The water use efficiency of rice (kg ha^{-1} of rice per kg ha^{-1} of water used) is much lower than for other crops. The benefits that can be gained from water saving techniques is enormous, as irrigation water is becoming more and more scarce for Asian rice farmers. In Chapter 7, a pre-tillage before reflooding rice fields before the next rice crop was introduced. The feasibility of such a new technology for different soil types and the likelihood that it will be accepted by the farmer can be investigated using simulation models and associated socio-economic analyses; the importance in terms of areas of land by combining the analysis with GIS.

Regional rice yield losses due to drought in the wet-season in the province of Tarlac, Philippines were estimated through combined use of GIS and the simulation model ORYZA1-DSTRESS-PADDY (Chapter 11). The analysis indicated which soil types were most susceptible to drought and would benefit most from improved irrigation facilities.

Simulation models can be used to investigate if shallow flooding of paddy rice fields increases water use efficiency as claimed by Tabal et al. (1992) and Hardjoamidjojo

(1992). Preliminary analyses using the differential SAWAH simulation model (ten Berge et al., 1992) showed that savings depend on the soil hydraulic conductivity of the subsoil and the thoroughness of puddling of the topsoil (Bouman et al., 1993).

Recent experiments conducted at IRRI (Tuong and Wopereis, unpublished data) showed that preferential flow through poorly puddled spots in a rice field and/or lateral flow to and down through bunds ('under-bund flow') may occur, especially in case of a relatively permeable subsoil. Under-bund percolation loss should be distinguished from lateral seepage, which is defined as horizontal flow through the bunds from one field to the other (Wickham and Singh, 1978; Chapter 9). While lateral seepage often results in no net loss to the field, except in peripheral fields, under-bund percolation may occur in every field, even in completely flat areas. Walker and Rushton (1984) identified under-bund percolation, which they called lateral percolation, as the main cause of low water use efficiency in certain irrigated rice fields. Under-bund percolation loss may be particularly important if the ratio between bund length and field surface area is large. Two-dimensional water balance models are needed to simulate lateral flow to and down through bunds. The PADDY soil water balance model can be used as well, provided a constant percolation rate is assumed, incorporating both lateral and vertical percolation losses.

These recent experimental results and those reported in Chapter 9 indicate that substantial water savings can be expected if shallow depths of ponded water are maintained in rice fields with a relatively permeable subsoil. Construction of 'seasonal bunds' after puddling a field, close to the bunds that are left undisturbed from year to year may also greatly reduce lateral percolation losses as it will prevent water from flowing toward and down through the bund. On a regional scale, such measures could have a major impact. In Chapter 11, the soil hydraulic properties of seven soil types under rice cropping in the Tarlac province were determined. Two of these soils have relatively permeable subsoils (as evidenced by a large hydraulic conductivity near saturation) occupying 50,000 ha or 40% of potentially suitable rice land within the province.

Dry seeding is more and more practiced as a means to increase the water use efficiency and thus the cropping intensity and productivity of rainfed rice ecosystems. Increased cropping intensity is possible due to early crop establishment and increased scope for a second rice crop. Dry seeding is already successfully used in Vietnam and Indonesia (Fujisaka et al., 1993). More experimental work and combined use of simulation modelling and GIS may identify other areas where this new technique may be adopted.

In Tamil Nadu, India, simulation models are being used to improve irrigation water conveyance efficiency and scheduling of centuries old tank irrigation systems. Evaluations of different cropping systems are conducted as well. (Palanisami, 1993; Kropff et al., 1993b).

Future challenges

Increasing the water use efficiency of rice-based cropping systems is becoming more and more important. This can be done through improvement of irrigation facilities, introduction of water savings techniques and adjustment of choice of crop and/or planting time. For any of these approaches, a thorough systems analysis is needed to evaluate different solutions for different environments. Research in rice-based cropping systems should move away from standard agronomy trials and recommendations based on analyses of variance. Results from such experiments usually cannot be extrapolated to other environments and are, therefore, of little use. The response of a rice crop to adverse environmental conditions, or the opportunities for a new water saving technology cannot be studied by one or two years experiments in one farmer's field or experimental station. What is needed is a systems approach to research, in which problems and opportunities for rice production are evaluated through a better understanding of the dynamic processes in the crop-soil-weather system rather than through trial and error. Numerous drought screening trials have been conducted where rice suffered from N deficiency rather than from drought stress. High fertilizer input, monitoring of the soil-water status of the root zone and the N content of the plant and interpretation of the data with validated simulation models would improve the efficiency of screening activities.

In this thesis several options for water saving techniques were identified. The introduction of a pre-tillage before reflooding a dry, cracked rice field may reduce the amount of water needed for land preparation (Chapter 7). Maintaining shallow depths of ponded water in the rice field and construction of extra bunds ('seasonal bunds') after puddling the field, close to the bunds that are left undisturbed from year to year, may also greatly reduce water use (Chapter 9, this chapter). GIS and simulation modelling may be used to identify areas that are expected to benefit from such technologies.

Unfortunately, what is lacking most for effective application of models at the regional level are suitable data. Data base development is far behind model development. Sophisticated extrapolation tools like GIS and kriging are readily available, but they depend on input data, derived from field surveys, meteorological stations, national soil survey institutes, research networks etc. National and international agricultural research centres should work together to optimize the number of field monitoring sites in research networks. Key sites in such consortia should be carefully selected. It is better to have fewer but well-maintained sites that are carefully monitored. Only if good data sets are available, simulation models can be used to extrapolate new technologies or to identify constraints to rice production. Minimum data sets for key site characterization and standard methodologies for collecting soil and climate data should be identified. One of the major problems for application of crop-soil models is the lack of data on soil hydraulic functions. Data bases are needed that relate these functions to soil characteristics that can be derived from soil survey data. Maintenance and installment of weather stations should be stimulated. More research is needed on how to deal with limited weather data in regional crop simulation studies.

Different applications often require models with different levels of complexity. Complex models can be used for in-depth research, and simple, but robust, rice crop models can be used for extrapolation. Usually simple models will be derived from carefully tested complex models. The rainfed rice model presented in this thesis can be used to investigate yield losses due to drought in rainfed environments and may be used to quantify the benefits of improved irrigation facilities. It is also a starting point for simulation studies on rice-upland crop rotations. The model still needs to be validated for a broader range of environmental conditions. Further research is required to study drought stress effects on sink size formation (i.e. spikelet formation, ratio filled-unfilled grains) and on root growth and soil cracking and ripening processes in puddled soils.

More and more agricultural land in rice growing countries in Asia is converted into industrial areas and housing compounds, and water available for agricultural use is getting scarce. Problems and opportunities in rice production will vary from one place to another. A systems approach to research, frequent field monitoring and interaction with farmers is essential in finding the appropriate solutions.

Summary

Population pressure and demand for water and land in rice-growing countries in Asia are growing rapidly. There is a strong need for an increase in production from existing rice fields. In rainfed environments, whether lowland or upland, water is the major factor that determines rice production. The same holds for irrigated ecosystems, because the volume of water that is required for land preparation and for maintaining adequate soil moisture conditions throughout the growing season determines the area of land that can be serviced by a particular irrigation facility. Efficient management of soil-water, whether its source is rainfall or irrigation, is thus vital to global rice production.

This study aimed at quantification of the impact of soil and climate variability on rainfed rice production. To meet this objective, measurement techniques and sampling strategies to characterize soil hydraulic properties in soils under rice cropping were identified and adapted (Chapters 2 - 6). Field and greenhouse experiments were conducted (Chapters 7 - 9), and a rainfed lowland rice model was developed (Chapter 10). The model was coupled to a Geographic Information System to predict rice yield losses due to drought at a regional level (Chapter 11).

Lowland rice, whether rainfed or irrigated, is usually grown in soils that have been puddled, i.e. plowed, harrowed and levelled under (near) water-saturated conditions. Puddling destroys soil structure, and transforms the topsoil into a muddy layer. Undisturbed soil samples are virtually impossible to take under such conditions and standard measurement techniques are often not applicable. In Chapter 2, a method was introduced for *in situ* measurement of water-percolation rate and soil-water pressure gradients in puddled rice soils. Such data can be used to calculate the soil's hydraulic conductivity at different depths. The method was tested by conducting 36 measurements in a submerged rice field. Results showed that the hydraulic resistance in a puddled topsoil is largest at the interface of puddled and non-puddled soil material. Corresponding average hydraulic conductivity was 0.36 mm d^{-1} . The formation of this least permeable layer was attributed to translocation of clay particles and compaction of the non-puddled subsoil by animal hooves. Especially if the non-puddled subsoil is relatively permeable, this layer is an important determinant of water economy and rice production.

Measurements of infiltration rate are time consuming and costly; their number of measurements should, therefore, be minimized. Percolation rates in puddled rice fields are expected to show little spatial variability and a standard geostatistical analysis, requiring 50 - 60 observations seems, therefore, redundant. In Chapter 3, the field average for infiltration rate in a 0.05 ha puddled experimental field was determined using a sequential *t*-test, thus reducing the number of measurements needed by 85% to only 8.

For rainfed rice, spatial and temporal variability of root zone water content strongly determines the yield response. Spatial variation of soil properties can be described by discrete and continuous spatial models (Chapter 1). Soil maps used in Chapters 4, 6 and

11 are examples of discrete spatial models; the geostatistical model is an example of a continuous spatial model (Chapter 2, 6). Temporal variation of soil properties can be described using simulation models. In this thesis a distinction is made between integral and differential models. Differential models describe water distribution in soils by solving the general flow equation; integral models use integrating (over time and/or depth) calculations instead (Chapter 1).

A differential model, like the SAWAH soil-water balance module (Chapters 4, 5, 6 and 9) requires knowledge of the soil's water retention and hydraulic conductivity characteristics. Measurement of such hydraulic functions should focus on soil horizons to allow extrapolation to other sites where no sampling has been carried out through simple knowledge of the soil profile (Chapter 4). Measurements of soil hydraulic conductivity and water retention functions are expensive and time consuming. Merging 'classical' soil horizons into broader, hydraulic functional horizons that are similar in terms of soil hydraulic functions is, therefore, attractive. In this study the feasibility of identifying hydraulic-functional horizons from visual appraisal of texture and structure during a field survey was demonstrated (Chapter 4).

A variability analysis in Chapter 4 showed that the effect of variation in soil hydraulic properties in a 50 ha dryland rice area on simulated rice yield was relatively small compared to the effect of variation in year to year weather conditions. In Chapter 5, three methods to derive soil hydraulic conductivity functions were compared for two 0.05 ha test sites within a 1.0 ha field used for dryland rice. Differences in hydraulic conductivity functions obtained by the three methods were large but differences in model performance were small because simulation results were relatively insensitive to hydraulic conductivity input data. In Chapter 9, simulated values of ponded water depth were very much affected by the differences in the saturated hydraulic conductivity of the least permeable layer in the puddled topsoil, whereas the variation in measured hydraulic properties of the subsoil had no effect. It was concluded that sampling strategies for soil hydraulic functions should be based on a first rough comparison of the impact of weather variability and soil heterogeneity on yield variability using simulation and sensitivity analyses.

In Chapters 4 and 6, a detailed soil survey conducted in a 50 ha dryland rice area (144 auger observations) is described. Nonsubmerged rice yield for this study area was simulated in two different ways. In Procedure 1, simulations were conducted for six sites, representative for the six soil units distinguished within the area. In Procedure 2, simulations were conducted for all auger observations and results were interpolated to areas of land using block kriging. It was concluded that sensitivity analyses, conducted for a number of clearly different years and based on expert knowledge on soil variability, are needed to determine if use of a soil map for spatial interpolation purposes is adequate. If the model is sensitive to spatial variability within a soil unit, use of the soil map for prediction purposes for specific sites cannot be recommended. Additional auger observations are then needed and kriging may be used to interpolate such extra point observations to areas of land. The best procedure for spatial interpolation of simulated rice yield should, therefore, follow from preliminary simulation and sensitivity analyses of the im-

impact of weather variability and soil heterogeneity on yield variability and associated cost-benefit calculations (Chapter 6).

Water flow into vertically continuous soil macropores (such as cracks or worm channels) that bypass a surrounding unsaturated soil matrix is termed 'bypass flow'. Reducing water losses through bypass flow is important in rice growing areas (rainfed and irrigated) where water losses during land preparation for rice are high due to soil cracking on the surface and a relatively permeable subsoil. Shallow surface tillage (0 - 5 cm) applied to a dry, cracked previously puddled experimental field using a rototiller, resulted in 45 - 60% water savings in a laboratory experiment. For rainfed rice areas, introduction of this tillage practice may lead to earlier transplanting and, therefore, reduced risk of late drought. In some areas this may broaden the scope for a second crop. In irrigated rice systems, water savings during land preparation may enable an increase in the command area of an irrigation system (Chapter 7).

In Chapter 9, the water use efficiency of a puddled rice field was studied by analyzing the components of the water balance in the field and through simulation modelling. Seepage and percolation (SP) losses were the main determinants of water use efficiency in a field experiment conducted in the Philippines. Seepage through and underneath bunds can greatly increase total water loss. SP rates in well-puddled soil varied between 0.4 cm d⁻¹ without seepage to 3.62 cm d⁻¹ with seepage, and cumulative SP losses varied between 88 and 350 cm per crop cycle. Maintaining shallow depth of ponded water and construction of extra bunds after puddling the field, close to bunds that are left undisturbed from year to year, may reduce water use (Chapters 9 and 12).

The responses of two lowland rice cultivars (IR20 and IR72) to temporary drought were studied in a greenhouse experiment using over 650 pots of 20 cm diameter and 25 cm height. Yield differences between plants that were temporarily stressed in the vegetative phase and well-watered plants were not significant. However, flowering and maturity were strongly delayed. Severe drought in the reproductive phase resulted in large yield reductions. The following morphological and physiological plant responses to soil moisture content were quantified for different growth stages: (1) rate of new leaf production; (2) rate of leaf rolling; (3) rate of senescence; and (4) relative transpiration rate (Chapter 8).

In this study, a new integral soil-water balance module (PADDY) suitable for puddled rainfed lowland soils and a module predicting the response of rice to drought (DSTRESS) were developed (Chapter 10). PADDY predicts changes in ponded water depth and root zone water content and accounts for root zone volume changes due to soil shrinkage. DSTRESS contains functions derived in the greenhouse study described in Chapter 8. DSTRESS and PADDY were coupled to a crop growth simulation model (ORYZA1) to simulate rice growth and production in rainfed lowland rice ecosystems. The combined PADDY-DSTRESS-ORYZA1 model was validated using two field experiments in the Philippines. The model satisfactorily predicted changes in ponded water depth, root zone water content, leaf area index, total above-ground dry matter and panicle dry weight across drought treatments over time.

The soil hydraulic properties of seven major soil types under rice cropping occurring within the province of Tarlac in the Philippines were determined (Chapter 11). The crop growth model ORYZA1-DSTRESS-PADDY, introduced in Chapter 10, was used to predict rainfed rice yield as a function of these soil characteristics and long-term weather information (25 years). Risk involved in growing rainfed rice was quantified by calculating yield probability distributions for each soil type. Spatial variability of simulated rainfed rice yield within the province was analyzed using a Geographic Information System (Chapter 11).

In Chapter 12, the results of this study are discussed in view of the increasing use of simulation models in rice growing countries for estimation of potential yields and yield gaps, priority setting in research and extrapolation of new technologies.

Samenvatting

Het gebruik van land en water voor niet agrarische doeleinden in rijstproducerende landen in Azië neemt de laatste jaren sterk toe. Tegelijkertijd is meer voedsel nodig voor een nog altijd groeiende bevolking. Dit betekent dat in de meeste landen de rijstteelt geïntensiveerd moet worden, aangezien een produktiestijging door het in gebruik nemen van meer grond niet tot de mogelijkheden behoort. Beschikbaarheid van water is één van de belangrijkste opbrengstbepalende factoren voor produktie in niet-geïrrigeerde rijstbouw. Dat geldt echter ook voor geïrrigeerde gebieden, omdat het volume water dat vereist is voor grondbewerking en het nat houden van de bodem gedurende het groeiseizoen het maximale areaal bepaalt dat een irrigatiesysteem kan omvatten. Efficiënt waterbeheer in zowel geïrrigeerde als niet-geïrrigeerde rijstbouw is dus van cruciaal belang voor de rijstproduktie.

Het onderzoek heeft zich gericht op het kwantificeren van de gevolgen van bodem- en klimaatsvariabiliteit voor de niet-geïrrigeerde rijstproduktie. Om aan deze doelstelling te voldoen zijn een aantal meetmethoden en bemonsteringsstrategieën getest en aangepast waarmee de bodemfysische karakteristieken kunnen worden bepaald van bodems in gebruik voor de natte rijstteelt (Hoofdstukken 2 - 6). Diverse kas- en veldproeven zijn uitgevoerd (Hoofdstukken 7 - 9) en een simulatiemodel voor niet-geïrrigeerde rijstbouw is ontwikkeld (Hoofdstuk 10). Dit model is gekoppeld aan een geografisch informatiesysteem om op regionaal niveau opbrengstredukties bij rijst als gevolg van droogte te kunnen voorspellen (Hoofdstuk 11).

Rijst wordt in Azië veelal verbouwd in 'gepuddelde' bodems, geploegd en geëgaliseerd onder waterverzadigde omstandigheden. Het proces van puddelen vernietigt de structuur van de bodem en verandert de bovengrond in een modderige laag. Ongestoorde bodemmonsters kunnen onder zulke omstandigheden nauwelijks gestoken worden en standaard meettechnieken zijn veelal niet toepasbaar. In Hoofdstuk 2 wordt een methode gepresenteerd die *in situ* bepaling toelaat van de infiltratiesnelheid en tevens van gradiënten in vochtspanning in gepuddelde gronden. Zulke gegevens kunnen gebruikt worden om de doorlatendheid van de bodem te berekenen op verschillende dieptes. De methode is getest door middel van 36 metingen in een onder water staand rijstveld. De resultaten geven aan dat de hydrologische weerstand in een gepuddelde bovengrond het grootst is op de grens van gepuddeld en niet-gepuddeld bodemmateriaal. De gemiddelde doorlatendheid van deze laag was slechts 0.36 mm per dag. Het ontstaan van deze buitengewoon slecht doorlatende laag wordt toegeschreven aan uitspoeling van kleideeltjes en verdichting van de bodem door het veelvuldig gebruik van waterbuffels voor ploegwerk in de natte rijstbouw. Deze ondoorlatende laag is erg belangrijk voor efficiënter gebruik van water en voor de rijstproduktie in het algemeen, vooral in het geval van een relatief doorlatende ondergrond.

Metingen van infiltratiesnelheden zijn tijdrovend en het aantal bepalingen moet

daarom beperkt gehouden worden. De verwachting is dat infiltratiesnelheden in gepuddelde gronden slechts een geringe mate van ruimtelijke variabiliteit zullen vertonen. Een standaard geostatistische analyse waarvoor 50 - 60 waarnemingen nodig zijn lijkt voor dit soort gronden dan ook overbodig. Daarom is (Hoofdstuk 3) een sequentiële *t*-test gebruikt om het minimale aantal metingen te bepalen dat noodzakelijk is om een veldgemiddelde voor de infiltratiesnelheid te berekenen. Toepassing van deze procedure bracht het aantal benodigde metingen terug van 56 tot 8, een reductie met 85%.

De variabiliteit van het watergehalte binnen de wortelzone in ruimte en tijd bepaalt in sterke mate het produktieniveau in de niet-geïrrigeerde rijstbouw. De ruimtelijke variabiliteit van bodemeigenschappen kan beschreven worden door discrete en continue ruimtelijke modellen (Hoofdstuk 1). Bodemkaarten zijn voorbeelden van discrete ruimtelijke modellen (Hoofdstukken 4, 6 en 11); het toepassen van geostatistische technieken leidt tot een continue beschrijving van een bodemvariabele (Hoofdstukken 2 en 6).

De variabiliteit van bodemeigenschappen in de tijd kan beschreven worden met simulatiemodellen. Het gebruik van het SAWAH bodem-water balans simulatiemodel (Hoofdstukken 4, 5, 6 en 9) vereist kennis van de waterretentie- en doorlatendheidskarakteristieken van de bodem. Het meten van zulke karakteristieken kan zich het beste richten op bodemhorizonten om het extrapoleren van bodemfysische informatie te vereenvoudigen (Hoofdstuk 4) maar metingen blijven duur en tijdrovend. Het samenvoegen van 'klassieke' bodemhorizonten, met vergelijkbare hydrologische eigenschappen, tot bredere, hydraulisch-funktionele horizonten, is daarom aantrekkelijk. In dit proefschrift wordt aangetoond dat het mogelijk is zulke funktionele horizonten al in een vroeg stadium in het veld te onderscheiden, op grond van overeenkomsten in textuur en structuur (Hoofdstuk 4).

In Hoofdstuk 4 wordt aangetoond dat het effect van de variatie in bodem-hydrologische eigenschappen in een rijstgebied van 50 ha op de gesimuleerde rijstproduktie relatief gering is vergeleken met de invloed van de weersvariabiliteit. In Hoofdstuk 5 worden drie methoden vergeleken voor het bepalen van de doorlatendheidskarakteristiek van twee rijstveldjes van 0.05 ha. De onderlinge verschillen zijn groot maar dit had weinig invloed op de uitkomsten van het model omdat dit relatief ongevoelig bleek voor de doorlatendheidskarakteristiek. Simulaties van de dikte van de waterlaag boven een rijstveld (Hoofdstuk 9) worden in sterke mate beïnvloed door de doorlatendheid van de gepuddelde bovengrond. Variatie in de doorlatendheidskarakteristiek van de ongepuddelde ondergrond had geen enkel effect. In dit proefschrift wordt daarom aangeraden bemonsteringsstrategieën te baseren op een eerste schatting van de invloed van bodem- en weersvariabiliteit op rijstopbrengst met behulp van simulatie- en gevoeligheidsanalyses.

In de Hoofdstukken 4 en 6 wordt een gedetailleerde bodemkartering (144 boringen tot 2.2 m diepte) beschreven, uitgevoerd in een rijstgebied van 50 ha. De rijstopbrengst voor dit studiegebied werd gesimuleerd op twee verschillende manieren. De simulaties in Procedure 1 werden uitgevoerd voor slechts 6 plekken. Deze worden echter represen-

tatief geacht voor de 6 bodemeenheden die in het studiegebied werden onderscheiden. Simulaties in Procedure 2 werden uitgevoerd voor alle boringen en de resultaten werden geïnterpoleerd naar landoppervlakte door middel van blokkering. Uit de studie werd afgeleid dat gevoeligheidsanalyses, uitgevoerd voor een aantal duidelijk verschillende jaren en gebaseerd op deskundige kennis, nodig zijn, om uit te maken of een bodemkaart voor interpolatiedoeleinden gebruikt kan worden. Indien het model gevoelig is voor ruimtelijke variabiliteit binnen bodemeenheden moet het gebruik van een bodemkaart worden afgeraden. Extra boringen zijn dan nodig, en kriging kan worden gebruikt voor interpolatie van simulatieresultaten van punt (boringen) naar vlak (rijstvelden). In Hoofdstuk 6 wordt aangeraden het kiezen van de interpolatieprocedure te laten afhangen van verkennende simulatie- en gevoeligheidsanalyses van de invloed van weers- en bodemvariabiliteit op de simulatieresultaten en van een kosten-baten analyse.

In Hoofdstuk 7 wordt ingegaan op het proces van kortsluiting van water in onverzadigde gronden ('bypass flow'). Hierbij stroomt water door macroporiën (scheuren en wormgangen) naar beneden zonder de bovengrond te bevochtigen. Herbevochtiging vindt pas plaats op enige diepte in de ondergrond. Het verminderen van bypass flow is belangrijk in zowel geïrrigeerde als niet-geïrrigeerde rijstbouw. Vooral tijdens de grondbewerking voor aanvang van het natte groeiseizoen, kunnen aanzienlijke waterverliezen optreden in het geval van een gescheurde bovengrond en een relatief doorlatende ondergrond. Eveneens in Hoofdstuk 7 worden experimenten beschreven om de omvang van bypass flow te kunnen vaststellen. Oppervlakkige grondbewerking (0 - 5 cm) van een droge, gescheurde en gepuddelde kleigrond resulteerde in een vermindering van waterverlies met 45 - 60% in een laboratorium experiment. Introductie van deze grondbewerking kan in niet-geïrrigeerde gebieden leiden tot vroegere verplanting en verkleint daarmee het risico van droogte aan het eind van het groeiseizoen. In sommige gevallen kan dit mogelijkheden bieden voor een tweede gewas. Voor de geïrrigeerde rijstteelt betekent een besparing op waterverbruik tijdens de grondbewerking dat het gebied dat een irrigatiesysteem bestrijkt aanzienlijk vergroot kan worden.

In Hoofdstuk 9 wordt de efficiëntie van watergebruik van een gepuddeld rijstveld geanalyseerd door middel van het kwantificeren van de componenten van de bodemwaterbalans. Verliezen als gevolg van wegzijging en percolatie (SP) bepaalden in belangrijke mate het waterverbruik in een veldexperiment uitgevoerd in de Filippijnen. SP snelheden in een goed gepuddelde grond varieerden van 0.4 cm d⁻¹ zonder wegzijging tot 3.62 cm d⁻¹ met wegzijging, en cumulatieve SP verliezen varieerden van 88 tot 350 cm per groeiseizoen. Het handhaven van een lage waterstand op het rijstveld en de aanleg van extra dijkjes ('bunds') na het puddelen, op enige afstand van bestaande, permanente bunds kan het waterverbruik verminderen (Hoofdstukken 9 en 12).

De response van twee rijstcultivars IR20 en IR72 op tijdelijke droogte is onderzocht in een kasexperiment, gebruik makend van 650 potten van 20 cm diameter en 25 cm hoogte. Opbrengstverschillen tussen planten die tijdelijk aan droogte werden blootgesteld in de vegetatieve fase, en continu natgehouden planten waren niet significant. Tijdstip van bloei en oogst werden door droogte echter sterk vertraagd. Ernstige droogte in de

reproductieve fase veroorzaakte grote opbrengstredukties. De volgende fysiologische en morfologische reacties op bodemvochtgehalte werden gekwantificeerd voor verschillende groeistadia van de plant: (1) snelheid van nieuwe bladproductie, (2) snelheid van het oprollen van blad, (3) snelheid van het afsterven van blad en (4) relatieve transpiratiesnelheid (Hoofdstuk 8).

In dit onderzoek is een nieuwe bodem-water balans model (PADDY) ontwikkeld, geschikt voor gepuddelde rijstbouw en een module (DSTRESS) dat de reactie van de rijstplant op droogte in verschillende groeistadia beschrijft (Hoofdstuk 10). PADDY voorspelt veranderingen in de dikte van de waterlaag op het veld, in vochtgehalte van de bewortelde laag en houdt rekening met volumeveranderingen als gevolg van krimp van de gepuddelde bovengrond. In DSTRESS zijn de functies opgenomen die afgeleid werden in Hoofdstuk 8. DSTRESS en PADDY zijn gekoppeld aan een gewasgroei model (ORYZA1) om rijstproductie te simuleren voor niet-geïrrigeerde gebieden. De combinatie PADDY-DSTRESS-ORYZA1 is gevalideerd met behulp van twee veldexperimenten uitgevoerd in de Filipijnen. Het model is in staat temporele veranderingen in dikte van de waterlaag op het veld, bodemvochtgehalte, bladoppervlak, en drogestof gewichten goed te voorspellen (Hoofdstuk 10).

In Hoofdstuk 11 wordt een case-study gepresenteerd naar de mogelijkheid om op regionaal niveau rijstopbrengstverliezen als gevolg van droogte te voorspellen. Hiervoor zijn de bodemfysische karakteristieken van de zeven belangrijkste bodemtypes in gebruik voor natte rijstbouw in de provincie Tarlac in de Filipijnen bepaald. Het gewasgroei model ORYZA1-DSTRESS-PADDY, geïntroduceerd in Hoofdstuk 10, is gebruikt om niet-geïrrigeerde opbrengsten te voorspellen als functie van bodemeigenschappen en weersgegevens (25 jaar). Het risico van opbrengstreduktie als gevolg van droogte werd gekwantificeerd door het berekenen van opbrengstkansverdelingen voor ieder bodemtype. De ruimtelijke variabiliteit van gesimuleerde niet-geïrrigeerde rijstopbrengsten werd geanalyseerd met behulp van een geografisch informatiesysteem.

In Hoofdstuk 12 worden de resultaten van dit onderzoek belicht in het kader van het toenemende gebruik van simulatiemodellen in rijstproducerende landen voor het schatten van potentiële opbrengsten, opbrengstverliezen, het stellen van onderzoeksprioriteiten en het extrapoleren van nieuwe teelttechnieken.

References

- Adachi, K., 1990. Effects of rice-soil puddling on water percolation. In: Transactions of the 14th International Congress of Soil Science. Vol. I. ISSS, Kyoto, Japan, pp. 146-151.
- Adachi, K. and Ishiguro, M., 1987. Water requirement and percolation. In: Physical measurements in flooded rice soils. The Japanese methodologies. International Rice Research Institute, Los Baños, Philippines, pp. 35-48.
- Ahuja, L.R., Naney J.W. and Williams, R.D., 1985. Estimating soil water characteristics from simpler properties or limited data. *Soil Sci. Soc. Am. J.* 49: 1100-1105.
- Anderson, J.R., 1991. A framework for examining the impacts of climatic variability. In: Muchow, R.C. and Bellamy, J.A. (Eds), *Climatic Risk in Crop Production: Models and Management for the Semiarid Tropics and Subtropics*. CAB International, Wallingford, UK, pp. 3-17.
- Angus, J.F., 1991. The evolution of methods for quantifying risk in water limited environments. In: Muchow, R.C. and Bellamy, J.A. (Eds), *Climatic Risk in Crop Production: Models and Management for the Semiarid Tropics and Subtropics*. CAB International, Wallingford, UK, pp. 39-53.
- Angus, J.F. and Zandstra, H.G., 1980. Climatic factors and the modelling of rice growth and yield. In: Proceedings of the WMO-IRRI symposium on Agrometeorology of the rice crop. International Rice Research Institute, Los Baños, Philippines, pp. 189-199.
- Aragon, E.L., De Datta, S.K., Buresh, R.J. and Evangelista, R.C., 1987. Increased lowland rice yield through improved fertilizer and water management practices. *Phil. J. Crop Sci.* 12: 151-161.
- Arya, L.M., Farrell, D.A. and Blake, G.R., 1975. A field study of soil water depletion patterns in presence of growing soybean roots. I. Determination of hydraulic properties of the soil. *Soil Sci. Soc. Am. Proc.* 39: 424-430.
- Belmans, C., Wesseling, J.G. and Feddes, R.A., 1983. Simulation model of the water balance of a cropped soil: SWATRE. *J. Hydrol.* 63: 271-286.
- Berge, H.F.M. ten, Jansen, D.M., Rappoldt, K. and Stol, W., 1992. The soil water balance module SAWAH: user's guide and outline. CABO-TPE Simulation Report Series, no. 22. CABO, Wageningen, The Netherlands, 78 pp. + appendices.
- Beven, K. and Germann, P.F., 1982. Macropores and water flow in soil. *Water Resour. Res.* 18: 1311-1325.
- Bhuiyan, S.I., 1987. Irrigation technology for Food Production: Expectations and Realities in South and Southeast Asia. In: Jordan, W.R. (Ed.), *Water and Water Policy in World Food Supplies*, Texas A&M University Press, pp. 325-334.
- Bloemen, G.W., 1980. Calculation of hydraulic conductivities of soils from texture and organic matter content. *Z. Pflanzenernähr. Bodenkd.* 143 (5): 581-615.

- Boels, D., van Gils, J.B.H.M., Veerman, G. and Wit, K.E., 1978. Theory and system of automatic determination of soil moisture characteristics and unsaturated hydraulic conductivities. *Soil Sci.* 126: 191-199.
- Bolton, F.R. and Zandstra, H.G., 1981. A soil moisture based yield model of wetland rainfed rice. IRRI Research Paper no. 62. International Rice Research Institute, Los Baños, Philippines.
- Booltink, H.W.G. and Bouma, J., 1991. Physical and morphological characterization of bypass flow in a well-structured clay soil. *Soil Sci. Soc. Am. J.* 55: 1249-1254.
- Booltink, H.W.G., Bouma, J. and Gimenez, D., 1991. A suction crust infiltrometer for measuring hydraulic conductivity of unsaturated soil near saturation. *Soil Sci. Soc. Am. J.* 55: 566-568.
- Bouma, J., 1982. Measuring the hydraulic conductivity of soil horizons with continuous macropores. *Soil Sci. Soc. Am. J.* 46: 438-441.
- Bouma, J., 1990. Using morphometric expressions for macropores to improve soil physical analysis of field soils. *Geoderma* 46: 3-13.
- Bouma, J. and Dekker, L.W., 1978. A case study of infiltration into dry clay soil. *Geoderma* 20: 27-51.
- Bouma, J. and Wösten, J.H.M., 1979. Flow patterns during extended saturated flow in two undisturbed swelling clay soils with different macrostructures. *Soil Sci. Soc. Am. J.* 43: 16-22.
- Bouma, J. and de Laat, P.J.M., 1981. Estimation of the moisture supply capacity of some swelling clay soils in The Netherlands. *J. Hydr.* 49: 247-259.
- Bouma, J. and van Lanen, H.A.J., 1987. Transfer functions and threshold values: from soil characteristics to land qualities. In: Beek, K.J. et al. (Eds), *Proceedings of the Workshop by ISSS/SSSA on Quantified Land Evaluation Procedures*. ITC Publication 6, Enschede, The Netherlands, pp. 106-111.
- Bouma, J., Dekker, L.W. and Muilwijk, C.J., 1981. A field method for measuring short-circuiting in clay soils. *J. Hydrol.* 52: 347-354.
- Bouma, J., Belmans, C., Dekker, L.W. and Jeurissen, W.J.M., 1983. Assessing the suitability of soils with macropores for subsurface liquid waste disposal. *J. Environ. Qual.* 12: 305-310.
- Bouma, J., Wopereis, M.C.S., Wösten, J.H.M. and Stein, A., 1993. Soil data for crop-soil models. In: Penning de Vries, F.W.T., Teng, P.S. and Metselaar, K., (Eds), *Systems Approaches for Agricultural Development*. Kluwer Academic Publishers, Dordrecht, and the International Rice Research Institute, Los Baños, pp. 207-220.
- Bouman, B.A.M., Wopereis, M.C.S., Kropff, M.J., ten Berge, H.F.M. and Tuong, T.P., 1993. Understanding the water use efficiency of flooded rice fields. II. Simulation and sensitivity analyses. Submitted to *Agric. Wat. Management*.
- Bregt, A.K., 1992. Processing of soil survey data. PhD Thesis, Wageningen Agricultural University, 167 pp.
- Bregt, A.K. and Beemster, J.G.R., 1989. Accuracy in predicting moisture deficits and

- changes in yield from soil maps. *Geoderma* 43: 301-310.
- Bregt, A.K., McBratney, A.B. and Wopereis, M.C.S., 1991. Construction of isolinear maps of soil attributes with empirical confidence limits. *Soil Sci. Soc. Am. J.* 55: 14-19.
- Brinkman, R. and Stein, A., 1987. Linking site information and geographically distributed data at different scales and levels of detail. In: Bunting, A.H. (Ed.), *Agricultural Environments. Characterization, classification and mapping*. CAB International, Wallingford, UK, pp. 119-125.
- Bronswijk, J.J.B., 1988a. Modeling of water balance, cracking and subsidence of clay soils. *J. Hydrol.* 97: 199-212.
- Bronswijk, J.J.B., 1988b. Effect of swelling and shrinkage on the calculation of water balance and water transport in clay soils. *Agric. Water Management* 14: 185-193.
- Bronswijk, J.J.B., 1989. Prediction of actual cracking and subsidence in clay soils. *Soil Sci.* 148: 87-93.
- Bronswijk, J.J.B., 1991. Relation between vertical soil movements and water-content changes in cracking clays. *Soil Sci. Soc. Am. J.* 55: 1220-1226.
- Bronswijk, J.J.B. and Evers-Vermeer, J.J., 1990. Shrinkage of Dutch clay soil aggregates. *Neth. J. Agric. Sci.* 38: 175-194.
- Brooks, R.H. and Corey, C.T., 1964. Hydraulic properties of porous media. *Hydrology Paper 3.*, Colorado State University, Fort Collins, USA.
- BSWM, 1992. Soils/land resources evaluation project Tarlac Province. Physical environment, agro-soci-economics and land evaluation. Department of Agriculture, Bureau of Soils and Water Management, Manila, Philippines.
- Bunting, A.H. (Ed.), 1987. *Agricultural Environments. Characterization, classification and mapping*. CAB International, Wallingford U.K.
- Burgess, T.M., Webster, R. and McBratney, A.B., 1981. Optimal interpolation and isarithmic mapping of soil properties. IV. Sampling strategy. *J. Soil Sci.* 32: 643-659.
- Burrough, P.A., 1986. Principles of geographical information systems for land resources assessment. Clarendon Press, Oxford, 194 pp.
- Burrough, P.A., 1992. Development of intelligent geographical information systems. *Int. J. Geographical Information Systems* 6: 1-11.
- Cruz, R.T., O'Toole, J.C., Dingkuhn, M., Yambao, E.G., Thangaraj, M. and De Datta, S.K., 1986. Shoot and root response to water deficit in rainfed lowland rice. *Aust. J. Plant Physiol.* 13: 567-575.
- Daamen, C.C., Xiao, Z. and Robinson, J.A., 1990. Estimation of water-retention function using scaling theory and soil physical properties. *Soil Sci. Soc. Am. J.* 54: 8-13.
- Dam, J.C. van, Stricker, J.N.M. and Droogers, P., 1990. From one-step to multi-step. Determination of soil hydraulic functions by outflow experiments. Report 7. Department of Hydrology, Soil Physics and Hydraulics, Wageningen Agricultural University, The Netherlands, 39 pp. + figures.

- De Datta, S.K., 1986. Technology development and spread of direct-seeded flooded rice in Southeast Asia. *Experimental Agriculture* 22: 417-426.
- De Datta, S.K., Abilay, W.P. and Kalwar, G.N., 1973. Water stress effects in flooded tropical rice. In: *Water management in Philippine irrigation systems: Research and operations*. International Rice Research Institute, Los Baños, Philippines, pp. 19-36.
- Dekker, L.W. and Jungerius, P.D., 1990. Water repellency in the dunes with special reference to the Netherlands. In: Bakker, T.W., Jungerius, P.D. and Klijn, J.A. (Eds), *Dunes of the European coasts: geomorphology - hydrology - soils*. Cremlingen-Destedt, Catena suppl. 18: 173-183.
- Di, H.J., Trangmar, B.B. and Kemp, R.A., 1989. Use of geostatistics in designing sampling strategies for soil survey. *Soil Sci. Soc. Am. J.* 53: 1163-1167.
- Diepen, C.A. van, Rappoldt, C., Wolf, J. and van Keulen, H., 1988. CWFS crop growth simulation model WOFOST. Documentation Version 4.1. Centre for World Food Studies, Amsterdam - Wageningen, The Netherlands, 299 pp.
- Diepen, C.A. van, van Keulen, H., Wolf, J., Berkhout, J.A.A., 1991. Land evaluation: from intuition to quantification. In: Stewart, B.A. (Ed.), *Advances in Soil Science* 15. Springer-Verlag, New York, pp. 139-204.
- Dobermann, A., 1993. Field variation of soil properties and the growth of direct-seeded flooded rice. *Geoderma*, in press.
- Doorenbos, J. and Kassam, A.H., 1979. Yield response to water. *FAO Irrigation and Drainage Paper* 33, FAO, Rome, 193 pp.
- ESRI, 1987. *ARC/INFO: The geographic information system software (user's guide)*. Environmental Systems Research Institute, California, USA.
- Falayi, O. and Bouma, J., 1975. Relationships between the hydraulic conductance of surface crusts and soil management in a Typic Hapludalf. *Soil Sci. Soc. Amer. Proc.* 39: 957-963.
- FAO, 1977. Crop water requirements. *FAO Irrigation and Drainage Paper* 24, 16 pp.
- FAO, 1979. Soil survey investigations for irrigation. *FAO Soil Bulletin* 42, App. B-2, Rome.
- Feddes, R.A. and van Wijk, A.L.M., 1990. Dynamic land capability model: a case history. *Phil. Trans. R. Soc. Lond.* 329: 411-419.
- Feddes, R.A., Kowalik, P.J. and Zaradny, H., 1978. Simulation of field water use and crop yield. *Simulation Monographs*, Pudoc, Wageningen, 195 pp.
- Feddes, R.A., de Graaf, M., Bouma, J. and van Loon, C.D., 1988. Simulation of water use and production of potatoes as affected by soil compaction. *Potato Res.* 31: 225-239.
- Feijen, J. (Ed.), 1987. Simulation models for cropping systems in relation to water management. *Proceedings of a symposium in the Community programme for coordination of agricultural research*. 26-28 November 1986, Louvain. EUR 10869. Commission of the European Communities, Luxembourg.
- Finke, P.A., Bouma, J. and Stein, A., 1992. Measuring field variability of disturbed soils for simulation purposes with geostatistical and morphological techniques. *Soil*

- Sci. Soc. Am. J. 56: 187-192.
- Ferguson, J.A., 1970. Effect of flooding depth on rice yield and water balance. *Arkansas Farm Research* 19(3): 4.
- France, J. and Thornley, J.H.M., 1984. *Mathematical models in agriculture*. Butterworths, London.
- Fujioka, Y. and Sato, K., 1986. On the drying of clayey paddy field (II). *Trans. ISIDRE*, 26, pp. 1-7. (in Japanese with English abstract).
- Fujisaka, J.S., Moody, K. and Ingram, K.T., 1993. A descriptive study of farming practices for dry seeded rainfed lowland rice in India, Indonesia, and Myanmar. *Agriculture, Environment and Ecosystems* (in press).
- Fukai, S., Kuroda, E. and Yamagishi T., 1985. Leaf gas exchange of upland and lowland rice cultivars. *Photosynthesis Res.* 7: 127-135.
- Gajem, Y.M., Warrick, A.W. and Myers, D.E., 1981. Spatial dependence of physical properties of a typical Torrifluent soil. *Soil Sci. Soc. Am. J.* 45: 709-715.
- Gardner, W.R., 1958. Some steady state solutions of the unsaturated moisture flow equation with application to evaporation from a water-table. *Soil Sci.* 85: 228-232.
- Genuchten, M.Th. van, 1980. A closed-form equation for predicting the hydraulic properties of unsaturated soils. *Soil Sci. Soc. Am. J.* 44: 892-898.
- Genuchten, M.Th. van, Leij, F.J. and Yates, S.R., 1991. The RETC code for quantifying the hydraulic functions of unsaturated soils. US-EPA, Ada, Oklahoma 74820, USA, 85 pp.
- Ghani, M.A., 1987. Improved irrigation water management for rice areas in Bangladesh. PhD Thesis, Utah State University, USA, 180 pp.
- Greenland, D.J., 1985. Physical aspects of soil management for rice-based cropping systems. In: *Soil Physics and Rice*. International Rice Research Institute, Los Baños, Philippines, pp. 1-16.
- Haraguchi, N., 1990. Effect of soil puddling on spatial variability of bulk density and soil moisture in the topsoil of paddy field. *Transactions of the 14th International Congress of Soil Science*, Vol. I ISSS, Kyoto, pp. 241-242.
- Hardjoamidjojo, S., 1992. The effect of depth of flooding and method of water application on water requirements and yield of wetland paddy. In: Murty, V.V.N. and Koga, K. (Eds), *Soil and Water Engineering for Paddy Field Management*. Irrigation Engineering and Management Program, Asian Institute of Technology, Bangkok, pp. 63-71.
- Hasegawa, S. and Woodhead, T., 1990. Problems and opportunities in soil physical management in rice-based cropping systems. In: *Transactions of the 14th International Congress of Soil Science*. Vol. I. ISSS, Kyoto, Japan, pp. 139-145.
- Hasegawa, S., Thangaraj, M. and O'Toole, J.C., 1987. Root behaviour: field and laboratory studies for rice and non rice crops. In: *Soil Physics and Rice*. International Rice Research Institute, Los Baños, Philippines, pp. 383-396.
- Haverkamp, R. and Parlange, J.Y., 1986. Predicting the water-retention curve from particle-size distribution: 1. Sandy soil without organic matter. *Soil Sci.* 142: 325-339.

- Hillel, D. and Gardner, W.R., 1969. Steady infiltration into crust-topped profiles. *Soil Sci.* 108: 137-142.
- Hillel, D. and Gardner, W.R., 1970. Measurement of unsaturated conductivity and diffusivity by infiltration through an impeding layer. *Soil Sci.* 109: 149-153.
- Hopmans, J.W. and Stricker, J.N.M., 1989. Stochastic analysis of soil water regime in a watershed. *J. Hydrol.* 105: 57-84.
- Hundal, S.S. and De Datta, S.K., 1984. In situ water transmission characteristics of a tropical soil under rice-based cropping systems. *Agric. Water Management* 8: 387-396.
- Hurbich, C.M. and Tsai, C., 1989. Regression and time series model selection in small samples. *Biometrika* 76: 297-307.
- IBSNAT, 1988. Experimental design and data collection procedures for IBSNAT. Technical Report no. 1 (3rd edition), University of Hawaii.
- Inthapan, P. and Fukai, S., 1988. Growth and yield of rice cultivars under sprinkler irrigation in south-eastern Queensland. 2. Comparison with maize and grain sorghum under wet and dry conditions. *Aust. J. Exp. Agric.* 28: 243-248.
- IRRI, 1965. Annual report 1964. International Rice Research Institute, Los Baños, Philippines, 335 pp.
- IRRI, 1978. Annual report for 1977. International Rice Research Institute, Los Baños, Philippines, 548 pp.
- IRRI, 1987. Physical measurements in flooded rice soils - the Japanese methodologies. International Rice Research Institute, Los Baños, Philippines, 65 pp.
- IRRI, 1988. Annual Report for 1987. International Rice Research Institute, P.O. Box 933, 1099 Manila, Philippines, 640 pp.
- IRRI, 1989. IRRI towards 2000 and beyond. International Rice Research Institute, Los Baños, Philippines, 66 pp.
- IRRI, 1991a. IRRI Toward 2000. International Rice Research Institute, P.O. Box 933, 1099 Manila, Philippines, 7 pp.
- IRRI, 1991b. Compilation of weather data for 1990. Annual Report Climate Unit IRRI. International Rice Research Institute, Los Baños, Philippines, 98 pp.
- IRRI, 1992. Program report for 1991. International Rice Research Institute, Los Baños, Philippines, 322 pp.
- IRRI, 1993. Rice Research in a Time of Change. IRRI's Medium-Term Plan for 1994-1998. International Rice Research Institute, Los Baños, Philippines, 79 pp.
- Ishiguro, M., 1992. Effects of shrinkage and swelling of soils on water management in paddy fields. In: Murty, V.V.N. and Koga, K. (Eds), *Soil and Water Engineering for Paddy Field Management*. Irrigation Engineering and Management Program, Asian Institute of Technology, Bangkok, pp. 258-267.
- Iwata, S., Tabuchi, T. and Warkentin, B.P., 1988. Soil-water interactions. Mechanisms and applications. Marcel Dekker, Inc., New York, pp. 362-363.
- Jones, A.C. and O'Toole, J.C., 1987. Application of crop production models in agro-ecological characterization: simulation models for specific crops. In: Bunting, A.H.

- (Ed.), *Agricultural Environments. Characterization, classification and mapping*. CAB International, Wallingford, UK, pp. 199-209.
- Journal, A.G. and Huijbregts, C.J., 1978. *Mining geostatistics*. Academic Press, London.
- Kafritsas, J. and Bras, R.L., 1981. *The practice of kriging*. Report No. 263. Mass. Inst. of Technol., Cambridge, Mass.
- Kampen, J., 1970. *Water losses and water balance studies in lowland rice irrigation*. PhD Thesis, Cornell University, USA, 416 pp.
- Kanwar, J.S., 1986. *Water management - the key to developing agriculture*. In: Kanwar, J.S. (Ed.), *National Seminar on Water Management - the Key to Developing Agriculture*. Agric. Publishing Academy, New Delhi, pp. 55-71.
- Keulen, van H. and Wolf, J. (Eds), 1986. *Modelling of agricultural production: weather, soils and crops*. Simulation Monographs, Pudoc, Wageningen, 479 pp.
- Keulen, H. van, Berkhout, J.A.A., van Diepen, C.A., van Heemst, H.D.J., Janssen, B.H., Rappoldt, C. and Wolf, J., 1987. *Quantitative land evaluation for agro-ecological characterization*. In: Bunting, A.H. (Ed.), *Agricultural Environments. Characterization, classification and mapping*. CAB International, Wallingford U.K, pp. 185-197.
- Khush, G.S. and Garrity, D.P., 1984. *Terminology for rice growing environments*. International Rice Research Institute, P.O. Box 933, 1099 Manila, Philippines.
- Klute, A., 1986. *Methods of soil analysis. Part 1. Physical and mineralogical methods*. Madison, Wisconsin, 1188 pp.
- Kneale, W.R. and White, R.E., 1984. *The movement of water through cores of a dry (cracked) clay-loam grassland topsoil*. J. Hydrol. 67: 361-365.
- Kool, J.B., Parker, J.C. and van Genuchten, M.Th., 1985. *Determining soil hydraulic properties from one-step outflow experiments by parameter estimation. I. Theory and numerical studies*. Soil Sci. Soc. Am. J. 49: 1348-1353.
- Kraalingen, D.W.G., 1991. *The FSE system for crop simulation*. Simulation Report CABO-TT no. 23, Centre for Agrobiological Research, P.O. Box 14, Wageningen, The Netherlands, 77 pp.
- Kropff, M.J., 1993. *Mechanisms of competition for water*. In: Kropff, M.J. and van Laar, H.H. (Eds), *Modelling Crop-Weed Interactions*. CAB International, Wallingford, UK, in press.
- Kropff, M.J. and Spiters, C.J.T., 1992. *An eco-physiological model for interspecific competition, applied to the influence of *Chenopodium album* L. on sugar beet. I. Model description and parameterization*. Weed Res. 32: 437-450.
- Kropff, M.J. and van Laar, H.H. (Eds), 1993. *Modelling Crop-Weed Interactions*. CAB International, Wallingford, UK, 274 pp.
- Kropff, M.J., Cassman, K.G. and van Laar, H.H., 1992. *Quantitative understanding of the irrigated rice ecosystem for achieving high yield potential in (hybrid) rice*. Paper presented at the International Rice Research Conference, 21-25 April 1992. International Rice Research Institute, P.O. Box 933, Manila, Philippines.

- Kropff, M.J., van Laar, H.H. and ten Berge, H.F.M. (Eds), 1993a. ORYZA1, a basic model for irrigated lowland rice production. International Rice Research Institute, Los Baños, Philippines, 78 pp.
- Kropff, M.J., ten Berge, H.F.M. and M.C.S. Wopereis (Eds), 1993b. Third phase of the SARP-network (1992-1995): Project outline and crop simulation research plans. International Rice Research Institute, P.O. Box 933, Manila, Philippines.
- Laar, H.H. van, Goudriaan, J. and van Keulen, H. (Eds), 1992. Simulation of crop growth for potential and water-limited production situations (as applied to spring wheat). CABO-TPE Simulation Report Series, no. 27. CABO, Wageningen, The Netherlands, 72 pp.
- Lanen, H.A.J. van, van Diepen, C.A., Reinds, G.J. and de Koning, G.H.J., 1992. A comparison of qualitative and quantitative physical land evaluations, using an assessment of the potential for sugar-beet growth in the European Community. *Soil Use and Management* 8(2): 80-89.
- Lauren, J.G., Wagenet, R.J. and Bouma, J., 1988. Variability of saturated hydraulic conductivity in a glossaquic Hapludalf with macropores. *Soil Sci.* 145: 20-28.
- Lilliefors, H.W., 1967. On the Kolmogorov-Smirnov test for normality with mean and variance unknown. *J. Am. Stat. Assoc.* 62: 399-402.
- Matheron, G., 1989. Estimating and choosing. Springer, Berlin.
- McBratney, A.B., Webster, R. and Burgess, T.M., 1981. The design of optimal sampling schemes for local estimation and mapping of regionalized variables. I. Theory and methods. *Computers and Geosciences* 7: 331-334.
- McBratney, A.B. and Webster, R., 1981. The design of optimal sampling schemes for local estimation and mapping of regionalized variables. II. Program and examples. *Computers and Geosciences* 7: 335-365.
- McCree, K.J. and Fernandez, C.J., 1989. Simulation model for studying physiological water stress responses of whole plants. *Crop Sci.* 29: 353-360.
- Miller, E.E. and Miller, R.D., 1955. Theory of capillary flow: I. Practical implications. *Soil Sci. Soc. Am. Proc.* 19: 267-271.
- Miller, E.E. and Miller, R.D., 1956. Physical theory for capillary flow phenomena. *J. Appl. Phys.* 27: 324-332.
- Moormann, F.R. and van Breemen, N., 1978. Rice: soil, water, land. International Rice Research Institute, Los Baños, Philippines, 185 pp.
- Muchow, R.C. and Bellamy, J.A. (Eds), 1991. Climatic risk in crop production: models and management for the semiarid tropics and subtropics. CAB International, Wallingford, UK, 548 pp.
- Muchow, R.C., Hammer, G.L. and Carberry, P.S., 1991. Optimising crop and cultivar selection in response to climatic risk. In: Muchow, R.C. and Bellamy, J.A. (Eds), *Climatic risk in crop production: models and management for the semiarid tropics and subtropics*. CAB International, Wallingford, UK, pp. 235-262.
- Murty, K.S. and Sahu, G., 1987. Impact of low-light stress on growth and yield of rice. In: *Weather and Rice*. International Rice Research Institute, Los Baños, Philippines,

pp. 93-101.

- Nix, H.A., 1976. Climate and crop productivity in Australia. In: *Climate and Rice*. International Rice Research Institute, Los Baños, Philippines, pp. 495-508.
- Nix, H.A., 1987. The role of crop modelling, minimum data sets, and geographic information systems in the transfer of agricultural technology. In: Bunting, A.H. (Ed.), *Agricultural environments. Characterization, classification and mapping*. CAB International, Wallingford, pp. 113-117.
- O'Toole, J.C., 1982. Adaptation of rice to drought-prone environments. In: *Drought Resistance in Crops with Emphasis on Rice*. International Rice research Institute, Los Baños, Philippines, pp. 195-213.
- O'Toole, J.C. and Chang, T.T., 1979. Drought resistance in cereals - Rice: a case study. In: Mussel, H. and Staples, R. (Eds), *Stress physiology in crop plants*. Wiley-Interscience New York, pp. 373-405.
- O'Toole, J.C. and Cruz, R.T., 1980. Response of leaf water potential, stomatal resistance and leaf rolling to water stress. *Plant Physiol.* 65: 428-432.
- O'Toole, J.C. and Moya, T.B., 1981. Water deficits and yield in upland rice. *Field Crops Res.* 4: 247-259.
- O'Toole, J.C. and Baldia, E.P., 1982. Water deficits and mineral uptake in rice. *Science* 22: 1144-1150.
- Painuli, D.K., Woodhead, T. and Pagliai, M., 1988. Effective use of energy and water in rice-soil puddling. *Soil and Tillage Res.* 12: 149-161.
- Palanisami, K., 1993. Optimization of cropping patterns in tank irrigation systems in Tamil Nadu, India. In: Penning de Vries, F.W.T., Teng, P.S. and Metselaar, K. (Eds), *Systems approaches for agricultural development*. Kluwer Academic Press, Dordrecht, pp. 413-425.
- Pathak, M.D. and Gomez, K.A., 1991. Rice production trends in selected Asian countries. IRRI Research Papers no. 147. International Rice Research Institute, Los Baños, Philippines.
- Peck, A.J., Luxmoore, R.J. and Stolzy, J.L., 1977. Effects of spatial variability of soil hydraulic properties in water budget modeling. *Water Resour. Res.* 13: 348-354.
- Penman, H.L., 1948. Natural evaporation from open water, bare soil and grass. *Proceedings of the Royal Society of London Series A* 193, 120-146.
- Penning de Vries, F.W.T. and van Laar, H.H. (Eds), 1982. Simulation of plant growth and crop production. *Simulation Monographs*, Pudoc, Wageningen, 308 pp.
- Penning de Vries, F.W.T., Jansen, D.M., ten Berge, H.F.M. and Bakema, A., 1989. Simulation of ecophysiological processes of growth in several annual crops. *Simulation Monographs* 29. IRRI, Los Baños and Pudoc, Wageningen, 271 pp.
- Price, W.L., 1979. A controlled random search procedure for global optimization. *The Computer Journal* 20: 367-370.
- Prihar, S.S., Ghildyal, B.P., Painuli, D.K. and Sur, H.S., 1985. Physical properties of mineral soils affecting rice-based cropping systems. In: *Soil Physics and Rice*. International Rice Research Insitute, Los Baños, Philippines, pp. 57-70.

- Puckridge, D.W. and O'Toole, J.C., 1981. Dry matter and grain production of rice, using a line source sprinkler in drought studies. *Field Crops Res.* 3: 303-319.
- Radulovich, R., Sollins, P., Baveye, P. and Solorzano, E., 1992. Bypass water flow through unsaturated microaggregated tropical soils. *Soil Sci. Soc. Am. J.* 56: 721-726.
- Richards, L.A., 1965. Physical condition of water in soil. In: Black, C.A. et al. (Eds), *Methods of Soil Analysis*. Agronomy 9: 131-137.
- Russo, D., 1984. Design of an optimal sampling network for estimating the variogram. *Soil Sci. Soc. Am. J.* 48: 708-716.
- Russo, D. and Bresler, E., 1980. Scaling soil hydraulic properties of a heterogeneous field. *Soil Sci. Soc. Am. J.* 44: 681-684.
- Sanchez, P.A., 1973. Puddling tropical rice soils. II. Effects of water losses. *Soil Sci.* 115(4): 303-308.
- Sattar, M.A. and Bhuiyan, S.I., 1985. Water utilization in a selected tubewell project in Bangladesh. *Bangladesh Journal of Agriculture* 10 (1): 23-33.
- Sharma, P.K. and De Datta, S.K., 1985a. Effects of puddling on soil physical properties and processes. In: *Soil Physics and Rice*. International Rice Research Institute, Los Baños, Philippines, pp. 217-234.
- Sharma, P.K. and De Datta, S.K., 1985b. Puddling influence on soil, rice development, and yield. *Soil Sci. Soc. Am. J.* 49: 1451-1457.
- Sinclair, T.R., 1986. Water and nitrogen limitations in soybean grain production. I. Model development. *Field Crops Res.* 15: 125-141.
- Sinclair, T.R. and Ludlow, M.M., 1986. Influence of soil water supply on the plant water balance of four tropical grain legumes. *Aust. J. Pl. Physiol.* 13: 329-341.
- Soil Survey Staff, 1975. Soil taxonomy. A basic system of soil classification for making and interpreting soil surveys. USDA-SCS Agric. Handb. 436. U.S. Government Printing Office. Washington, DC.
- Spitters, C.J.T., van Keulen, H. and van Kraalingen, D.W.G., 1989. A simple and universal crop growth simulator: SUCROS87. In: Rabbinge, R., Ward, S.A. and van Laar, H.H. (Eds), *Simulation and Systems Management in Crop Protection*. Simulation Monographs, Pudoc, Wageningen, pp. 147-181.
- Starks, T.H. and Fang, J.H., 1982. On the estimation of the generalized covariance function. *Mathematical Geology* 14: 57-64.
- Steel, R.G.D. and Torrie, J.H., 1980. Principles and procedures of statistics. A biometrical approach. McGraw-Hill, Inc., New York, 95 pp.
- Steenhuis, T.S. and Muck, R.E., 1988. Preferred movement of non adsorbed chemicals on wet, shallow, sloping soils. *J. Environ. Qual.* 17: 376-384.
- Stein, A., 1991. Spatial interpolation. PhD Thesis, Wageningen Agricultural University, The Netherlands, 236 pp.
- Stein, A., Hoogerwerf, M. and Bouma, J., 1988. Use of soil-map delineations to improve (co-)kriging of point data on moisture deficits. *Geoderma* 43: 163-177.
- Stein, A., Bouma, J., Kroonenberg, S.B. and Cobben, S., 1989. Sequential sampling

- to measure the infiltration rate within relatively homogeneous soil units. *Catena* 16: 91-100.
- Stein, A., van Eijnsbergen, A.C. and Barendregt, L.G., 1991. Cokriging non-stationary data. *Mathematical Geology* 23: 703-719.
- Stein, A., Staritsky, I.G., Bouma, J., van Eijnsbergen, A.C. and Bregt, A.K., 1992. Simulation of moisture deficits and areal information by universal cokriging. *Water Resour. Res.* 27: 1963-1973.
- Stiphout, T.P.J. van, van Lanen, H.A.J., Boersma, O.H. and Bouma, J., 1987. The effect of bypass flow and internal catchment of rain on the water regime in a clay loam grassland soil. *J. Hydrol.* 95: 1-11.
- Stroosnijder, L., 1982. Simulation of the soil water balance. In: Penning de Vries, F.W.T. and van Laar, H.H. (Eds), *Simulation of plant growth and crop production. Simulation Monographs*. Pudoc, Wageningen, pp. 175-193.
- Supit, I., 1986. Manual for generation of daily weather data. *Simulation Reports CABO-TT No. 7*, CABO, Wageningen, the Netherlands, 47 pp.
- Sur, H.S., Prihar, S.S. and Jalota, S.K., 1981. Effect of rice-wheat and maize-wheat rotations on water transmission and wheat root development in a sandy loam of the Punjab, India. *Soil and Tillage Res.* 1: 361-371.
- Tabal, D.F., Lampayan, R.M. and Bhuiyan, S.I., 1992. Water-efficient irrigation techniques for rice. Paper presented at the International Workshop on Soil and Water Engineering for Paddy Field Management, Asian Institute of Technology, Bangkok, 28-30 January, 1992.
- Tabuchi, T., 1985. Underdrainage of lowland rice fields. In: *Soil Physics and Rice*. International Rice Research Institute, Los Baños, Philippines, pp. 147-159.
- Tabuchi, T., Yamafuji, I. and Kuroda, H., 1990. Effect of puddling on percolation rate and nitrogen concentration in percolating water. *Transactions of the 14th International Congress of Soil Science. Vol. I* ISSS, Kyoto, Japan, pp. 287-288.
- Takagi, S., 1960. Analysis of the vertical downward flow of water through a two-layered soil. *Soil Sci.* 90: 98-103.
- Trangmar, B.B., Yost, R.S., Wade, M.K., Uehara, G. and Sudjadi, M., 1987. Spatial variation of soil properties and rice yield on recently cleared land. *Soil Sci. Soc. Am. J.* 51: 668-674.
- Turner, N.C., 1986. Crop water deficits: a decade of progress. *Adv. Agron.* 39: 1-51.
- Turner, N.C., O'Toole, J.C., Cruz, R.T., Namuco, O.S. and Ahmad S., 1986. Responses of seven diverse rice cultivars to water deficits. I. Stress development, canopy temperature, leaf rolling and growth. *Field Crops Res.* 13: 257-271.
- Valera, A., 1977. Field studies on water use and duration for land preparation for lowland rice. MSc Thesis, University of the Philippines, Los Baños, 126 pp.
- Vereecken, H., Maes, J. and Feyen, J., 1990. Estimating unsaturated hydraulic conductivity from easily measured soil properties. *Soil Sci.* 149(1): 12-32.
- Villaruz, M.S., 1986. The floating power tiller in the Philippines. In: *Small Farm Equipment for Developing Countries*. International Rice Research Institute, Los

- Baños, Philippines, pp. 173-178.
- Wagenet, R.J., Bouma, J. and Grossman, R.B., 1991. Minimum data sets for use of taxonomic information in soil interpretive models. In: Mausbach, M.J. and Wilding, L.P. (Eds), *Spatial variabilities of soils and landforms*. Soil Sci. Soc. Am. Spec. Publication 28: 161-183.
- Wald, A., 1947. *Sequential analysis*. Wiley, New York.
- Walker, S.H. and Rushton, K.R., 1984. Verification of lateral percolation losses from irrigated rice fields by a numerical model. *J. Hydrol.* 71: 335-351.
- Warrick, A.W., Mullen, G.J. and Nielsen, D.R., 1977. Scaling field measured soil hydraulic properties using a similar media concept. *Water Resour. Res.* 13, 355-362.
- Warrick, A.W. and Myers, D.E., 1987. Optimization of sampling locations for variogram calculations. *Water Resour. Res.* 23: 496-500.
- Webster, R., 1985. Quantitative spatial analysis of soil in the field. In: Stewart, B.A. (Ed.), *Advances in Soil Science 3*. Springer Verlag, New York, pp. 1-70.
- Wetherill, G.B. and Glazebrook, K.D., 1986. *Sequential methods in statistics*. Chapman and Hall, London.
- Wickham, T.H. and Singh, V.P., 1978. Water movement through wet soils. In: *Soils and Rice*. International Rice Research Institute, Los Baños, Philippines, pp. 337-358.
- Wild, A., 1972. Nitrate leaching under bare fallow at a site in northern Nigeria. *J. Soil Sci.* 23: 315-324.
- Wind, G.P., 1968. Capillary conductivity data estimated by a simple method. In: Rijtema, P.E. and Wassink, H. (Eds), *Water in the Unsaturated Zone*. Vol. 1. Proceedings of the Wageningen Symposium, June 1966. IASH Gentbrugge / UNESCO Paris, pp. 181-191.
- Wit, C.T. de and Penning de Vries, F.W.T., 1982. L'analyse des systèmes de production primaire. In: Penning de Vries, F.W.T. and Djitéye, M.A. (Eds), *La Productivité des Pâturages Sahéliens*. Agricultural Research Reports 918, Pudoc, Wageningen, pp. 20-27.
- Wit, C.T. de and van Keulen, H., 1987. Modelling production of field crops and its requirements. *Geoderma* 40: 253-265.
- Wit, C.T. de, Goudriaan, J., van Laar, H.H., Penning de Vries, F.W.T., Rabbinge, R., van Keulen, H., Sibma, L. and de Jonge, C., 1978. Simulation of assimilation, respiration and transpiration of crops. *Simulation Monographs*, Pudoc, Wageningen, 141 pp.
- Wolfram, S., 1991. *Mathematica*. A system for doing mathematics by computer. Second edition. Addison-Wesley Publishing Company, Inc., Redwood City, California, 961 pp.
- Woodhead, T., ten Berge, H.F.M. and de San Agustin, E.M., 1991. Modeling upland rice hydrology. In: Penning de Vries, F.W.T., Kropff, M.J., Teng, P.S. and Kirk, G.J.D. (Eds), *Systems Simulation at IRRI*. International Rice Research Institute, P.O. Box 933, 1099 Manila, Philippines, pp. 53-60.

- Wopereis, M.C.S., Kropff, M.J., Bouma, J., van Wijk, A.L.M. and Woodhead, T. (Eds), 1993. Manual for soil hydraulic measurements, field monitoring techniques and sampling strategies for rice based cropping systems. International Rice Research Institute, Los Baños, Philippines, in press.
- Wösten, J.H.M., 1991. Use of scaling techniques to quantify variability in hydraulic functions of soil in The Netherlands. In: K. Roth, H. Flühler, W.A. Jury and J.C. Parker (Eds), Proceedings of the International Workshop on 'Field-scale Water and Solute Flux in Soils', Sept. 25-29, Monte Verità, Switzerland. Birkhäuser Verlag, Basel-Boston-Berlin.
- Wösten, J.H.M. and van Genuchten, M.Th., 1988. Using texture and other soil properties to predict the unsaturated soil hydraulic functions. *Soil Sci. Soc. Am. J.* 52: 1762-1770.
- Wösten, J.H.M., Bouma, J. and Stoffelsen, G.H., 1985. Use of soil survey data for regional soil water simulation models. *Soil Sci. Soc. Am. J.* 49: 1238-1244.
- Wösten, J.H.M., Bannink, M.H., de Gruijter, J.J. and Bouma, J., 1986. A procedure to identify different groups of hydraulic-conductivity and moisture-retention curves for soil horizons. *J. Hydrol.* 86: 133-145.
- Wösten, J.H.M., Bannink, M.H. and Beuving, J., 1987a. Water retention and hydraulic conductivity characteristics of top- and subsoils in the Netherlands: The Staring Series. Report No. 1932, Soil Survey Institute, Wageningen, The Netherlands.
- Wösten, J.H.M., Bannink, M.H. and Bouma, J., 1987b. Land evaluation at different scales: you pay for what you get! *Soil Survey and Land Evaluation* 7: 13-24.
- Wösten, J.H.M., Schuren, C.H.J.E., Bouma, J. and Stein, A., 1990. Functional sensitivity analysis of four methods to generate soil hydraulic functions. *Soil Sci. Am. J.* 54: 827-832.
- Wijk, A.L.M. van and Feddes, R.A., 1986. Simulating effects of soil type and drainage on arable crop yield. In: van Wijk, A.L.M. and Wesseling, J.G. (Eds), *Agricultural water management. Proceedings of the symposium on agricultural water management, Arnhem, 18 - 21 June 1985.* A.A. Balkema, Rotterdam, pp. 97-112.
- Yoshida, S., 1981. Fundamentals of rice crop science. International Rice Research Institute, Los Baños, Philippines, 269 pp.

Other related publications of the author

- Wopereis, M.C.S., M.J. Kropff, J. Bouma, A.L.M. van Wijk and T. Woodhead (Eds), 1993. Measurement and use of soil physical properties in rice based cropping systems. International Rice Research Institute, Los Baños, Philippines, in press.
- Wopereis, M.C.S., 1993. Introduction. In: Wopereis, M.C.S. et al. (Eds), Measurement and use of soil physical properties in rice based cropping systems. International Rice Research Institute, Los Baños, Philippines, in press.
- Stein, A., Wopereis, M.C.S. and Bouma, J., 1993. Soil sampling strategies and geostatistical techniques. In: Wopereis, M.C.S. et al. (Eds), Measurement and use of soil physical properties in rice based cropping systems. International Rice Research Institute, Los Baños, Philippines, in press.
- Stolte, J., Veerman, G.J. and Wopereis, M.C.S., 1993. Measurement of soil hydraulic properties. In: Wopereis, M.C.S. et al. (Eds), Measurement and use of soil physical properties in rice based cropping systems. International Rice Research Institute, Los Baños, Philippines, in press.
- Wopereis, M.C.S., 1993. Field monitoring techniques. In: Wopereis, M.C.S. et al. (Eds), Measurement and use of soil physical properties in rice-based cropping systems. International Rice Research Institute, Los Baños, Philippines, in press.
- Wopereis, M.C.S., Kropff, M.J. and Bouma, J., 1993. Soil data needs for regional studies of yield constraints in water-limited environments using modeling and GIS. In: Wopereis, M.C.S. et al. (Eds), Measurement and use of soil physical properties in rice-based cropping systems. International Rice Research Institute, Los Baños, Philippines, in press.
- Bouma, J., Wopereis, M.C.S., Wösten, J.H.M. and Stein, A., 1993. Soil data for crop-soil models. In: F.W.T. Penning de Vries, F.W.T., Teng, P.S. and Metselaar, K. (Eds), Systems approaches for agricultural development. Kluwer Academic Publishers, pp. 207-220.
- Stolte, J., Veerman, G.J. and Wopereis, M.C.S., 1992. Manual soil physical measurements, version 2.0. Wageningen (The Netherlands), DLO Winand Staring Centre. Technical Document 2. 49 pp. ISSN 0928-0944.
- Bregt, A.K., McBratney, A.B. and Wopereis, M.C.S., 1991. Construction of isolinear maps of soil attributes with empirical confidence limits. *Soil Sci. Soc. Am. J.* 55: 14-19.
- Bregt, A.K. and Wopereis, M.C.S., 1990. Comparison of complexity measures for choropleth maps. *The Cartographic Journal* 27: 85-91.
- Wopereis, M.C.S. and Bregt, A.K., 1989. Complexity measures for choropleth maps. *Kartografisch Tijdschrift* 15: 25-30. (In Dutch).
- Wopereis, M.C.S., Gascuel-Oudoux, C., Bourrie, G. and Soignet, G., 1988. Spatial variability of heavy metals in soil on a one-hectare scale. *Soil Science* 146: 113-118.

Curriculum vitae

Marco Cletus Sebastiaan Wopereis was born August 15, 1962, in Ede, The Netherlands. He began his study in soil science and fertilizer use at the Wageningen Agricultural University, The Netherlands in September 1980. From March to September 1986, he worked as a research student at the Institute National de Recherche Agronomique (INRA) in Rennes, France on spatial variability of heavy metals in soil. In January 1988, he graduated from the Wageningen Agricultural University (cum laude) with specializations in soil survey and land evaluation, soil chemistry and soil fertility, computer science, and public administration (at the Erasmus University, Faculty of Management, Rotterdam). After his study, he first worked as a computer programmer at the Biogeographic Information Centre in Utrecht. In November 1988, he joined the Winand Staring Centre for Integrated Land, Soil and Water Research in Wageningen as soil scientist. From April 1989 to June 1992, he worked for the research project 'Soil management for increased and sustainable rice production' at the International Rice Research Institute (IRRI) in Los Baños, Philippines. Since June 1992, he is employed by the Department of Theoretical Production Ecology of the Wageningen Agricultural University as theme coordinator Crop and Soil management for the project 'Simulation and systems analysis for rice production' (SARP), stationed at IRRI. The research conducted in the Philippines for both projects was partly financed by the Netherlands' Ministry for Development Co-operation and resulted in this thesis.